Iterative Multiuser Receivers for Coded DS-CDMA Systems

José Martín Luna Rivera

A thesis submitted for the degree of Doctor of Philosophy.
The University of Edinburgh.
October 2002

Abstract

The introduction of cellular wireless systems in the 1980s has resulted in a continuous and growing demand for personal communication services. This demand has made larger capacity systems necessary. With the interest from both the research community and industry in wireless code-division multiple-access (CDMA) systems, the application of multiuser detection (MUD) techniques to wireless systems is becoming increasingly important. MUD is an important area of interest to help obtain the significant increase in capacity needed for future wireless services.

The standardisation of direct-sequence CDMA (DS-CDMA) systems in the third generation of mobile communication systems has raised even more interest in exploiting the capabilities and capacity of this type of technology. However, the conventional DS-CDMA system has the major problem of multiple-access interference (MAI). The MAI is unavoidable because receivers deal with information which is transmitted not by a single source but by several uncoordinated and geographically separated sources. As a result, the capacity of these systems is inherently interference limited by other users. To overcome these limitations, MUD emerges as a promising approach to increase the system capacity.

This thesis addresses the problem of improving the downlink capacity of a coded DS-CDMA system with the use of MUD techniques at the mobile terminal receiver. The optimum multiuser receiver scheme is far too computational intensive for practical use. Therefore, the aim of this thesis is to investigate sub-optimal multiuser receiver schemes that can exploit the advantages of MUD but also simplify its implementation. The attention is primarily focused on iterative MUD receiver schemes which apply the turbo multiuser detection principle. Essentially this principle consists of an iterative exchange of extrinsic information among the receiver modules to achieve improved performance.

In this thesis, the implementation of an iterative receiver based on a linear MUD technique and a cancellation scheme over an additive white Gaussian noise (AWGN) channel is first proposed and analysed. The interference analysis shows that good performance is achieved using a low-complexity receiver structure. In more realistic mobile channels, however, this type of receiver suffers from the presence of higher levels of interference resulting in poor receiver performance. The reason for this is that in such scenarios the desired signals are no longer linearly separable. Therefore, non-linear detection techniques are required to provide better performance. With this purpose, a hybrid iterative multiuser receiver is investigated for the case of a stationary multipath channel. The incorporation of antenna arrays is an effective and practical technique to provide a significant capacity gain over conventional single-antenna systems. In this context, a novel space-time iterative multiuser receiver is proposed which achieves a large improvement in spectral efficiency and performance over multipath fading channels. In addition, it is shown that this architecture can be implemented without a prohibitive complexity cost. The exploitation of the iterative principle can be used to approach the capacity bounds of a coded DS-CDMA system. Using the Shannon's sphere packing bound, a comparison is presented to illustrate how closely a practical system can approach the theoretical limits of system performance.

Declaration of originality

I hereby declare that the research recorded in this thesis and the thesis itself was composed and originated entirely by myself in the School of Engineering and Electronics at The University of Edinburgh.

The software program used to perform the simulations was written by myself with the following exceptions:

- The routines used to generate Gaussian distributed noise, uniform distributed deviates, and to perform the inverse matrix operation were obtained from *Numerical recipes in C* [1]

José Martín Luna Rivera

Acknowledgements

There are numerous people that contributed to the completion of this thesis. First and foremost, a sincere thanks is extended to my supervisors Dr. David G. M. Cruickshank and Dr. John S. Thompson for their guidance, support and invaluable advice. I am personally grateful to Dr. David G. M. Cruickshank for reading and correcting this thesis but also for his remarkable availability during a difficult period.

I would like to thank the National Council for Science and Technology (CONACYT-Mexico) for the financial support of this work.

Thanks are also extended to my colleagues in the Signals and System Group for their assistance in one way or another during the last three years.

I would like to express my deepest gratitude to my parents Noradino and Maria de los Angeles for giving me the opportunity to build a successful career. Finally, I wish also to thank my brothers and sisters Gerardo, Yolanda, Noradino, Eduardo, Francisco, Rosalba and Cristóbal, for their constant and unconditional support.

Contents

List of figures

List of tables

Acronyms and abbreviations

3G	third generation
ACI	adjacent channel interference
ACTS	Advanced Communications Technologies Services
AMPS	Advance Mobile Phone Service
APP	*a posteriori* probabilities
AWGN	additive white Gaussian noise
BCJR	Bahl *et al.* [2]
BER	bit error rate
BPSK	binary phase shift keying
BS	base station
CCI	co-channel interference
CDMA	code division multiple acces
CLPC	closed-loop power control
CP	cyclic prefix
DS	direct sequence
DS-CDMA	direct sequence code division multiple access
ETSI	European Telecommunications Standars Institute
FCC	Federal Communications Comision
FDMA	frequency division multiple access
FEC	forward error correction
FFT	Fast Fourier Transform
FH	frequency hopping
FIR	finite impulse response
FLOP	floating point operations
GD	greedy detector
GSM	Global System for Mobile communications
HIC	hybrid interference cancellation
HIMR	hybrid iterative multiuser receiver
IC	interference cancellation

IIR	infinite impulse response
IMT-2000	International Mobile Communications
ISI	intersymbol interference
ITU	International Telecommunication Union
JD	joint detection
LLR	logarithm of likelihood ratio
MAI	multiple access interference
MAP	maximum a posteriori
MC-CDMA	multi-carrier code division multiple access
MF	matched filter
ML	maximum likelihood
MLSE	maximum likelihood sequence estimator
MMSE	minimum mean squared error
MRC	maximum ratio combining
MS	mobile user
MSC	mobile switching center
MUD	multiuser detection
NMT450	Nordic Mobile Telephone
NSC	non-systematic convolutional code
NTT	Nippon Telephone and Telegraph
OFDM	Orthogonal frequency division multiplexing
OLPC	open-loop power control
PCCC	parallel concatenated convolutional codes
PCS	Personal Communication Service
PIC	parallel interference cancellation
PN	pseudo-noise
PSK	phase shift keying
PSML	pre-selection maximum likelihood
PSTN	public switching telephone network
QPSK	quadrature phase shift keying
RBF	radial basis functions
RF	radio frequency
RSC	recursive systematic convolutional code

SCCC	serial concatenated convolutional codes
SIC	successive interference cancellation
SISO	soft input soft output
SNR	signal to noise ratio
SOVA	soft output Viterbi algorithm
SRBF	sub-optimal radial basis function
SS	spread spectrum
STC	space time coding
STTC	space time trellis coding
STTD	space time transmit diversity
TACS	Total Access Communication System
TD	transmit diversity
TDMA	time division multiple access
TH	time hoping
UMTS	Universal Mobile Telecommunication Systems
VA	Viterbi algorithm
WCDMA	wideband code division multiple access
ZF-DF	zero forcing decision feedback

List of Symbols

$\mathbf{A}$	users' amplitude matrix
A_c	amplitude of the SNR per channel symbol
$\mathbf{A}_m$	$(N+\alpha)\times N$ precoding matrix for the signal transmission through the *m*th antenna
$\mathbf{A}_m^0$	$\alpha \times N$ precoding matrix that incorporates the cyclic prefix
$\mathbf{A}_m^1$	$N \times N$ precoding matrix
$\bar{\mathbf{A}}_m$	$(N\times l+\alpha)\times(N\times l)$ block precoding matrix for the signal transmission through the *m*th antenna
$\bar{\mathbf{A}}_m^0$	$\alpha\times(N\times l)$ block precoding matrix that incorporates the cyclic prefix
$\bar{\mathbf{A}}_m^1$	$(N\times l)\times(N\times l)$ block diagonal matrix
B	available bandwidth
B_t	bandwidth of the transmitted signal
B_i	bandwidth of the information signal
C	capacity in an AWGN channel
$\mathbf{C}$	matrix of spreading codes at time t
$\underline{\mathbf{C}}$	matrix of spreading codes which considers the ISI information from the previous and next symbols
$\bar{\mathbf{C}}$	block diagonal matrix with the matrix $\mathbf{C}$ as its diagonal and next symbols
C_T	total system capacity for the AWGN channel
C_u	channel capacity of the *u*th user for the AWGN channel
D	diagonal matrix representing the normalised power of the users according to the number of transmit antennas
E	variable representing the computational complexity of the exponential operation
E_b	energy per data bit
$F[\underline{\mathbf{b}}(t)]$	$(3U\times 1)$ vector of absolute values for the LLRs of the elements in $\underline{\mathbf{b}}(t)$
G_1, G_2	polynomial generators
$\bar{\mathbf{H}}_m$	channel response matrix to the signal sent from the *m*th transmit antenna
$\mathbf{H}_t$	channel response matrix to the transmission of $\mathbf{x}(t)$ without ISI

$\underline{\mathbf{H}}_t$	channel response matrix to the transmission of $\mathbf{x}(t)$ with ISI
$\mathbf{H}_{t-1}^{ISI}$	Toeplitz matrix with the ISI effect from $\mathbf{x}(t-1)$
$H(z)$	z-transform of the channel impulse response
$\mathbf{I}$	identity matrix
K	number of users in a group
L	total number of data bits per block transmitted
M	number of transmit antennas
N	processing gain or spreading factor
N_p	number of paths out of each state in the trellis
P	users' average power
$\mathbf{P}$	diagonal matrix representing the received power of the users
$\mathbf{P}'$	modified matrix with the received power of the users
$PM_s(i)$	path metric for state s at time i
$\mathbf{P}_a[d]$	input vector of *a priori* LLRs for the SISO MAP decoder
$\mathbf{P}_o[d]$	output vector of *a posteriori* LLR from the SISO MAP decoder
$P_e[b_u(t)]$	*extrinsic* LLR at the multiuser detector output for $b_u(t)$
$P_a[b_u(t)]$	*a priori* LLR for $b_u(t)$ at the input of the *u*th FEC decoder
$\hat{P}_e[b_u(t)]$	*extrinsic* LLR at the output of the *u*th FEC decoder for $b_u(t)$
$\hat{P}_a[b_u(t)]$	*a priori* LLR at the multiuser detector input for $b_u(t)$
$\hat{P}_e[d_u(i)]$	*extrinsic* LLR at the output of the *u*th FEC decoder for $d_u(i)$
$P_a^1[d(i)]$	*a priori* LLR of turbo codes at the input of the SISO MAP decoder 1 for the *i*th data bit
$P_c[d(i)]$	reliability constant [3]
$P_e^1[d(i)]$	*extrinsic* LLR of turbo codes at the output of the SISO MAP decoder 1 for the *i*th data bit
$P_o^1[d(i)]$	*a posteriori* LLR of turbo codes at the output of SISO MAP decoder 1 for the *i*th data bit
$P_a^2[d(i)]$	*a priori* LLR of turbo codes at the input of SISO MAP decoder 2 for the *i*th data bit
$P_e^2[d(i)]$	*extrinsic* LLR of turbo codes at the output of the SISO MAP decoder 2 for the *i*th data bit
$P_o^2[d(i)]$	*a posteriori* LLR of turbo codes at the output of SISO MAP decoder 2 for the *i*th data bit

P_u	transmitted power of the *u*th user
Q	number of users in a group
R	data rate at the symbol level
$\mathbf{R}$	correlation matrix of a synchronous system
R_0	FEC encoder rate
R_c	data rate at the chip level
R_s	signalling code rate of a DS-CDMA system with FEC coding
S	set of states that have transitions to state s
S_i	state at time i
S_i^d	set of all state transitions for which the input data bit $d(i)$ is $d = 0$ or $d = 1$
S_i^b	set of all state transitions for which the output FEC coded bit $b(i)$ is $b = -1$ or $b = 1$
T	one symbol duration
$\mathbf{T}$	linear transformation matrix
T_c	one chip duration
$TM_{s',s}(i)$	transition metric between states s' and s at time i (Euclidean distance)
U	number of active users in the system
$\mathbf{V}$	covariance matrix for the vector $\mathbf{r}(t)$
$\mathbf{V}_s tc$	covariance matrix for the vector $\boldsymbol{\varphi}_p$
$\mathbf{W}$	matrix with the FFT basis vectors
$\mathbf{Y}_1^{i-1}$	noisy received vector of codewords from time 1 to time $i-1$
$\mathbf{Y}_i$	noisy received codeword at time i
$\mathbf{Y}_{i+1}^{L}$	noisy received vector of codewords from time $t+1$ to time L
$\mathbf{Y}_i^{L}$	noisy received codeword at time i
$\mathbf{a}_l(t)$	*l*th centre of the RBF detector (noise free input vector for $\mathbf{b}(t)$)
$\mathbf{a}_l^{+1}(t)$	*l*th centre of the RBF detector when $b_u(t) = +1$ in $\mathbf{b}(t)$
$\mathbf{a}_l^{-1}(t)$	*l*th centre of the RBF detector when $b_u(t) = -1$ in $\mathbf{b}(t)$
$b(t)$	*t*th FEC coded bit
$\mathbf{b}(t)$	$(U \times 1)$ vector with the users' FEC coded bits at time t
$\underline{\mathbf{b}}(t)$	$(3U \times 1)$ vector with the users' FEC coded bits at time $t-1$, t and $t+1$
$\bar{\mathbf{b}}(p)$	$(3U \times 1)$ vector with the users' FEC coded bits at the it pth time slot
$\hat{\mathbf{b}}(t)$	vector with the estimates of the users' FEC coded bits at time t
$\mathbf{b}(i)$	*i*th codeword transmitted

$b_{s',s}(t)$	*t*th FEC coded bit in the transition from state s' to state s
$b_u(t)$	FEC coded bit of the *u*th user at time t
$\hat{b}_u(t)$	FEC coded bit estimate of the *u*th user at time t
$c_{u,n}$	*n*th chip of the spreading code for user u
$\mathbf{c}_u(t)$	spreading code for user u
$\mathbf{d}$	input vector of data bits
$\hat{\mathbf{d}}$	SISO MAP decoder output vector with an estimate of the data bits
$d(i)$	input data bit at time i
$d_u(i)$	data bit of the *u*th user at time i
$\hat{d}_u(i)$	data bit estimate of the *u*th user at time i
h_a	*a*th coefficient of the channel impulse response
l	number of information bits at the FEC encoder input
n_c	FEC codeword length
n_o	number of coded symbols per block (length L) of input information symbols
$\mathbf{n}(t)$	$N \times 1$ AWGN noise vector at time t
$\underline{\mathbf{n}}(t)$	$(N+\alpha) \times 1$ time span AWGN noise vector
$n_n(t)$	*n*th noise component at time t (chip rate)
$\bar{\mathbf{r}}_p$	received signal which includes the cyclic prefix at the *p*th time slot
$\hat{\mathbf{r}}_p$	received signal neglecting the first α samples of $\bar{\mathbf{r}}_p$
$\mathbf{r}(t)$	received signal at time t
$\underline{\mathbf{r}}(t)$	received signal at time t that captures all the energy from the transmitted data symbol in a multipath channel
$r_{t,n}$	*n*th component of the received signal at time t (chip rate)
$\mathbf{s}_1, \mathbf{s}_2$	group separation codes
$\mathbf{s}(t)$	output of the convolutional between the channel response and the transmitted signal at time t
$s(j)$	output of the convolutional between the channel response and the transmitted signal sampled at the chip rate
$\mathbf{w}_u$	vector of weights of the Wiener detector for the *u*th user
w_l	weight associated with $\mathbf{a}_l(t)$
$\mathbf{x}(t)$	transmitted signal at time t

$\hat{\mathbf{x}}(t)$	*STC symbol* at time t with the incorporation of a cyclic prefix
$\bar{\mathbf{x}}(p)$	virtual *STC symbol* at time *p*th time slot
$x_{t,n}$	*n*th component of the noise free received signal at time t (chip rate)
$x(j)$	transmitted signal sampled at the chip rate
$y(t)$	*t*th noisy received FEC coded bit
$\mathbf{y}(t)$	vector with the conventional detector output for all users in the system
$\bar{\mathbf{y}}(p)$	concatenated vector with the spreading signals for the FEC coded at the *p*th time slot
$\hat{\mathbf{y}}(p)$	estimate of $\bar{\mathbf{y}}(p)$
$y_u(t)$	Wiener detector output for the *u*th user at time t
$\hat{y}_u(t)$	PIC detector output for the *u*th user at time t
$\mathbf{z}(t)$	noise vector at the output of the conventional detector
z^{-1}	delay of one data symbol
$\mathbf{z}^{dec}(t)$	noise vector at the output of the decorrelator detector
z_c^{-1}	delay of one chip
$z_u(t)$	*u*th component of the noise vector at the output of the conventional detector
$\mathbf{\Lambda}_m$	diagonal matrix with the channel response to signal transmitted from the *m*th antenna
$\mathbf{\Phi}_{rr}$	autocorrelation matrix of the Wiener input signal $\mathbf{r}(t)$
Ω_1	set of states s' at time $i-1$ that are connected to the state s at time i
Ω_2	set of states s' at time $i+1$ that are connected to the state s at time i
Ω_b	set of vectors $\mathbf{b}(t)$ where $b_u(t) = b$ for $b \epsilon \{-1, 1\}$
$\alpha + 1$	number of the multipath components in the channel
$\alpha_i(s)$	forward probability of state s at time i
$\beta_i(s)$	backward probability of state s at time i
$\gamma_i(\mathbf{Y}_i, s', s)$	transition probability from state s' to state s at time i
$\boldsymbol{\zeta}(t)$	noise vector at the STTD decoder output in a multipath fading channel
$\boldsymbol{\eta}(t)$	$N \times 1$ vector with complex Gaussian noise samples
$\bar{\boldsymbol{\eta}}(t)$	$(N+\alpha) \times 1$ vector with complex Gaussian noise samples
$\bar{\boldsymbol{\eta}}(p)$	$2N \times 1$ vector with complex Gaussian noise samples
θ	half angle of an n_o-dimensional cone
$\lambda_i(s)$	joint probability of state s at time i
$\lambda_i(s', s)$	joint probability from state s' to state s at time i

$\mu_u(t)$	noise sample at the PIC output for the ìt uth user at time t
ν	constraint length
$\pi(t)$	random permutation function
$\rho_{u,k}$	cross-correlation between $\mathbf{c}_u(t)$ and $\mathbf{c}_k(t)$
σ^2	variance of the AWGN samples
σ^2_{stc}	noise variance at the STTD decoder output
$\sigma^2_w(u)$	variance of the Wiener detector output for user u
$\sigma^2_\mu(u)$	variance of the noise sample $\mu_u(t)$
$\phi_l()$	radially symmetric scalar non-linear function (Gaussian kernel function)
$\boldsymbol{\varphi}_p$	$(2N \times 1)$ noise vector with complex Gaussian samples
ϕ^u_{rb}	cross-correlation between $\mathbf{r}(t)$ and $b_u(t)$
$\psi_u(t)$	complex Gaussian noise sample
$\boldsymbol{\omega}(t)$	noise vector at the STTD decoder output in a flat fading channel
$\|\|.\|\|$	Euclidean norm

Chapter 1
Introduction

The need to communicate with others has always existed. In primitive times different civilisations found different ways to cope with their problems. We can guess that man used drawing on walls, grunts and possible hand signs to communicate with others. Man found that voice had a limited distance. Thus one of the first long distance communication was maybe done by using drums where the sound could be heard a long distances providing a warning of danger or other sort of messages.

In 1837 Samuel Morse invented the telegraph and by the end of the 19th century Gugliemo Marconi established what is considered the first successful and practical radio system. Nevertheless, it was not until the 1940s when commercial mobile telephony began and then the point where we can establish the first roots of cellular communications. What it is certain is that every major telecommunications company and manufacturer knew about the cellular idea by the middle 1960s.

The first generation analog cellular system began in 1978 when The Bahrain Telephone Company operated a commercial cellular telephone system. It was the first time in the world that individuals started using what we think of as traditional, mobile cellular radio. Then in 1981 the first multinational cellular system took place in Europe, when the Nordic Mobile Telephone System (NMT450) began operating in Denmark, Sweden, Finland and Norway. Few years later other European countries were also operating radio telephone systems but with a major problem of incompatibility between each other. As a result, it brought about a new technology called Global System for Mobile communications (GSM) [4, 5] to build a uniform European wide cellular system in a new radio band (900 MHz). The system was designed to be fully digital with a new service that would incorporate the best thinking of the time. On the other hand, around 1990 North America carriers were facing problems of capacity due to the significant increase of customers and the few resources available. A partial solution to this problem soon came up when the North America cellular network incorporated the IS-54B standard (updated afterwards as IS-136) [6]. The IS-54 increased capacity by digital means: sampling,

digitising, and the multiplexing conversations, using a technique called time-division multiple-access (TDMA). This method separated calls by time, placing parts of individual conversations on the same frequency, one after the next. It tripled call capacity.

In the early 1990s the cellular telephone deployment was already world wide offering a wide variety of wireless services. In America the leading technology was IS-54 while GSM dominated in Europe and many other countries. With a slightly different direction Japan went with Japanese Digital Cellular (or Personal digital Cellular) in 1991 [5, 6]. All these early digital schemes were using TDMA. Nevertheless, as a result of the booming of cellular business, by 1993 in North America were again running out of capacity, despite the movement to IS-54. In 1994 Qualcomm proposed a cellular system and standard based on spread spectrum technology to increase capacity. It was called IS-95 [7]. This code-division multiple-access (CDMA) based system would be all digital and promised a significant increased in capacity over existing cellular systems.

In late 1990s even more wireless channel were needed in America. Existing cellular bands had no more room. New services and many more frequencies were needed to handle all the customers. So a new block of higher frequencies in the radio spectrum was licensed for wireless use. After much study the Federal Communications Commission (FCC) started auctioning spectrum in the newly PCS (Personal Communication Service) band [8]. PCS were all digital using TDMA or CDMA.

By now the trend is to form a global standard for mobile communications [9]. In this direction different regulatory organisations such as the International Telecommunication Union (ITU) and European Telecommunications Standards Institute (ETSI) are coordinating global telecommunication networks and services. As a result huge importance has been given to the development of new technology such as the third generation of mobile communications systems known as Universal Mobile Telecommunication Systems (UMTS) in Europe and International Mobile Communications (IMT-2000) elsewhere, or with the generic term 3G worldwide [10–17]. 3G systems aim to provide enhanced voice, text and data services to the user. The main benefit of the 3G technologies will be substantially enhanced capacity, quality and data rates than are currently available. This will enable the provision of advanced services transparently to the end user (irrespective of the underlying network and technology, by means of seamless roaming between different networks) and will bridge the gap between the wireless world and the computing/Internet world, making inter-operation apparently seamless. The third generation networks

should be in a position to support real-time video, high-speed multimedia and mobile Internet access. All this should be possible by means of highly evolved air interfaces, packet core networks, and increased availability of spectrum. Currently programs such as ACTS (Advanced Communications Technologies Services) will strive to ensure that current mobile services are extended to include multimedia and broadband services and that convenient light weight, compact and power efficient terminals adapt automatically to whatever air-interference parameters are appropriate to the user's location, mobility and desired services.

The remaining of this chapter is organised in the following sections: Firstly, Section 1.1 will present a general overview of wireless communications with a primary emphasis on mobile cellular communications which is the main area of study in this thesis. Following this, in Section 1.2 is addressed the motivation of the work. And finally, the thesis layout and the main results of this work are discussed in Sections 1.3 and 1.4 respectively.

1.1 Wireless mobile communications

Nowadays wireless communication is used widely in many communication systems: mobile telephony, satellite networks, digital radio/television broadcasting, fixed wireless local loops, etc. Particularly, wireless mobile communications has exploded in popularity because of the fact that it simplifies and revolutionises communications. The success of mobile communications lies in the ability to provide instant connectivity anytime and anywhere and the ability to provide high-speed data services to the mobile user. The quality and speeds available in the mobile environment must match the fixed networks if the convergence of the mobile wireless and fixed communication networks is to happen in the real sense. So, the challenges for the mobile networks lie in making the movement from one network to another as transparent to the user as possible and the availability of high speed reliable data services along with high quality voice. A range of successful mobile technologies exists today in various parts of the world and every technology must evolve to fulfill all these requirements. In this work we are particularly interested in the cellular mobile environment, therefore, our attention will be primarily focused to this research area. Next section gives a brief introduction to the cellular concepts describing the general idea behind of this type of wireless communications.

1.1.1 Cellular communications

In the early mobile radio systems a large coverage was attained by placing an antenna with a high-power transmitter in one of the highest point of the coverage area for instance, on top of a hill or a high building. Nevertheless, it meant that only a small number of users could be allocated in a large area due to the few available radio frequencies. So any attempt to reuse the same frequencies throughout the system would result in interference.

Thus, the need of higher capacity with limited radio channel brought into the cellular concept [18]. A cellular mobile communications system uses a large number of low-power wireless transmitters to create cells which are the basic geographic service area of a wireless communications system. Figure 1.1 illustrates the structure of a cellular communication system. Each cell consists of a base station (BS) transmitting over a small geographic area usually depicted as an hexagon (the true shape of a cell is not a perfect hexagon due to constraints impose by the terrain). According to the density and demand of mobile users (MS) within a certain region, the cell size is determined. The base stations in turn are connected to a central called the mobile switching centre (MSC) which provides connectivity between the public switched telephone network (PSTN) and the base stations. Thus a global communication network is formed with PTSNs which connects the conventional telephone switching centres with MSCs all over the world.

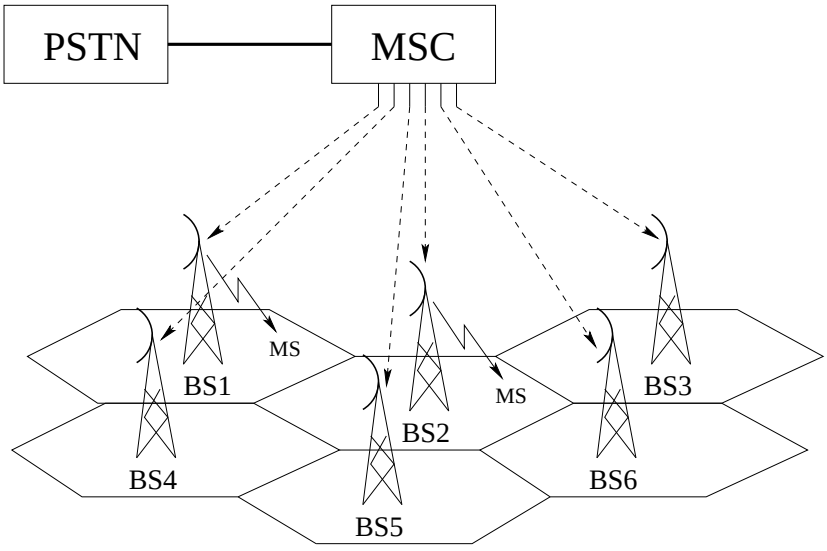

Figure 1.1: *Structure of a cellular communication system*

An obstacle in the cellular network arises when a mobile user travel from one cell to another

during a call. To ensure that mutual interferences between users remains low, adjacent cells do not use the same radio frequency channel, then when a user moves out from a cell the call has to be transferred to another stronger frequency channel (which becomes the new cell where the user is moving in). This process is known as hand-off or hand-over, changing a call from one cell to another without being notice by the users.

Another important concept inside the established cellular systems is the frequency planning or frequency reuse. Due to the reduce number of radio frequency channels available for mobile systems, a reuse of the frequency channels had to be implemented into the cellular concept. This reuse process means that the radio frequency channels used in one cell can also be reused in another cell some distance away. Usually clusters of cells (no frequency channels are reused in a cluster) are reused in a regular pattern during the entire coverage area as it shown in Figure 1.2. Hence, the frequency reuse factor in a system is determined by the available frequency channels, *i.e* for the particular case depicted in Figure 1.2 the frequency reuse factor of the system is 1/7.

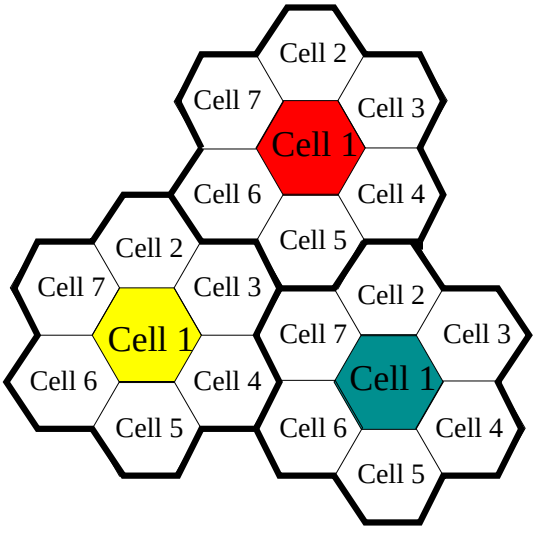

Figure 1.2: *Frequency reuse pattern in a cellular system*

1.1.2 Mobile cellular environment

A cellular communication system provides with a full duplex communication between the mobile user and the base stations to carry through a normal conversation talk (back and forth). To achieve this type of radio transmission the mobile users and the base station both need circuitry

to transmit on one frequency while receiving on another. The radio link from the base station to the mobile phone (BS→MS) is usually referred as downlink (or forward link) and the inverse process (MS→BS) is called uplink (or reverse link), see Figure 1.3. In the downlink, all the users' signals are transmitted by the same single source, base station, therefore the signals received at each mobile terminal are synchronous. On the other hand, in the uplink the signals received in the base station are asynchronous as now the transmissions are yielded by several uncoordinated and geographical separated sources (mobile users).

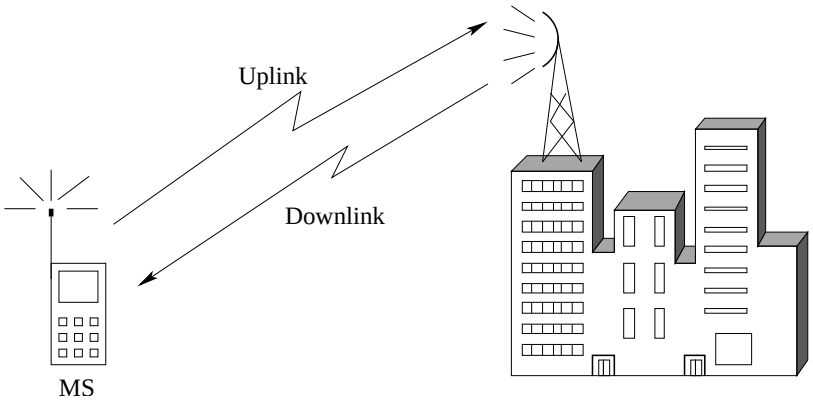

Figure 1.3: *Radio channels used in the transmission of information inside a cell.*

In a cellular system interference is the major limiting factor in increasing capacity. Some of the interference sources are for example: other base station transmitting in the same frequency band, another mobile user in the same cell, a call in progress in a neighbouring cell, impairments caused by the propagation of radio waves, etc. As a result, different type of system interference are yielded in the network. Among those interferences the most important are the following:

Co-channel interference (CCI). This type of interference is caused by the interference between co-channel cells (cells with the same frequency channel) due to the frequency reuse. To reduce CCI, co-channel cells must be separated by a minimum distance to provide sufficient isolation due to propagation distance.

Adjacent channel interference (ACI). This other type of interference results when two frequency channel are adjacent in the frequency spectrum and one of them is leaking into the passband causing interfering into the adjacent channel. ACI is mainly provoked by imperfect receiver filters. This problem can be minimised with a careful filtering and channel assignments (assigning channels to a cell which are not adjacent in frequency).

Intersymbol interference (ISI). When the signal travels through a channel, objects in the transmission path can create multiple echoes of the transmitted signal. These echoes occur at the receiver and overlap in successive time slots. This is known as intersymbol interference. Equalisers at the receiver can be used to compensate the effect of ISI created by multipath within time dispersive channels.

Fading. One consequence of transmitting a signal through a time-varying multipath channel is to confront at the receiver with a signal fading (amplitude variations in the received signal). Hence not only the propagation delays but also the random impulse responses of the channel will provoke some attenuation and time spread of the signal transmitted.

Thermal noise. Finally, the additive thermal noise is a factor that always corrupts a transmitted signal through a communication channel. Generally this thermal noise is assumed to be an additive white Gaussian noise (AWGN).

Therefore, not only sophisticated systems are needed but also advanced signal processing techniques in the receivers are required to overcome these type of interferences. Many mobile technologies exist today each having influence in specific parts of the world. GSM, TDMA (IS 136), and CDMA (IS 95) are the main technologies in the second generation mobile market [4], [6, 7]. GSM by far has been the most successful standard in terms of its coverage. All these systems have different features and capabilities. Although both GSM and TDMA based networks use time division multiplexing on the air interfaces, their channel sizes, structures and core networks are different. CDMA has an entirely different air interface.

In the following sections a brief description of the existing standards in multiple access technologies is presented.

1.1.3 Multiple access channels

A multiuser communication system is a multiple access channel where a large number of users share a common communication channel to transmit information to a receiver. In general, multiple access systems require that messages corresponding to different transmitting sources, which are sent simultaneously through the same communication channel, be separated in some fashion so that they do not interfere with one another. This is usually accomplished by making the messages orthogonal to one another in the dimensions of frequency, time or space.

Within the wireless communication there are several different ways in which multiple users can send information through the communication channel. The first multiple access technique implemented in cellular radio environment is known as *frequency division multiple access* (FDMA). FDMA is a method that divides the frequency band allocated for wireless cellular communication into frequency non-overlapping sub-channels. Each individual sub-channel can carry a voice conversation, or with digital service, carry digital data. Therefore, each sub-channel can be assigned to only one user at a time (during the whole period of time for the call) as is shown in Figure 1.4. Although FDMA is the only multiple access technique which can handle both analog and digital transmissions, an obvious disadvantage in FDMA is that the frequency spectrum is not used efficiently as no user can share the same frequency band at the same time and guard bands have to be maintained between adjacent signals spectra to minimise cross talk between sub-channels. Clearly, it yields a constraint in the maximum bit rate per channel (an essential characteristic in future communication services) as increasing the bit rate requires to allocate more frequency channels for a user.

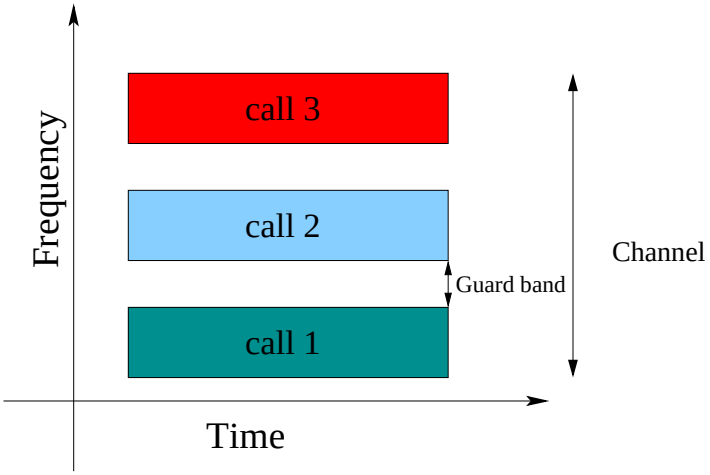

Figure 1.4: *Frequency division multiple access (FDMA)*

FDMA is a basic technology in the analog Advance Mobile Phone Service (AMPS), the most widely installed cellular phone system in North America. Also it is used in other systems as the UK's Total Access Communication system (TACS), Nordic Mobile Telephone System (NMT450) and Nippon Telephone and Telegraph (NTT). These systems are often referred as the first generation analog cellular systems [18, 19].

A second generation of mobile communications brought along the technology to deploy digital communication to cellular radio environment. With this generation another method of

multiple access appeared, namely *time division multiple access* (TDMA). TDMA is a digital transmission technology that allows a number of users to access and share a common radio-frequency (RF) channel without interfering by allocating unique time slots to each user within each channel. So different users can transmit or receive messages, one after the next in the same bandwidth but in different time slots. Figure 1.5 shows a general TDMA system structure. In addition to increasing the efficiency of transmission, TDMA offers a number of other advantages over standard cellular technologies. First and foremost, it can be easily adapted to the transmission of data as well as voice communication. Furthermore, it permits utilisation of all the advantages of digital techniques: digital speech interpolation, source and channel coding, etc. Nevertheless, one of the disadvantages is that it requires a significant amount of signal processing for synchronisation as the transmission of all users must be exactly synchronised. Additionally, TDMA needs guard times (the equivalent to guard bands in FDMA) between time intervals to reduce clock instabilities and transmission time delay.

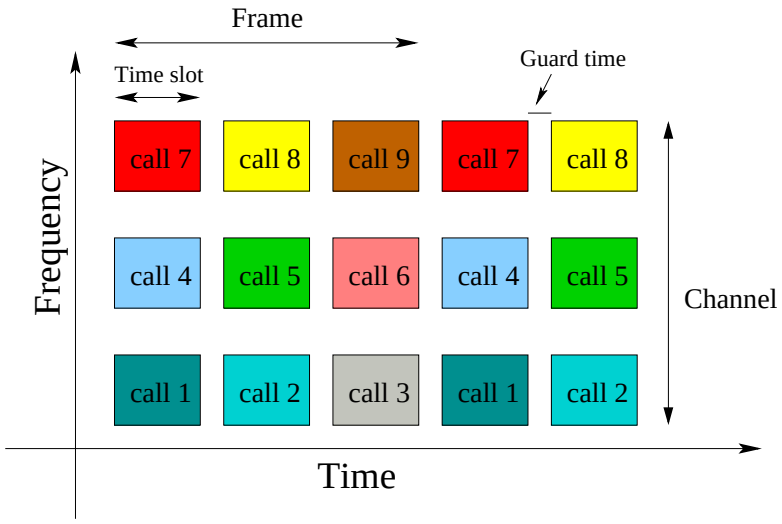

Figure 1.5: *Time division multiple access (TDMA)*

Second generation of cellular systems are based on TDMA. Among those systems are the European Global System for Mobile communications (GSM) [4], the North America cellular network with the standard IS-54 and the Japanese Digital Cellular (or Personal Digital Cellular) [19].

Another multiple access technology which was designed to increase both the system capacity and the service quality is called *code-division multiple access* (CDMA). CDMA is a form of spread spectrum technology, a family of digital communication techniques that have been used

in military applications for many years [20–22]. It spreads the information contained in a particular signal of interest over a much greater bandwidth than the original signal at the same data rate. The capabilities of the spread spectrum technique for both anti-jam and low probability of undesired interception, make this technology suitable for multi-user applications.

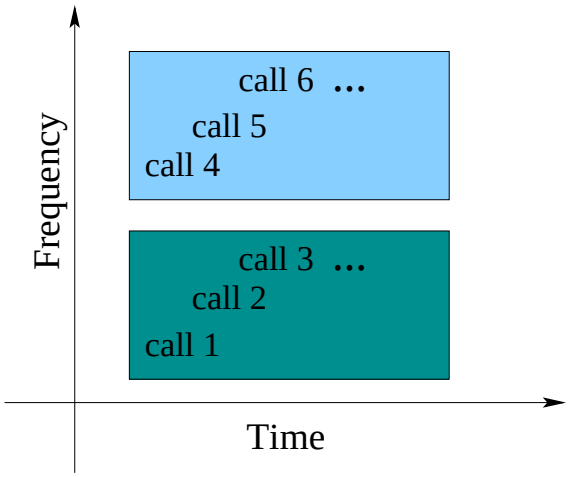

Figure 1.6: *Code division multiple access (CDMA)*

When CDMA is implemented in cellular systems, all users share a common channel in time and frequency. Figure 1.6 shows a general scheme of a CDMA system. CDMA has many forms, however direct sequence (DS) CDMA has been the method of choice as it is showed with its standardisation (IS-95) [7]. In this scheme, each user modulates its data with a special and unique code or spreading sequence (pseudo-random modulation), which allows the users' data to be distinguished at the receiver. In contrast to FDMA and TDMA, where the users' communication channels are separated in frequency or time, in a DS-CDMA system the users' data are distinguished by the separation (cross-correlation) between their spreading sequences. Then as long as there is sufficient separation between the codes the noise level, called multiple access interference or simply MAI, will be low enough to recover the desired user's signal. Therefore, DS-CDMA can be either orthogonal or non-orthogonal depending on the spreading sequences. If orthogonal spreading sequences are used and it is assumed that there is no time delay caused by the communication channel, the received signals of the users appear as orthogonal. However, in practice this orthogonality is a very difficult task, if not impossible to achieve, due to the lack of precise synchronism and impairments in the communication channel.

CDMA systems are the latest technology on the market and are already taking the shine off TDMA in terms of cost and call quality [23]. Since CDMA offers greater capacity and variable

data rates depending on the audio activity, many more users can be fit into a given frequency spectrum and higher audio quality can be provided. The current CDMA systems boast at least three times the capacity of TDMA and GSM systems. The fact that CDMA shares frequencies with neighbouring cell base stations allows for easier installation of extra capacity, since extra capacity can be achieved by simply adding extra cell sites and shrinking power levels of nearby sites. However, the downside of CDMA is the complexity of deciphering and extracting the received signals, especially if there are multiple signal paths (reflections) between the mobile user and the cell base station which yields ISI. As a result, CDMA phones and cell site equipment are more expensive than TDMA equivalents.

1.2 Motivation of the work

As we look toward the future the demand of new mobile wireless services such as video phones, orbiting satellites repeaters, wrist watch sized radio and especially the mobile Internet upon us, seems to be limited only by our imaginations. Thus, an increasingly demand of further developments in the field of wireless communications are required to satisfied those services. And even more efforts are required in order to provide a communication service from one person to another in any place at any time by only using a flexible and small unit at minimum cost, with good quality and security [9], *i.e* converting the world into a global communication village. Tremendous potential exists but until networks are built and other problems are solved that potential remain unfulfilled.

Over the last years, DS-CDMA technology has not been just another option for the second generation of digital systems (together with TDMA and GSM) but it is also the basis of third generation systems due to its capabilities to support enhanced capacity and data services, two key elements of third generation wireless [24]. By the time this thesis was written, Wideband CDMA (WCDMA) and CDMA2000 were the third generation systems about to be launched into the market. These two systems support much higher data rate ($>$ 128 kbps) and both are compatible with current CDMA systems. Therefore, this research work will be mainly focused on DS-CDMA systems throughout as this technology will be a driving force in the wireless revolution.

Thus, the DS-CDMA's standardisation has raised even more interest in exploiting the capabilities and capacity of this type of technology. Nevertheless, it has the major problem of multiuser

interference which limits significantly the system capacity. Multiuser detection techniques are essential for achieving near optimal performance in communication systems. Therefore the addition of multiuser detection capabilities to the various elements of networks promises to be key for enabling the significant increases in capacity needed for future network services.

As the field has matured, non-ideal situations have been gradually incorporated into analysis and simulations to assess their impact on system performance. With the advent of high performance mixed-signal devices, high-speed processors, reconfigurable computing devices, and the incorporation of advance receiver concepts, the practical implementation of advance multiuser receivers will be more feasible into future systems. Today, a significant research activity is carrying out to solve several of the practical and theoretical open issues that still exists in the field of multiuser detection. Then motivated by this growing demand of requirements, in this thesis is presented an investigation on various multi-user receiver structures with focusing primarily in structures that apply the turbo multiuser detection principle to improve the spectral efficiency and performance of cellular systems. The objective of the work presented is to investigate and develop signal processing methods which can provide a final multiuser receiver structure with a satisfactory tradeoff between complexity and performance.

1.3 Thesis outline

This thesis is organised in eight chapters as it is described in the flow diagram of Figure 1.7. The introduction chapter of this thesis gives a general overview of wireless mobile communications with a primary interest in the cellular mobile environment. The general ideas behind the cellular concepts, which includes the existing standards in multiple access techniques, are discussed. Due to its capabilities to support enhanced capacity and data services, CDMA systems are the basis technology for the third generation of mobile systems. However, it has the major problem of multiuser interference. The motivation for the work developed in this thesis is then addressed.

Chapter two develops a framework for understanding the DS-CDMA communication system. It begins presenting the fundamentals of spread spectrum techniques which represent the basis of CDMA technologies. Since DS-CDMA systems are the main concern in this work, direct-sequence spread spectrum technique is only discussed. A general DS-CDMA system model with FEC coding is then introduced. A description of the basic elements in a DS-CDMA sys-

tem, *i.e* transmitter, communication channel and receiver, are presented in detail. FEC coding using convolutional codes is a popular choice in current communication systems. A description of this type of FEC coding is then given. It is also included a detailed discussion of a sub-class of convolutional codes, namely turbo codes, due to its direct implication in the development of this research work. A general description of the communication channel model is also covered. The receiver element is described next. In this chapter the conventional detector is only discussed. Due to the single-user strategy followed by the conventional detector, it is shown that

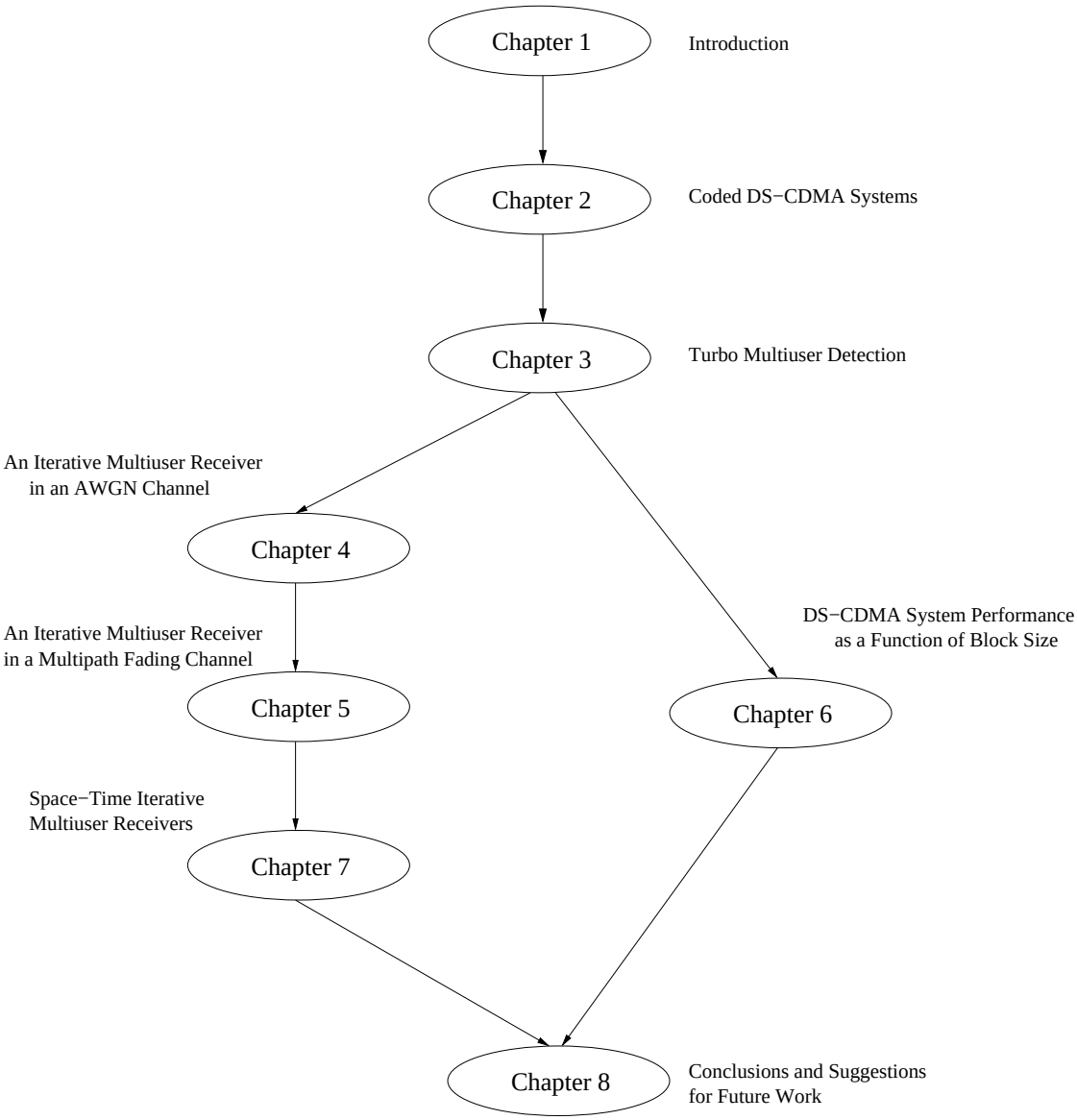

Figure 1.7: *Thesis structure*

the correlation with other users give rise to MAI. Finally, the decoding process for the type of FEC codes considered are described.

Chapter three addresses the turbo multiuser detection principle. Firstly, it is shown that the capacity of a conventional DS-CDMA system is inherently interference limited by other users. Therefore, MUD techniques represent a potential scheme to overcome this interference and consequently to increase the system capacity. A general overview of MUD is then presented. Various MUD techniques are reviewed and compared. In a DS-CDMA system with FEC coding, the optimal multiuser receiver structure uses an optimal mapping from the received signals to the original uncoded symbols (multiuser detection and FEC decoding jointly). However, this optimum scheme has a prohibitive computational complexity. To mitigate this complexity issue a sub-optimal multiuser receiver scheme based on a partitioned structure is considered. It is then shown that the serial concatenation of the channel coding with the DS-CDMA channel can perform well using the iterative principle as proposed in turbo codes. Following this, the turbo multiuser detection principle is introduced.

In chapter four an iterative multiuser receiver for the downlink of a FEC coded DS-CDMA system operating in a AWGN channel is introduced. Similar to turbo codes, this receiver performs signal detection and decoding separately, but exchanging soft information in an iterative fashion. Based on a linear detection technique, two approaches are proposed and investigated: firstly, a Wiener detector is considered for the signal detection. Traditionally, it is assumed that single FEC coded bits are independent between each other but it is shown that the turbo principle can be introduced if this condition is removed. Secondly, the iterative receiver structure is investigated by incorporating a single stage of parallel interference cancellation scheme after the Wiener detector. In this case the turbo principle is introduced via the cancellation scheme. Simulations results using pseudo-random spreading codes are discussed.

The model of the synchronous DS-CDMA channel developed to this point assumes that a single path is received from the transmitted signal at the mobile receiver. A more realistic model is, however, one which receives multiple signal paths from the transmitted signal. Chapter five takes the model introduced in chapter four and extends it to incorporate multipath propagation. A hybrid iterative multiuser receiver for this scenario is then introduced. It is assumed that the multipath channel spans only one neighbouring data bit. The approach proposed combines a linear MUD technique at the first iteration with a non-linear technique on further iterations. Performance and complexity of this receiver are analysed via simulation results.

Chapter 6 exploits the turbo multiuser detection principle to approach to the capacity bounds of a FEC coded DS-CDMA system in a AWGN channel. Using the Shannon's sphere packing bound, the capacity limits for a FEC coded DS-CDMA system are formulated for a given data rate and a given data block size. The achievable performance of a simulated FEC coded DS-CDMA system using an iterative multiuser receiver is also investigated. A comparison between the performance of the simulated system using pseudo-random codes and its theoretical limits are presented. This is analysed and discussed in detail.

A novel space-time architecture for the downlink of a FEC coded DS-CDMA system is proposed in chapter seven. It is shown that the synchronous DS-CDMA model with FEC coding can be extended to incorporate antenna arrays. Due to the constraints in size, cost and weight at the mobile receiver only one receive antenna is considered. In particular this architecture exploits the spatial and temporal capabilities of the system to design the transmitter and receiver. In this chapter MUD, transmit diversity via space time coding and the turbo multiuser detection principle are combined in an efficient way to enhance the system capacity over flat and multipath fading channels. In addition, the reuse of orthogonal codes are suggested as a method to enhance further the system capacity. Analysis and simulation results are provided to demonstrate the spectral efficiency and performance improvement in the system. The complexity of the multiuser receiver scheme is also analysed in detail and is found that this architecture can be implemented without a prohibitive complexity cost.

Finally, chapter eight concludes this thesis. It reviews and highlights the contributions that have been presented in this thesis and the importance of these to solving the DS-CDMA multiple access interference problem. Suggestions for future work are also discussed in this final chapter.

Chapter 2
FEC coded DS-CDMA systems

The interest of this thesis is the analysis and design of advanced multiuser receivers for DS-CDMA systems with forward error correction (FEC) coding. The main concern in this thesis is the application of the turbo multiuser detection principle in the receiver design to increase the system capacity. Hence, in order to establish and discuss the contributions of this thesis, it is necessary to present a description of the communication system of interest. This chapter gives a review of key concepts from the existing literature in order to firmly establish the setting for the following chapters.

First, section 2.1 presents the fundamentals of spread spectrum techniques. Section 2.2 introduces a general DS-CDMA system model with forward error correction (FEC) coding which consists of three basic elements: transmitter, communication channel and receiver. A description of these elements are given in sections 2.3, 2.4 and 2.5 respectively. Finally, Section 2.6 finishes the chapter with a summary.

2.1 Spread spectrum systems

Spread spectrum (SS) is defined as a communication technique in which the intended data signal occupies a much larger bandwidth than the minimum required to transmit that signal. This is accomplished by means of spreading the data signal with a unique code (wideband signal) which is independent of the data signal. The receiver, which is synchronised with the transmitter and with knowledge about the code, is then capable of despreading and recovering the desired signal [22], [25, 26].

The main parameter in a spread spectrum system is the processing gain or spreading factor (N) which is the ratio of the transmitted bandwidth to the information bandwidth $N = B_t/B_i$. This parameter determines the number of users that can be allowed in a system, the amount of multi-path effect reduction, the difficulty to jam or detect a signal, etc. For spread spectrum

systems it is advantageous to have a processing gain as high as possible. A number of important properties in spread spectrum systems are discussed below:

Multiple access capabilities. In a multiuser system where all users transmit spread spectrum signals at the same time, the receiver can still distinguish between users, providing that there is sufficiently low cross-correlation among the users spreading codes. When correlating the received signal with the code of a particular user, the data signal of that user is only despread as its power is much larger than the remaining interfering power (other spread spectrum signals).

Interference rejection. At the receiver, the effect of cross-correlating the spreading code with a narrowband interference signal is to spread the power of the narrowband signal. Therefore, a rejection capability is achieved as the power of the interfering signal appears as background noise compared with the despread data signal.

Reduction of multipath effects. High time resolution is attained by the correlation detection of wideband signals. Differences in the time of arrival of the wideband signal, on the order of the reciprocal of the signal bandwidth, are detectable. This property can be used to suppress multipath effects.

Low power spectral density. As the data signal is spread over a large frequency band, the power spectral density is getting very small, so other communications systems do not suffer from this kind of communications. However the Gaussian noise level is the same as that of a narrowband signal of bandwidth B_i.

Privacy and low probability of interception. The probability that an undesired user can detect the message of another user is very low as the spreading codes are unknown. Also due to its low power spectral density, the spread spectrum signal is difficult to detect.

Random access possibilities. In any situation the whole frequency spectrum is used and users can have access at any arbitrary time.

Different spread spectrum techniques can be used in communications systems such as: Direct-Sequence (DS), Frequency-Hopping (FH), Time-Hopping (TH), Multi-Carrier CDMA (MC-CDMA) and chirp modulation. As DS-CDMA systems are the main concern in this work, a brief description of this technique is presented here, an overview of more general spread spectrum techniques can be found in [22], [25], [27, 28].

2.1.1 Direct-sequence systems

A direct sequence (DS) spread spectrum technique is performed by multiplying a radio frequency (RF) carrier and a pseudo-noise (PN) digital signal. Figure 2.1 shows a basic DS/SS system for both the transmitter and the receiver. First the PN code is modulated onto the data signal, using one of several modulation techniques (*e.g* BPSK, QPSK, etc). Then the PN modulated data signal and the RF carrier are multiplied. This process causes that the RF signal to be replaced with a very wide bandwidth signal with the spectral equivalent of a noise signal. In the reception of the signal, the receiver must not only know the code sequence to despread the signal but also it requires to be synchronised with the code generator in the transmitter.

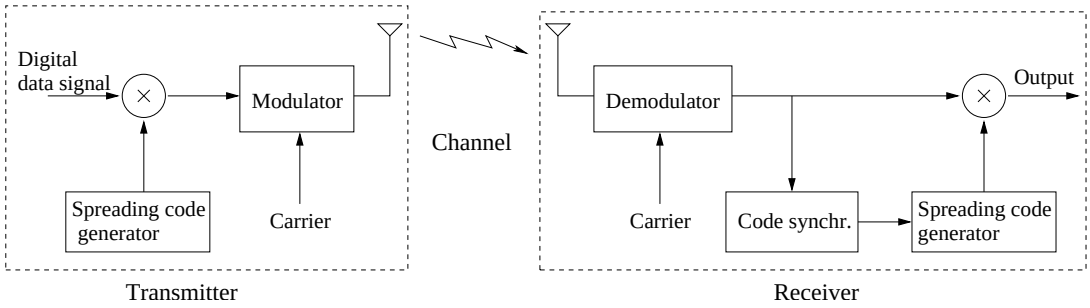

Figure 2.1: *DS/SS system.*

The multiplication in the time domain of the data signal by the PN code sequence results in a signal with a frequency spectrum similar to the spectrum of the PN code signal (due to the fact that $T_c < T$, where T_c and T represent the duration of one chip in the PN code and one symbol in the data signal respectively). Therefore, the effects of increasing the data rate from R (symbol level) to R_c (chip level) are a reduction in the amplitude spectrum (from T to T_c) and an expansion of the signal in the frequency domain. Since the wide bandwidth of the PN codes allows us to reduce the amplitude spectrum to noise levels (without loss information), the generated signals appears as background noise in the frequency domain. From another perspective, the bandwidth of the data signal is basically spread by a factor $N = T/T_c$, which corresponds to the processing gain in the DS/SS system. In this type of systems the length of the code is the same as the processing gain. Several families of PN codes exist and some of them will be addressed in section 2.3.2. To illustrate the spread spectrum concepts, Figure 2.2 and Figure 2.3 show a sketch of the time-domain and frequency-domain representation of the signals in the DS/SS system of Figure 2.1.

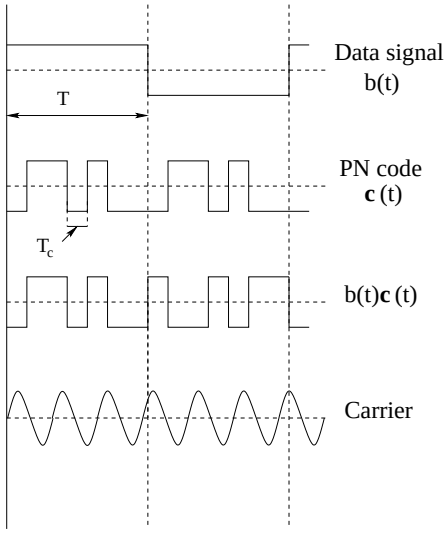

Figure 2.2: *Time domain representation of the signals at the transmitter of a DS system.*

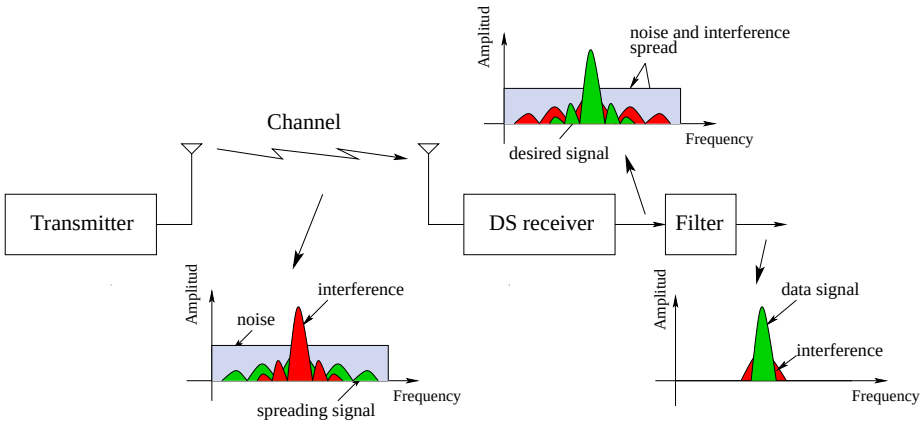

Figure 2.3: *Frequency domain representation of the received signal in a DS system.*

From the viewpoint of a CDMA system, the most important properties of a spread spectrum technique are: multiple access capabilities, multipath interference rejection, narrowband interference rejection, and secure and privacy capabilities. For simplicity and a better understanding, the carrier will be omitted for all further discussions and then our analysis will be centred only on the baseband equivalent system.

2.2 FEC Coded DS-CDMA System

The capabilities of the spread spectrum techniques make of this a technology suitable for multiuser application. Particularly, a DS-CDMA system is one of the most widely used schemes. In a DS-CDMA system all users share the same communication channel overlapping the transmitted signals both in time and frequency. To separate and detect the intended data signal a unique spreading waveform is assigned to each of the users in the system. A general scheme of a FEC coded DS-CDMA system model for downlink is depicted in Figure 2.4. The scheme shows a discrete-time DS-CDMA communication system with FEC coding for U active users. FEC coded signals are treated in this work not only as a medium of resistance to the degradations introduced by the communication channel (physical medium) but also because it plays an essential role in the iterative multiuser receiver structures which will be discussed from chapter 3 onwards.

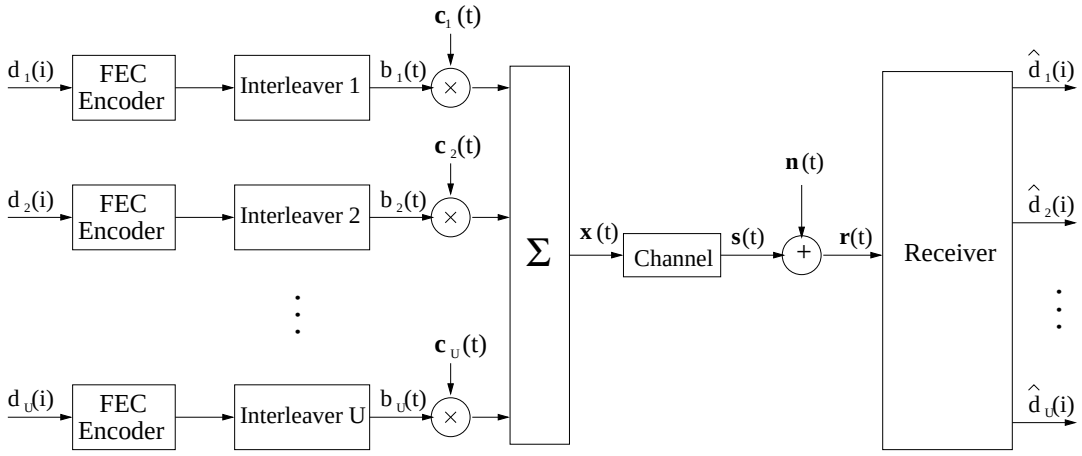

Figure 2.4: *Coded DS-CDMA system model for the downlink (base station to mobile).*

In this model each user transmits an input data stream, $\{d_u(i)\} \epsilon \{0,1\}$; with $u \epsilon \{1,2,\ldots,U\}$ and $i \epsilon \{1,2,\ldots,L\}$, where each individual data bit is first encoded with a rate R_0 and then passed through a modulation function. At the encoder output each user transmit L/R_0 coded bits $b_u(t) \epsilon \{-1,1\}$ where $t \epsilon \{1,2,\ldots,L/R_0\}$ identifies the coded bit interval and u as defined before. To reduce the effect of error bursts at the input of the decoder channel, interleaving (π) is incorporated at the encoder output as is shown in Figure 2.4. The resulting interleaved coded bits are then spreading by a unique PN code sequence, $\mathbf{c}_u(t)$. The *n*th chip of the spreading code $\mathbf{c}_u(t)$ is defined as $c_{u,n}(t) \epsilon \{\frac{-1}{\sqrt{N}}, \frac{1}{\sqrt{N}}\}$, where N is the processing gain of the system and $n \epsilon \{1,2,\cdots,N\}$. A mathematical representation of the transmitted signal at time t is

expressed as

$$\mathbf{x}(t) = \sum_{u=1}^{U} \sqrt{P_u}\mathbf{c}_u(t)b_u(t). \tag{2.1}$$

where P_u denotes the transmitted power of the *u*th user. For the downlink, the signals are passed synchronously through the same communication channel since the users' signals are transmitted by the same source (base station). At the receiver side, the received signal, $\mathbf{r}(t) = \mathbf{s}(t) + \mathbf{n}(t)$, results from the convolution of the the channel response and the transmitted signal, represented by $\mathbf{s}(t)$, plus the additive white Gaussian noise (AWGN), $\mathbf{n}(t)$. Finally, the intended signal is extracted from $\mathbf{r}(t)$ by despreading the signal with the same code used in the transmitter. If orthogonal spreading codes are used, *i.e.* $\mathbf{c}_u^T(t)\mathbf{c}_k(t) = 0$ for $u, k \,\epsilon\, \{1, 2, \cdots, U\}$ where $u \neq k$, no mutual interference exist between users in the system and then only the impairments from the channel are the noise sources. However, in practical systems this orthogonality is destroyed by the communication channel (section 2.4 addresses this problem) generating CCI for other users in the system. This type of interference is called multiple access interference (MAI). Unfortunately, the MAI increases proportionally with the number of users which degrades significantly the system performance. To reduce complexity, MAI from a single cell is only considered in this work.

The major problem in a DS-CDMA system is then of interference due to the fact that both channel impairments and mutual interference between users are the principal impediments to reliable communication. Work in this area is mainly at mitigating these effects. Only the conventional detector, which follows a single user detection strategy, is discussed in this chapter. Multiuser detection however could achieves a significant capacity improvement over the conventional detector. However, the receiver design from the multiuser detection viewpoint is not addressed until next chapter. A description of each element that comprises the DS-CDMA system is given in the following sections.

2.3 Transmitter

As shown in Figure 2.4, a basic transmitter scheme consists primarily of the FEC encoder and spreading functions for each of the users in the system. Nowadays, fundamental signal processing operations in any communication system are modulation and FEC coding. One of the reasons of using FEC coding is to increase the robustness of data transmission over the

distortions and disturbances of the physical channel (propagation of radio waves in free space). Since the physical channel provokes a degradation in the system performance, in terms of the bit error rate (BER), FEC coding is used to reduce the required signal to noise ratio (SNR) for a fixed BER. A measure of the advantage between a FEC coded system and an uncoded system is given by the FEC *coding gain* [29]. From another perspective, it means that the system capacity is incremented since a relaxation in the power budget is attained (*i.e.* a reduction in hardware costs, less transmitted power required, etc.).

2.3.1 Channel coding

There exist several channel coding schemes, however, we are only concern of those with an error control scheme. The basic function of error control coding in a digital communication system is to reduce the number of errors in the reception of a signal. The quantification of this is obtained by taking the ratio of the number of error bits to the total number of bits received (BER). A type of error control coding (or FEC coding) is widely used in current communication systems which includes several cellular systems such as GSM [4]. Hence, this work will be focused only to use this type of error control coding.

The FEC encoder consists of the addition of redundant bits (called check or parity bits) to the transmitted data signal. This is done in such a way that at the receiver the channel decoder uses these redundant bits to correct errors yielded by the communication channel. The proportion of information bits, l, in the code sequence, n_c, is called the code rate, $R_0 = l/n_c$. FEC coding has been classified into block codes and convolutional codes. In the case of block codes, the codewords are built by adding $n_c - l$ redundant bits to blocks of l data bits. These redundant bits can be obtained from a linear transformation that depends on the l data bits. Therefore, it results in an encoder that does not have memory since each block is treated independently. Commonly, these codes are referred as (n_c, l) block codes. Some of the commonly used block codes are Hamming codes, Golay codes, BCH codes, and Reed Solomon codes. There are many ways to decode block codes and estimate the l information bits. However, these type of codes will not be discussed here but can be studied in Coding Theory [29]. On the other hand, convolutional codes different to block codes does have memory due to the dependency of the codewords with not only the current data block but also on one or more previous blocks. This dependency is yielded by the convolution operation performed in the encoder between the input data block and the impulse response of the encoder. Convolutional coding has been more widely accepted

in wireless communication for its properties in continuous transmission (primarily used for real time error correction). Hence, convolutional codes are only of interest in this thesis. Since the realisation of this thesis has its fundamentals in a subclass of convolutional codes, namely turbo codes, a special attention is focused in this powerful FEC coding technique.

The remaining of this section is only devoted to describe the channel encoding. The decoding process for this sort of codes is addressed in section 2.5.2.

2.3.1.1 Convolutional codes

In general, a convolutional encoder consists of a ν stages shift register and associated combinatorial logic that performs module two addition (binary codes). The combinatorial logic is usually composed of exclusive-or gates. The convolutional codes are generated by shifting blocks of l input binary bits at a time into a shift register. Then by using a number of algebraic function generators (sets of exclusive-or gates), a number of n_c output binary bits (codeword length) are yielded from each block of l bits. This results in an encoder with a rate, $R_0 = l/n_c$. The total number of input data blocks in the shift register, ν, is known as the *constraint length*

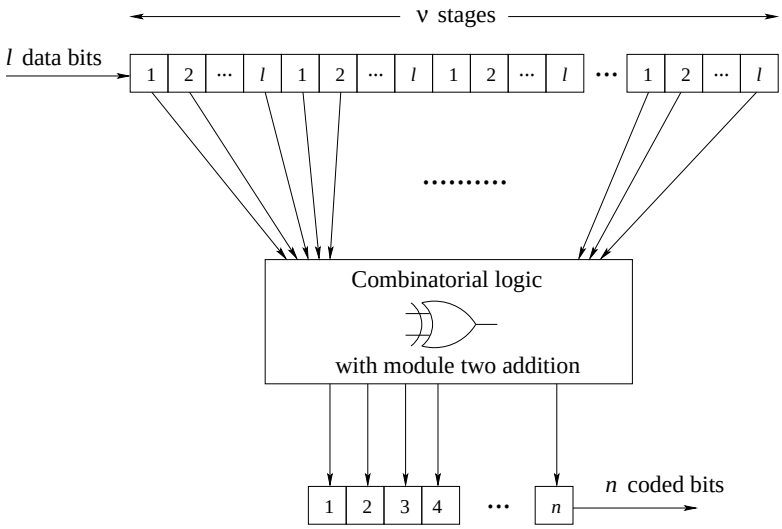

Figure 2.5: *General convolutional encoder structure.*

of the code and the term $\nu - 1$ is the memory of the code. In addition, the codes are said to be linear since only delays (shift register) and module-2 adders are implemented in the encoder structure. Figure 2.5 illustrates the general structure of a convolutional encoder which in a short form can be described as (n_c, l, ν) code.

For a better understanding of the encoder structure, let us consider the following example. This particular example consists in encoding the data input 10011 using a convolutional code of rate $1/2$ with constraint length 3. Figure 2.6 shows the two different ways that the $(2, 1, 3)$ code can be illustrated, where z^{-1} represents a delay of one data symbol. The algebraic function

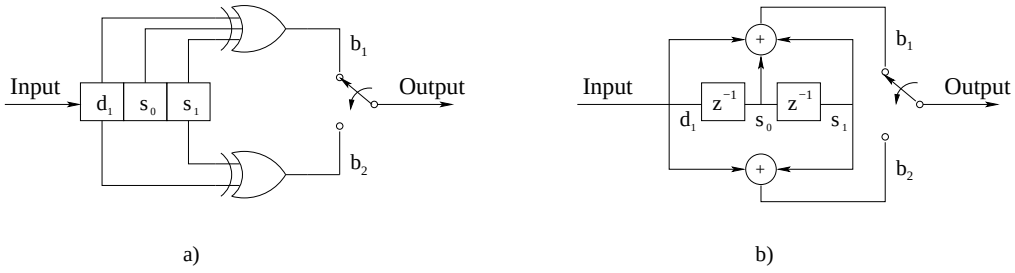

Figure 2.6: *Illustration of the convolutional encoder (2,1,3) with: a) exclusive-or gates b) simplified version of a).*

generators of this encoder are represented by $G_1 = 111$ and $G_2 = 101$ or simply $(7, 5)$ in octal notation. These generators, also called polynomial generators, correspond to the connections of the shift register with the upper and lower modulo-two adders, respectively. The binary representation of the generators means simply the omission or inclusion of a connection to the relevant shift register element. To demonstrate its operation, the state of various parts of the encoder during successive clock periods is shown in Table 2.1. It is assumed that the encoder starts with zeros in the shift register.

d_1	s_0	s_1	b_1	b_2
1	0	0	1	1
1	1	0	0	1
0	1	1	0	1
0	0	1	1	1
1	0	0	1	1

Table 2.1: *NSC encoding process for an input sequence 11001*

Also a convolutional encoder can be classified as a *systematic* or *non-systematic*. While *systematic* codes are accomplished when the current input block appear unchanged in the current code block, in the case of the *non-systematic* codes this restriction is not applied. In the previous example a *non-systematic* convolutional code (NSC) was analysed.

A more complex structure in the convolutional encoder is implemented by including feedback in the encoder (in a similar way to an infinite impulse response filter (IIR)). Again for simplicity

a (2,1,3) code is shown in Figure 2.7, the corresponding status of the encoding process is given in Table 2.2. This form of encoding is known as *recursive* convolutional code . Note that a *recursive* convolutional code can be *systematic* or *non-systematic*. In the example a *recursive* and *systematic* convolutional (RSC) code with polynomial generators $(7, 5)$ is illustrated.

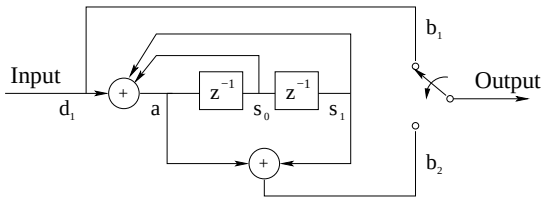

Figure 2.7: *RSC encoder*

d_1	a	s_0	s_1	b_1	b_2
1	1	0	0	1	1
0	1	1	0	0	1
0	0	1	1	0	1
1	0	0	1	1	1
1	1	0	0	1	1

Table 2.2: *RSC encoding process for an input sequence 10011*

2.3.1.2 Turbo codes

Perhaps the most important development in channel coding theory, in recent years, has been the introduction of *turbo codes* [30]. This error correcting code is able to transmit information across the channel with arbitrary low bit error rate (BER). It has been shown that a turbo code can achieve performance within 0.7 dB of the AWGN channel capacity. This code is a parallel concatenation of two component convolutional codes separated by a random interleaver that combines concepts such as iterative decoding and soft input soft output (SISO) decoding [3, 31–36].

The original turbo encoder scheme consists of a combination of two convolutional codes in a parallel concatenation [37]. A more general structure is extended to include more than two convolutional codes either in a parallel or serial concatenation [38–41]. In Figure 2.8 is presented the turbo encoder scheme as given in its original form. This turbo encoder consists of two RSC codes in a parallel concatenation. Both encoders (RSC 1 and RSC 2) receive the same binary data bits in a continuous or block fashion but arranged in a different sequence due to

the presence of a random interleaver. The reason for using an interleaver is to "randomise" the locations of errors introduced in transmission (burst errors) which are generated by the first decoder, allowing them be corrected by the second decoder [35, 42]. The output of the turbo encoder is formed by multiplexing the data bits and the parity bits of the two RSC encoders. The basic rate of the overall code is a rate $R_0 = 1/3$ but it can be increased by puncturing, as it is done in the original turbo codes [30].

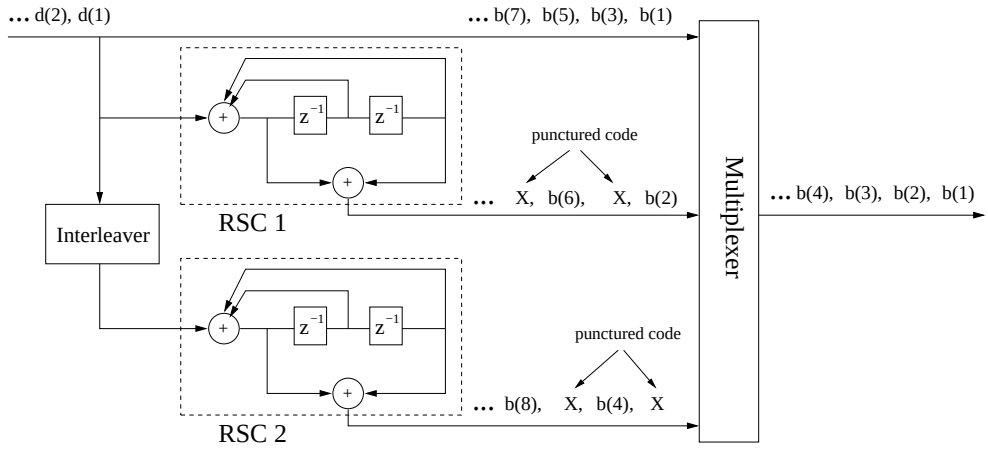

Figure 2.8: *Turbo encoder structure for a rate* $1/2$.

The description for the decoding structures is addressed in section 2.5.2.3.

2.3.2 Spreading sequences

The spreading sequences generation is the first step in understanding CDMA mobile communications. In cellular radio communication, the autocorrelation and the cross-correlation properties of the spreading sequences are used to achieve multiple access communications. A receiver for a DS-CDMA system uses a synchronised replica of the spreading sequence used for a desired transmitter to recover the original information. This operation will cause that other transmitters' signals (using different spreading sequences) to remain spread over the communication channel and will cause minimal interference to the desired signal due to the noise like properties of the spreading sequences. However, this emphasises the need for low cross-correlation between the spreading sequences, otherwise the MAI term will dominate the correlator output. The MAI also increases with the number of users active in the system and is very susceptible to power variation among users using the conventional detector. MAI can cause high bit error rates and ultimately decrease system capacity. Although orthogonal se-

quences can be applied to eliminate totally the MAI term because of the zero cross-correlation property, this is a very difficult task to maintain in a practical DS-CDMA system due to the presence of a dispersive communication channel. Even in synchronous systems the multipath effect does not allow us to ensure orthogonality at the receiver front end.

In practice, pseudo-random or pseudo-noise (PN) sequences are used to spread the signal spectrum because they achieve several signalling properties such as, are easy to generate and are difficult to reconstruct from a short segment. To simplify the implementation, periodic PN sequences are employed. Hence, a PN sequence is a sequence of chips, *e.g* ± 1, which appears to be random but is in fact perfectly deterministic. The randomness property is treating in the sense that a PN sequence appears to have been generated from a random or non deterministic experiment such as a fair coin tossing experiment (head could result in $+1$ and tail in -1). In this class of sequences, there are maximal length sequences (m-sequences), gold codes and Kasami sequences which are used in current wireless systems. In this thesis we shall think about a DS-CDMA system with the use of short PN sequences. This comes from the fact that systems with long sequences are relatively unsuited for multiuser detectors.

Although PN sequences are the choice for practical systems, unless otherwise stated, we will consider instead random codes as the main spreading sequences for the work presented in this thesis. This type of sequences are chosen due to the following characteristics:

- Statistically a random sequence is equivalent to using PN sequence of period much greater than the spreading length (N).
- The multipath effect in the properties of a spreading sequence (inter-chip interference) can be modelled by random sequences.
- The performance of a synchronous system with random sequences is on average the same that of an asynchronous system.

A random sequence can be generated by selecting independently each chip of the sequence which can take the value ± 1 with equal probability. With the purpose of comparison in the analysis and simulations to assess the system performance, orthogonal codes will be incorporated for some discussions. One of the most common orthogonal sequences are the Walsh codes [43]. In general, the spreading code vector will be defined throughout this thesis as $\mathbf{c}_u^T(t) = [c_{u,1}(t), c_{u,2}(t), \cdots, c_{u,N}(t)]$ where u relates the user in the system, N the processing

gain and T denotes the transpose. The chips of the spreading will be normalised to a signal level of $\pm 1/\sqrt{N}$ to obtain between any two spreading codes of a DS-CDMA system the following correlation properties

$$\mathbf{c}_u^T(t)\,\mathbf{c}_k(t) = \begin{cases} 1 & \text{if } u = k \text{ (autocorrelation)} \\ \rho_{u,k} & \text{if } u \neq k \text{ (cross-correlation)} \end{cases}$$

where u, k are the indexes that identify any two users in the system.

2.4 Communication channel

The radio propagation channel is often the dominant factor limiting the performance of any wireless system. Modelling of wave propagation phenomena is the key to a successful state of the art design, because it provides mechanism to test and evaluate methods for mitigating the impairment effects before a single piece of expensive hardware has to be built and validated in the field. In current systems such as in IMT 2000 and cdmaone, the impulse response of the channel is estimated in several different ways, for example using pilot channels. Therefore, the channel impulse response can be assumed to be known mainly because the radio propagation characteristics is not a problem tackled in this work. Studies in the effect of multipath for the downlink in a DS-CDMA system can be found in [44, 45]. In this work we have reduced the complexity of the problem by giving to all users the same channel conditions and thereby the same spreading code length. A general description of the communication channel model

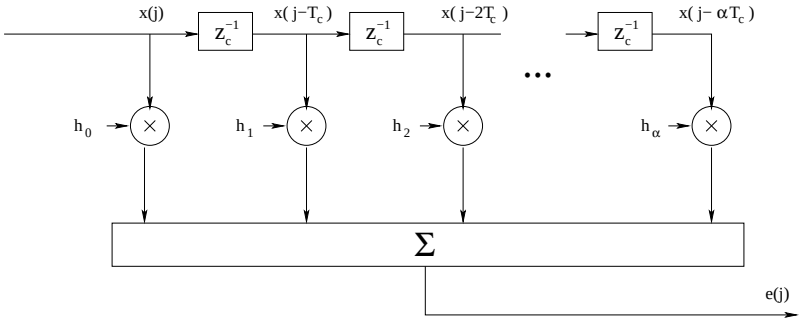

Figure 2.9: *Communication channel model.*

is illustrated in Figure 2.9, where z_c^{-1} represents a delay of one chip. Denoting the channel

input by the time series $x(j), x(j - T_c), x(j - 2T_c), \cdots$, and the impulse response of the channel by $h_0, h_1, h_2, \cdots$, the channel output $s(j)$ at discrete time j (chip level) is given as $s(j) = \sum_{a=0}^{\alpha} h_a x(j - aT_c)$, where α comprises the duration of the channel impulse response in chips. Assuming perfect time synchronisation between the transmitter and the receiver, the mathematical model for the received signal at discrete time t (bit level) can be expressed in a matrix notation as follow

$$\mathbf{r}(t) = \mathbf{H}_t \mathbf{x}(t) + \mathbf{H}_{t-1}^{ISI} \mathbf{x}(t-1) + \mathbf{n}(t) \tag{2.2}$$

where the channel response matrix to the transmission of the $N \times 1$ vector $\mathbf{x}(t)$ is given by the $N \times N$ Toeplitz matrix

$$\mathbf{H}_t = \begin{bmatrix} h_0 & 0 & 0 & 0 & \cdots & 0 \\ h_1 & h_0 & 0 & 0 & \cdots & 0 \\ \vdots & & \ddots & & \ddots & \vdots \\ 0 & \cdots & h_\alpha & h_{\alpha-1} & \cdots & h_0 \end{bmatrix}.$$

The term $\mathbf{H}_{t-1}^{ISI} \mathbf{x}(t-1)$ in (2.2) represents the effect of ISI from the signal at the preceding discrete time, where $\mathbf{H}_{t-1}^{ISI}$ denotes an $N \times N$ Toeplitz matrix given as

$$\mathbf{H}_{t-1}^{ISI} = \begin{bmatrix} 0 & \cdots & 0 & h_\alpha & h_{\alpha-1} & \cdots & h_1 \\ 0 & \cdots & 0 & 0 & h_\alpha & \cdots & h_2 \\ \vdots & & \ddots & & & \ddots & \vdots \\ 0 & \cdots & 0 & 0 & 0 & \cdots & h_\alpha \\ 0 & \cdots & 0 & 0 & 0 & \cdots & 0 \\ \vdots & & \ddots & & & \ddots & \vdots \\ 0 & \cdots & 0 & 0 & 0 & \cdots & 0 \end{bmatrix}.$$

Considering the particular case of $\alpha = 0$ and the amplitude of the channel response as the unit, equation (2.2) is reduced to the conventional DS-CDMA system over an AWGN channel given as

$$\begin{aligned} \mathbf{r}(t) &= \mathbf{x}(t) + \mathbf{n}(t) \\ &= \sum_{u=1}^{U} \sqrt{P_u} \mathbf{c}_u(t) b_u(t) + \mathbf{n}(t) \end{aligned} \tag{2.3}$$

where $\mathbf{n}(t)$ denotes the white Gaussian noise with double sided power spectral density $\sigma^2 = N_0/2$.

2.5 Receiver

In this section we describe the conventional DS-CDMA detector structure with FEC decoding. In the particular case where the signals from different users are uncorrelated, the conventional detector (or single-user detector) is optimum [46]. However, in practise the signals from different users will be correlated which means that the conventional detector will be suboptimum.

2.5.1 Single-user detector

The conventional detector or RAKE detector [47] for the received signal given in (2.2) is a bank of $\alpha + 1$ correlators (called fingers) for each user, as shown in Figure 2.10 where z_c^{-1} is a delay of one chip. The outputs of the fingers provide with $\alpha + 1$ replicas of the same transmitted

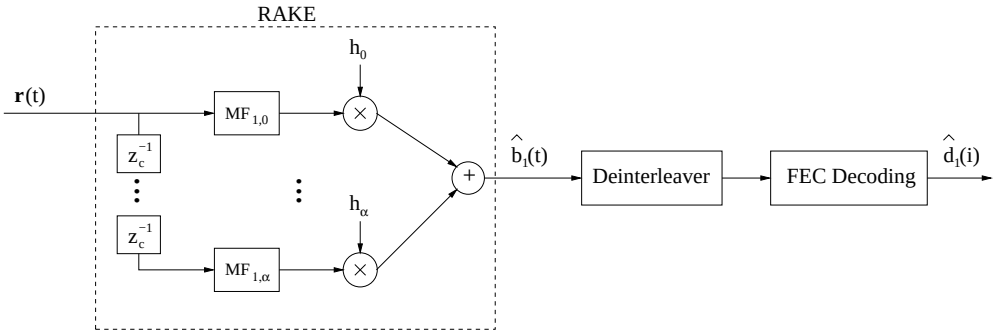

Figure 2.10: *The conventional DS-CDMA detector for user* 1 *with FEC decoding*

signal at the receiver but with a delay of one chip between each other. These replicas are then combined to yield a single soft estimate of the transmitted data symbols. Since each finger detects one user without regard to the existence of the other users whose interference is assumed to be Gaussian, the optimal combining weights are the path coefficients of the channel. This is equivalent to an $\alpha + 1$ branch diversity system with maximum ratio combining (MRC) [48]. Therefore, the output of the RAKE detector for the *u*th user is mathematically represented as

$$\hat{b}_u(t) = \sum_{a=0}^{\alpha} h_a \mathbf{c}_u^T(t)\mathbf{r}(t - aT_c) \tag{2.4}$$

where $\mathbf{r}(t - aT_c)$ is a delay version of the received signal $\mathbf{r}(t)$ (with T_c as the chip period). Considering that each transmitted signal arrives at the receiver over a single path (no multipath, *i.e* $\alpha = 0$) and with a channel coefficient amplitude $h_0 = 1$, the conventional detector for the *u*th user is reduced to implement a single matched filter detector which gives as an output

$$\begin{aligned}
\hat{b}_u(t) &= \mathbf{c}_u^T(t)\mathbf{r}(t) \\
&= \mathbf{c}_u^T(t)\mathbf{x}(t) + \mathbf{c}_u^T(t)\mathbf{n}(t) \\
&= \mathbf{c}_u^T(t)\sum_{k=1}^{U}\sqrt{P_k}\mathbf{c}_k(t)b_k(t) + \mathbf{c}_u^T\mathbf{n}(t) \\
&= b_u(t) + \sum_{\substack{k=1 \\ k\neq u}}^{U}\rho_{u,k}\sqrt{P_k}b_k(t) + z_u(t)
\end{aligned} \tag{2.5}$$

where the correlations with all the others users ($\rho_{u,k}$) give rise to the MAI term and the correlation with the thermal noise yields the noise term $z_u(t)$. In the particular case of uncorrelated users, $\rho_{u,k} = 0$ for all $k \neq u$. Nevertheless, the existence of MAI ($\rho_{u,k} \neq 0$) has a significant impact in the capacity and performance of the conventional detector. This drawback arises as the conventional detector follows a single-user strategy which treats other users as noise. Due to the problem with the conventional detector mentioned above, a different type of detector has been derived. These detectors, which do not treat other users as noise, but as digital signals are called multiuser detectors. The study of multiuser detection techniques will be addressed in the next chapter.

2.5.2 FEC decoding

Following the encoder descriptions in section 2.3.1 for convolutional codes and turbo codes, this section presents the decoding algorithms for this type of codes. The main decoding strategy for convolutional codes is based on the widely used Viterbi algorithm (VA) [49],[50]. However, the introduction of turbo codes [30] have brought an increased interest to another method of decoding, namely the maximum *a posteriori* (MAP) algorithm [2] (also known as the BCJR algorithm). There are a few important difference between these two approaches. For instance, the VA is a maximum likelihood algorithm that finds the most probable data sequence that was transmitted, while the MAP algorithm finds the most probable data bit to have been transmitted given a coded sequence. The MAP algorithm is considerably more complex than the VA.

On the other hand, there are two primary decoding strategies for turbo codes. They are based on the MAP algorithm or a soft input VA (SOVA). Regardless of which algorithm is implemented, the turbo decoder requires the use of two component decoders that operate in an iterative manner. In this thesis, the MAP will be adopted for the turbo decoder structure. An outline of VA and MAP algorithms is given in sections 2.5.2.1 and 2.5.2.2 respectively. Lastly, the turbo decoder structure is presented in section 2.5.2.3. Special attention is given to this scheme since it represents the basis of the work presented in this thesis.

2.5.2.1 Viterbi algorithm

The task of a decoder is to recover the transmitted coded bit stream from the received noisy signal. Since the original transmitted signal can never be recovered with certainty, the VA is a means of tracing all the possible data sequences and selecting the one which is most likely to have been transmitted, hence the term maximum likelihood sequence estimation (MLSE) [49]. Perhaps the single most important concept to aid in understanding the VA is the trellis diagram [51]. Figure 2.11 shows the trellis diagram for the example of the convolutional encoder illustrated in Figure 2.6, *i.e* a $(2, 1, 3)$ NSC code with generators $(7, 5)$. It is assumed that the initial condition of the encoder is the state 00. Convolutional codes with VA decoding is particularly

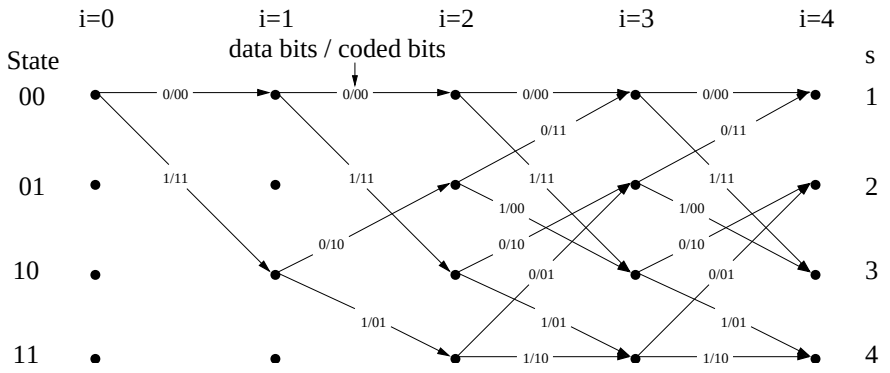

Figure 2.11: *Trellis diagram for a convolutional code* $(2, 1, 3)$ *and generators* $(7, 5)$.

suited to a channel in which the transmitted signal is mainly corrupted by AWGN. Given a received sequence of symbols corrupted by AWGN, the VA searches every path through the trellis diagram and determines the sequence that is closest in distance to the received sequence of noisy symbols. The decoder can perform either soft (Euclidean distance) or hard (Hamming distance) decisions as the distance measure, if soft decisions are used the VA is the optimal MLSE in AWGN.

To keep things simple we describe the VA for our example rate with $R_0 = 1/2$. Let assume that each time the pair of received noisy symbols corresponding to one transmitted data bit are $y(2i-1), y(2i)$ where $i \epsilon \{1, 2, \cdots, L\}$ indicates the stage in the trellis diagram with L as the number of transmitted data bits. To compute the sequence that most closely resemble the received signal sequence, the VA first recursively computes the survivor path entering each state. The survivor path for a given state is the sequence of symbols, entering the given state, that is closest in distance to the received noisy symbols. The distance between the survivor path and the sequence with the noisy symbols is called the path metric for that state. Assuming soft decoding decisions, the transition metric between state s' to state s at time i is defined as the Euclidean distance

$$TM_{s',s}(i) = \sum_{t=2i-1}^{2i} (y(t) - \sqrt{E_b} b_{s',s}(t))^2 \qquad s', s \ \epsilon \ \{1, \cdots, 2^{\nu-1}\} \tag{2.6}$$

where $b_{s',s}(t) \epsilon \{-1, 1\}$ is the tth output coded bit in the transition from state s' to state s with $s', s = 1, 2, \cdots, 2^{\nu-1}$ and E_b is the energy of each coded bit. If $PM_s(i)$ defines the path metric for state s at time i and S the set of states that have transitions to state s, then

$$PM_s(i) = min(PM_{s'}(i-1) + TM_{s',s}(i)). \tag{2.7}$$

Let $s_m \epsilon S$ be the state that results in the minimum metric. Then the transition from state s_m to state s at time i is appended to the survivor path of state s_m at time $i-1$ in order to form the updated survivor path of state s at time i. Following the same process, the path metrics and the survivor path are updated for all states at each stage of the trellis. Hence, at the end of the trellis, the survivor path can be traced from the state that has the minimum path metric backward. If the register in the encoder is flushed with zeros, the most likely path is traced from the state 00 (s=1). For long data sequences, or continuous data ($L \rightarrow \infty$), the VA is neither practical or desirable due to the memory constraints and decoder delay. Therefore, the length of the survivor path is usually kept to practical values according to the application. Research has shown [52] that any traceback depth of $L > 5\nu$ increases delay and decoder memory requirements, while not significantly improving the performance of the decoder.

The VA has been frequently used in different applications such as space communications, satellites, detection in digital communications, etc. Many radio channels are AWGN channels, but many, particularly terrestrial radio channels also have other impairments, such as multipath, se-

lective fading and interference. Transmitters and receivers can add noise signals to the desired signal as well. Although convolutional coding with VA decoding might be useful in dealing with those other problems, it may not be the most optimal technique. For a deeper understanding of the VA the reader is advised to consult [29, 46, 49].

2.5.2.2 MAP algorithm

The MAP algorithm [2] estimates the *a posteriori* probabilities (APP) of the states and transitions of a Markov source observed through a noisy discrete memoryless channel. The decoding algorithm for convolutional codes is then shown to be a special case of this problem as shown in Figure 2.11.

To describe the operation of the MAP algorithm consider a convolutional code of rate $R_0 = 1/n_c$ with constraint length ν. Let $d(i) \; \epsilon \; \{0, 1\}$; $i \; \epsilon \; \{1, \cdots, L\}$ be the *i*th data bit in the data block and $b(t) \; \epsilon \; \{-1, 1\}$; $t \; \epsilon \; \{1, \cdots, n_c L\}$ be the *t*th coded bit. Given the noise observation vector $\mathbf{Y}_1^L = \mathbf{Y}_1, \cdots, \mathbf{Y}_L$, the MAP decoder can compute the following APPs

$$P\{d(i) = d\} = P\{d(i) = d|\mathbf{Y}_1^L\} \qquad d \; \epsilon \; \{0, 1\} \tag{2.8}$$

$$P\{b(t) = b\} = P\{b(t) = b|\mathbf{Y}_1^L\} \qquad b \; \epsilon \; \{-1, 1\}. \tag{2.9}$$

The APPs in (2.8) and (2.9) can be computed as the sum of the probabilities of all trellis transitions from time $i-1$ to time i that are generated by $d(i) = d$ (data bit) or produce $b(t) = b$ (coded bit). If S_i defines the state at time i and s, s' the indexes for any of the $2^{\nu-1}$ possible states, the APP for a data bit at time i is given as

$$P\{d(i) = d|\mathbf{Y}_1^L\} = \sum_{S_i^d} P\{S_{i-1} = s', S_i = s|\mathbf{Y}_1^L\} \tag{2.10}$$

where S_i^d represents the set of all state transitions for which the input bit $d(i)$ is d, *i.e* S_i^0 if $d = 0$ or S_i^1 if $d = 1$. On the other hand, the APP for a coded bit at time t is denoted by

$$P\{b(t) = b|\mathbf{Y}_1^L\} = \sum_{S_t^d} P\{S_{i-1} = s', S_i = s|\mathbf{Y}_1^L\} \tag{2.11}$$

where similarly S_t^b represents the set of all state transitions for which the output coded bit $b(t)$

is equal to $b \epsilon \{-1, 1\}$.

By using the Bayes' theorem each valid state transition in the trellis diagram can be computed as

$$P\{S_i = s, S_{i-1} = s' | \mathbf{Y}_1^L\} = \frac{\lambda_i(s', s)}{P\{\mathbf{Y}_1^L\}} \tag{2.12}$$

where

$$\lambda_i(s', s) = P\{S_{i-1} = s', S_i = s, \mathbf{Y}_1^L\} \tag{2.13}$$

is the joint probability of $S_i = s$ and $S_{i-1} = s'$. The properties of the Markov process can be used to partition the joint probability which becomes

$$\lambda_i(s', s) = \alpha_{i-1}(s')\gamma_i(\mathbf{Y}_i, s', s)\beta_i(s) \tag{2.14}$$

$$\begin{aligned} \alpha_{i-1}(s') &= P\{S_{i-1} = s', \mathbf{Y}_1^{i-1}\} \\ \gamma_i(\mathbf{Y}_i, s', s) &= P\{S_i = s, \mathbf{Y}_i | S_{i-1} = s'\} \\ \beta_i(s) &= P\{\mathbf{Y}_{i+1}^L | S_i = s\} \end{aligned} \tag{2.15}$$

and where $\alpha_{i-1}(s')$ (also known as the forward recursion) computes the probability of state $S_{i-1} = s'$ based on the values received before time i, $\mathbf{Y}_1^{i-1}$. The function $\gamma_i(\mathbf{Y}_i, s', s)$ computes the transition probability based on the current received values, $\mathbf{Y}_i$, and $\beta_i(s)$ (known as the backward recursion) is the probability of state $S_i = s$ based on the values received after time i, $\mathbf{Y}_{i+1}^L$.

Assuming that S_{i-1} is a known condition, events after time $i - 1$ do not depend on $\mathbf{Y}_1^{i-1}$ and

then the forward probability $\alpha_i(s)$ can be recursively calculated as follow

$$\begin{aligned}
\alpha_i(s) &= \sum_{s' \epsilon \Omega_1} P\{S_{i-1} = s', S_i = s, \mathbf{Y}_1^{i-1}, \mathbf{Y}_i\} \\
&= \sum_{s' \epsilon \Omega_1} P\{S_i = s, \mathbf{Y}_i | S_{i-1} = s', \mathbf{Y}_1^{i-1}\} P\{S_{i-1} = s', \mathbf{Y}_1^{i-1}\} \\
&= \sum_{s' \epsilon \Omega_1} P\{S_i = s, \mathbf{Y}_i | S_{i-1} = s', \mathbf{Y}_1^{i-1}\} \alpha_{i-1}(s') \\
&= \sum_{s' \epsilon \Omega_1} P\{S_i = s, \mathbf{Y}_i | S_{i-1} = s'\} \alpha_{i-1}(s') \\
&= \sum_{s' \epsilon \Omega_1} \gamma_i(\mathbf{Y}_i, s', s) \alpha_{i-1}(s')
\end{aligned} \tag{2.16}$$

where Ω_1 implies the set of states s' at time $i-1$ that are connected to the state s at time i.

Similarly, the values for the backward probabilities $\beta_i(s)$ are computed recursively starting with the values of $\beta_L(s)$,

$$\begin{aligned}
\beta_i(s) &= \sum_{s' \epsilon \Omega_2} P\{S_{i+1} = s', \mathbf{Y}_{i+1}^L | S_i = s\} \\
&= \sum_{s' \epsilon \Omega_2} P\{\mathbf{Y}_{i+2}^L | S_{i+1} = s', S_i = s, \mathbf{Y}_{i+1}\} P\{S_{i+1} = s', \mathbf{Y}_{i+1} / S_i = s\} \\
&= \sum_{s' \epsilon \Omega_2} P\{\mathbf{Y}_{i+2}^L | S_{i+1} = s', S_i = s, \mathbf{Y}_{i+1}\} \gamma_{i+1}(\mathbf{Y}_{i+1}, s, s') \\
&= \sum_{s' \epsilon \Omega_2} P\{\mathbf{Y}_{i+2}^L | S_{i+1} = s'\} \gamma_{i+1}(\mathbf{Y}_{i+1}, s, s') \\
&= \sum_{s' \epsilon \Omega_2} \beta_{i+1}(s') \gamma_{i+1}(\mathbf{Y}_{i+1}, s, s')
\end{aligned} \tag{2.17}$$

where Ω_2 implies the set of states s' at time $i+1$ that are connected to the state s at time i. The initial conditions for the α's and β's are defined as follow

$$\alpha_1(s) = \begin{cases} 1 & \text{if } s = 1 \\ 0 & \text{otherwise} \end{cases} \tag{2.18}$$

$$\beta_L(s) = \begin{cases} 1 & \text{if } s = 1 \\ 0 & \text{otherwise} \end{cases} \tag{2.19}$$

these conditions basically states that the encoding process starts from the state $S_1 = 1$ and

finishes in the state $S_L = 1$. In the case that the trellis termination is not performed, the β recursion probability can be initialised either using $\beta_L(s) = 1/2^{\nu-1}$ or $\beta_L(s) = \alpha_L(s)$ for all s.

The transition probability at time i can also be determined by using Bayes' theorem

$$\begin{aligned}\gamma_i(\mathbf{Y}_i, s', s) &= P\{S_i = s, \mathbf{Y}_i | S_{i-1} = s'\} \\ &= P\{S_i = s | S_{i-1} = s'\} P\{\mathbf{Y}_i | S_i = s, S_{i-1} = s'\} \\ &= P\{S_i = s | S_{i-1} = s'\} \prod_{t=n_c(i-1)+1}^{n_c i} p(y(t)|b(t) = d) \end{aligned} \tag{2.20}$$

where the noisy received symbols at time i are denoted as $\mathbf{Y}_i = y(n_c(i-1)+1), \cdots, y(n_c i)$ and $p(y(n_c(i-1)+1)|b(n_c(i-1)+1) = d), \cdots, p(y(n_c i)|b(n_c i) = d)$ determine the conditional probabilities of the output coded bits associated with the transition from state $S_{i-1} = s'$ to state $S_i = s$. The transition state probabilities $P\{S_i = s | S_{i-1} = s'\}$ of the trellis are defined by the encoder input statistics. Generally, $Pr\{d(i) = 1\}$=$Pr\{d(i) = 0\} = 1/2$ and since there are two possible transitions from each state, $P\{S_i = s | S_{i-1} = s'\} = 1/2$.

Once the joint probability of each state transition, $\lambda_i(s)$, is calculated from (2.14), the APP for the *i*th data bit under the hypothesis of $d(i) = 1$ is computed as

$$\begin{aligned} P\{d(i) = 1 | \mathbf{Y}_i^L\} &= \frac{\sum_{S_i^1} \lambda_i(s', s)}{P\{\mathbf{Y}_1^L\}} \\ &= \frac{\sum_{S_i^1} \lambda_i(s', s)}{\sum_{S_i^0} \lambda_i(s', s) + \sum_{S_i^1} \lambda_i(s', s)} \end{aligned} \tag{2.21}$$

where the term $P\{\mathbf{Y}_1^L\}$ in (2.21) can be seen as a normalising factor. Based on the fact that $P\{d(i) = 1\} + P\{d(i) = 0\} = 1$ it can be observed that this term cancels out as shown in (2.21). Similarly, the APP for the hypothesis $d(i) = 0$ is obtained. Using also equation (2.21), the APP for the coded bits can be determined; however, they are calculated for a different set of state transitions which are given by S_i^b instead of S_i^d.

Therefore, an outline of the decoder operation is then:

1) Initialisation of $\alpha_1(s)$ and $\beta_L(s)$; $s = 1, \cdots, 2^{\nu-1}$, according to (2.18) and (2.19).

2) Given $\mathbf{Y}_i$, the decoder computes the transition probability $\gamma_i(\mathbf{Y}_i, s', s)$ using (2.20) and the forward probability $\alpha_i(s)$ using (2.16). The calculated values of $\alpha_i(s)$ are stored for

all i and s.

3) Once the complete sequence $\mathbf{Y}_i^L$ has been received, the decoder can then recursively computes the backward probability $\beta_i(s)$ using (2.17). When the $\beta_i(s)$ have been computed for all i and all s, the joint probabilities $\lambda_i(s', s)$ are obtained using (2.14). Finally, the APP for a decoded bit is then calculated using (2.21). Thus if a hard decision is performed in the decoder, the output for a decoded bit at time i is given as

$$\hat{d}(i) = \begin{cases} 1 & \text{if } P\{d(i) = 1|\mathbf{Y}_i^L\} > P\{d(i) = 0|\mathbf{Y}_i^L\} \\ 0 & \text{otherwise.} \end{cases} \tag{2.22}$$

A comparison of the Viterbi and MAP algorithms in decoding convolutional codes is presented in Figure 2.12. The figure shows the bit error rate (BER) performance for a AWGN channel as a function of the signal to noise ratio, measured in terms of the E_b/N_0, for a $(2, 1, 3)$ NSC code with generators $(7, 5)$. The size of the data block is $L = 200$ data bits. Monte Carlo simulations are provided to obtain the numerical results.

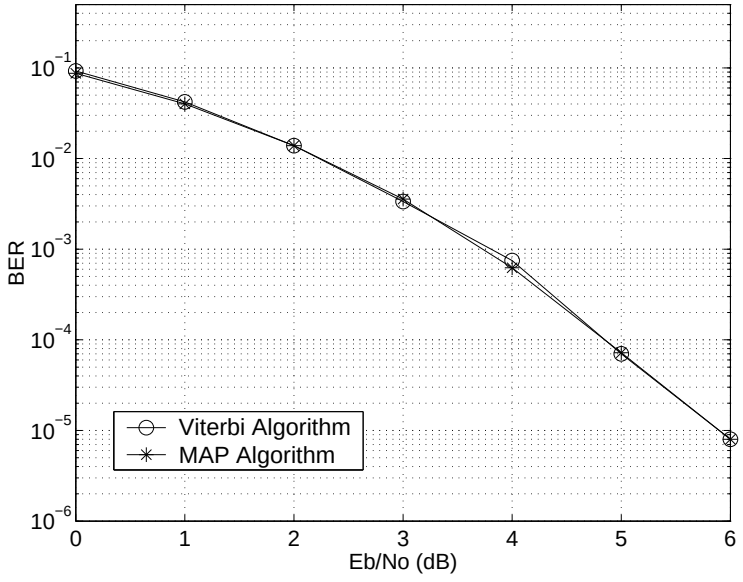

Figure 2.12: *Performance comparison of Viterbi and MAP algorithms for a* $(2, 1, 3)$ *nsc code with generators* $(7, 5)$.

The simulations show that both algorithms perform identically although the MAP algorithm is more computationally intensive than the VA. Recently, the introduction of turbo codes have brought an increased interest to the MAP algorithm which is very well suited in the iterative

decoding scheme. A description of the turbo decoder structure is presented in next section.

2.5.2.3 Turbo decoding

The particular success of turbo codes relies essentially on its powerful decoding structure which achieves performance close to the theoretical Shannon capacity limits. As described in section 2.3.1.2, the turbo encoder consists of two or more components codes (parallel or serial), separated by interleavers. This section presents the decoding strategy of turbo codes for the parallel concatenation of two components codes, other type of turbo codes structures can be found in [53]. The turbo code decoder iterates between the decoders for the component codes, improving data estimates on each iteration. The concept behind turbo decoding is to pass soft decisions (called *extrinsic information*) rather than hard decisions from the output of one decoder to the input of the other. The MAP decoder algorithm provides the best decoding method of determining soft-input soft-output (SISO) decisions. The preferred form for this SISO information is as the log likelihood ratio (LLR). Alternative SISO decoders are the SOVA [54], the log-MAP and the max-log-MAP algorithms [55] which are simplified versions of the MAP algorithm which was described in the previous section.

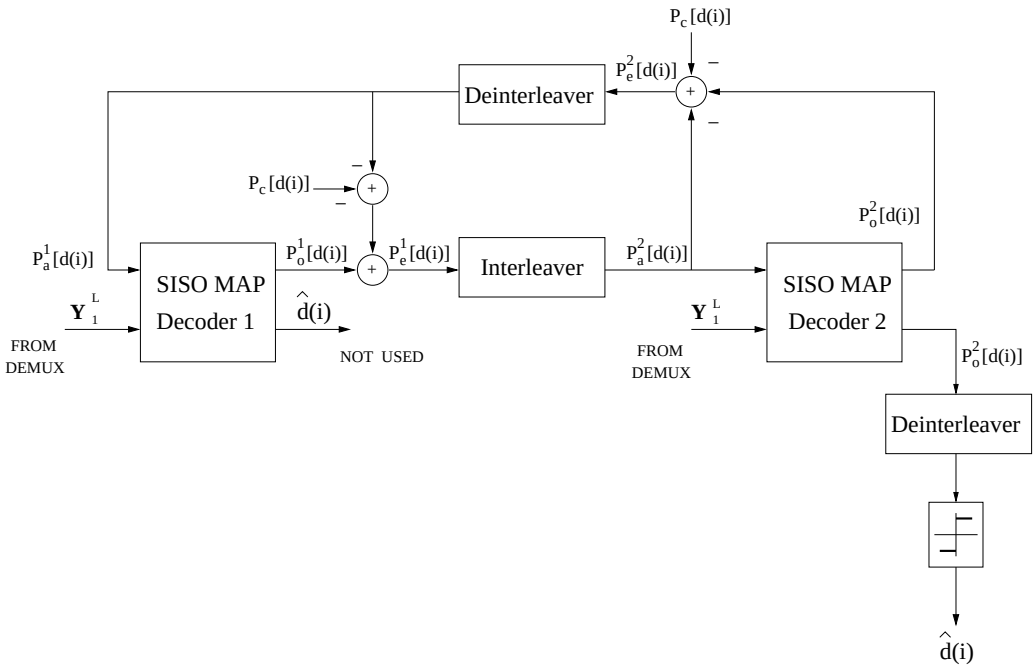

Figure 2.13: *Block diagram of a turbo code decoder.*

In Figure 2.13, the block diagram of the iterative decoder is shown. It is based on two SISO MAP decoders, an interleaver and deinterleaver operations. The SISO MAP decoders are a four-port device, with two inputs and two outputs. It accepts as inputs a vector of received symbol values from the channel, $\mathbf{Y}_1^L$, and a vector of *a priori* LLRs, $\mathbf{P}_a[d]$, for the corresponding data bits. As its outputs, it delivers a vector with an estimate of the data bits, $\hat{\mathbf{d}}$, and a vector of *a posteriori* LLRs after decoding, $\mathbf{P}_o[d]$. The estimates $\hat{\mathbf{d}}$ are given by the sign of the *a posteriori* LLRs.

Consider a turbo code of rate $R_0 = 1/2$, as described in section 2.3.1.2, where $d(i) \epsilon \{0, 1\}$; $i \epsilon \{1, \cdots, L\}$ is the *i*th data bit in the data block and $\mathbf{b}(i) = b(2i-1), b(2i)$ is the *i*th codeword transmitted with $b(t) \epsilon \{-1, 1\}$; $t \epsilon \{1, \cdots, nL\}$. Notice that puncturing is considered and therefore some output bits from the component codes are deleted as shown in Figure 2.8. When the redundant information of a given encoder is not transmitted (punctured code), the corresponding decoder LLR input is set to zero. Let $\mathbf{Y}_1^L = \mathbf{Y}_1, \cdots, \mathbf{Y}_L$ be the noise observation vector with $\mathbf{Y}_i = y(2i-1), y(2i)$ as the noisy received codeword at time i. The generalised form of the *a posteriori* LLR for the *i*th data bit, $d(i)$, is defined as

$$\begin{aligned} P_o[d(i)] &= ln\left\{\frac{P\{d(i)=1|\mathbf{Y}_1^L\}}{P\{d(i)=0|\mathbf{Y}_1^L\}}\right\} \\ &= ln\left\{\frac{P\{\mathbf{Y}_1^L|d(i)=1\}}{P\{\mathbf{Y}_1^L|d(i)=0\}}\right\} + ln\left\{\frac{P\{d(i)=1\}}{P\{d(i)=0\}}\right\} \end{aligned} \tag{2.23}$$

SISO MAP decoder. The inputs to the SISO MAP decoder 1 at time i becomes $\mathbf{Y}_i$ and $P_a^1[d(i)]$, where $P_a^1[d(i)]$ represents the *a priori* LLR information provided by the SISO MAP decoder 2. The output *a posteriori* LLR for the *i*th data bit $d(i)$ is

$$P_o^1[d(i)] = ln\left\{\frac{P\{d(i)=1|\mathbf{Y}_1^L\}}{P\{d(i)=0|\mathbf{Y}_1^L\}}\right\}. \tag{2.24}$$

In the case of the SISO MAP decoder 1, the estimates of the data bits are not performed. The APPs required in eq. (2.24) are obtained by using the MAP algorithm described earlier in section 2.5.2.2. However, these estimates also take into account the *a priori* information, $P_a^1[d(i)]$. The transition probability $P\{S_i = s|S_{i-1} = s'\}$, as required in (2.20), depends directly on the *a priori* probability of the data bit $d(i)$. In conventional decoders it is assumed that $P\{d(i)=1\} = P\{d(i)=0\}$ and therefore the second term in (2.23) does not contribute in the output LLR. For turbo decoding, a deinterleaved version of the *a posteriori* LLRs from

the SISO MAP decoder 2 ($P_o^2[d(i)]$ which becomes $P_a^1[d(i)]$) is used as *a priori* information in the following form

$$P\{S_i = s|S_{i-1} = s'\} = \frac{\exp(P_a^1[d(i)])}{1 + \exp(P_a^1[d(i)])} \tag{2.25}$$

if $P\{d(i) = 1|S_i = s, S_{i-1} = s'\} = 1$, and

$$P\{S_i = s|S_{i-1} = s'\} = \frac{1}{1 + \exp(P_a^1[d(i)])} \tag{2.26}$$

if $P\{d(i) = 0|S_i = s, S_{i-1} = s'\} = 1$. In the first iteration this information is not available, therefore $P_a^1[d(i)]$ is set to 0, *i.e* $P\{S_i = s|S_{i-1} = s'\} = 1/2$ for any transition in the trellis. Note that the MAP decoder requires estimates of the noise variance.

The operation of the second SISO MAP decoder is identical to the first but where the input *a priori* LLR, $P_a^2[d(i)]$, is provided from the output of the SISO MAP decoder 1, $P_o^1[d(i)]$.

Extrinsic information. Exchanging soft information, $P_e^1[d(i)]$ and $P_e^2[d(i)]$, in the iterative decoding does improve the performance of turbo codes with iterations, however, a better performance can be obtained if correlations between the constituent codes of the turbo decoder can be mitigated. Since the RSC codes are systematics ($b(2i-1) = d(i)$), the transition probability $p(y(2i-1)|b(2i-1) = d)$ in (2.20) is independent of the trellis structure and states. Therefore, for the first SISO MAP decoder equation (2.24) can be decomposed into

$$P_o^1[d(i)] \quad = \quad P_e^1[d(i)] + P_c[d(i)] + P_a^1[d(i)] \tag{2.27}$$

where $P_e^1[d(i)]$ is called the *extrinsic* LLR information and $P_c[d(i)]$ is known as the reliability constant [3]. The variables $P_e^1[d(i)]$ and $P_c[d(i)]$ are defined as

$$\begin{aligned} P_e^1[d(i)] &= ln\left\{\frac{p(y(2i)|d(i)=1)}{p(y(2i)|d(i)=0)}\right\} \\ P_c[d(i)] &= ln\left\{\frac{p(y(2i-1)|d(i)=1)}{p(y(2i-1)|d(i)=0)}\right\}. \end{aligned}$$

and $P_a^1[d(i)]$ is the *a priori* LLR which is provided by the second SISO MAP decoder. Thus, a less correlated decoder components can be obtained by only exchanging *extrinsic* LLR information $P_e[d(i)]$ instead of the *a posteriori* LLR information, $P_o[d(i)]$, since it represents extra knowledge that is gleaned from the decoding process. Also due to the presence of interleaving

between decoders, *extrinsic* information and channel observations are weakly correlated. The *extrinsic* LLR information of bit $d(i)$ from the SISO MAP decoder 1 is therefore

$$P_e^1[d(i)] \quad = \quad P_o^1[d(i)] - P_c[d(i)] - P_a^1[d(i)] \tag{2.28}$$

Similarly, the *extrinsic* information of bit $d(i)$ for the SISO MAP decoder 2 is

$$P_e^2[d(i)] \quad = \quad P_o^2[d(i)] - P_c[d(i)] - P_a^2[d(i)]. \tag{2.29}$$

The difference between the decoding exchanging *extrinsic*, $P_e[d(i)]$, or complete $P_o[d(i)]$ information is that using complete information the BER performance saturates on a floor much higher that the one using *extrinsic* information [53].

Iterative decoding. As shown in Figure 2.13 the SISO MAP decoder 1 computes $P_o^1[d_i]$, then the reliability constant, $P_c[d(i)]$, and the *a priori* LLR information, $P_a^1[d(i)]$, are subtracted to provide with the *extrinsic* information from the first SISO MAP decoder, $P_e^1[d(i)]$, see (2.28). On the other hand, the SISO MAP decoder 2 takes as input the channel observations and the *extrinsic* information $P_e^1[d(i)]$, which after interleaving, becomes the *a priori* information $P_a^2[d(i)]$ to the SISO MAP decoder 2. Note that the received systematic information for the second SISO MAP decoder is an interleaved version of $y(2i-1)$, see Figure 2.8. The SISO MAP decoder 2 generates $P_o^2[d(i)]$. The *extrinsic* information $P_e^2[d(i)]$ from the SISO MAP decoder 2 is obtained by using (2.29). The deinterleaving version of $P_e^2[d(i)]$ yields the *a priori* information $P_a^1[d(i)]$ which is fed to the SISO MAP decoder 1. The iterative process then continues. When a desired number of iteration have been performed in the turbo decoder, a decision is made using $P_o^2[d(i)]$, to yield the estimate output $\hat{d}(i)$

$$\hat{d}(i) = \begin{cases} 1 & \text{if } P_o^2[d(i)] > 0 \\ 0 & \text{otherwise} \end{cases} \tag{2.30}$$

Figure 2.14 shows the performance of Berrou *et al.* code [30] for a AWGN channel, after $1, 2, 3, 6$ and 18 decoder iterations. This particular codes is implemented for a rate $R_0 = 1/2$ (see Figure 2.8), constraint length $\nu = 5$ and generators $(37, 21)$ in octal notation. The interleaver consists of a 256×256 matrix where bits are written and read following the nonuniform rule given in [30]. The SISO MAP decoders are used with a data block length of $L = 65536$ bits.

The channel capacity [46] formula for an AWGN channel is given as

$$C = B\log_2\left(1 + \frac{C}{B}\frac{E_b}{N_0}\right) \tag{2.31}$$

where B is the available bandwidth, and E_b/N_0 is the information to noise energy ratio. Alternatively the channel capacity can be expressed in terms of the E_b/N_0 as follow

$$\frac{E_b}{N_0} = \frac{2^{C/B} - 1}{C/B}. \tag{2.32}$$

The capacity limits in (2.32) show basically the lowest possible bit signal-to-noise ratio (SNR), E_b/N_0, required to achieve arbitrarily small error probability over the AWGN channel using codes with a particular rate. For example, the channel capacity for a code with a rate $1/2$ is then give as

$$\frac{E_b}{N_0} = \frac{2^1 - 1}{1} = 1 = 0dB. \tag{2.33}$$

where this theoretical limit is obtained by assuming no constraint on block size, *i.e* approaching this limit require that the block size grows arbitrarily large. Therefore, it is then evident that the error performance of a turbo code with a rate $1/2$ and a block size of $L = 65536$ bits is within 1 dB from the Shannon limit as is shown in Figure 2.14.

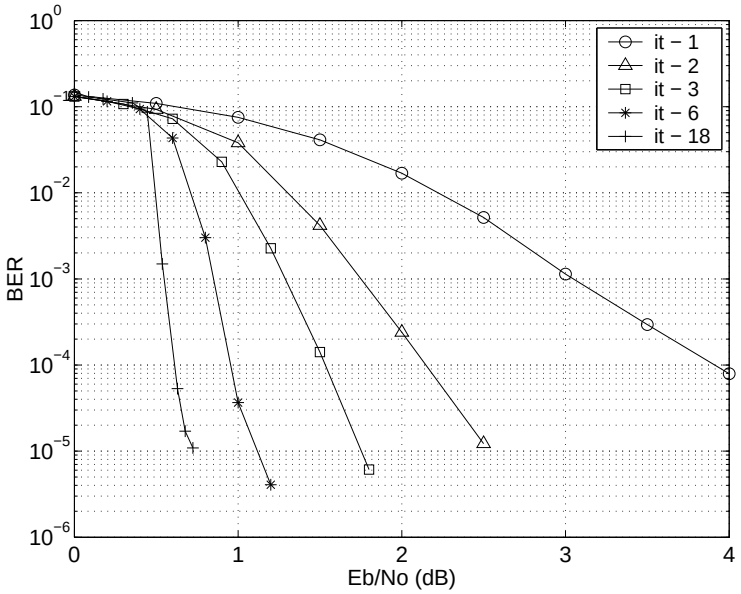

Figure 2.14: *BER vs E_b/N_0 for Berrou et al. code with different number of decoder iterations.*

2.6 Summary

In this chapter, a brief review of the basic principles of spread spectrum technology was presented. Particularly, we have focused our attention to DS-CDMA systems which represent one of the main spread spectrum technologies for the third generation of wireless communications. A general scheme for the downlink of a DS-CDMA system together with the mathematical models of the signals have been defined. The structure of the transmitter has also been described which comprises the channel coding and the spreading sequences. Random codes and orthogonal codes have been discussed as the spreading codes in the system. The communication channel, which represents the main limiting factor in the performance of any wireless system, has also been described. Finally, the receiver structure is addressed where the conventional DS-CDMA detector structure with FEC decoding is described. The study of multiuser detection techniques will be presented in next chapter. The FEC channel coding has also been reviewed but limited only to convolutional codes. Since the basis of this thesis has its fundamentals in a subclass of convolutional codes, *i.e* turbo codes, a special attention has been given to this type of FEC coding technique. Two type of decoding methods have been discussed which are the VA and MAP algorithms. When the decoding of a single convolutional code is considered, it is shown that MAP and VA perform identically. Originally the VA [49] appeared as a simplified version (less computationally intensive) of the MAP algorithm and then became a better choice for practical applications. However, MAP has shown to be more suitable in the decoding of turbo codes. Since the VA neglects some of the information during the decoding process, a loss in performance is obtained when the VA is implemented in the turbo decoder structure. Therefore and in order to exploit all the potential at the receiver, we will make use of the MAP algorithm in the FEC decoding on subsequent chapters.

Chapter 3
Turbo Multiuser Detection

The objective of this chapter is to introduce the turbo multiuser detection principle. Mainly this chapter aims to provide the fundamentals of multiuser detection. The first section (3.1) presents an introduction to multiuser DS-CDMA communication systems. Since the capacity of a multiuser DS-CDMA system is mainly limited by interference, mitigating this effect will provide a significant increase in capacity. A promising approach to combat this interference is to use multiuser detection. A general overview of this area is given in section 3.2. Due to the high complexity of the optimal multiuser detector, sub-optimum multiuser detector structures are needed. A brief description of several multiuser detection techniques which includes the optimum detector is also presented in section 3.2. Reviewing the turbo decoding structure, it is established that the application of the serial turbo coding structure into the multiuser detection area with the name of turbo multiuser detection. Replacing the inner code of a serial turbo codes with a DS-CDMA channel results in an encoder structure that can perform well using the iterative principle. This new type of multiuser receiver for FEC coded DS-CDMA systems is introduced in section 3.3.

3.1 Introduction

In a DS-CDMA communication system with U users, the capacity of the system depends on the level of cooperation among the users in the system. When the receiver of each user follows a single-user detection strategy (conventional detector), other users' signals appear as interference at the receiver of each user. Assuming a memoryless channel where each user transmits a pseudo-random signal of average power P, it is clear, therefore, that each user is corrupted by interference of power $(U-1)P$. The channel capacity formula per user for the AWGN channel is then

$$C_u = B\log_2\left[1+\frac{P}{(U-1)P+BN_0}\right] \qquad u \in \{1,2,\cdots,U\} \tag{3.1}$$

where B is the available bandwidth. Since C_u is the rate in bits/s, then $P = C_u E_b$. If the number of users is large it can be shown [46] that using the conventional detector the total system capacity $C_T = UC_u$ does not increased with U.

On the other hand, spreading codes and timing information of multiple users can be jointly used to detect each individual user. This is called multiuser detection (cooperative users). Assuming that each user is assigned a rate C_u the achievable capacity for U users with equal power in an AWGN channel is

$$\sum_{u=1}^{U} C_u \quad < \quad B \log_2 \left[1 + \frac{UP}{BN_0} \right]. \tag{3.2}$$

When all rates in the DS-CDMA system are identical to C_u, equation (3.2) reduces to

$$C_T \quad < \quad \log_2 \left[1 + C_T \frac{E_b}{N_0} \right]$$

where $C_T = UC_u/B$ is the total rate achieved by the U users per unit of bandwidth. Note that C_T increases as E_b/N_0 increases and therefore, it can be shown [46] that the total system capacity goes to infinity with U.

The conventional detector described in section 2.5.1, is a bank of correlators as shown in Figure 2.10. For synchronous transmissions, the cross-correlation between pairs of spreading codes is defined as

$$\rho_{u,k} \quad = \quad \mathbf{c}_u(t)^T \mathbf{c}_k(t) \tag{3.3}$$

where $\mathbf{c}_u(t)$ and $\mathbf{c}_k(t)$ are defined as in section 2.3.2 with $u, k \; \epsilon \; \{1, 2, \cdots, U\}$. Under the assumption of a memoryless channel, the output of the conventional detector for user u as given in equation (2.5) is

$$\begin{aligned} \hat{b}_u(t) \quad &= \quad b_u(t) + \sum_{\substack{k=1 \\ k \neq u}}^{U} \rho_{u,k} \sqrt{P_k} b_k(t) + z_u(t) \\ &= \quad b_u(t) + MAI + z_u(t) \qquad u, k \; \epsilon \; \{1, 2, \cdots, U\} \end{aligned} \tag{3.4}$$

the success of this detector depends on the correlation properties between the spreading codes. If $\rho_{u,k} = 0$ for all $u \neq k$ (orthogonal codes) the conventional detector becomes optimal. However, orthogonality is a difficult task to maintain in practical DS-CDMA systems mainly

because of two factors:

1) Since several uncoordinated and geographically separated users transmit information at the same time (asynchronous transmissions), orthogonality is difficult to achieve.

2) In DS-CDMA systems the presence of intersymbol interference (ISI) due to the multipath nature of the wireless channels makes it impossible to maintain the orthogonality in the system.

When the number of interfering users increases, the contribution of MAI becomes the limiting factor on the capacity and performance of the system. One way of suppressing this interference is to increase the processing gain when the number of users is large. However, this also increases the bandwidth required.

Another important factor that contributes to MAI is the presence of users with unequal levels of power. This problem arises when all mobile users transmit signals toward the base station with the same power, without taking into account the propagation loss from the base station. Mobile users that are closer to the base station will cause significant interference to the mobile users that are further from the base station because of the non zero cross-correlation between spreading codes assigned to users. This effect is known as near/far effect. Because of this effect, well-defined power control is essential for proper functioning of the conventional DS-CDMA system.

Since the conventional DS-CDMA system is mainly limited by interference, mitigating the effect of MAI can provide a significant increase in the system capacity. Research efforts to mitigate this effect embrace several areas such as:

- **Code Waveform Design**. This approach leads to the design of spreading codes with low levels of cross-correlation properties. As noted earlier, the asynchronism and multipath problems of practical conventional DS-CDMA communication systems, make is impossible to maintain orthogonality between the users' signals even if orthogonal codes are used. Time shifts of most orthogonal waveforms are not self-orthogonal.

- **Power Control**. In conventional DS-CDMA systems, power control allows users to share resources of the system equally between themselves to mitigate the near/far effect. In most modern systems, both base stations and mobiles have the capability to dynamic

adjustment their transmit powers. Power control techniques can be mainly classified as follows: 1) Open-loop power control (OLPC) and 2) Closed-loop power control (CLPC). OLPC technique is used initially for the mobiles to adjust their transmitted power according to the power levels received from the base station. CLPC is used by the base station to send power control instructions to the mobile based on the power level it receives from the mobile. In the event that power control is not used, the capacity of the DS-CDMA mobile system is very low, even lower than that of mobile systems based on FDMA. Therefore, power control is an essential feature for a proper operation of a modern CDMA high-capacity cellular radio system using the conventional detector.

- **FEC coding**. The design of more powerful forward error correction codes allows more acceptable error rate performance at lower signal to interference ratio levels.
- **Sectored/Adaptive Antennas**. By directing the reception of the desired signal over a narrow angle, the antenna enhances only the desired signal and attenuates the MAI from the other incident angles. The direction of the antenna can be fixed (sectored antennas), or adjusted dynamically (adaptive antennas). In the latter case, the antennas are directed to a desired user by using adaptive signal processing.
- **Multiuser detection**. Multiuser receivers for DS-CDMA systems aim to jointly detect signals to increase the capacity of such systems. The conventional DS-CDMA detector treats other user as noise, but multiuser receivers attempt to mitigate the interference from other users for their mutual benefit. Multiuser detection is also used to alleviate the near far problem. This allows the use of less power control updates. The complexity problem of the optimum multiuser receiver leads us to investigate sub-optimum approaches. This research has focused on finding approaches with the best possible trade off between complexity and performance.

3.2 Multiuser detection

Multiuser detection (MUD) is a promising approach to provide more efficient use of the available frequency spectrum and overcoming the limitations of the conventional DS-CDMA detector.

Potential benefits of using MUD in a cellular system are significant increase in capacity. However, there are two main limitations on the benefits of MUD which are: 1) inter-cell interference and

2) multiuser receiver complexity on the downlink. In cellular DS-CDMA systems, the uplink and the downlink utilise different frequency bands. However, due to the frequency planning (see section 1.1) the same pair of frequencies are reused in neighbouring cells, resulting in inter-cell interference which is added to the interference within a cell (intra-cell interference). Significant reduction in capacity can occur if this interference is not mitigated. For the sake of simplicity, we assume null inter-cell interference in the work presented in this thesis, *i.e* only intra-cell interference is considered. A second limitation of MUD is the receiver complexity. With respect to downlink transmissions, a major concern is the constraints in cost, size and weight of the receiver. Therefore, there is a need to provide mobile multiuser receivers that have reasonable computational complexity and acceptable performance to ensure practical implementation. On the other hand, for uplink transmissions (where the detection of multiple users is required in any case) these issues are relaxed since base stations of current systems allow the extra signal processing required. Hence, improving the capacity of the uplink does not improve the overall capacity of the system. In the work presented here, multiuser receivers are only considered for the downlink of a DS-CDMA system.

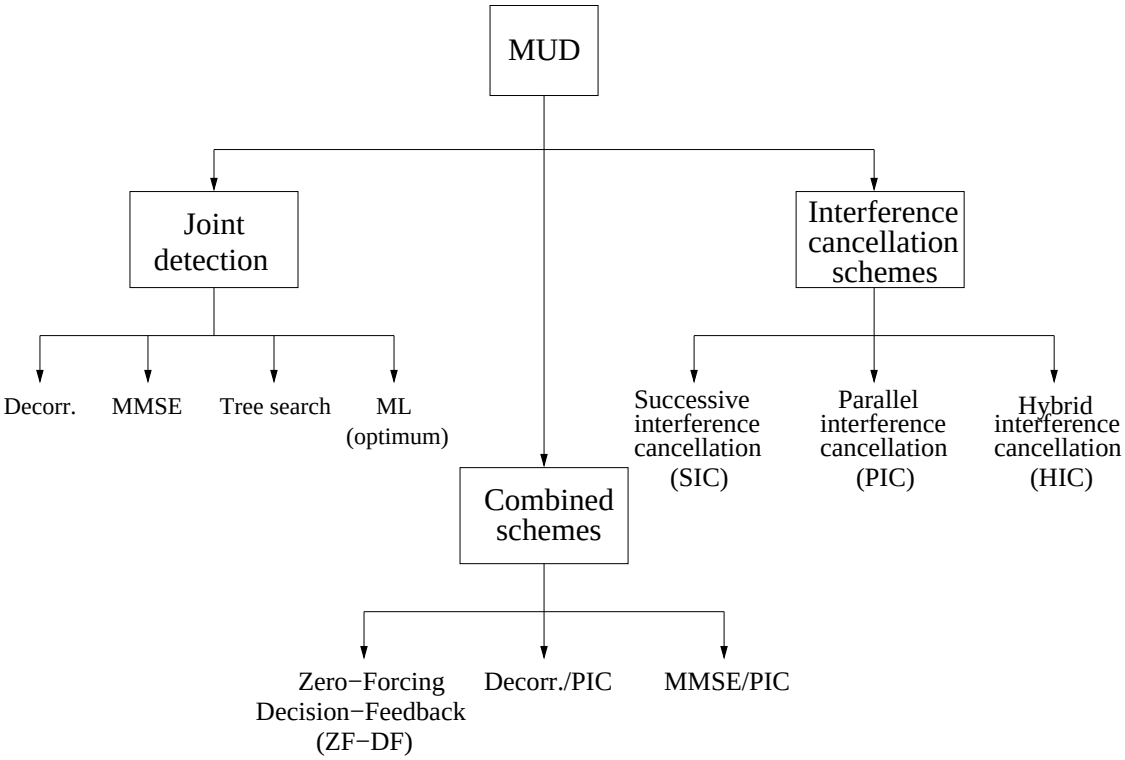

Figure 3.1: *General classification of multiuser detection structures.*

A general overview of MUD is presented in Figure 3.1. This area of research can be divided mainly into three categories: joint detection (JD), interference cancellation (IC) schemes and structures with combined schemes. The first category is usually a bank of conventional detectors followed by filters that performs linear or non-linear transformations. As compared to the conventional detector, joint detection structures are generally computationally more expensive due to complex matrix calculations and inversions. The IC schemes are mainly characterised by the regeneration and subtraction of interference based on the data estimates. Finally, a third category of MUD can be considered as the group of multiuser detectors that combine detection techniques from the two groups of MUD mentioned above.

To simplify the discussion on the multiuser detector structures, we will assume throughout this chapter a conventional synchronous DS-CDMA system model over an AWGN channel (no multipath). Thus equation (2.3) which represents the AWGN channel output can be expressed in a matrix notation as follow

$$\mathbf{r}(t) \quad = \quad \mathbf{CAb}(t) + \mathbf{n}(t) \tag{3.5}$$

where the $N \times U$ matrix of codes $\mathbf{C}$ is given as

$$\mathbf{C} = \begin{bmatrix} c_{1,1} & c_{2,1} & \cdots & c_{U,1} \\ c_{1,2} & c_{2,2} & \cdots & c_{U,2} \\ \vdots & \vdots & \vdots & \vdots \\ c_{1,N} & c_{2,N} & \cdots & c_{U,N} \end{bmatrix}$$

$\mathbf{A}$ is the users' amplitude matrix of dimensions $U \times U$ denoted by

$$\mathbf{A} = \begin{bmatrix} \sqrt{P_1} & 0 & \cdots & 0 \\ 0 & \sqrt{P_2} & \cdots & 0 \\ \vdots & \vdots & \vdots & \vdots \\ 0 & 0 & \cdots & \sqrt{P_U} \end{bmatrix}$$

and the vectors $\mathbf{b}(t) = [b_1(t), b_2(t), \cdots, b_U(t)]^T$ and $\mathbf{n}(t) = [n_1(t), n_2(t), \cdots, n_N(t)]^T$ are the users' data and noise components respectively. The elements of the noise vector are considered independent and identically distributed (i.i.d) Gaussian noise samples with zero mean and two-sided power spectral density equals to $\sigma^2 = N_0/2$. During the following sections

we will present some of the established multiuser detector structures. Later on this thesis, the model given in (3.5) will be extended to include multipath propagation.

3.2.1 Joint detection

In this section a concise summary is given of some of the most important JD techniques proposed in the literature. The most widely recognised joint multiuser receiver so far, is the optimal multiuser detector or maximum likelihood (ML) detector introduced by Verdú in 1986 [56]. However, its prohibitive computational complexity which grows exponentially with the number of users, $O(2^U)$, makes of this structure much too complex for practical DS-CDMA systems. Due to the large differences in performance and complexity between the conventional detector and the ML detector, over the last 15 years or so, most of the search has been in finding sub-optimal multiuser detectors that show good performance/complexity tradeoffs. Despite the high complexity of the ML, its performance serves as a benchmark for the comparison with other sub-optimal multiuser detector structures. These sub-optimal structures are divided into two classes, namely linear and non-linear detection methods. A brief description of these detector are given in the following sections.

3.2.1.1 Optimum multiuser detector

The optimum multiuser detector are divided into two detection categories, namely jointly optimum and individually optimum multiuser detector. The jointly optimum multiuser detector is defined as the receiver that selects the most likely transmitted vector of symbols $\mathbf{b}(t)$, given that $\mathbf{r}(t)$ was received. In other words, the minimum probability of sequence error decision is obtained by selecting the vector $\mathbf{b}(t)$ that maximises the joint *a posteriori probability* (APP) $p(\mathbf{b}(t)|\mathbf{r}(t))$. The objective of the individually optimum multiuser detector, on the other hand, is to find the most likely transmitted symbol $b_u(t)$; $u \in \{1, 2, \cdots, U\}$, *i.e* to maximise the APP $p(b_u(t)|\mathbf{r}(t))$. The two decision criteria either for jointly or individually detection are the MAP and the ML criteria. Since the individually optimum multiuser detector achieves the minimum probability of error for each user, we focus our attention to the analysis on only this type of

detector structure. Mathematically, the MAP decision criterion is given as

$$\begin{aligned} \hat{b}_u(t) &= \arg\max_{b\epsilon\{-1,1\}} p(b_u(t)=b|\mathbf{r}(t)) \\ &= \arg\max_{b\epsilon\{-1,1\}} \sum_{\Omega_b} p(\mathbf{b}(t)|\mathbf{r}(t)) \end{aligned} \tag{3.6}$$

where Ω_b is the set of vectors $\mathbf{b}(t)$ with $b_u(t)=b$. Using Bayes' theorem the APP in (3.6) can be expressed as

$$\hat{b}_u(t) = \arg\max_{b\epsilon\{-1,1\}} \sum_{\Omega_b} \frac{p(\mathbf{r}(t)|\mathbf{b}(t))pr(\mathbf{b}(t))}{pr(\mathbf{r}(t))} \tag{3.7}$$

where $p(\mathbf{r}(t)|\mathbf{b}(t))$ is the conditional probability of the observed signal, $\mathbf{r}(t)$, given $b_u(t)$, and $pr(\mathbf{b}(t))$ is the *a priori* probability of $\mathbf{b}(t)$ being transmitted. Since $pr(\mathbf{r}(t))$ is not dependent on $b_u(t)$, it can be neglected from equation (3.7) resulting

$$\hat{b}_u(t) = \arg\max_{b\epsilon\{-1,1\}} \sum_{\Omega_b} p(\mathbf{r}(t)|\mathbf{b}(t))pr(\mathbf{b}(t)). \tag{3.8}$$

The probability function $p(\mathbf{r}(t)|\mathbf{b}(t))$ can be computed as

$$p(\mathbf{r}(t)|\mathbf{b}(t)) = \frac{1}{(2\pi\sigma^2)^{N/2}} \exp\left(-\frac{||\mathbf{r}(t)-\mathbf{x}(t)||^2}{2\sigma^2}\right) \tag{3.9}$$

where

$$||\mathbf{r}(t)-\mathbf{x}(t)||^2 = \sum_{n=1}^{N}(r_{t,n}-x_{t,n})^2. \tag{3.10}$$

with $\mathbf{r}(t) = [r_{t,1}, r_{t,2}, \cdots, r_{t,N}]^T$ as the received vector at time t and $\mathbf{x}(t) = [x_{t,1}, x_{t,2}, \cdots, x_{t,N}]^T$ is the channel input when transmitted $\mathbf{b}(t)$.

In the case of the ML criterion, the *a priori* probability of $\mathbf{b}(t)$, *i.e* $pr(b_u(t))$ for all $u \epsilon \{1, 2, \cdots, U\}$, is not taken into account as it is assumed that all symbols occur with equal probability. Therefore, (3.8) is simplified to

$$\hat{b}_u(t) = \arg\max_{b\epsilon\{-1,1\}} \sum_{\Omega_b} p(\mathbf{r}(t)|\mathbf{b}(t)). \tag{3.11}$$

where Ω_b is defined as before. It is clear, however, that if the *a priori* probabilities are equal,

the result of both the MAP and the ML criteria will be the same.

In other words, the optimum multiuser detector searches through all possible combinations in $\mathbf{b}(t)$ and selects the one closest to the received signal $\mathbf{r}(t)$ based on the Euclidean distance. This Euclidean distance can be calculated either at the chip level (3.10) or at the bit level. The decision rule of the ML multiuser detector with equal *a priori* information and using (3.10) can be then written as

$$\hat{b}_u(t) = \begin{cases} 1 & \text{if } \sum_{\Omega_1} \exp\left(-\frac{||\mathbf{r}(t)-\mathbf{x}(t)||^2}{2\sigma^2}\right) > \sum_{\Omega_{-1}} \exp\left(-\frac{||\mathbf{r}(t)-\mathbf{x}(t)||^2}{2\sigma^2}\right) \\ -1 & \text{otherwise.} \end{cases} \tag{3.12}$$

The resulting complexity of the ML multiuser detector is therefore $O(2^U)$ for a synchronous DS-CDMA system in a AWGN channel.

RBF detector. In [57] it was shown that the individually optimum multiuser detector for a synchronous DS-CDMA system can be implemented with a radial basis function (RBF) network when all of the system parameters are known (number of users and their spreading codes). The RBF network or detector outputs a linear combination of 2^U, with U as the number of users, non-linear weighted basis functions, each of which is applied to the received vector $\mathbf{r}(t)$. The structure of the RBF detector is shown in Figure 3.2. Mathematically, the RBF detector output can be expressed as

$$f(\mathbf{r}(t)) = \sum_{l=1}^{2^U} w_l \phi_l \left(||\mathbf{r}(t) - \mathbf{a}_l(t)||\right)$$

where $\phi_l()$; $l \in \{1, 2, \cdots, 2^U\}$ is a radially symmetric scalar non-linear function (normally a Gaussian kernel function [58]) with $\mathbf{a}_l(t)$ and w_l as the *l*th centre and *l*th weight that optimise some performance criterion. The vector norm $||.||$ is the Euclidean distance between the vectors $\mathbf{r}(t)$ and $\mathbf{a}_l(t)$. The vector of centres $\{\mathbf{a}_l(t)\}$; $l \in \{1, 2, \cdots, 2^U\}$ represents the noise free received vectors for all possible combinations of the data vector $\mathbf{b}(t)$. The decision rule for the RBF detector is then given as

$$\hat{b}_u(t) = \text{sgn}\left[\sum_{l=1}^{2^U} w_l \exp\left(-\frac{||\mathbf{r}(t) - \mathbf{a}_l(t)||^2}{2\sigma^2}\right)\right] \tag{3.13}$$

where w_l is substituted by the value of $b_u(t)$ (either $+1$ or -1) associated with the *l*th centre $\mathbf{a}_l(t)$.

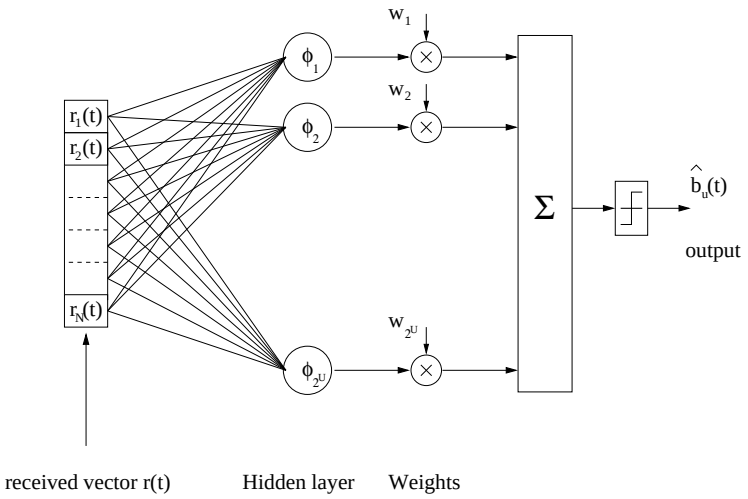

Figure 3.2: *Chip rate structure of the radial basis function detector.*

The optimum RBF multiuser detector can also be applied when the received signal are pre-processed by the conventional detector, *i.e* detection at the bit rate. Without pre-processing the received signal, the noise components are neither correlated with the signal nor other noise components, therefore, the Euclidean distance is the optimum measure for the chip rate RBF detector. However, due to pre-processing the noise components becomes correlated [46, 58] and then the Euclidean distance measure non-optimum. Hence, the bit rate RBF detector, using the Mahalanobis distance [59] rather than Euclidean distance, will reflect the correlated nature of the noise components. Thus,

$$\hat{b}_u(t) \quad = \quad \text{sgn}\left[\sum_{l=1}^{2^U} w_l \exp\left(-\frac{(\mathbf{r}(t)-\mathbf{a}_l(t))^T\mathbf{V}^{-1}(\mathbf{r}(t)-\mathbf{a}_l(t))}{2}\right)\right] \tag{3.14}$$

where

$$V \quad = \quad E[(\mathbf{r}(t)-\mathbf{a}_l(t))(\mathbf{r}(t)-\mathbf{a}_l(t))^T].$$

Similarly to the ML detector, the complexity of the RBF detector (either at the chip or bit rate) is $O(2^U)$ for an AWGN channel.

3.2.1.2 Linear multiuser detectors

Due to the complexity of the optimum multiuser detector, a number of reduced complexity detectors based on linear techniques have been proposed. This group of detectors mitigate interferences by applying a linear transformation to the output vector of the conventional DS-CDMA detector. In this section we review the two most common linear detectors, the decorrelator and minimum mean squared error (MMSE) detectors. First, the decorrelator detector [60–64] (which is analogous to the zero-forcing equaliser [46]) is a transformation which applies the inverse of the correlation matrix leaving the received signal without interference. However, a drawback of this detector is that it causes noise enhancement. The second detector is the MMSE detector [63–65] which takes into account the background noise and utilises knowledge of the received signal powers.

To represent the output vector of the conventional detector (bank of U matched filters), equation (3.5) is multiplied by $\mathbf{C}^T$ resulting

$$\mathbf{y}(t) = \mathbf{R}\mathbf{A}\mathbf{b}(t) + \mathbf{z}(t) \tag{3.15}$$

where $\mathbf{R}$ is the correlation matrix, and $\mathbf{z}(t)$ is the vector with the correlated noise created by the bank of matched filters.

Decorrelator detector. By inspection of (3.15) and considering that the correlation matrix $\mathbf{R}$ is positive definite (*i.e* invertible), it is clear that by multiplying both sides of (3.15) with the inverse of $\mathbf{R}$ the users signals in the system can be decoupled. Thus, the soft estimate of the decorrelator detector is

$$\begin{aligned} \mathbf{R}^{-1}\mathbf{y}(t) &= \mathbf{A}\mathbf{b}(t) + \mathbf{R}^{-1}\mathbf{z}(t) \\ \hat{\mathbf{b}}(\mathbf{t}) &= \mathbf{A}\mathbf{b}(t) + \mathbf{z}^{dec}(t) \end{aligned} \tag{3.16}$$

where now $\mathbf{z}^{dec}(t)$ is a noise vector with zero mean and covariance matrix $\mathbf{V}^{dec} = \sigma^2\mathbf{R}^{-1}$, and $\hat{\mathbf{b}}(t) = [\hat{b}_1(t), \hat{b}_2(t), \cdots, \hat{b}_U(t)]^T$. Reviewing (3.16), we can see that the user u (uth component of $\hat{\mathbf{b}}(t)$) does not contain interference from other users in the system, therefore, the MAI is completely eliminated by the decorrelator detector. Substantial performance gain is provided by this detector over the conventional detector. Another significant feature is that it does not need to estimate the received users amplitudes. Moreover, since the level power of the users are independent from each other, the decorrelator detector yields the optimum near-far resistance

performance metric. Furthermore, its complexity, which is linear with the number of users $O(U)$ (excluding the cost of re-computation of $\mathbf{R}^{-1}$), is significantly lower that the optimum multiuser detector.

On the other hand, there are two significant disadvantages of this detector. Firstly, it causes noise enhancement which can be observed from the term $\mathbf{R}^{-1}\mathbf{z}(t)$ in (3.16). It has been shown in [66] that the noise power associated with the noise term $\mathbf{R}^{-1}\mathbf{z}(t)$ is always greater or equal to the noise term at the output of the conventional detector. Therefore, it can occur that if the MAI is weak, the conventional detector can outperform the decorrelator. This is simply because the MAI terms is smaller than the noise enhanced term in (3.16). The second and more significant drawback, is the need to invert the matrix $\mathbf{R}$ (usually a difficult operation in real time). For synchronous systems, where detection can be performed at a bit basis, the problem is somewhat simplified to invert a $U \times U$ matrix. However, for asynchronous systems, the dimensions of this matrix increase with the message length which could be very large. Consequently, the computation required is substantially increased. This situation can even get worse in multipath channels where the paths are treated as separate users. Several suboptimal approaches to implementing the decorrelator detector have already been suggested [67–69].

Minimum mean squared error (MMSE) detector. Similar to the decorrelator detector, the MMSE detector applies a linear transformation to the output of the conventional detector (3.15). However, as distinct from the decorrelator, the MMSE detector takes into account the background noise and utilises knowledge of the received signal power. The MMSE detector attempts to strike a balance between the residual interference and the noise enhancement. This transformation is chosen to minimise the mean-square error between its output and the data, *i.e*

$$\min_{\mathbf{T}\epsilon R^{U\times U}} E[||\mathbf{b}(t) - \mathbf{T}\mathbf{y}(t)||^2]$$

where $\mathbf{T}$ is the $U \times U$ transformation matrix. Thus, the soft estimate vector of the MMSE detector is given as [70]

$$\hat{\mathbf{b}}(t) \quad = \quad (\mathbf{R} + \sigma^2\mathbf{A}^{-2})^{-1}\mathbf{y}(t). \tag{3.17}$$

The MMSE detector minimises the squared error in the presence of channel noise, and becomes the decorrelator detector when no noise is present. Performance is very similar to the decorrelator solution when the SNR is relatively high ($\sigma^2 \rightarrow 0$), but MMSE is better at low SNR's. On

the other hand, if the MAI is small as compared with the noise, the MMSE detector approaches the conventional detector. The analogy to the MMSE detector is the MMSE linear equaliser [46], used to combat ISI for a single-user channel.

Some of the important drawbacks of this detector are that it requires an estimate of the received amplitudes and that its performance depends on the power of the interfering users (there is some loss in resistance to the near-far problem). In terms of complexity, the MMSE detector faces, like the decorrelator detector, the problem of implementing matrix inversion. Therefore, most of the sub-optimal approaches to implementing the decorrelator detector are applicable to the MMSE detector as well.

From another perspective, the DS-CDMA receiver structure can alternatively be confined to being a finite impulse response (FIR) filter. Therefore, the MMSE detector can also be implemented with a single-user FIR filter without the need of pre-processing the received signal with the conventional detector. Considering the received signal as given in (3.5), the Wiener filter theory [71, 72] states that the optimal set of weights for a FIR $\mathbf{w}_u$ is given by

$$\mathbf{w}_u = \mathbf{\Phi}_{rr}^{-1} \boldsymbol{\phi}_{rb}^{u} \tag{3.18}$$

where the $N \times N$ matrix $\mathbf{\Phi}_{rr}$ is the autocorrelation matrix of the input signal $\mathbf{r}(t)$. Assuming that the data from different users are independent, *i.e* $E[b_k(t)b_u(t)] = 0$ with $k \neq u$ and $k, u \, \epsilon \, \{1, 2, \cdots, U\}$, then it can be shown [73] that

$$\begin{aligned} \mathbf{\Phi}_{rr} &= E[\mathbf{r}(t)\mathbf{r}^T(t)] \\ &= \mathbf{C}\mathbf{P}\mathbf{C}^T + \sigma^2\mathbf{I} \end{aligned} \tag{3.19}$$

where $\mathbf{C}$ is the $N \times U$ matrix with the codes, $\mathbf{P} = \mathbf{A}^2$ is a $U \times U$ diagonal matrix with $\mathbf{A}$ as defined in (3.5), and $\mathbf{I}$ is the identity matrix with dimensions $N \times N$. The $N \times 1$ vector $\boldsymbol{\phi}_{rb}$ represents the desired response, *i.e* $\boldsymbol{\phi}_{rb}^{u} = P_u \mathbf{c}_u(t)$ for the *u*th user. The soft estimate of the Wiener detector output for the *u*th user is then given as

$$\begin{aligned} \hat{b}_u(t) &= \mathbf{w}_u^T \mathbf{r}(t) \\ &= P_u \mathbf{c}_u(t)^T (\mathbf{C}\mathbf{P}\mathbf{C}^T + \sigma^2\mathbf{I})^{-1} \mathbf{r}(t). \end{aligned} \tag{3.20}$$

3.2.1.3 Non-linear multiuser receivers

Linear multiuser detection techniques generally overcome the problem of complexity, however, the presence of high levels of MAI and/or ISI generates poor performance in the receiver. This degradation is mainly caused by the fact that in such scenarios the desired signals are no longer linearly separable [74]. Therefore, non-linear detection approaches have to be considered. Recently, a new family of detectors, based on a tree search technique, have been studied extensively. In general, tree search based sub-optimal detectors provide with the next best performance to the optimum multiuser detector but with a significant reduction in complexity. A number of this type of detectors have been proposed for improving performance. These include the following detector structures:

Pre-selection maximum likelihood (PSML) multiuser detector. This approach is a reduced-complexity ML detector that uses two distinct stages in approximating the ML solution [75]. Figure 3.3 shows the structure of the PSML detector. As distinct from the optimum multiuser

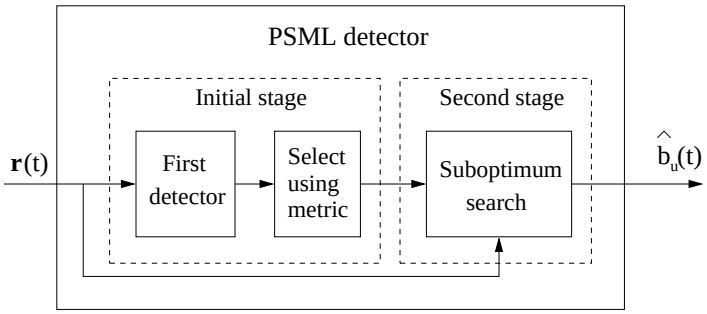

Figure 3.3: *PSML multiuser detector structure.*

detector, the PSML detector uses an initial stage to assess the received signal in order to confine the search to a smaller number of possible combinations. The function of the initial stage is to generate soft estimates of the interfering users which are used to provide with a measure of how likely they can be correctly detected. The initial detector, which provides with the soft estimates of the users' symbols, is implemented by a linear detection technique, *i.e* the conventional detector, decorrelator, or MMSE detectors. Based on these estimates, a metric of how likely each symbol can be detected correctly is obtained by using the magnitude of the likelihood ratio $|LLR|$. This metric is then used to establish an order of precedence between the users. After the initial stage, a hard decision is made on those users' symbols with the highest metrics (more likely to be correct). On the other hand, those symbols with lower $|LLR|$

values are kept as soft estimates for the second stage of the detector. The second stage of the detector is the optimum multiuser detector with reduced complexity as the number of possible combinations have been reduced by the hard decision made by the initial stage. It was shown in [75] that the PSML detector approximated the ML solution with significant less complexity at the expense of small degradation performance.

M-Algorithm and T-Algorithm detectors. Like the VA, the M or T algorithms [76] are breadth-first trellis search algorithms that differ only in the criterion used to discard paths. At a particular trellis depth, the VA discards all but the minimum metric path to each trellis stage. The M-algorithm instead maintains the M paths of minimum metrics. Then a search through all M remaining paths is applied to yield the soft outputs of the M-algorithm detector. In the case of the T-algorithm, the criterion to discard paths is different. It first finds the overall best path of minimum metric and then rejects all paths whose metrics exceed this minimum metric by more than a threshold T. The number of paths kept by the T-algorithm is variable. A derivative from this two techniques can be found in the hybrid MT-algorithm detector [76]. As the number of surviving paths may occasionally be very large, the hybrid MT-algorithm is normally a good compromise as it ensures that the number of paths is kept within a maximum threshold that maintains the complexity at a manageable level.

Greedy detector. One of the most recent multiuser detector algorithm is the greedy detector (GD) which was proposed in [77]. This algorithm utilises the coefficients of the user's symbols in the maximum likelihood metric as weights to indicate the order in which symbols can be estimated. Based on theses coefficients, this detector forms a modified trellis tree with complexity much lower than that needed for the optimum multiuser detector. Significant performance gain is achieved by the GD with a complexity only of the order of $U^2 \log U$ as compared to the 2^U of the optimum multiuser detector.

3.2.2 Interference cancellation schemes

A second way to perform MUD is using an interference cancellation scheme. This category of detectors can be classified mainly into three sub-categories: parallel interference cancellation (PIC), successive interference cancellation (SIC) and hybrid interference cancellation (HIC). The basic principle of these schemes is to estimate at the receiver the MAI generated by each user in order to subtract it.

PIC detector. If the power and codes of all interfering users are known, the PIC detector [64, 78] yields an estimate of all MAI for each user and then subtracts them in a parallel scheme. Figure 3.4 shows one stage of a PIC detector for U users. The initial bit estimates, $\hat{b}_u(t)$ for $u \in \{1, 2, \cdots, U\}$, are provided by the output of a bank of conventional detectors. These estimates are then re-spreaded and added to regenerate the MAI estimates for each user. As shown in

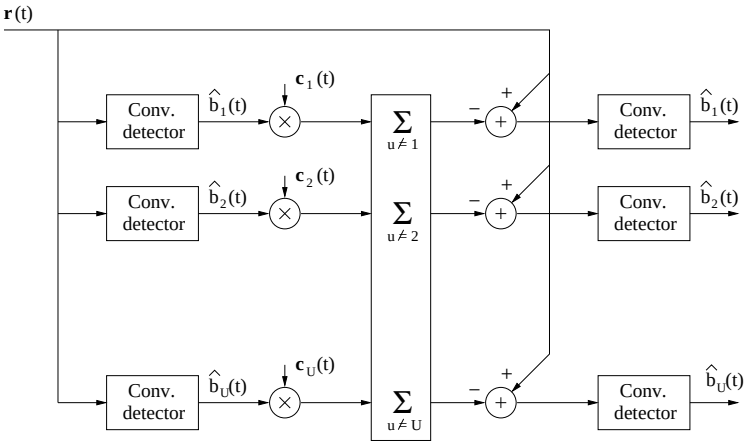

Figure 3.4: *First stage of a PIC detector for U users.*

Figure 3.4, interference cancellation is then performed on the received signal to provide the input to a second bank of conventional detectors. Thus, a new set of soft estimates are yielded by the second bank of conventional detectors in this first stage of parallel cancellation. The process can be repeated for multiple stages by taking the estimates at the output of one stage as the input of a new stage of parallel cancellation.

SIC detector. As distinct from PIC detector, the SIC detector [61, 64] takes a serial approach to cancelling interference as shown in Figure 3.5. The first operation in the SIC detector consists of sorting the users' signals out in a descending order according to theirs powers (not shown) which are estimated from the output of the conventional detector. The first stage in this detector is to regenerate the transmitted signal of the strongest user (in terms of powers and assuming knowledge of the spreading code). This regenerated signal provides an estimate of the MAI caused by the strongest user, $b_1(t)$, which is then subtracted from the total received signal $\mathbf{r}(t)$, yielding a partially cleaned version of the received signal $\mathbf{r}_1(t)$. If the user estimate is accurate, the remaining users see less MAI in the next stages. Thus, this new version of the received signal can be used to detect the next strongest user in the system. This process is repeated until all users are detected. Note that in each stage the estimate of the users are obtained by

making a decision at the output of the conventional detector. The benefit of sorting the signals out in a descending order is because the strongest users can give the most accurate estimate and consequently the removal of this signal will provide the most benefit to the remaining users.

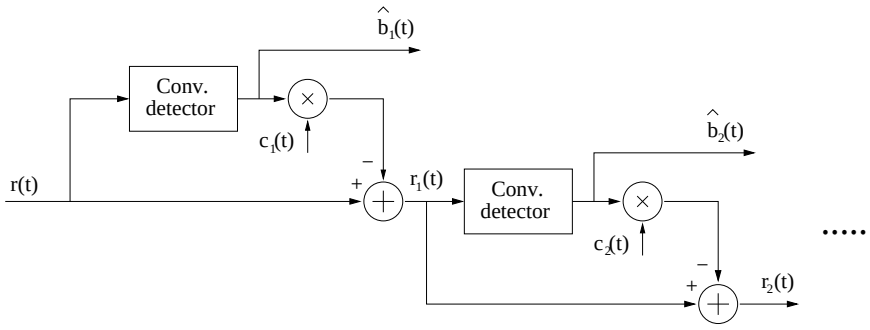

Figure 3.5: *First stage of a SIC detector.*

The SIC detector can provide a significant improvement over the conventional detector. However, its performance is poor under equal power conditions since a wrong order of users results in drastic performance loss. Furthermore, for every stage of cancellation a delay of one bit is required, therefore, the scheme must operate is such a way that the delays can be tolerated. A comparison between the PIC and SIC detectors can be found in [79]. Also for a more detailed discussion in the advantages/disadvantages of these detectors, the reader is referred to [61, 64, 67–69, 79].

Hybrid detector. This group of subtractive interference cancellation schemes combine certain positive features of the SIC and PIC detector into a hybrid scheme. The main advantage of these schemes is that at the expense of some performance degradation, they offer significant delay and hardware reduction over the conventional SIC and PIC. Some examples of this type of structures are the schemes proposed in [61, 64, 67–69, 79].

3.2.3 Combined schemes

A third group of multiuser detectors embraces those schemes that combine a linear transformation with subtractive cancellation schemes. Examples of this detection schemes are: the zero-forcing decision-feedback (ZF-DF) detector, decorrelator/PIC, MMSE/PIC , etc, [61, 64, 69, 78–81] .

The ZF-DF detector is analogous to the decision-feedback equalisers in ISI channels [46]. That

is, a linear transformation is performed at an initial stage followed by a form of SIC detection. Using Cholesky decomposition, the linear operation is able to partially decorrelates the users without enhancing the noise. The SIC operates by making decision and subtracting the interference in a descending order of the signal strength. It is clear that the success of any cancellation scheme relies on the initial data estimates. If these estimates are not reliable, error propagation will occur and consequently the system will collapse. Therefore, as compared to the conventional SIC detector, the ZF-DF provides with a more powerful SIC operation since a more reliable initial stage is considered. Ranking the users prior to filtering is important so that the most reliable user is the first to be cancelled.

The decorrelator/PIC is another approach to combine detection structures. This form of detector is a multistage PIC scheme that uses a decorrelator at the first stage in order to generate the initial decision statistics. This type of receiver has shown to outperform the conventional decorrelator in a number of situation of practical interest. However, the performance of these detection schemes depends heavily on the initial data estimates, other combined schemes with a more powerful initial stage may provide better improvements, for example, MMSE/PIC detector.

3.2.4 Discussion

Due to the poor BER performance of the conventional detector and the prohibitive complexity of the optimum multiuser detector for DS-CDMA systems, a significant number of sub-optimal multiuser receiver have been proposed to provide with better performance/complexity tradeoffs [64, 65, 70, 82]. Firstly, multiuser receivers based on linear techniques were proposed such as the decorrelator and MMSE detectors [63]. A second multiuser receiver approach is that based on an interference cancellation scheme [61]. This type of structures are for example, the PIC and SIC detectors. A comparison in BER performance and computationally complexity of this type of receivers can be found in [79]. Hybrid or combined structures between linear detection techniques and interference cancellation schemes normally provides an enhanced receiver performance. This improvement is obtained from the combination of certain positive features from two or more of these detection techniques. All of these receivers give significant improvement over the conventional detector and under certain conditions they can even give a performance close to that of the optimum multiuser detector. Recently, multiuser detector structures based on a tree-search have been proposed in the literature [75–77]. In general, these are low-complexity

sub-optimal multiuser detector structures which provide with good performance, comparable to the optimum detector but with a much lower complexity. In this thesis, we will investigate those MUD techniques that can be implemented together with the turbo multiuser detection principle. In next section the turbo multiuser detection principle will be defined.

3.3 Turbo multiuser detection principle

In early years, the design of a multiuser receiver had only considered FEC coding has an additional gain but not until recently has this become as part of the multiuser receiver structure [83]. Similarly to the optimum detector [70], the optimal multiuser receiver can be formulated for a DS-CDMA system with FEC coding as shown in [84]. However, the even higher complexity of this receiver $O(2^{U\nu})$ which depends not only exponentially with the number of users but also with the constraint length of the encoder, makes this receiver too complex for implementation. It points to the use of sub-optimal multiuser approaches with FEC coding to attempt to attain high performance levels in the system.

First, the multiuser receiver with FEC coding can be partitioned to mitigate complexity, as proposed in [83], but where coding is considered by generating suitable input metrics for the decoding function. This will be discussed in more detail in section 3.3.2. As noted earlier, turbo codes is now widely recognised as a very general and powerful concept in communication theory, with applications that go beyond the practical decoding of these near channel capacity codes. The turbo principle is used to describe the iterative exchange of soft information between different blocks in a communication receiver in order to improve the overall system performance. There are two main type of codes that have been developed, parallel turbo codes [30] and serial turbo codes [39]. Reviewing the turbo decoding techniques it can be established that the serial turbo coding structure is easy to adapt to the multiuser detection area. In order to introduce the turbo MUD principle we will briefly overview the serial turbo encoder and decoder in next section. This will lead us to introduce in section 3.3.2 the turbo multiuser detection principle.

3.3.1 Serial turbo codes

A serial turbo code is the serial concatenation of two convolutional codes, referred to as the inner and outer codes, which are separated by a random interleaver. The output of the outer

encoder is fed to the interleaver and the output of the interleaver is input to the inner encoder. The output of the inner encoder is then transmitted over the communication channel. The product of the rates of the two convolutional encoders is the overall rate of the serial encoder. Figure 3.6 shows the structure of this encoder.

Figure 3.6: *Serial turbo encoder structure.*

Similar to the decoding of parallel turbo codes (see section 2.5.2.3), the serial turbo decoding structure utilises concepts of soft-input/soft-output (SISO) decoding and random interleaving. The important difference is that each individual FEC decoder, which is implemented by a SISO MAP decoder [85], computes the LLRs not only of the data bits but also for the coded bits which are used as *a priori* information for the next decoding component in the scheme.

The serial turbo decoding structure receives the channel output bits and first decodes them with the inner SISO MAP decoder as shown in Figure 3.7. The inner SISO MAP decoder also takes as input the *a priori* LLR, $P_a^1[b(t)]$, which are set to zero for the first iteration (on subsequent iterations this is provided by the outer SISO MAP decoder). The inner SISO MAP decoder computes the *extrinsic* LLRs for every coded bit $b(t)$ labelled as $P_e^1[b(t)]$. After deinterleaving, this *extrinsic* LLRs are then taken as *a priori* information to the outer SISO MAP decoder which are denoted by $P_a^2[b(t)]$ in Figure 3.7. Unlike the inner SISO MAP decoder, the outer SISO MAP decoder is provided with only the LLR's of the coded bits. This input is the *a priori* input from the inner SISO MAP decoder. As the outer SISO MAP decoder does not transmit data directly over the channel there is no input metric information available. The outer SISO MAP decoder takes the *a priori* LLR information, $P_a^2[b(t)]$, and uses it to yield both the final hard output on the data bits, $\hat{d}(i)$ (after enough iterations have been performed), as well as soft *a posteriori* probability information for the coded bits, $P_e^2[b(t)]$. After interleaving, the LLRs of the *a posteriori* probabilities for the coded bits from the outer SISO MAP decoder, $P_a^1[b(t)]$, are fed into the inner SISO MAP decoder as the *a priori* information on the next iteration. Once a desired number of iterations have been completed or a desired performance is achieved, the outer SISO MAP decoder outputs the LLRs for the data bits $P_e^2[d(i)]$ and then a hard decision

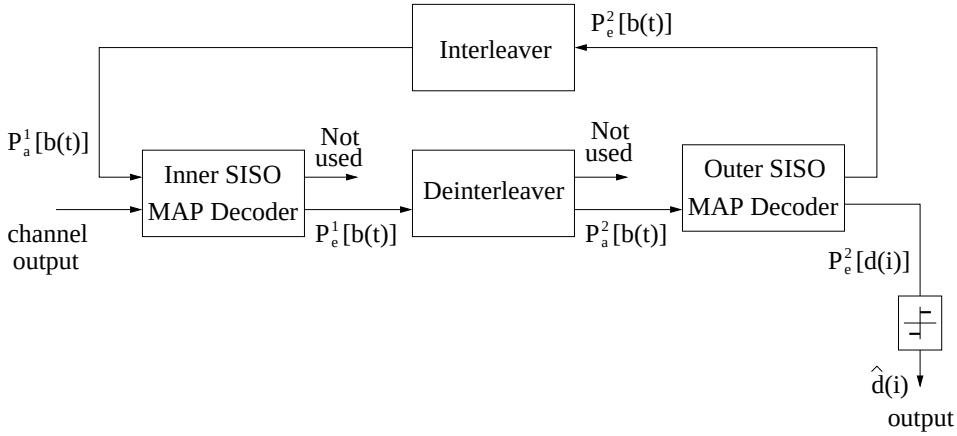

Figure 3.7: *Serial turbo decoder structure.*

is made according to

$$\hat{d}(i) = \begin{cases} 1 & \text{if } P_e^2[d(i)] > 0 \\ 0 & \text{otherwise} \end{cases} \tag{3.21}$$

3.3.2 Turbo principle applied to MUD

In the context of this thesis, MUD refers to the detection of data from multiple users when observed in a non-orthogonal multiplexed wireless channel (DS-CDMA system). The basic idea of MUD is to exploit the cross-correlations among the signals to be detected in order to improve the data detection process. On the other hand, FEC coding exploits the dependencies among successive channel symbols to improve the detection of a single stream of data symbols. Currently many of the wireless systems, such as the third generation systems, involve both FEC coding and non-orthogonal multiplexed channels. A typical configuration of this is a convolutional encoder followed by an interleaver and a DS-CDMA modulator for the channel symbols. In the previous section, we discussed the use of convolutional codes in the serial turbo code structure. However, a number of channels can also be represented by a linear sequential operation rather than convolutional codes. Particularly, it can be viewed that by replacing the inner code of the serial turbo codes with a DS-CDMA system results in an encoder structure that can perform well using the iterative principle. Figure 3.8 shows such an encoder structure.

The decoding process for this concatenation is also similar to the serial turbo decoder as is

Figure 3.8: *Channel coding concatenation with a DS-CDMA channel.*

shown in Figure 3.9. First the DS-CDMA signals are despread (using the conventional detector or a multiuser detector) and deinterleaved to provide the input to the channel decoder. In a similar way to the serial turbo decoder, the FEC decoder generates a final output decision after a desired number of iterations. It also outputs *extrinsic* soft *a posteriori* information which is interleaved and input to the multiuser detector as *a priori* information on the next iteration. The process repeats for the desired number of iterations, after which the FEC decoder outputs a hard decision of the uncoded data. Similar to turbo codes, the turbo multiuser detection prin-

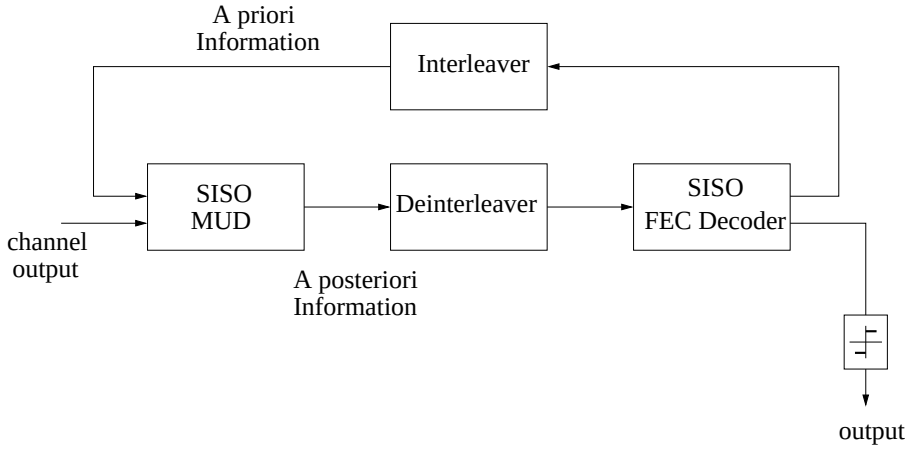

Figure 3.9: *Iterative detector/decoder structure (turbo multiuser detection principle).*

ciple refers to joint the channel coding (outer code) and multiuser detection (inner code) using an iterative exchange of soft information [86–93]. Thus we have established the application of the turbo principle into the area of multiuser detection. Like turbo decoding, the iterative approach to joint multiuser detection and channel coding have shown considerable promise for achieving performance close to the Shannon limit. The main purpose in this thesis is then to investigate the application of the turbo multiuser detection principle on some of the multiuser receiver structures already established. This approach taken aims to look for an advance multiuser receiver that can achieve superior performance while requiring structures with reasonable complexity.

3.3.3 Iterative multiuser receiver

As mentioned earlier, an overall optimal detector/decoder uses an optimal mapping from the received signals to the original data symbols (multiuser detection and FEC coding jointly) [84]. However, this results in a prohibitive complexity, $O(2^{U\nu})$, which rises exponential in the product of the the number of users U and the constraint length of the convolutional code ν. In [83] a sub-optimal scheme that perform symbol detection and decoding separately is proposed, see also Figure 3.10. The complexity of this partitioned structure is reduced to $O(2^{U}) + O(2^{\nu})$. Both multiuser detection and channel decoding typically involve very complex algorithms, and so complexity issues often dominate the study of these problems. In particular this complexity can be mitigated by applying the turbo multiuser detection principle as we will show later in this thesis.

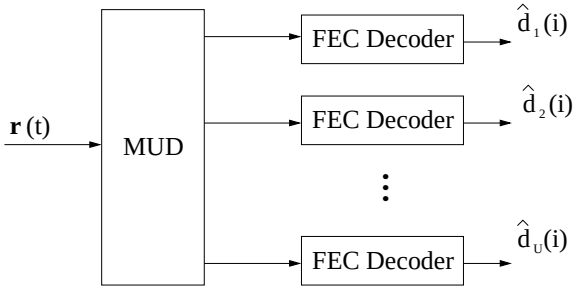

Figure 3.10: *Partitioned multiuser receiver structure.*

In [88] an iterative multiuser receiver for DS-CDMA system with FEC coding is presented. This receiver is derived from the serial concatenation of a metric generator (MAP criterion) for the joint received signal and a block of U single-user turbo decoders. Figure 3.11 shows this iterative multiuser receiver system. The receiver takes the conventional detector output and generates the conditional channel probabilities $p(\mathbf{r}(t)|\mathbf{b}(t))$ which are multivariate Gaussian conditional probabilities [46]. Then the metric generator calculates the marginal probabilities $p(\mathbf{r}(t)|b_u(t))$ for the *u*th decoder. The FEC decoders generate the *a posteriori* coded bit probabilities, $p(b_u(t)|\mathbf{r}(t))$, which are then used as *a priori* information for the metric generator on the next iteration. After a number of desired iterations a hard decision of the *u*th user data bit at time t, $d_u(t)$, is output by the single-user FEC decoder. The implementation of the MAP criterion for the metric generator provides with the optimum multiuser detector performance while turbo codes are the most powerful FEC coding scheme proposed so far. Therefore, the use of this iterative scheme will achieve the lowest BER performance for a partitioned multiuser

receiver. Although the complexity of this structure is still too high for a practical implementation, especially for a large number of users, it is useful for understanding the turbo multiuser detection principle but also as a benchmark in the receiver performance/complexity tradeoff. In [88] is shown that this scheme approaches single-user performance for large system loads.

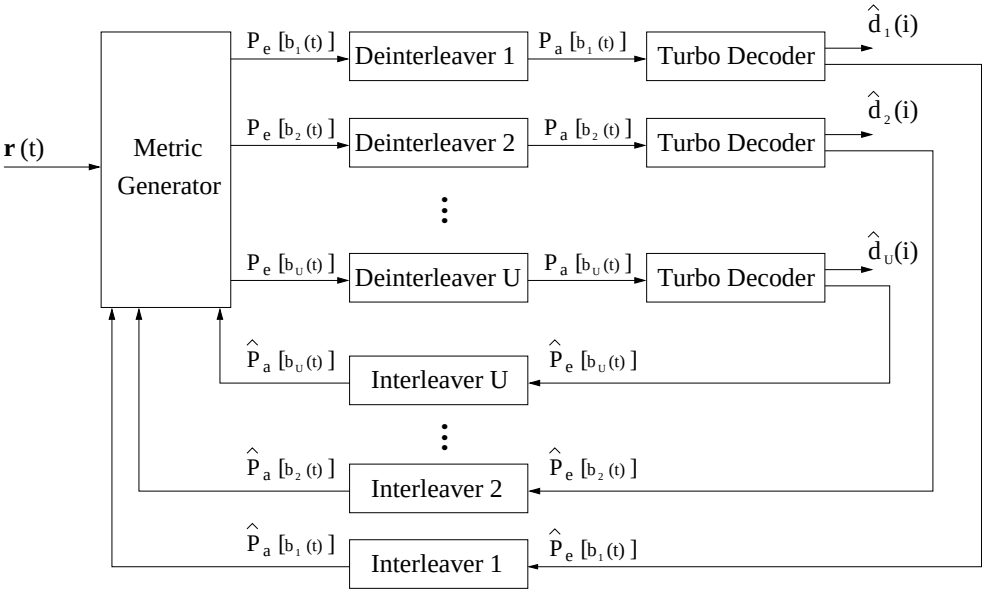

Figure 3.11: *Iterative multiuser receiver.*

Like turbo decoding, an essential issue in an iterative scheme is the way of exchanging information between the detection stage and the block of FEC decoders. Given the received signal, $\mathbf{r}(t)$ see (3.5), the metric generator detector outputs single-user *a posteriori* information (LLRs) which are then supplied, after deinterleaving, as *a priori* information to the FEC decoders, $P_a[b_u(t)]$; $u \in \{1, 2, \cdots, U\}$. Equally, every single-user FEC decoder provides with *a posteriori* information, $\hat{P}_e[b_u(t)]$, which are used after interleaving as *a priori* information, $\hat{P}_a[b_u(t)]$, into the metric generator on each iteration. Similar to turbo codes the main idea is to exchange soft information (across the users and across the FEC coded bits) by using a SISO multiuser detector and a block of single-user FEC decoders.

3.3.3.1 Metric generator

The MAP decision rule for the metric generator sets

$$\hat{\mathbf{b}}(t) = \arg\max_{\mathbf{b}(t)} p(\mathbf{r}(t)|\mathbf{b}(t))pr(\mathbf{b}(t)). \tag{3.22}$$

However, the metric generator requires to generate single-user decoder metrics for the block of FEC decoders. This soft information can be obtained by computing the LLR of the conditional probabilities given as

$$P_e[b_u(t)] = ln\left(\frac{p(\mathbf{r}(t)|b_u(t)=+1)}{p(\mathbf{r}(t)|b_u(t)=-1)}\right). \tag{3.23}$$

Using Bayes theorem the metric generator output (LLR) for user u as shown in [88] is given by the conditional probabilities $p(\mathbf{r}(t)|b_u(t)=b)$ with $b\,\epsilon\,\{-1,+1\}$ which are expressed as

$$p(\mathbf{r}(t)|b_u(t)=b) = \sum_{\substack{\mathbf{b}(t)\\(b_u(t)=b)}} p(\mathbf{r}(t)|\mathbf{b}(t)) \prod_{\substack{k=1\\k\neq u}}^{U} pr(b_k(t)) \tag{3.24}$$

where $pr(b_k(t))$ is the *a priori* probability in the metric generator on each iteration and $p(\mathbf{r}(t)|\mathbf{b}(t))$ is the joint likelihood generated by the multivariate Gaussian probability density function as given below

$$p(\mathbf{r}(t)|\mathbf{b}(t)) = \frac{\exp\left(-\frac{||\mathbf{r}(t)-\mathbf{a}_l(t)||^2}{2\sigma^2}\right)}{(2\pi)^{N/2}\sigma^N} \tag{3.25}$$

$\mathbf{a}_l(t)$ is the noise free input vectors for the input data vector **b**(t).

3.3.3.2 Single-user turbo decoder

Using turbo codes as the FEC coding gives a very powerful decoding stage. A description of this decoding structure has already been given in section 2.5.2.3. However, the turbo decoder structure needs to be modified slightly to accept soft input probabilities and produce suitable soft output probabilities for the *a priori* input to the metric generator. Since we are considering exactly the same FEC decoder for each user in the system, the following discussion is based solely on the decoding process for the *u*th user.

The turbo decoder for the *u*th user receives as input and after interleaving the LLR, $P_a[b_u(t)]$,

which is generated by the multiuser detector. This information is used directly into the first SISO MAP decoder as follow

$$\gamma_i(\mathbf{Y}_i, s', s) = P\{S_i = s | S_{i-1} = s'\} \prod_{t=n_c(i-1)+1}^{n_c i} p(\mathbf{r}(t)|b_u(t) = b) \tag{3.26}$$

where

$$p(\mathbf{r}(t)|b_u(t) = b) = \begin{cases} \frac{\exp(P_a[b_u(t)])}{1+\exp(P_a[b_u(t)])} & \text{if } b = 1 \\ \frac{1}{1+\exp(P_a[b_u(t)])} & \text{if } b = -1 \end{cases} \tag{3.27}$$

the noisy received symbols at time i are denoted as $\mathbf{Y}_i = \mathbf{r}(n_c(i-1)+1), \cdots, \mathbf{r}(n_c i)$ and where the product is over all coded bits that produce the transition of the SISO decoder from state s to state s'. In turbo codes the first SISO MAP decoder does not take any *a priori* information on the first iteration of the turbo decoding scheme, *i.e* $P\{S_i = s|S_{i-1} = s'\} = 0.5$. On subsequent iterations of the turbo decoder, the second SISO MAP decoder provides with *a priori* information for the systematic bits in the first SISO MAP decoder. Note that in the multiuser receiver structure there are two iterative processes, one for the FEC coding using turbo codes and a second for the multiuser receiver where the latter corresponds to the turbo multiuser detection principle.

As an output the turbo decoder must produce an update of the LLRs for the coded bits, $\hat{P}_e[b_u(t)]$, as well as for the data bits, $\hat{P}_e[d_u(i)]$. The LLRs of the coded bits after interleaving are used as the *a priori* probabilities in the metric generator output, see (3.24). As described in section 2.5.2.3, all bits that were input to the turbo decoder (not just the data bits) can also be updated with the SISO MAP decoder modules. Then after a desired number of iterations in the turbo decoder, the output LLRs $\hat{P}_e[b_u(t)]$ are calculated using the outputs of both SISO MAP decoders, that is, as the turbo code is punctured, the redundant LLRs codes bit are taken alternately from the first and second SISO MAP decoders according to the punctured scheme described in [30]. The LLRs for the data bits are taken from the output of the second SISO MAP decoder.

3.3.3.3 Iterative scheme in the multiuser receiver

In a similar fashion than turbo codes, the single-user turbo decoder output probabilities, $p(b_u(t) = b|\mathbf{r}(t))$, after interleaving are assigned as the *a priori* probabilities in the metric generator (see (3.24)) on every iteration, *i.e* $p(b_u(t) = b) = p(b_u(t) = b|\mathbf{r}(t))$ for $u \in \{1, 2, \cdots, U\}$ and

$b \in \{1, -1\}$. On the first iteration the *a priori* probabilities in the metric generator are set to $p(b_u(t) = b) = 0.5$, *i.e* all coded bit sequences are assumed to be equiprobable. At the last multiuser iteration at the receiver, the FEC decoders computes the *a posteriori* LLR of the data bits which are used to make a decision on the decoded bit as follow

$$\hat{d}(i) = \begin{cases} 1 & \text{if } \hat{P}_e[d(i)] > 0 \\ 0 & \text{otherwise.} \end{cases} \tag{3.28}$$

3.4 Summary

This chapter has shown that using the conventional detector the capacity of a DS-CDMA system does not increase with the number of users. Therefore, multiuser detection emerges as a very promising area to increase the capacity of a DS-CDMA system. A general review in this area has been presented with a description of various of the existing multiuser detectors. MUD can be divided into joint detection, cancellation schemes and combined schemes. Firstly, joint detection techniques are introduced, starting from the optimum multiuser detector. Due to the complexity of the optimal multiuser detector sub-optimal structures are also discussed which include those with linear (Decorrelator, MMSE) and non-linear (PSML, Greedy, M and T algorithms) detection methods. Multiuser detector structures based on cancellation scheme (PIC and SIC) or combined detection schemes (Decorrelator/PIC, MMSE/PIC) are also addressed. Recently a new type of multiuser receiver based on the turbo decoding principle has been proposed. In this chapter the principles of the serial turbo code encoding and decoding have been explained. It is shown that by replacing the inner code of the serial turbo codes with a DS-CDMA channel results in an encoder structure that can perform well using the iterative principle. The application of the turbo principle can be then established in the area of multiuser detection with the turbo multiuser detection principle. An overview of this principle together with its fundamentals are discussed. This class of receivers exploits the iterative technique of turbo codes to exchange soft information between the detection process and the FEC decoders.

Chapter 4
An Iterative Multiuser Receiver in a AWGN Channel

In chapter 3 the turbo multiuser detection principle is introduced. Due to the prohibitive complexity of an overall multiuser receiver (detection/decoding), the turbo multiuser detection principle emerges as a very promising approach to mitigate this issue of complexity. As stated earlier in this thesis, we are interested in developing a multiuser receiver based on the turbo principle.

In the downlink of a DS-CDMA system the signals received at each mobile terminal are synchronous due to the fact that the base station broadcasts to all users simultaneously. When orthogonal codes arrive at the mobile terminal the conventional detector achieves the single-user performance under these ideal conditions, *i.e* no multiple access interference and no multipath. However, time dispersive channels are common in wireless mobile channels which destroys the orthogonal property in the system. Under this scenario pseudo-random spreading codes can be a better choice to model the channel conditions as they provide an average interference level which is noise like when the number of users is large.

Therefore, in this chapter we investigate the downlink of DS-CDMA system with FEC coding that employs pseudo-random spreading codes in an AWGN channel. The description of this channel model is presented in the next section. Following the next section (4.2) we investigate the implementation of linear detection techniques in order to provide a sensible detection stage that can incorporate the turbo multiuser detection principle in its structure. Based on this search, we propose a new iterative multiuser receiver. This new structure has not only the benefit of reducing complexity at the receiver but also exploits the iterative principle to improve the receiver performance in a similar way to turbo codes.

4.1 System model

We model the downlink of a discrete-time DS-CDMA communication system with FEC coding for U active users. It is assumed both bit and chip synchronous with the samples taken at the chip rate. Figure 4.1 depicts the system model. The *u*th user transmits data blocks of i.i.d[1] binary data, $\{d_u(i)\}$; $i \in \{1, 2, \cdots, L\}$, $u \in \{1, 2, \cdots, U\}$, where $d_u(i)$ will be referred to as the *i*th data bit of user u. To reduce the complexity in the receiver, the FEC coding considered here is limited to one convolutional code. To mitigate the effect of error bursts at the input of every FEC decoder, the sequence of coded bits at the output of each encoder is interleaved using a distinct random pattern. The random interleaver is a permutation that maps the sequence of L/R_0 FEC coded bits into the same sequence of data but with a new order, *i.e.*, for each t there is a corresponding random integer $\pi(t)$ without repetition ($t \rightarrow \pi(t)$) [32, 33, 35, 42]. Every interleaver has a corresponding deinterleaver that acts on the interleaved sequence of FEC coded bits and puts them back into its original order. On the other hand, the spreading codes are reselected independently in a pseudo-random fashion on a bit by bit basis (channel coded bits) for every user. This is statistically equivalent to using random sequences. It is

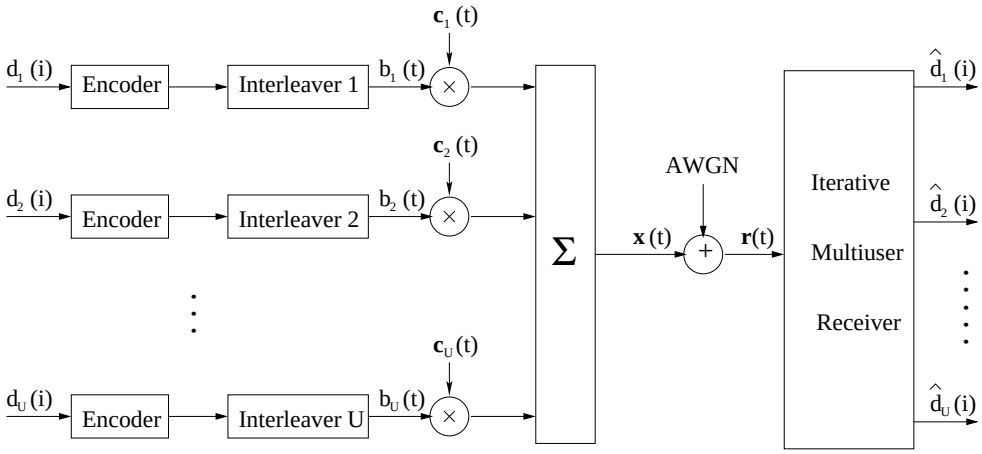

Figure 4.1: *DS-CDMA system model with FEC coding in a AWGN channel.*

assumed that all the users transmit with equal and constant power. At time t the output of the channel is given exactly as denoted in (3.5).

[1] independent and identically distributed

4.2 Iterative multiuser receiver

In [84] an optimal iterative multiuser detector for synchronous coded CDMA, based on iterative techniques for cross-entropy minimisation is introduced. A practical suboptimal implementation is also presented. However, the computational complexity of this practical structure is $O(2^U + 2^\nu)$ which is still prohibitive for systems with large number of users. In section 3.3.3, a similar structure is described but where the complexity is even higher due to the utilisation of turbo codes as the FEC coding. Therefore, the purpose of this section is to develop a low complexity iterative multiuser receiver based on a partitioned structure for a FEC coded DS-CDMA system over an AWGN channel as shown in Figure 4.2.

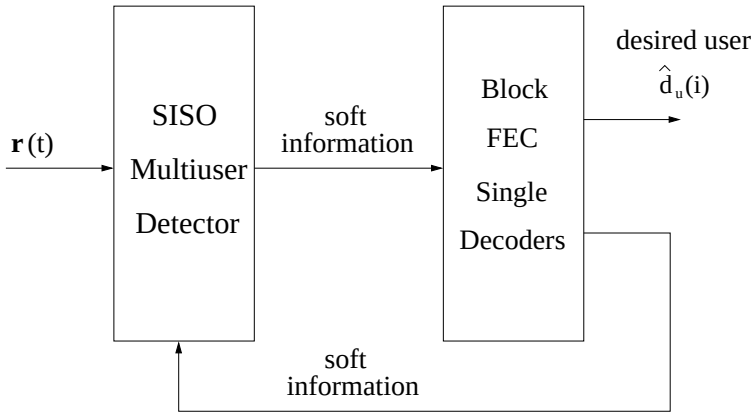

Figure 4.2: *Iterative multiuser receiver structure.*

4.2.1 Multiuser detector

It is clear that when the RBF detector is applied in the partitioned multiuser detector/decoder structure, the complexity in the receiver for medium to large number of users is mainly determined by the detection stage, $O(2^U)$. Therefore, a number of reduced complexity multiuser detectors based on linear techniques have been proposed. The conventional detector is the optimal detector only in an AWGN channel but has a very poor performance when the level of MAI from other users in the system is high. On the other hand, it is well known that the Wiener detector gives better performance than any other linear detection in isolation and that combined with a single stage of parallel interference cancellation (PIC) scheme can give even better performance that either technique on is own [94]. Therefore, in this chapter we investigate the structure of a multiuser receiver based on two detection schemes, Wiener detector and Wiener

detector followed by a single stage of a PIC scheme.

4.2.1.1 Wiener detector

Figure 4.3 shows an iterative multiuser receiver using the Wiener detector at the front end of the receiver. The Wiener detector is an N tap FIR filter, where N is the processing gain, with the weights of this filter given by

$$\mathbf{w}_u = \mathbf{\Phi}_{rr}^{-1}\boldsymbol{\phi}_{rb}^{u}. \tag{4.1}$$

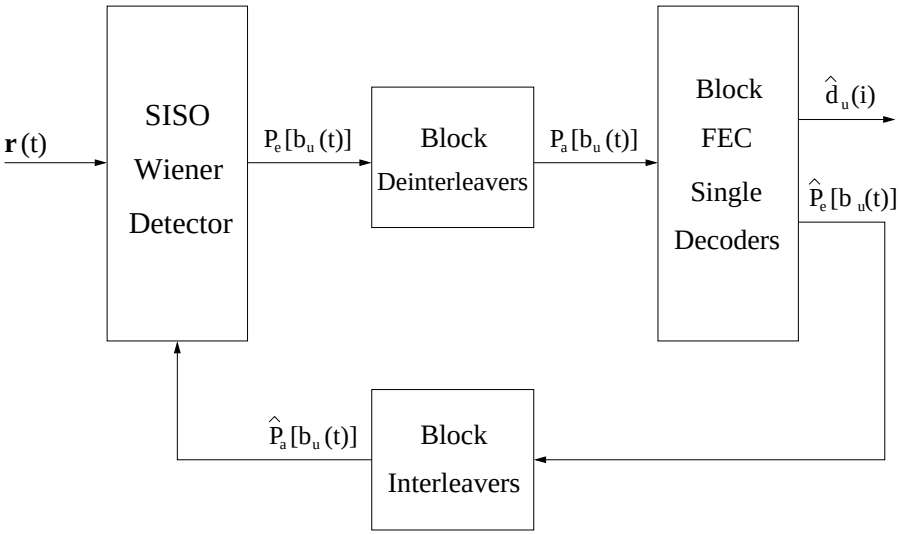

Figure 4.3: *Iterative multiuser receiver structure using only the Wiener detector.*

$\mathbf{\Phi}_{rr}$ is the autocorrelation matrix of the input signal, $\mathbf{r}^T(t) = [r_1(t), r_2(t), \cdots, r_N(t)]^T$, which is given as $\mathbf{\Phi}_{rr} = E[\mathbf{r}(t)\mathbf{r}^T(t)]$, *i.e*

$$\mathbf{\Phi}_{rr} = E\begin{bmatrix} r_1^2(t) & r_1(t)r_2(t) & \cdots & r_1(t)r_N(t) \\ r_1(t)r_2(t) & r_2^2(t) & \cdots & r_2(t)r_N(t) \\ \vdots & & \ddots & \vdots \\ r_1(t)r_N(t) & r_2(t)r_N(t) & \cdots & r_N^2(t) \end{bmatrix} \tag{4.2}$$

where $E[]$ denotes the expected value. Traditionally, it is assumed that the data modulation on each coded bit is independent, *i.e* $E[b_u(t)b_k(t)] = E[b_u(t)]E[b_k(t)] = 0$ with $u \neq k$;

$u, k \in \{1, 2, \cdots, U\}$, however, in this scheme we remove such assumption and therefore, $E[b_u(t)]E[b_k(t)] \neq 0$ for all u and k. This condition will allow us to introduce the turbo multiuser detection principle as it will be shown later on this chapter. Consequently, the auto-correlation matrix Φ_{rr} is then defined as

$$\mathbf{\Phi}_{rr} = \mathbf{C}\mathbf{P}'\mathbf{C}^T + \sigma^2\mathbf{I} \tag{4.3}$$

with $\mathbf{C}$, $\mathbf{C}^T$, $\mathbf{I}$ and σ^2 as given in section 3.2.1.2 but where now the diagonal matrix representing the received power of the users, $\mathbf{P}$, becomes (see appendix A.1)

$$\mathbf{P}' = \begin{bmatrix} b_1^2(t) & E[b_1(t)]E[b_2(t)] & \cdots & E[b_1(t)]E[b_U(t)] \\ E[b_1(t)]E[b_2(t)] & b_2^2(t) & \cdots & E[b_2(t)]E[b_U(t)] \\ \vdots & & \ddots & \vdots \\ E[b_1(t)]E[b_U(t)] & E[b_2(t)]E[b_U(t)] & \cdots & b_U^2(t) \end{bmatrix}. \tag{4.4}$$

The vector $\boldsymbol{\phi}_{rb}^u$ in (4.1) denotes the cross-correlation between the received signal, **r**(t), and the desired user data bit, $b_u(t)$, which is given by

$$\boldsymbol{\phi}_{rb}^u = E\left[b_u(t) \begin{bmatrix} r_1(t) \\ r_2(t) \\ \vdots \\ r_N(t) \end{bmatrix} \right]. \tag{4.5}$$

Under the same assumptions that in (4.2), that is, $E[b_u(t)b_k(t)] \neq 0$ for all u and k, the cross-correlation vector $\boldsymbol{\phi}_{rb}$ is modified to (see appendix A.2)

$$\boldsymbol{\phi}_{rb}^u = \begin{bmatrix} E[b_u(t)]E[b_1(t)]c_{1,1} + \cdots + b_u^2(t)c_{u,1} + \cdots + E[b_u(t)]E[b_U(t)]c_{U,1} \\ E[b_u(t)]E[b_1(t)]c_{1,2} + \cdots + b_u^2(t)c_{u,2} + \cdots + E[b_u(t)]E[b_U(t)]c_{U,2} \\ \vdots \\ E[b_u(t)]E[b_1(t)]c_{1,N} + \cdots + b_u^2(t)c_{u,N} + \cdots + E[b_u(t)]E[b_U(t)]c_{U,N} \end{bmatrix} \tag{4.6}$$

The Wiener detector output for the *u*th user can be therefore defined as follow

$$y_u(t) = \mathbf{w}_u^T\mathbf{r}(t) \tag{4.7}$$

A comprehensive review of this multiuser detector can be found in [73].

Single-user Wiener detector output. The problem faced when designing a partitioned multiuser detector/decoder with an iterative structure is that of generating the correct single-user input probability information for the FEC decoders and of supplying appropriate *a priori* information to the multiuser detector on each iteration.

Using the Wiener detector, the single-user output probability information is obtained from the conditional probabilities, $p(y_u(t)|b_u(t) = b)$, with $b \in \{1, -1\}$. These probabilities are calculated assuming Gaussian noise at the Wiener detector output. The scalar $y_u(t)$ denotes the Wiener detector output for the uth user with mean $\mathbf{w}_u^T \boldsymbol{\phi}_{r,b}^u$ and variance $\sigma_w^2(u) = -(\mathbf{w}_u^T \boldsymbol{\phi}_{r,b}^u)^2 + \mathbf{w}_u^T \boldsymbol{\phi}_{r,b}^u$ (see appendix B.1). Therefore the single-user input probability information for the FEC decoders is provided in the form of LLR as follow

$$P_e[b_u(t)] = ln\left(\frac{p(y_u(t)|b_u(t)=1)}{p(y_u(t)|b_u(t)=-1)}\right). \tag{4.8}$$

4.2.1.2 Wiener detector with a single stage of PIC

A second multiuser detector structure comprises the Wiener detector followed by a single stage of a PIC scheme. We exploit this combined scheme not only to improve performance in the multiuser receiver but also as an alternative structure to bring forward the multiuser detection principle as it will be shown later on this chapter. Therefore, the Wiener detector together

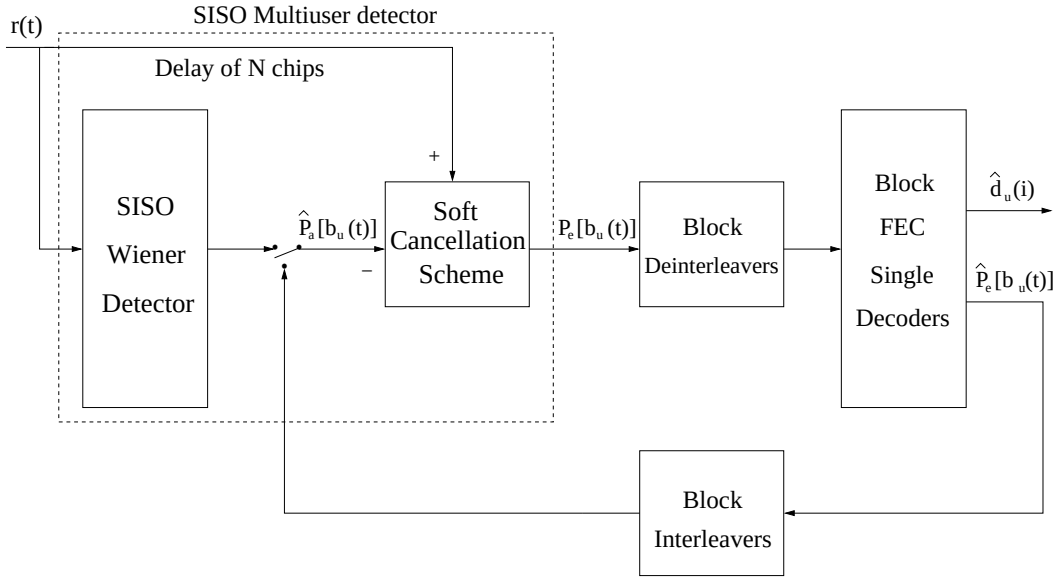

Figure 4.4: *Iterative multiuser receiver structure using Wiener detector and a single stage of parallel cancellation scheme.*

with a PIC scheme is also investigated in the structure of the iterative multiuser receiver whose structure is depicted in Figure 4.4.

Like in turbo decoding, an essential issue in an iterative structure is not to perform any hard decisions during the detection/decoding process. If a user coded bit is detected incorrectly, a hard decision will increase the multiple access interference caused by this detection error. Hence, in the structure of Figure 4.4 the Wiener detector delivers an initial soft estimates of the users FEC coded bits, $\{\hat{b}_u(t)\}$; $u \,\epsilon\, \{1, 2, \cdots, U\}$, $t \,\epsilon\, \{1, 2, \cdots, L/R_0\}$, which are then passed to the PIC scheme. For the *u*th user this soft estimate is obtained by forming the expectation of the users' coded bits as follow

$$\hat{b}_u(t) = E[b_u(t)] = \sum_{b\epsilon\{1,-1\}} bp(b) \tag{4.9}$$

where $p(b)$ represents the *a priori* probability of transmitted either $b = 1$ or $b = -1$. The conditional probabilities at the Wiener detector output, $p(y_u(t)|b_u(t) = b)$; $u \,\epsilon\, \{1, 2, \cdots, U\}$, $b \,\epsilon\, \{1, -1\}$, are calculated similarly to section 4.2.1.1 but in this case we assume that $E[b_u(t)b_k(t)] = 0$ with $u \neq k$, $u, k \,\epsilon\, \{1, 2, \cdots, U\}$. These conditional probabilities are then assigned as the *a priori* probabilities required in (4.9).

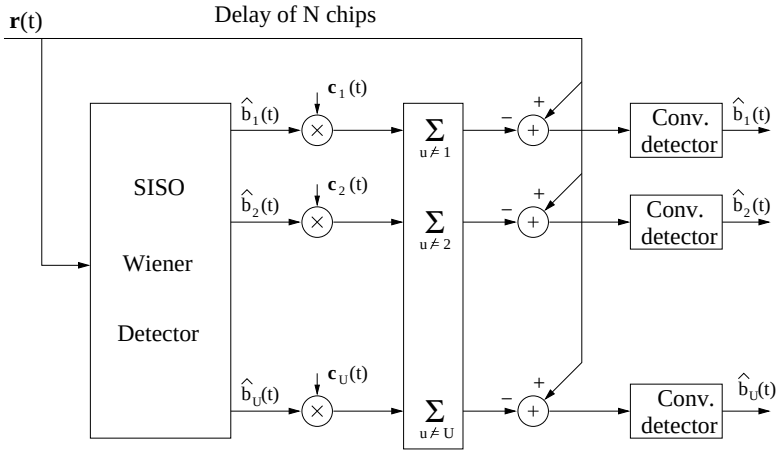

Figure 4.5: *Wiener detector followed by the PIC scheme.*

Using the PIC scheme the soft estimate of the interfering users coded bits (MAI) are spreading and then subtracted from the received signal $\mathbf{r}(t)$. The resulted signal is passed through the

conventional detector whose output is denoted as

$$\hat{y}_u(t) = \mathbf{q}_u[\mathbf{b}(t) - \hat{\mathbf{b}}_u(t)] + z_u(t) \tag{4.10}$$

where $\mathbf{q}_u$ denotes the *u*th row of the autocorrelation matrix, $\mathbf{R} = \mathbf{C}^T\mathbf{C}$, the vector $\hat{\mathbf{b}}_u(t)$ corresponds to the soft estimates of the interfering users which are given as $\mathbf{b}_u(t) = [\hat{b}_1(t), \cdots, \hat{b}_{u-1}(t), 0, \hat{b}_{u+1}(t), \cdots, \hat{b}_U(t)]$. Lastly, $z_u(t)$ denotes a Gaussian noise sample with zero mean and variance σ^2.

Single-user PIC detector output. In the case of the PIC detector, the single-user output *extrinsic* information is given in terms of the following LLRs

$$P_e[b_u(t)] = \ln\left(\frac{p(\hat{y}_u(t)|b_u(t)=1)}{p(\hat{y}_u(t)|b_u(t)=-1)}\right) \tag{4.11}$$

where $p(\hat{y}_u(t)|b_u(t) = b)$ is the conditional probability at the output of the PIC scheme. Since the PIC scheme output for the *u*th user can be modelled on the first iteration by an equivalent AWGN channel, this output can then be written as follow

$$\hat{y}_u(t) = b_u(t) + \mu_u(t) \tag{4.12}$$

with $\mu_u(t)$ is a Gaussian noise sample with zero mean and variance (see appendix B.2)

$$\sigma_\mu^2(u) = \sum_{\substack{k=1 \\ k\neq u}}^{U} \rho_{u,k}^2 + \sigma_n^2 \tag{4.13}$$

ρ_{u,k_1} denotes the cross-correlation factor between user u and user k_1.

4.2.2 FEC coding

To reduce the complexity in the iterative multiuser receiver convolutional codes are chosen for the channel coding. Thus the FEC decoder for the *u*th user consists of a single SISO MAP decoder. As shown in Figure 4.2, the multiuser detector output for the *u*th user after deinterleaving, $P_a[b_u(t)]$, is fed as input to a single SISO MAP decoder. This information is used

directly in the MAP's branch decoder metric calculation which is modified as in [87–92] to

$$\gamma_i(\mathbf{Y}_i, s', s) \quad = \quad P\{S_i = s | S_{i-1} = s'\} \prod_{t'=n_c(i-1)+1}^{n_c i} p(\hat{y}_u(t') | b_u(t')) \tag{4.14}$$

where the product is over all the n_c FEC coded bits, $b_u(t)$, value that produce the transition of the MAP decoder from state s' to state s. Like the SCCC solution [39] the SISO MAP decoder does not take any *a priori* information for the data bits, *i.e* $P\{S_j = s | S_{j-1} = s'\} = 0.5$. As shown in section 2.5.2.2, the SISO MAP decoder algorithm outputs the *a posteriori* LLRs of the coded bits, $\hat{P}_e[b_u(t)]$; $u \, \epsilon \, \{1, 2, \cdots, U\}$, based on the soft information provided from the multiuser detector. This *extrinsic* information is the information about the coded bits gleaned from the *a priori* information about the other code bits based on the trellis structure of the code. Also the SISO MAP decoder computes the *a posteriori* LLRs of the uncoded bits, $\hat{P}_e[d_u(i)]$. Note that the LLR of the uncoded bits is computed only at the last iteration. Finally, the data bit of user u, $d_u(i)$, is then decoded according to (3.28).

4.2.3 Iterative principle

The general structure of a partitioned iterative multiuser receiver consists of a SISO multiuser detector followed by a block of U SISO FEC decoders. These two modules are separated by interleavers and deinterleavers. When users share information suitably, a joint detection process results with an improved performance over a system without joint detection. In the turbo decoding scheme, the output *a posteriori* probability of the first SISO MAP decoder is used as *a priori* information for the second SISO MAP decoder. Equally the output *a posteriori* probability from the second SISO MAP decoder is fed to the first SISO MAP decoder during each iteration in. In a similar fashion, the SISO multiuser detector in the iterative multiuser receiver scheme delivers single-user probabilities (given in the form of LLR, $P_e[b_u(t)]$) for every user coded bit which are fed to the SISO MAP decoders. The iterative principle is thus incorporated in the receiver structure by using the *a posteriori* probabilities (interleaving version) of the users coded bits from the SISO MAP decoders output, $\hat{P}_a[b_u(t)]$; $u \, \epsilon \, \{1, 2, \cdots, U\}$, as *a priori* probabilities in the SISO multiuser detector.

4.2.3.1 Iterative multiuser receiver with Wiener detection

Considering only the Wiener detector in the iterative multiuser receiver structure, as shown in Figure 4.3, the turbo multiuser detection principle can be incorporated by using the *a posteriori* LLRs, $\hat{P}_a[b_u(t)]$ (provided from the SISO MAP decoders and after interleaving), to obtain the expectation value of the users' coded bits, *i.e* $\hat{b}_u(t) = E[b_u(t)]$. Using (4.9), we can compute these expectation values where the *a priori* probabilities required are derived from *a posteriori* LLRs, $\hat{P}_a[b_u(t)]$ as follow

$$p(b_u(t) = b) = \begin{cases} \frac{\exp(\hat{P}_a[b_u(t)])}{1+\exp(\hat{P}_a[b_u(t)])} & \text{if } b = 1 \\ \frac{1}{1+\exp(\hat{P}_a[b_u(t)])} & \text{if } b = -1. \end{cases} \tag{4.15}$$

The resulted expectation values are then substituted into (4.4) and (4.6) to compute an updated version of the autocorrelation matrix Φ_{rr} and cross-correlation vector $\boldsymbol{\phi}^u_{rb}$ which are used to estimates the users' coded bits on subsequent iterations. For the first iteration, we set the multiuser receiver *a priori* information to $p(b_u(t) = b) = 0.5$, that is, $\hat{P}_a[b_u(t)] = 0$ for all $u \in \{1, 2, \cdots, U\}$. Finally, after a desired number of iterations the SISO MAP decoders performs a hard decision on the LLRs of the data bits, $\hat{P}_e[d_u(i)]$ to recover the original uncoded data stream, that is

$$\hat{d}_u(i) = \begin{cases} 1 & \text{if } \hat{P}_e[d_u(i)] > 0 \\ 0 & \text{otherwise.} \end{cases} \tag{4.16}$$

4.2.3.2 Iterative multiuser receiver with Wiener detection and a single stage of PIC

Figure 4.4 shows the iterative multiuser receiver structure with the incorporation of the PIC scheme in the detection stage. For the first iteration, the Wiener detector provides the initial probabilities which are then used as *a priori* probabilities ($p(y_u(t)|b_u(t) = b) = p(b_u(t) = b)$) in (4.9) to compute soft estimates of the interfering users coded bits at the PIC output. Similar to the previous section, the iterative principle is incorporated by using the interleaving version of the *a posteriori* LLRs for the users coded bits at the SISO MAP decoders output, $\hat{P}_a[b_u(t)]$, with $u \in \{1, 2, \cdots, U\}$, as *a priori* probabilities in the PIC scheme rather than the Wiener detector output as shown in Figure 4.4. These *a priori* probabilities, $\hat{P}_a[b_u(t)]$, are then used to produce soft estimates at the PIC output for the interfering users coded bits on subsequent iterations. At the last iteration, the SISO MAP decoder computes the *a posteriori* LLR of every

data bit, $\hat{P}_e[d_u(i)]$, which is then used to make a decision on the decoded data bit based on equation (4.16).

4.3 Complexity analysis

In this section an analysis of the complexity is presented for the two iterative multiuser detector/decoder structures presented in this chapter. This is important to determine those parts of the receiver which require more computational resources. The complexity analysis consists of determining the number of operations (measured in terms of multiplications and divisions) required for the multiuser detector, SISO MAP decoder and LLR calculation per data bit transmitted and per iteration. We assign the variable E to be the equivalent to the computational complexity of the exponential operation, the number of users equal to U, the processing gain equal to N, the number of paths out of each code state equal to N_p, and R_0 as the code rate of the FEC coding. Table 4.1 and 4.2 show the complexity of the iterative multiuser receiver structures in terms of those variables.

Procedure	multiplications and divisions per data bit
Wiener detector	$O(N^2) + N^2(U+1) + N(U^2+2U+1) + (U-1)^2$
LLR calculation	$U(E+N) + 4U$
SISO MAP decoder	$\frac{1}{R_0}(E + 2^{\nu-1}N_p + 3)$

Table 4.1: *Iterative multiuser receiver using Wiener detection*

Table 4.1 shows the complexity of the modules in the proposed iterative multiuser receiver illustrated in Figure 4.3. A major concern in the complexity of the Wiener detector is the inversion of the matrix, Φ_{rr}, whose complexity is denoted as $O(N^2)$. This matrix requires knowledge of the spreading users codes and the noise variance σ^2. Since the users codes are known, it can be seen that Φ_{rr}^{-1} mainly changes according to the value of σ^2 and the expectation values $E[b_u(t)]$. Therefore, the inverse of Φ_{rr} is required every time the expectation values are updated. Secondly, the complexity of a single SISO MAP decoder for a constituent convolutional codes of constraint length ν is in the order of $O(2^{\nu-1})$. Normally ν is chosen small to reduce the complexity of the channel decoder. Finally, the LLR calculations are linearly dependent on the number of users and the processing gain.

Table 4.2 shows the complexity of the iterative multiuser receiver structure proposed in Figure 4.4. This structure assumes that $E[b_u(t)] = 0$, $u \epsilon \{1, 2, \cdots, U\}$, therefore, the autocorrelation

Procedure	multiplications and divisions per data bit
Wiener detector	$O(N^2) + N^2(U+1) + 3N$
PIC scheme	$UN(1+2U)$
LLR calculations	$U(E+U+1)$
SISO MAP decoder	$\frac{1}{R_0}(E + 2^{\nu-1}N_p + 3)$

Table 4.2: *Iterative multiuser receiver complexity using Wiener detection and a PIC scheme*

matrix $\mathbf{\Phi}_{rr}$ and the cross-correlation vector $\boldsymbol{\phi}_{rb}^{u}$ do not require the calculation of the expectation values for the users' coded bits. This will reduce the complexity in the Wiener detector as compare with the structure in Figure 4.3. Thus Φ_{rr}^{-1} will change only according to the noise variance parameter σ^2. Although an extra stage is incorporated (PIC scheme), for a number of iteration > 1 the complexity of the iterative multiuser receiver is reduced to the complexity only in the PIC scheme and the block of SISO MAP decoders.

4.4 Simulation results

Monte Carlo simulations are used to illustrate the performance of the iterative multiuser receiver structures proposed in this chapter for the downlink of a DS-CDMA system over an AWGN channel. Equal-power users are assumed in the system. Simulation results throughout

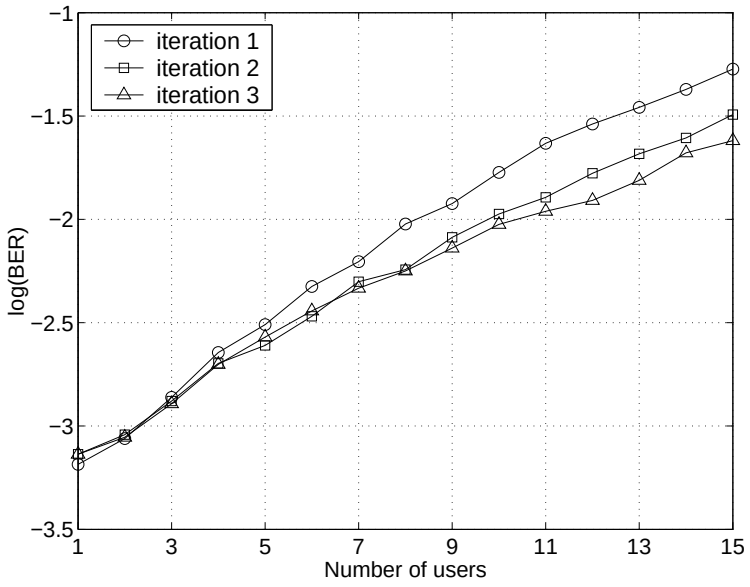

Figure 4.6: *Number of users against BER for $E_b/N_0 = 4dB$ and $N = 15$ using Wiener detector as the detector of the the iterative multiuser detector/decoder.*

this section show the average BER performance over all the users in the system. The FEC coding technique employed for each user consists of a non-recursive non-systematic convolutional code (nsc) with rate $R_0 = 1/2$, constraint length $\nu = 3$, and generators $(7, 5)$ in octal notation. The channel decoder is implemented by the SISO MAP algorithm. The constituent MAP decoder assumes a starting state of zero with the convolutional codes are not terminated (that is an equiprobable final state). The data block size is set to $L = 128$ data bits. In the simulations, the spreading codes of length N are chosen in a pseudo-random fashion on a bit by bit bit basis. Also a unique random interleaver of length $L/R_0 = 256$ coded bits is assigned to each user. It is assumed that the receiver knows the noise variance σ^2 and the user spreading codes exactly.

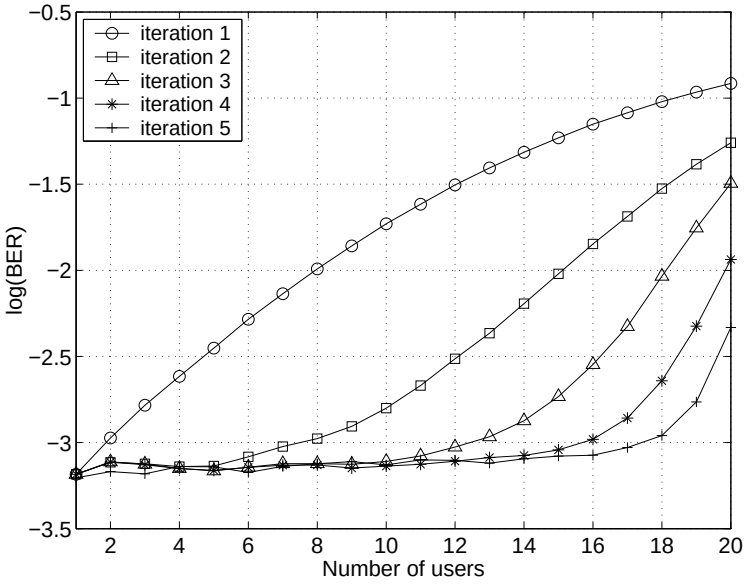

Figure 4.7: *Number of users against BER for $E_b/N_0 = 4dB$ and $N = 15$ using Wiener detector with soft cancellation scheme in the iterative multiuser receiver.*

Figure 4.6 show the BER performance as a function of the number of users for 1, 2 and 3 iterations in the multiuser receiver structure proposed in Figure 4.3. Similarly, 4.7 show the performance corresponding to the scheme in Figure 4.4 but where up to 5 iterations are applied. Comparing the results, it is clear that using the Wiener detector followed by the PIC scheme provides with a much better performance gain that using only the Wiener detector on its own. Although an improvement is obtained by increasing the number of iterations in the scheme of Figure 4.3, the gain is small compared with the performance using the scheme in 4.4. From the latter, we can observe that for a multiuser iteration number > 3 the multiuser receiver performance remains closely to a constant value (single-user bound) up to a number of users

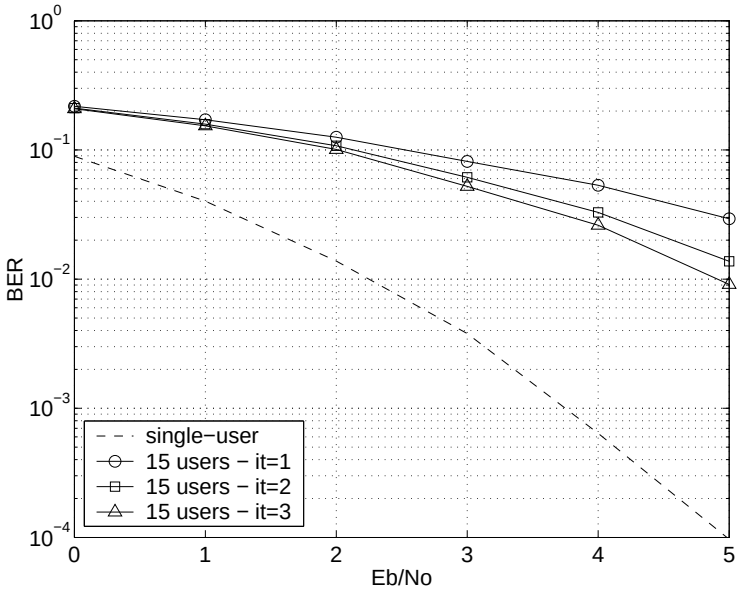

Figure 4.8: *Iterative multiuser receiver performance using a Wiener detector.*

equal to the processing gain, *i.e* $U = N$. The incorporation of more users in the system $(U/N > 1)$ pushes the receiver performance away from the single-user bound, as is expected.

On the other hand, Figures 4.8 and 4.9 show the BER performance of the system as a function of the E_b/N_0 and the number of iterations on the receiver. The simulations are performed with a processing gain $N = 15$ and with $U = 15$ active users. Figure 4.8 presents the simulation results using the scheme proposed in Figure 4.3. It can be seen that with 2 and 3 iterations in the receiver the performance is improved slightly. However, the gain achieved is not significant. The performance for the scheme proposed in Figure 4.4 is shown in Figure 4.9. These simulation results show that the multiuser receiver achieves near single-user performance in this highly loaded system, a result within 0.4 dB of single-user performance is obtained at a BER of 10^{-3}. Similar to turbo codes, the major improvement of the receiver occurs in the second and third multiuser iterations. It is important to highlight the crucial effect of the receiver performance at the first multiuser iteration since it indicates whether it will converge to the single-user performance.

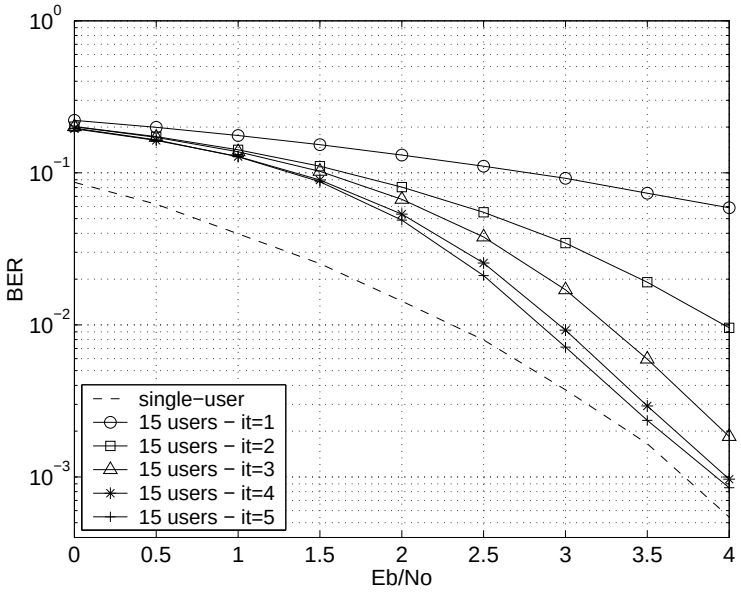

Figure 4.9: *Iterative multiuser receiver performance using Wiener detector with a soft cancellation scheme.*

4.5 Summary

In this chapter, an iterative multiuser receiver technique is proposed. In a similar fashion to turbo codes, this receiver performs signal detection and decoding separately, but exchanging soft information in an iterative fashion. Due to the complexity of the optimal joint receiver, an iterative multiuser receiver has been analysed using low-complexity detection techniques.

Firstly, an iterative receiver with Wiener detection is proposed in order to apply the turbo principle. However, simulation results indicate that a small gain is obtained by iterating between the Wiener detector and a block of FEC decoders. The reason for this is a weak multiuser detection stage.

A second iterative multiuser receiver structure is investigated using a more powerful detection technique which consists of the Wiener detector followed by a single stage of PIC. It is shown that this scheme performs close to the single-user performance even for large system loads. The complexity of the optimal joint receiver is well known to be exponential with the number of users and the constraint length of the FEC code. By applying this low-complexity multiuser receiver, the complexity reduces then from $O(2^{U\nu})$ to a factor proportional to $\left(O(N^2) + O(U^2) + O(UN) + O(2^{\nu-1})\right)$ as shown in table 4.2. Thus, the main con-

tribution in this chapter is the application of the turbo multiuser detection principle in the receiver of a synchronous FEC coded DS-CDMA system that employs pseudo-random spreading codes in an AWGN channel.

Chapter 5
An Iterative Multiuser Receiver in a Multipath Fading Channel

In the previous chapter we have discussed the design of an iterative receiver for a FEC coded DS-CDMA system over an AWGN channel. It was shown that the proposed receiver structure achieves good performance with a low-complexity structure. In a more realistic mobile channel, however, multiple paths are received from the signal that is transmitted through the channel. This phenomenon introduces ISI which is another of the major interference factors for a DS-CDMA system that significantly degradates the system performance. In this chapter we investigate the structure of an iterative multiuser receiver with the distortion of a multipath fading channel.

The next section introduces the FEC coded DS-CDMA system model for a multipath fading channel. Section 5.2 looks at the hybrid iterative multiuser receiver (HIMR) which is a partitioned receiver that iterates between multiuser signal detection and channel coding using two different MUD schemes and a block of single-user FEC decoders. A linear MUD structure is applied in the first iteration of the scheme then a sub-optimum RBF detector is incorporated for the MUD on subsequent iterations. In section 5.3 the complexity of the proposed HIMR is analysed. Finally, simulation results and conclusions are drawn in section 5.4 and 5.5 respectively.

5.1 System model

In this section the downlink of a DS-CDMA with FEC coding over a stationary multipath channel is described. The system model is shown in Figure 2.4 of section 2.1. Denoting the channel input by the time series $x(j), x(j-T_c), x(j-2T_c), \cdots$, and the impulse response of the channel by $h_0, h_1, h_2, \cdots$, the output of the channel sampled at the chip rate can be denoted as

$$s(j) = \sum_{a=0}^{\alpha} h_a x(j - aT_c) \tag{5.1}$$

where α comprises the duration of the channel impulse response in chips. Following a similar approach to the model described in section 2.1, a DS-CDMA system with U active users is considered. Each user transmits data blocks of length L, $\{d_u(i)\}$; $i \in \{1, 2, \cdots, L\}$, $u \in \{1, 2, \cdots, U\}$. The FEC coding for the *u*th user consists of a convolutional codes of rate R_0 and constraint length ν. Every user's encoder output is then interleaved and modulated using the mapping $0 \rightarrow$ -1, $1 \rightarrow +1$. This produces the coded, interleaved and modulated stream of bits, $\{b_u(t)\}$; $t \in \{1, 2, \cdots, L/R_0\}$. Before transmission, the coded bits for user u are then spread by random codes of length N. At time t, the spreading code for the *u*th user is denoted by the vector $\mathbf{c}_u(t)$ whose elements are given as $c_{u,n}(t) \in \{+1/\sqrt{N}, -1/\sqrt{N}\}$ with $n \in \{1, 2, \cdots, N\}$. Assuming perfect time synchronisation between the transmitter and the receiver, the transmitted signal propagates through the multipath fading channel. Assuming also that the multipath channel spans only one neighbouring data bit, the receiver signal at time t is then given by (2.2). However, the energy from the current data bit continues α chips after the current bit has been transmitted as shown in Figure 5.1. Therefore, an alternative mathematical model that has a time span to capture all the energy from the current information bit transmitted can be expressed as

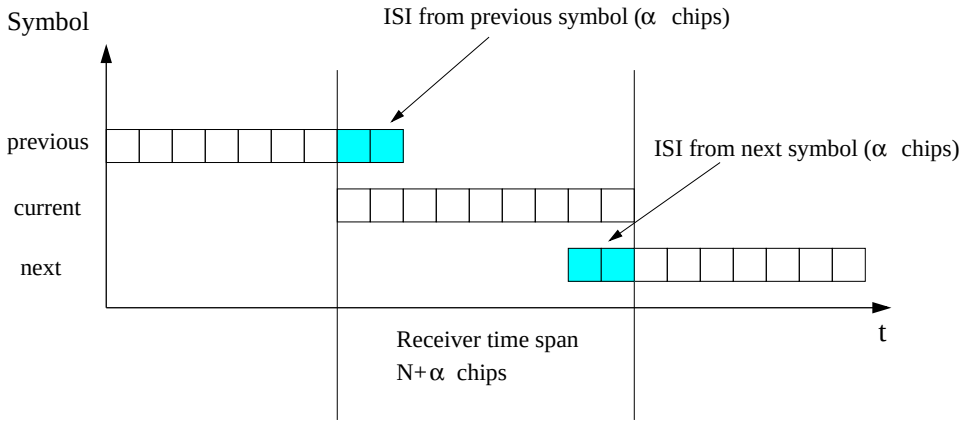

Figure 5.1: *ISI effect when the multipath channel spans only one neighbouring data symbol.*

$$\underline{\mathbf{r}}(t) = \underline{\mathbf{H}}_t \, \underline{\mathbf{C}} \, \underline{\mathbf{b}}(t) + \underline{\mathbf{n}}(t) \tag{5.2}$$

where all the energy corresponding to the current data symbol transmitted is in the vector $\underline{\mathbf{r}}(t)$ with dimensions $(N + \alpha) \times 1$. The channel matrix $\underline{\mathbf{H}}_t$ with dimensions $(N + \alpha) \times (N + 2\alpha)$

and the $(N+2\alpha)\times 3U$ matrix $\underline{\mathbf{C}}$ with the spreading codes are given as follows:

$$\underline{\mathbf{H}}_t = \begin{bmatrix} h_\alpha & h_{\alpha-1} & \cdots & h_0 & 0 & \cdots & 0 \\ 0 & h_\alpha & \cdots & h_1 & h_0 & \cdots & 0 \\ \vdots & & \ddots & & & \vdots & 0 \\ 0 & \cdots & 0 & 0 & h_\alpha & \cdots & h_0 \end{bmatrix}$$

and

$$\underline{\mathbf{C}} = \begin{bmatrix} c_{1,N-\alpha}(t-1) & 0 & 0 & \cdots & c_{U,N-\alpha}(t-1) & 0 & 0 \\ \vdots & \vdots & \vdots & \cdots & \vdots & \vdots & \vdots \\ c_{1,N}(t-1) & 0 & 0 & \cdots & c_{U,N}(t-1) & 0 & 0 \\ 0 & c_{1,1}(t) & 0 & \cdots & 0 & c_{U,1}(t) & 0 \\ 0 & c_{1,2}(t) & 0 & \cdots & 0 & c_{U,2}(t) & 0 \\ \vdots & \vdots & \vdots & \cdots & \vdots & \vdots & \vdots \\ 0 & c_{1,N}(t) & 0 & \cdots & 0 & c_{U,N}(t) & 0 \\ 0 & 0 & c_{1,1}(t+1) & \cdots & 0 & 0 & c_{U,1}(t+1) \\ \vdots & \vdots & \vdots & \cdots & \vdots & \vdots & \vdots \\ 0 & 0 & c_{1,\alpha}(t+1) & \cdots & 0 & 0 & c_{U,\alpha}(t+1) \end{bmatrix}.$$

Finally the vectors $\underline{\mathbf{b}}(t)$ and $\underline{\mathbf{n}}(t)$ both with dimensions $(N+\alpha)\times 1$ are the information and noise vectors respectively. These vector are represented by

$$\underline{\mathbf{b}}(t) = \begin{bmatrix} b_1(t-1) \\ b_1(t) \\ b_1(t+1) \\ \vdots \\ b_U(t-1) \\ b_U(t) \\ b_U(t+1) \end{bmatrix}$$

and

$$\underline{\mathbf{n}}(t) = \begin{bmatrix} n_1(t) \\ n_2(t) \\ \vdots \\ n_N(t) \\ n_1(t+1) \\ \vdots \\ n_\alpha(t+1) \end{bmatrix}.$$

The noise samples in $\underline{\mathbf{n}}(t)$ are assumed to be Gaussian with mean zero and variance σ^2.

5.2 Iterative multiuser receiver

In a DS-CDMA system the presence of ISI due to the multipath nature of the wireless channels and together with MAI constitute the major impediments to the overall system performance. In [84], the optimal multiuser receiver for the asynchronous Convolutionally coded DS-CDMA was formulated on a non-dispersive AWGN channel. However, the prohibitive complexity of this receiver, $O(2^{U\nu})$, which rises exponentially with the number of users U and the encoder constraint length ν, makes this structure far from practical. This complexity can be reduced to $O(2^U)+O(2^\nu)$ by performing symbol detection and decoding separately (partitioned receiver). Since v is normally small, the receiver complexity is basically dominated by the multiuser detector structure ($O(2^U)$). Therefore, even with a small number of users in the system the complexity of this structure becomes impractical.

Linear multiuser detection techniques generally overcome the complexity problem in the receiver, but the presence of high levels of MAI and/or ISI results in a poor receiver performance. This degradation is mainly caused by the fact that in such scenarios the desired signals are no longer linearly separable [74]. Therefore, non-linear receiver techniques are required to provide better performance. However, non-linear receivers usually involve a high complexity which motivates the current research into a search for sub-optimum non-linear receiver structures of comparable performance to that of the full complexity receiver but at a significantly reduced complexity.

In the last few years, several sub-optimal multiuser detectors, based on non-linear structures,

have been proposed [76, 77, 95, 96]. It has been shown that the next best performance to the optimum multiuser detector, but with a much lower complexity, is achieved by sub-optimal multiuser detectors based on a tree-search structure [77, 95, 97]. Since the full complexity RBF multiuser detector is based on searching through all the possible combinations of inputs to find the nearest match to the received data, tree-search detectors confines the search to only a subset of these combinations. An attractive tree-search structure based on a pre-selection technique was proposed in [95], a brief description of the PSML detector is also given in section 3.2.1.3. The PSML detector uses an initial stage to establish the preliminary information of all the coded bits belonging to the unwanted users. Then this information is used to provide a measure of how likely the user's coded bits can be correctly detected, as shown in Figure 3.3. This metric is then passed on to a second stage of the PSML detector where a reduced search is performed over those coded bits which are most likely incorrectly detected by the initial stage. There are different criteria that can be used to implement the PSML detector, those are defined in [95].

In [57], it was shown that the RBF detector can be implemented as the optimal multiuser detector for a synchronous DS-CDMA system over an AWGN channel. However, for a multipath channel and under the assumption that ISI spans only one neighbouring symbol, the complexity of the RBF detector is proportional to 2^{3U} [98]. This choice comes from the fact that the influence of the bits beyond one neighbouring symbol is just too small to be worth considering. In this manner, the RBF detector structure becomes sub-optimal for the multipath channel . With this in mind, in this chapter we investigate an iterative multiuser receiver based on a reduced-complexity RBF detector. Similar to [95], we make use of a pre-selection scheme to reduced the search in the RBF detector for the most likely data transmitted. On the other hand, in order to exploit fully the turbo multiuser detection principle, instead of using powerful FEC coding techniques, for example turbo codes, it may in fact be better to use a simpler FEC coding channel combined with a more advanced MUD techniques to overcome the system interference. Therefore, we investigate here an iterative multiuser receiver structure with a particular emphasis on the detection process rather than on the channel coding.

In this chapter, we propose a hybrid iterative multiuser receiver that exploits the turbo multiuser detection principle not only to improve the BER performance but also to reduce the receiver complexity. This hybrid structure uses a moderate-complexity multiuser detector structure at the first iteration and then a sub-optimal RBF (SRBF) detector for further iterations in the receiver as shown in Figure 5.2. The objective of the first stage is to identify by means of a

pre-selection technique those users' coded bits that are most likely to be correctly detected. Based upon these confidence values a reduced-complexity method is applied to the multiuser detector for subsequent iterations. The structure of the HIMR consists of a SISO multiuser detector followed by a block of SISO MAP decoders which operate separately but exchanging information in an iterative fashion. The implementation of this multiuser receiver can be viewed

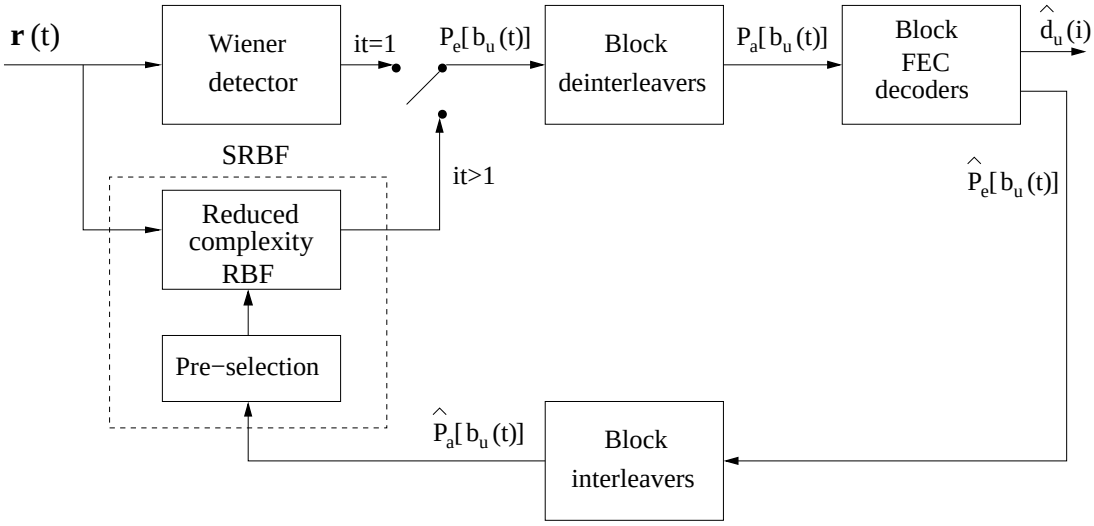

Figure 5.2: *Hybrid iterative multiuser receiver.*

as a structure that uses two different multiuser detection schemes: a moderate-complexity linear detector at the first iteration and the non-linear SRBF detector for subsequent iterations.

5.2.1 Multiuser detection for the first iteration

The initial SISO multiuser detector, which comprises a moderate-complexity detector, can be implemented using any linear detection technique, that is, MF, Decorrelator or Wiener detector. This initial detector is used to provide LLR information of the users' coded bits to the FEC decoders at the first iteration in the receiver. The SRBF detector consists of a pre-selection stage which is used to establish *a priori* information about the users' coded bits. This *a priori* information is then fed into the reduced-complexity RBF detector to simplify the search for the most likely bits transmitted. Therefore, the better the performance of the initial stage the more reliable the information provided to the SRBF detector. In Figure 5.2 we consider the initial stage to be the moderate-complexity detector followed by the FEC decoding channel. This will give more reliable information to feed into the SRBF detector which is applied on subsequent

iteration.

It is well known that Wiener detector provides the best performance among those linear detection techniques and this is what we will use as the moderate-complexity linear detector. Similar to section 4.2.1.1 the output of the *u*th user using the Wiener detector is defined as in (4.7), *i.e*, $y_u(t) = \mathbf{w}_u^T \mathbf{r}(t)$ where $\mathbf{r}(t)$ is the received signal and $\mathbf{w}_u$ the vector with the weights of the Wiener detector. Assuming that the FEC coded bits are independent, the weights are calculated following the same procedure as in section 4.2.1.1 but where $\mathbf{P}'$ is replaced by $\mathbf{P}$ in the calculation of the autocorrelation matrix $\mathbf{\Phi}_{rr}$. Therefore, the single-user LLR outputs for the Wiener detector are then expressed as

$$P_e[b_u(t)] = ln\left(\frac{p(y_u(t)|b_u(t)=1)}{p(y_u(t)|b_u(t)=-1)}\right). \tag{5.3}$$

where the conditional probabilities $p(y_u(t)|b_u(t) = b)$ with $b \,\epsilon\, \{1, -1\}$ are calculated under the assumption of Gaussian noise at the Wiener detector output. The scalar $y_u(t)$ represents the Wiener detector output corresponding to the *u*th user with mean $\mathbf{w}_u^T \boldsymbol{\phi}_{r,b}^u$ and variance $\sigma_u^2(t) = -(\mathbf{w}_u^T \boldsymbol{\phi}_{r,b}^u)^2 + \mathbf{w}_u^T \boldsymbol{\phi}_{r,b}^u$ (see appendix B.1).

5.2.2 FEC coding

The channel decoding consists of a block of U single-user SISO MAP decoders. The input sequence to the *u*th single-user SISO MAP decoder is given as $\{P_a[b_u(t)]\}$ which corresponds to the deinterleaved version of $\{P_e[b_u(t)]\}$ with $t\,\{1, 2, \cdots, L/R_o\}$. The LLR at time t, $P_a[b_u(t)]$, is then used directly into the MAP's branch decoder metric calculation which is modified to

$$\gamma_i(\mathbf{Y}_i, s', s) \;=\; P\{S_i = s|S_{i-1} = s'\} \prod_{t'=n_c(i-1)+1}^{n_c i} p(y_u(t')|b_u(t')) \tag{5.4}$$

where the product is over all the n_c FEC coded bits, $b_u(t)$, values that produce the transition of the MAP decoder from state s' to state s. The conditional probabilities in (5.4) are obtained from $P_a[b_u(t)]$ by using (4.15). The SISO MAP decoder does not take any *a priori* information for the data bits, *i.e* $P\{S_i = s|S_{i-1} = s'\} = 0.5$. As shown in section 2.5.2.2, the SISO MAP decoder algorithm computes as outputs the *a posteriori* LLRs of the FEC coded bits, $\hat{P}_e[b_u(t)]$; $u \,\epsilon\, \{1, 2, \cdots, U\}$, based on the information provided from the multiuser detector, $\{P_a[b_u(t)]\}$. This *extrinsic* information about the users coded bits is gleaned from the *a priori* information

about the other code bits based on the trellis structure of the code. Also the SISO MAP decoder can compute the *a posteriori* LLRs of the uncoded bits, $\hat{P}_e[d_u(i)]$ which is performed only at the last iteration. The data bit $d_u(t)$ is then decoded according to

$$\hat{d}_u(i) = \begin{cases} 1 & \text{if } \hat{P}_e[d_u(i)] > 0 \\ 0 & \text{otherwise.} \end{cases} \tag{5.5}$$

5.2.3 Pre-selection technique

A pre-selection technique is applied to reduced the complexity of the SRBF detector. We make use of the pre-selection technique to reduce the complexity of the RBF detector at time t based upon the LLRs $\{\hat{P}_a[b_u(t)]\}$ of the users coded bits provided from the FEC decoders. The absolute value of these LLRs, are used to yield *confidence* values for each of the FEC coded bits in the vector $\underline{\mathbf{b}}(t)$ at time t. These *confidence* values are then supplied to the multiuser detector so they can be used to reduce the complexity. Under the assumptions given in section 5.2, the ISI spans only to the previous and next symbols, then the dimensions of $\underline{\mathbf{b}}(t)$ is $3U$ .The basic idea is to treat every component in $\underline{\mathbf{b}}(t)$ as a virtual user, and therefore there are $3U$ virtual users in the vector $\underline{\mathbf{b}}(t)$. In the multipath scenario the vector used to obtain the centres of the RBF detector is then given as

$$\underline{\mathbf{b}}(t) = \begin{bmatrix} b_1(t-1) \\ b_1(t) \\ b_1(t+1) \\ \vdots \\ b_U(t-1) \\ b_U(t) \\ b_U(t+1) \end{bmatrix}$$

The *confidence* of each coded bit provides a measure of how likely these bits can be correctly detected. The function of this stage is then to establish an order of precedence among all these *confidence* values. A large *confidence* value will mean that that bit can be detected correctly with a very high probability. Therefore, those bits with a high *confidence* value can be fixed to $+1$ in the case that $\hat{P}_a[b_u(t)] > 0$ or -1 otherwise. To illustrate this technique an example for the case of two users (6 virtual users) is examined, we shall consider that the vector $\underline{\mathbf{b}}(t)$ has

been received with the following *confidence* values

$$\mathbf{F}[\underline{\mathbf{b}}(t)] = \begin{bmatrix} |\hat{P}_a[b_1(t-1)]| \\ |\hat{P}_a[b_1(t)]| \\ |\hat{P}_a[b_1(t+1)]| \\ |\hat{P}_a[b_2(t-1)]| \\ |\hat{P}_a[b_2(t)]| \\ |\hat{P}_a[b_2(t+1)]| \end{bmatrix} = \begin{bmatrix} |-10.38| \\ |5.33| \\ |9.18| \\ |1.20| \\ |-3.16| \\ |-6.38| \end{bmatrix} \begin{matrix} \\ \leftarrow \\ \\ \leftarrow \\ \leftarrow \\ \end{matrix} . \tag{5.6}$$

In this particular example a full search in the SRBF detector to find the most likely transmitted information would consider 2^6 possible combinations. However, a constraint in complexity can be given to allow only a desired level of complexity in the detector. For example, fixing the search to only 3 bits in the vector $\underline{\mathbf{b}}(t)$ (those virtual users with the lowest *confidence* values as indicated in (5.6)), the total search would be reduced to complexity 2^3. Therefore, the search in the SRBF detector is done only for those bits with the lowest *confidence* of being correctly detected, in our example the vector $\underline{\mathbf{b}}(t) = [-1, b_1(t), 1, b_2(t-1), b_2(t), -1]$ would be sent to the reduced-complexity RBF detector as shown in Figure 5.2.

5.2.4 Multiuser detection for an iteration > 1

The structure of the receiver for an iteration > 1 is obtained by replacing the Wiener detector with the SRBF detector which includes the *pre-selection* technique and a reduced-complexity RBF detector as shown in Figure 5.2. On the first iteration all FEC coded bits for every user are assumed to be equiprobable and therefore it is not convenient to use the SRBF at this point because it would be required to implement the SRBF with full complexity.

As shown in section 3.2.1.1, the decision rule of the RBF detector is given by (3.13). To provide the input probabilistic requirements of the single-user decoders, the SRBF delivers the LLR of a transmitted $+1$ and a transmitted -1 for every FEC coded bit of every user

$$\frac{p(\underline{\mathbf{r}}(t)|b_u(t)=+1)}{p(\underline{\mathbf{r}}(t)|b_u(t)=-1)} = \frac{\sum_{l=1}^{2^{3U-1}} \exp\left(-\frac{||\underline{\mathbf{r}}(t)-\mathbf{a}_l^{+1}(t)||^2}{2\sigma^2}\right)}{\sum_{l=1}^{2^{3U-1}} \exp\left(\frac{-||\underline{\mathbf{r}}(t)-\mathbf{a}_l^{-1}(t)||^2}{2\sigma^2}\right)} \tag{5.7}$$

where the conditional probabilities are generated by the multivariate Gaussian probability dens-

ity function [46] as given below

$$p(\underline{\mathbf{r}}(t)/b_u(t)=b)=\frac{1}{2^{3U-1}}\sum_{l=1}^{2^{3U-1}}\frac{\exp\left(-\frac{||\underline{\mathbf{r}}(t)-\mathbf{a}_l^b(t)||^2}{2\sigma^2}\right)}{(2\pi)^{N/2}\sigma^N} \tag{5.8}$$

where $b\,\epsilon\,\{+1,-1\}$. The received input vector consisting of $N+\alpha$ chips spaced input samples is denoted as

$$\underline{\mathbf{r}}(t)=\begin{bmatrix} r_1(t) \\ r_2(t) \\ \vdots \\ r_N(t) \\ r_1(t+1) \\ \vdots \\ r_N(t+1) \end{bmatrix} \tag{5.9}$$

while the *l*th centre in the SRBF network for $b_u(t)=b$, $b\,\epsilon\,\{+1,-1\}$, is given as

$$\mathbf{a}_l^b(t)=\begin{bmatrix} a_{l,1}^b \\ a_{l,2}^b \\ \vdots \\ a_{l,(N+\alpha)}^b \end{bmatrix} \tag{5.10}$$

and σ^2 is the noise variance.

5.2.5 Turbo multiuser detection principle

The iterative scheme for the multiuser receiver is shown in Figure 5.2. For the first iteration the moderate-complexity detector is performed by the Wiener detector. The detector takes as input the channel output, $\underline{\mathbf{r}}(t)$, and generates as its outputs the LLR for every user coded bit, *i.e* $P_e[b_u(t)]$; $t\,\epsilon\,\{1,2,\cdots,L/R_0\}$ and $u\,\epsilon\,\{1,2,\cdots,U\}$ which are obtained using (5.3). The input to the *u*th SISO MAP decoder, after deinterleaving, is given by the LLR $P_a[b_u(t)]$. It delivers as output an update of the LLR's of the coded bits, $\hat{P}_e[b_u(t)]$, as well as the LLR's of the data bits, $\hat{P}_e[d_u(t)]$. The *a posteriori* FEC coded bit probabilities, $\hat{P}_e[b_u(t)]$, obtained

from the output of the SISO MAP decoders are then used as *a priori* information for the SRBF detector. The SRBF detector is then applied as the multiuser detector on subsequent iterations, see Figure 5.2. The turbo multiuser detection principle can be applied to the SRBF detector by using (3.24) to express the conditional probability $p(\underline{\mathbf{r}}(t)|b_u(t)=d)$, *i.e*

$$p(\underline{\mathbf{r}}(t)|b_u(t)=b) = \sum_{\substack{\mathbf{b}(t) \\ (b_u(t)=b)}} p(\underline{\mathbf{r}}(t)|\mathbf{b}(t)) \prod_{\substack{k=1 \\ k\neq u}}^{U} pr(b_k(t)) \tag{5.11}$$

where the *a priori* probabilities for the FEC coded bits, $pr(b_k(t)=b)$; $k \,\epsilon\, \{1,2,\cdots,U\}$, are taken from the the output of the SISO MAP decoders from the previous iteration, *i.e*

$$p(b_u(t)=b) = \begin{cases} \frac{\exp(\hat{P}_a[b_u(t)])}{1+\exp(\hat{P}_a[b_u(t)])} & \text{if } b=1 \\ \frac{1}{1+\exp(\hat{P}_a[b_u(t)])} & \text{if } b=-1. \end{cases} \tag{5.12}$$

Therefore, for an iteration > 1 the LLRs required at the single-user SISO MAP decoders are provided from the output of the SRBF detector which are obtained using (5.7). When the required number of iterations have been completed a hard decision is output by the single-user SISO MAP decoders to recover the original uncoded data stream, that is

$$\hat{d}(i) = \begin{cases} 1 & \text{if } \hat{P}_e[d(i)] > 0 \\ 0 & \text{otherwise.} \end{cases} \tag{5.13}$$

5.3 Complexity analysis

In this section the computational complexity of the hybrid iterative multiuser receiver is described. The receiver complexity is determined by the number of operations required per information bit per bit transmitted for the Wiener detector, SRBF detector, FEC decoders and LLR calculations. As considered in chapter 4, an operation is defined as a real multiplication or division. Due to the significant number of comparisons required, we have also included this operation in the complexity analysis. Table 5.1 shows the complexity of the iterative multiuser receiver structure where we have assigned the variable E to be the equivalent to the computational complexity of the exponential operation, U the number of active users, N the spreading code length, N_p the number of paths out of each state in the trellis, R_0 the FEC encoder rate and α the duration of the channel impulse response in chips.

Procedure	multiplications, divisions and comparisons per data bit
Wiener detector	$O(N+\alpha)^2 + (N+\alpha)^2(U+1) + 3(N+\alpha)$
LLR calculation	$U(N+5)$
SISO MAP decoder	$(E + 2^{\nu-1}N_p + 3)\frac{1}{R_0}$
SRBF detector	$U^2 - 2U + 2^e(U + (N+\alpha) + 2E + 6)$

Table 5.1: *Complexity of iterative multiuser receiver components*

In terms of complexity the Wiener detector has a complexity proportional to $O((N+\alpha)^2)$. The FEC decoder which consists of a single SISO MAP decoder has a complexity that increases exponentially with the encoder memory $O(2^{v-1})$, but v is normally chosen small to reduce this complexity. On the other hand, the LLR calculations have a complexity in the order $O(UN)$. It can then be shown that the full complexity in the hybrid iterative multiuser receiver is mainly dominated by the complexity of the SRBF detector which comprises the pre-selection stage and the reduced-complexity RBF detector. Although in the pre-selection stage only comparisons are required, the structure in the SRBF detector has a complexity proportional to 2^e operations per information bit interval where e is the desired level of complexity in the SRBF detector. By taking the number of centres (2^e) in the SRBF detector as the measure of complexity, we will show in next section that using the pre-selection technique and the turbo multiuser detection principle, we not only get good performance but a significant complexity reduction is obtained in the SRBF detector structure as compared with the full complexity of SRBF detector. As mentioned before, the full complexity of the SRBF is in the order of 2^{3U} as the influence of bits beyond one neighbouring symbol are neglected.

5.4 Simulation results

In this section Monte Carlo simulations are presented to illustrate the performance of the hybrid iterative multiuser receiver in terms of the BER averaged over all users. It is assumed that the channel model is both chip and bit synchronous (downlink) with perfect power control. It is also assumed that every user employs a non-recursive nsc code of rate $R_0 = 1/2$, constraint length $\nu = 5$, and generators $(37, 21)$ in octal notation. Each user transmits a block of $L = 200$ data bits. A unique pseudo-random interleaver is used for each of the users. In the simulations, the spreading codes of length N are chosen in a pseudo-random fashion on a bit by bit basis. A

stationary multipath channel with impulse response,

$$H(z) = 0.3482 + 0.8704z^{-1} + 0.3482z^{-2}. \tag{5.14}$$

is considered in the simulations.

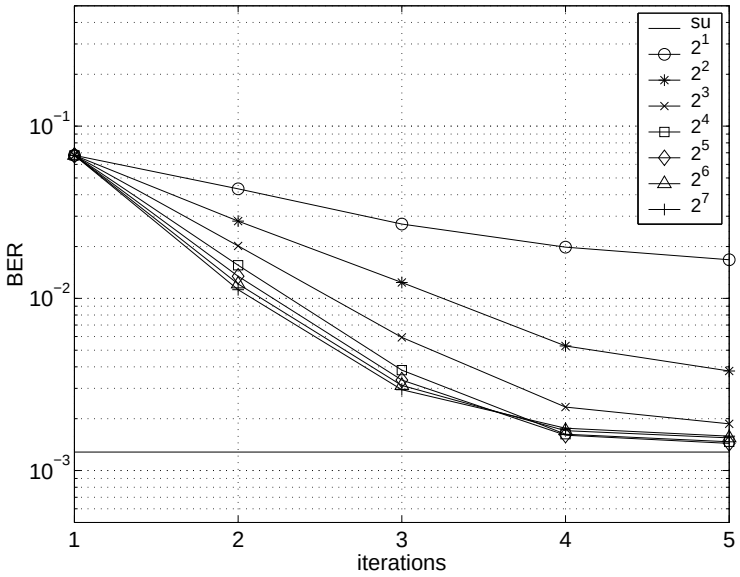

Figure 5.3:

Figure 5.3 shows the BER performance of the HIMR against number of iterations. The simulations were performed with a spreading code length of $N = 7$ and with $U = 5$ active users for $E_b/N_0 = 4dB$. We show the cases when the complexity in the SRBF detector is kept constant at 2^e where $e \, \epsilon \, \{1, 2, \cdots, 7\}$. Note that the full complexity of the SRBF detector for the multipath channel is 2^{15} when 5 users are considered in the system. In Figure 5.3 the simulation indicated by *su* refers to the single-user performance with full complexity in the SRBF detector. From the simulations it can be seen that the SRBF suffers performance degradation if the complexity is set too low. For example, the curve corresponding to 2^1 refers to the case when the complexity (number of centres) in the SRBF detector is kept constant at 2. Clearly, a large number of hard decisions in the vector of virtual users $\underline{\mathbf{b}}(t)$ increases the probability of making a wrong decision. This causes a significant degradation in the performance of the receiver. Therefore, by reducing the number of hard decisions in the vector $\underline{\mathbf{b}}(t)$, *i.e* increasing the number of centres in the SRBF detector, a better BER performance is expected by the iterative multiuser receiver as it is shown in Figure 5.3. It is also evident that a negligible im-

provement in performance is achieved in the HIMR when the number of centres considered in the SRBF detector goes beyond 2^4. This indicates that the performance of the SRBF detector with full complexity can be achieved despite some of the centres in the RBF network have not been considered at all. Therefore, by applying the hybrid structure proposed in Figure 5.2 we are avoiding many unnecessary operations.

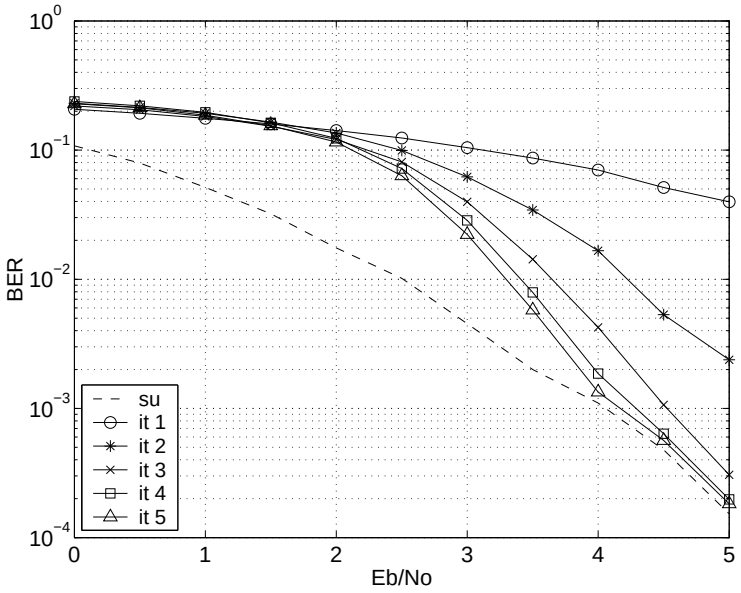

Figure 5.4:

A second simulation is carried out to illustrate the HIMR BER performance as a function of E_b/N_0. The HIMR performance is presented in Figure 5.4 for different number of multiuser iterations. Based on the results obtained in Figure 5.3, the desired complexity for the SRBF detector is kept constant at 2^4 in a system with $N = 7$ and $U = 5$. Again the simulation indicated by *su* refers to the case of the single-user performance with full complexity in the SRBF detector. From the results it can be seen that with only 4 iterations in the receiver, the system performance approaches to the single-user performance in a system with 5 users and $N = 7$ providing an $E_b/N_0 \geq 4dB$.

5.5 Summary

In this chapter, a hybrid iterative multiuser receiver for a multipath DS-CDMA system with FEC coding is derived. This receiver performs signal detection and decoding separately, but

exchanging information in an iterative fashion. A hybrid scheme is proposed to replace the full complexity SRBF detector in the signal detection stage. This scheme uses a linear detector (Wiener detector) on the first iteration of the receiver and then for further iterations a sub-optimal reduced complexity RBF detector is applied. The implementation of a linear detector on the first iteration is used to establish a level of confidence related to how likely the transmitted information can be correctly detected. Based on a pre-selection technique this information is used to reduce the complexity of the SRBF detector which is applied in subsequent iterations of the receiver. It is shown that the complexity in the hybrid receiver is mainly dominated by the complexity in the SRBF detector. Simulation results show that the hybrid receiver can still perform close to the full complexity SRBF detector despite the large reduction in complexity. For example, in the case presented in section 5.4, the complexity of the SRBF is reduced from $2^{15} = 32768$ to $2^4 = 16$ operations per bit detected.

Chapter 6
DS-CDMA System Performance as a Function of Block Size

The development of the turbo multiuser detection principle has attracted new interest in trying to understand how closely practical systems can approach the theoretical limits on system performance. This chapter considers Shannon's sphere-packing bound for analysing the theoretical and practical performance of a DS-CDMA system. These limits will serve as a useful performance benchmark where practical systems of a given rate R_s and information block size L can be compared.

A brief introduction to this chapter is given in the first section (6.1). In section 6.2.1 an outline of the fundamentals of the Shannon's sphere packing lower bound is presented. The formulation of the capacity bounds for a DS-CDMA system, based on Shannon's bound, are developed in section 6.2.2. In section 6.3 the performance evaluation of a simulated DS-CDMA system which applies the turbo multiuser detection principle in the receiver structure is considered. A comparison between the theoretical bounds and the performance achieved by the simulated DS-CDMA system is shown in section 6.4. Finally, a summary of the chapter is given in section 6.5.

6.1 Introduction

A synchronous CDMA system based on direct sequence spread spectrum technique offers considerable advantage over narrowband systems in terms of robustness to multipath. The development of such schemes are mainly for capacity reasons, therefore, in the information theory of a multiple access channel one of the principal goals is to find its capacity limit. This limit represents the set of information rates at which simultaneous reliable communication of the messages of each user is possible. However, practical applications impose constraints on the maximum block length of the information data bits. It is well known that the Shannon's sphere packing bound establishes a lower bound on the error probability for codes with a particular

block size. In this chapter, we reformulate Shannon's bound for a DS-CDMA system and compare the behaviour of this bound to the simulated error probabilities achieved by a practical DS-CDMA communication system.

With the advent of turbo codes, a significant amount of work has been carried out in iterative techniques for multiuser receivers. We make use of this approach to show the comparison between the theoretical bounds and the performance achieved by the DS-CDMA system. We compare the E_b/N_0 required to achieve a particular codeword error probability, P_w, operating over an AWGN channel.

6.2 Capacity limits

It is well known that the Shannon's sphere packing bound establishes a lower bound on the error probability for codes with a particular block size [99]. The development of this bound assumes a spherical block code that consists of a collection of 2^L equal power codewords where L is the number of information symbols. Each codeword is represented by a sequence of n_o code symbols (geometrically it represents a point in an n_o-dimensional Euclidean space) with a signal power n_oP per codeword (each codeword is on the surface of a hypersphere of radius $\sqrt{n_oP}$). The communication channel adds to each channel symbol a Gaussian random variable with distribution $\mathcal{N}(0,\sigma^2)$.

In a typical communication system, additional functions such as error control coding (channel coding) and a suitable modulation scheme are both enveloped in Shannon's bound, as shown in Figure 6.1. Therefore, the code rate, R_0, can then be defined as the ratio of the number of information symbols, L, to the number of channel symbols, n_o, where the amount of information, L, is measured in bits. Thus, the code rate, $R_0 = L/n_o$, is the number of information bits per channel symbol.

6.2.1 Shannon's bound

In what follows, an outline of the fundamentals of the Shannon's sphere packing lower bound is discussed. In this section we present only those expressions of interest to our problem, the more general development of these bounds is analysed in [99].

The fundamental sphere packing lower bound can be expressed in the following form

(a)

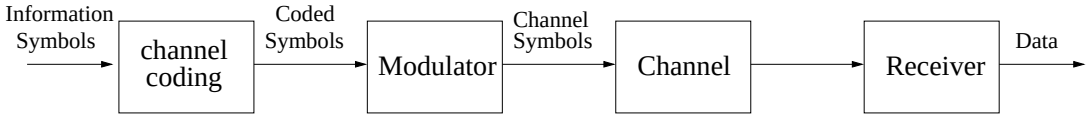

(b)

Figure 6.1: *(a) Shannon's model and (b) a typical communication system model*

$$P_w \geq Q(\theta_1, A_c, n_o) \tag{6.1}$$

where P_w is the codeword error probability, $A_c = \sqrt{2R_0E_b/N_0}$ is the amplitude corresponding to the signal to noise ratio per channel symbol. The scalar $Q(\theta, A_c, n_o)$ is the probability that an n_o-dimensional Gaussian random vector with mean $(A_c, 0, \cdots, 0)$ and covariance $\mathbf{I}_{n_o \times n_o}$ (identity matrix of dimension $n_o \times n_o$) falls outside an n_o-dimensional cone of half angle θ around its mean and θ_1 is the angle such that the n_o-dimensional cone of half angle θ_1 satisfies

$$\begin{aligned} \Omega_{n_o}(\theta_1) &= \frac{\Omega(\theta_1)}{\Omega(\pi)} \\ &= \frac{1}{2^L} \end{aligned} \tag{6.2}$$

where $\Omega(\theta_1)/\Omega(\pi)$ denotes the ratio of the solid angle within an n_o-dimensional cone of half angle θ_1 to the total solid angle of n_o-dimensional Euclidean space (full solid angle of a hypersphere). As given in [99], the expressions for the solid angle function, $\Omega_{n_o}(\theta)$, and the probability function, $Q(\theta, A_c, n_o)$, are denoted by

$$\Omega_{n_o}(\theta) = \int_0^{\theta} \frac{n_o - 1}{n_o} \frac{\Gamma(\frac{n_o}{2} + 1)}{\Gamma(\frac{n_o+1}{2})} (sin\phi)^{n_o-2} d\phi \tag{6.3}$$

and

$$Q(\theta, A_c, n_o) = \int_{\theta}^{\phi} \frac{n_o - 1}{2^{n_o/2}} \frac{(sin\phi)^{n_o-2}}{\sqrt{\pi}\Gamma(\frac{n_o+1}{2})} \int_0^{\infty} x^{n_o-1} \exp^{-(x^2+n_o A_c^2 - 2x\sqrt{n_o}A_c cos\phi)/2} \, dx d\phi \tag{6.4}$$

where $\Gamma(a)$ is the gamma function defined by the integral

$$\Gamma(a) \quad = \quad \int_0^{\infty} e^{-t} t^{(a-1)} dt.$$

Rather than the integrals in (6.3) and (6.4) where no closed form expression exists, asymptotic expressions can be derived for these bounds when n_o is large, [99]. These approximations are denoted in the following form

$$\Omega_{n_o}(\theta) \quad \approx \quad \frac{\Gamma(\frac{n_o}{2}+1)(sin\theta)^{n_o-1}}{n_o\Gamma(\frac{n_o+1}{2})\sqrt{\pi}cos\theta} \tag{6.5}$$

and

$$Q_{n_o}(\theta, A_c, n_o) \quad \approx \quad \frac{(G(\theta, A_c)sin\theta e^{-(A_c^2 - A_c G(\theta, A_c)cos\theta)/2})^{n_o}}{\sqrt{n_o\pi}\sqrt{1+G^2(\theta, A_c)}} \cdot \frac{1}{sin\theta(A_c G(\theta, A_c)sin^2\theta - cos\theta)} \tag{6.6}$$

where $G(\theta) = \frac{1}{2}(A_c cos\theta + \sqrt{A_c^2 cos^2\theta + 4})$. Therefore, a lower bound on the error performance of a code of rate R_0 can be computed using (6.2), (6.5) and (6.6).

6.2.2 Bounds in a CDMA channel

The incorporation of the CDMA channel into the communication model, where the spreading is imposed, yields a multiple access communication channel that can be interpreted in a similar manner to Shannon's model as shown in Figure 6.2. However, this representation instead yields an overall "code" rate that is now defined as the ratio of the number of information symbols produced for all users in the system, UL, to the number of channel symbols, $n_o N$, where the channel symbols are given at the chip rate. Therefore, the code rate of this new representation is given by

$$R_s = \frac{UL}{n_o N} = \frac{U}{N} R_0 \tag{6.7}$$

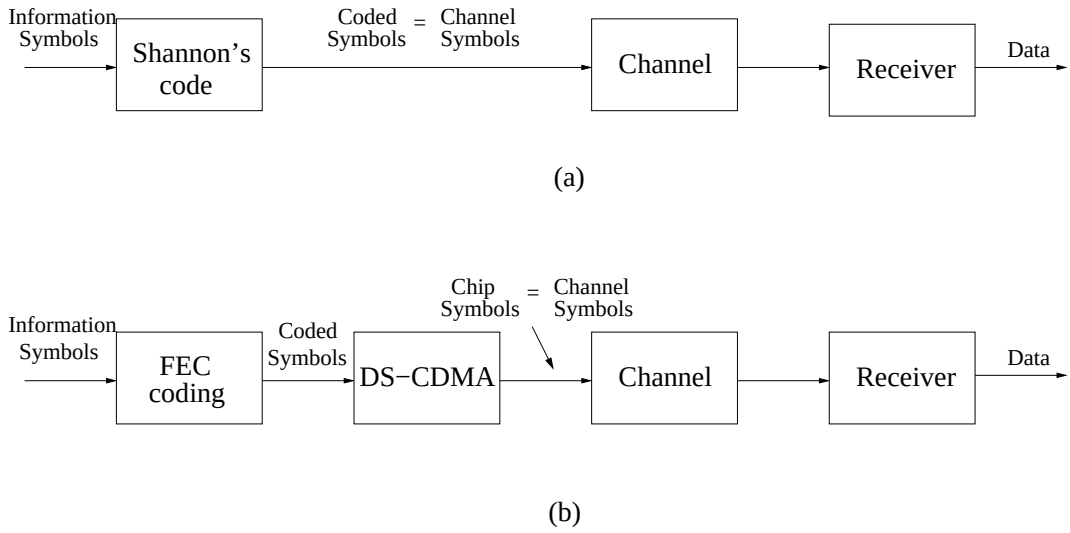

Figure 6.2: *(a) Shannon's model without spreading (b) a DS-CDMA communication system model with FEC coding*

where U is the number of users in the system, L represents the information block size (in bits) per user, n_o the number of FEC coded symbols per information block and N is the number of chips per coded symbol (spreading factor). Assuming a multiuser detection strategy where the multiuser receiver knows exactly the spreading codes of all users and jointly demodulates and detects all users' signals, each channel symbol is then corrupted only by Gaussian noise with variance σ^2. Consequently, the Shannon's sphere packing bound is also applicable to this multiple access model but with a signalling rate R_s instead of R_0 as presented in its original derivation.

A lower bound for the communication model illustrated in Figure 6.2 can be obtained by applying the Shannon's sphere packing lower bound for a code rate R_s. Therefore, using equations (6.2), (6.5), (6.6) the bounds for a FEC coded DS-CDMA system with a rate R_s are obtained. These asymptotic bounds allow us to determine the minimum E_b/N_0 required given a particular signalling rate (R_s) and a desired codeword error probability (P_w) as a function of the information block length (L). In section 6.4 these bounds will be showed as a function of the information block size and the number of users in the DS-CDMA system.

6.3 Performance of a simulated DS-CDMA system

In this section we consider the simulation of a discrete time FEC coded DS-CDMA system in an AWGN channel as shown in Figure 4.1. The communication model consists of U active users that transmit simultaneously and synchronous (both chip and coded bit) through the channel. Every user transmits blocks of L data bits, that is, $\{\mathbf{d}_u(i)\}$; $i \epsilon \{1, 2, \cdots, L\}$ and $u \epsilon \{1, 2, \cdots, U\}$. The information data bits, $\{\mathbf{d}_u(i)\}$, for user u, $u = 1, 2, \cdots, U$, are Convolutionally encoded with a code rate R_0 and then interleaved using a pseudo-random pattern. The interleaved coded bits of the *u*th user are BPSK symbol mapped, yielding the coded bits $\{\mathbf{b}_u(t)\}; t \epsilon \{1, 2, \cdots, L/R_0\}$ where $b_u(t) \epsilon \{1, -1\}$. Each coded bit, $b_u(t)$, is then modulated by a spreading code $\mathbf{c}_u(t)$, whose components are given as $c_{u,n}(t) \epsilon \{1/\sqrt{N}, -1/\sqrt{N}\}$ with $n \epsilon \{1, 2, \cdots, N\}$. The received signal, $\mathbf{r}(t)$, at the bit rate is represented by equation (3.5).

6.3.1 Iterative multiuser receiver

As mentioned earlier, an overall optimal detector/decoder in a DS-CDMA system with FEC coding is using an optimal mapping from the received signals to the original data symbols (multiuser detection and FEC coding jointly) [84]. However, this results in a prohibitive complexity, $O(2^{U\nu})$, which rises exponential in the product of the the number of users U and the constraint length of the convolutional code ν. The analysis of a jointly optimum multiuser receiver and FEC coding will yield the minimum achievable error probability and optimum asymptotic multiuser efficiency in this type of scheme. However, the implementation of this structure is far too complex even for simulation purposes. Therefore, due to this complexity restriction we consider a sub-optimal multiuser receiver based on an iterative scheme as shown in Figure (6.3).

In this section we implement the iterative multiuser receiver with the serial concatenation of the RBF detector and a block of U single-user turbo decoders as presented in Figure (6.3). The use of this scheme will achieve the lowest BER performance for a sub-optimal multiuser receiver with a partitioned structure. The use of the RBF detector will provide us with the best performance for a multiuser detector. On the other hand, turbo codes is one of the most powerful FEC coding scheme proposed so far and therefore we make use of it in the iterative scheme. The complexity of this structure is still too high for real implementation, especially for a large number of users, however it will be useful for understanding the gaps between a

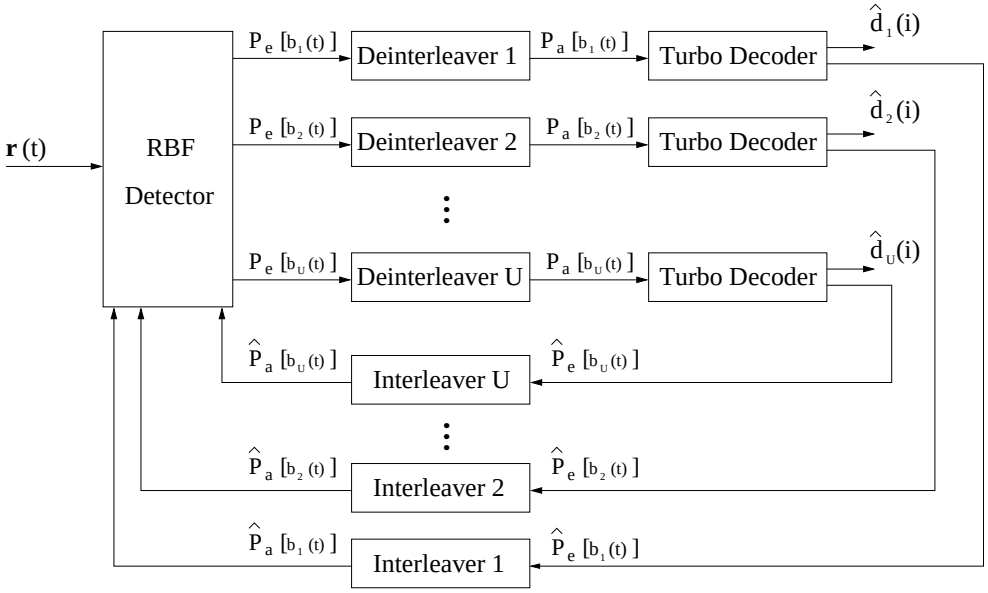

Figure 6.3: *Iterative multiuser receiver.*

practical system and its theoretical bounds. Also this structure can be used as a benchmark in the performance/complexity tradeoff of sub-optimal multiuser receivers.

Similar to previous chapters, a particular attention is focused on the exchange of information through the iterative scheme. Given the received signal, $\mathbf{r}(t)$ (see (3.5)), the RBF detector outputs single-user *a posteriori* information (LLRs) which are then supplied, after deinterleaving, as *a priori* information to the FEC turbo decoders, $P_a[b_u(t)]$; $u \in \{1, 2, \cdots, U\}$. Equally, every single-user FEC turbo decoder provides *a posteriori* information, $\hat{P}_e[b_u(t)]$, which are used after interleaving as *a priori* information, $\hat{P}_a[b_u(t)]$, into the multiuser detector on each iteration.

6.3.1.1 RBF detector

As described in section 3.2.1.1, the RBF detector can be implemented as the optimum multiuser detector over the AWGN channel. Using (3.13) and setting w_l to either $+1$ or -1 subject to the value of $b_u(t)$ in $\mathbf{b}(t)$, a binary decision at the output of the RBF detector would be

$$\hat{b}_u(t) = sgn\left(\sum_{l=1}^{2^{U-1}} \exp\left(-\frac{||\mathbf{r}(t) - \mathbf{a}_l^1(t)||^2}{2\sigma^2}\right) - \sum_{l=1}^{2^{U-1}} \exp\left(-\frac{||\mathbf{r}(t) - \mathbf{a}_l^{-1}(t)||^2}{2\sigma^2}\right)\right) \qquad (6.8)$$

where $\mathbf{a}_l^1(t)$ and $\mathbf{a}_l^{-1}(t)$ (centres of the RBF network) are the noise free input vectors for all possible input data bits given $b_u(t) = 1$ and $b_u(t) = -1$ respectively. The noise variance is denoted by σ^2. However, single-user input probability information is required for the FEC turbo decoders. This probability information is obtained in the RBF detector by computing the LLR of the conditional probabilities given as

$$P_e[b_u(t)] = ln\left(\frac{p(\mathbf{r}(t)|b_u(t)=+1)}{p(\mathbf{r}(t)|b_u(t)=-1)}\right). \tag{6.9}$$

Using Bayes theorem, the conditional probability $p(\mathbf{r}(t)|b_u(t)=b)$ with $b \,\epsilon\, \{-1,+1\}$ can be expressed as

$$p(\mathbf{r}(t)|b_u(t)=b) = \sum_{\substack{\mathbf{b}(t) \\ (b_u(t)=b)}} p(\mathbf{r}(t)|\mathbf{b}(t)) \prod_{\substack{k=1 \\ k\neq u}}^{U} pr(b_k(t)) \tag{6.10}$$

where the conditional probability $p(\mathbf{r}(t)|\mathbf{b}(t))$ is the likelihood of the received sequence, **r**(t), based on the hypothesis that **b**(t) is transmitted. This joint likelihood is generated by the multivariate Gaussian probability density function [46] as given below

$$p(\mathbf{r}(t)|\mathbf{b}(t)) = \frac{\exp\left(-\frac{||\mathbf{r}(t)-\mathbf{a}_l^b(t)||^2}{2\sigma^2}\right)}{(2\pi)^{N/2}\sigma^N} \tag{6.11}$$

where $\mathbf{a}_l^b(t)$ is the noise free input vectors for the input data vector $\mathbf{b}(t)$ in the case that $b_u(t) = b$ with $b \,\epsilon\, \{1,-1\}$. It can be shown that (6.8) and (6.9) are equivalent if a hard decision is performed (in (6.9) $\hat{b}_u(t) = 1$ if $P_e^1[b_u(t)] > 0$, otherwise $\hat{b}_u(t) = -1$). In (6.10) $pr(b_k(t))$ represents the *a priori* information in the multiuser detector on each iteration. In turbo decoding, the output probability of the first MAP decoder is used as *a priori* information for the second MAP decoder.

6.3.1.2 Single-user turbo decoder

The turbo decoder for the *u*th user receives as input and after interleaving the LLR, $P_a[b_u(t)]$, which is generated by the RBF detector. This information is used directly in the first SISO MAP decoder as follows:

$$\gamma_i(\mathbf{Y}_i, s', s) = P\{S_i = s|S_{i-1} = s'\} \prod_{t=n_c(i-1)+1}^{n_c i} p(\mathbf{r}(t)|b_u(t)=b) \tag{6.12}$$

where

$$p(\mathbf{r}(t)|b_u(t)=b)=\begin{cases}\frac{\exp(P_a[b_u(t)])}{1+\exp(P_a[b_u(t)])} & \text{if } b=1\\ \frac{1}{1+\exp(P_a[b_u(t)])} & \text{if } b=-1.\end{cases} \tag{6.13}$$

The noisy received symbols at time i are denoted as $\mathbf{Y}_i = \mathbf{r}(n_c(i-1)+1),\cdots,\mathbf{r}(n_c i)$ and where the product is over all n_c FEC coded bits that produce the transition of the SISO decoder from the state at time $i-1$, s', to the state at time i, s. Since the implementation of the single-user turbo decoders for the scheme in Figure (6.3) is equivalent to that given in section 2.5.2.3, we omit the description of this stage.

6.3.1.3 Iterative principle

In a similar fashion to turbo codes, the single-user turbo decoder output probabilities, $p(b_u(t)=b|\mathbf{r}(t))$, after interleaving are assigned as the *a priori* probabilities in the RBF detector on every multiuser iteration, *i.e* $p(b_u(t)=b)=p(b_u(t)=b|\mathbf{r}(t))$ for $u\,\epsilon\,\{1,2,\cdots,U\}$ and $b\,\epsilon\,\{1,-1\}$. Notice that the iterative multiuser receiver structure in Figure (6.3) comprises two different iterative schemes in its structure; one in the FEC decoder (turbo decoder iterations) and a second one in the multiuser receiver (multiuser iteration between the detector and the decoders). On the first multiuser iteration the *a priori* probabilities in the RBF detector are set to $p(b_u(t)=1)=p(b_u(t)=-1)=0.5$, *i.e* all FEC coded bit sequences are assumed to be equiprobable. At the last multiuser iteration at the receiver, the FEC turbo decoders computes the *a posteriori* LLR of the data bits which are used to make a decision on the decoded bit as follow

$$\hat{d}(i)=\begin{cases}1 & \text{if } \hat{P}_e[d(i)]>0\\ 0 & \text{otherwise.}\end{cases} \tag{6.14}$$

6.3.2 Simulations

In this section, the performance of the iterative multiuser receiver is presented for the DS-CDMA system in an AWGN channel. Figure 6.4 shows the average BER performance of the iterative multiuser receiver as a function of the E_b/N_0 and the multiuser iterations. In the simulations, a DS-CDMA system with $U=5$ active users and processing gain $N=7$ are considered. FEC is provided to every user by using a turbo code of rate $R_0=1/2$ and

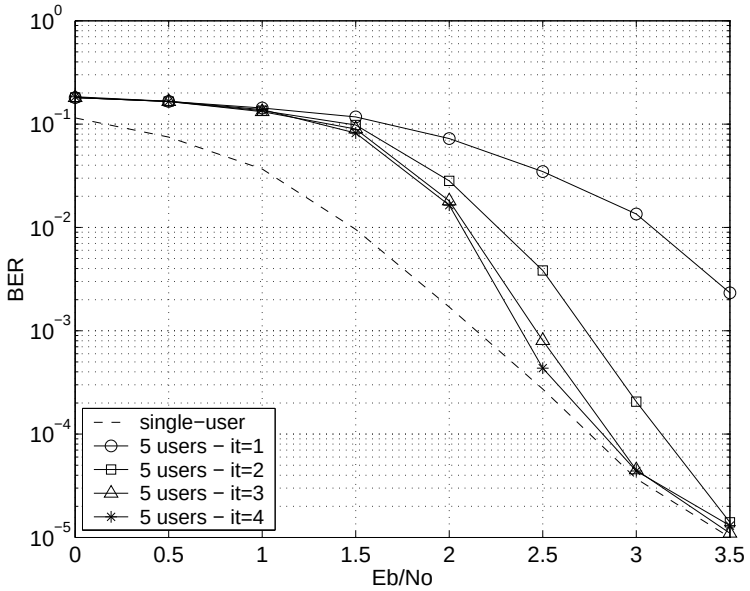

Figure 6.4: *Receiver performance for $U = 5$, $N = 7$ synchronous DS-CDMA channel.*

generators $G_1 = 37$ and $G_2 = 21$ in octal notation. The block size of the data bits for each user is $L = 200$. In the decoder structure the number of turbo decoder iterations was set to 4. Thus, it can be seen in Figure 6.4 that with 5 users in the system the iterative multiuser receiver can achieve a performance near to the single-user bound after 4 multiuser iterations. The simulations were performed with random spreading codes. For this example no effort is made to determine the best combination of turbo decoder iterations and multiuser iterations, instead we would rather highlight the turbo multiuser detection principle.

6.4 Comparison

To enable us to compare with the bounds derived in section 6.2, we analyse and simulate the DS-CDMA system introduced in the previous section in an identical scenario. For practical applications, it is clear that the computational complexity of the iterative multiuser receiver is still prohibitive, however it will be useful to get on understanding how closely a practical system can approach the theoretical limits.

The simulation results are shown in Figure 6.5. The parameters used to compare the achievable performance of this practical system with the theoretical bounds are: $R_0 = 1/3$, $N = 7$, with $U = 5$, 7 and 9 attaining a $P_w = 10^{-2}$. Pseudo-random sequences are employed to spread the

signals of the users. The FEC coding includes a turbo encoder with constraint length $\nu = 5$ and generators $G_1 = 37$, $G_2 = 21$. The same turbo encoder is employed for all users. A combination of 5 turbo decoder iterations and 5 multiuser iterations are applied in the receiver structure. This choice of iterations number was considered after several tests where it was shown that the influence of higher number of iterations was too small to be worth considering. The performance is measured by averaging the codeword error rate (or frame error rate FER) across all the users. Because of the large number of calculations required some simulations for the case of 9 users in the system could not be obtained in a reasonable time.

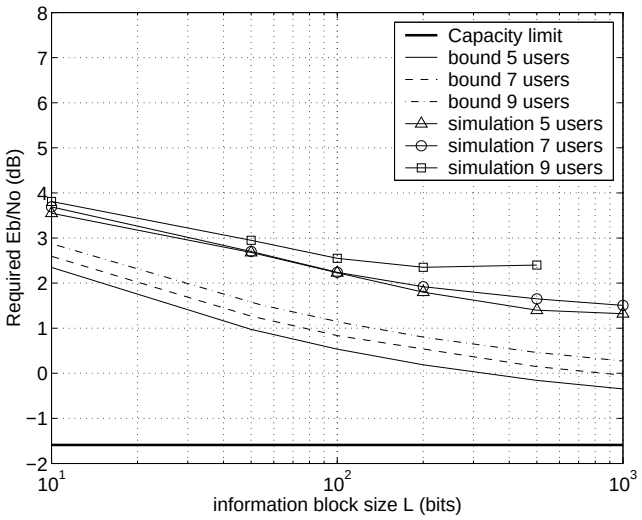

Figure 6.5: *Asymptotic bounds for a DS-CDMA system as a function of the information block length for $R_0 = 1/3$, $N = 7$ and $U = 5, 7$ and 9 achieving a $P_w = 10^{-2}$.*

These results show us that a small block length for these systems puts up the minimum E_b/N_o required for reliable communications. Also it is illustrated that increasing U (the number of users) also increases the minimum E_b/N_0 required for reliable communications. From the simulation results it can be noted that for $U > N$ (*i.e.* 9 users) the minimum E_b/N_o required does not show a similar behaviour as the cases when $U \leq N$. The reason for this is the behaviour of the FEC coding performance when the multiuser interference gets very high. The improvement in the BER performance with larger block sizes is a well known characteristic of turbo codes (also for the FER is illustrated). However, it does not continue at low signal to interference plus noise ratios, which is the case in our simulation results for 9 users in the system.

6.5 Summary

In this chapter we have derived and examined the capacity bounds for a FEC coded DS-CDMA system in an AWGN channel. Using the Shannnon's sphere packing lower bound, the capacity limits for a DS-CDMA system are formulated given the rate R_s and the information block size L. These limits are compared with the achievable capacity of a simulated DS-CDMA system based on an iterative multiuser receiver. The structure of this iterative multiuser receiver comprises the serial concatenation of the RBF detector and a block of FEC turbo decoders that exchange information in an iterative fashion. This approach shows that the performance of this type of system has a similar relationship between block length and required E_b/N_0 as that given by Shannon's sphere packing bound. It has also been found that by using the iterative multiuser receiver the total spectral efficiency in the system is similar to an orthogonal DS-CDMA system. Even though the computational complexity of the suggested iterative multiuser receiver is far too complex to be practical it does show how closely a practical system can approach the theoretical bounds.

Chapter 7
Space-Time Iterative Multiuser Receiver

The increasing demand for wireless services is driving the development of enhanced mobile communication systems in order to address current and future wireless service needs. Improvement of downlink capacity is one of the main challenges facing the effort towards 3G evolution. Poor performance due to the communication channel conditions is one of the problems associated with this type of model. Therefore, research efforts embraces techniques that enhance system performance. Multiuser detection (MUD) and transmit diversity (TD) are two of the key contributing technologies to addressing this problem. In this chapter, we investigate a novel space-time architecture for the downlink of a FEC coded DS-CDMA system that combines these two technologies to increase the system capacity.

The next section gives an introduction to this chapter. Section 7.2 introduces the suggested space-time communication system architecture. Section 7.3 looks into a particular technique to reduce the ISI effect which is faced in most practical systems. A description of the encoder/decoder schemes that provides with the desired transmit diversity gain in the system is given in Section 7.4. Section 7.5 shows the structure of the iterative scheme implemented in the multiuser receiver. The complexity of the proposed system architecture is analysed in Section 7.6. Simulation results are presented in Section 7.7. Finally, in Section 7.8 some conclusions are drawn.

7.1 Introduction

The rapid growth in mobile wireless communications creates the need for increasing system capacity, data rates, and multimedia services. Antenna array techniques and multiuser detection are very promising approaches for obtaining substantial capacity increases in wireless channels. In the last few years, MUD techniques based on iterative schemes have shown to provide a significant performance gain compared to the conventional receiver as demonstrated

in previous chapters. On the other hand, antenna arrays have also shown to be an effective and practical technique to provide spatial diversity, allowing a significant capacity gain over conventional single-antenna systems [100–105]. This spatial diversity is introduced into the signal by transmitting through multiple antennas. For downlink transmissions a major concern is with constraints in cost and size of the receiver. Therefore, transmit diversity techniques tend to provide an effective solution to these scenarios. In this work, transmit diversity is suggested via space time coding (STC) [106–109]. STC is a method for enhancing the level of diversity presented to the receiver in a wireless link, using transmit diversity in order to more efficiently combat the signal fading inherent in wireless communication channels. In general, coding with space and time redundancy is accomplished by finding an efficient way to allocate different symbols to different antennas while containing some type of redundancy for forward error correction.

Recently, an efficient STC scheme [110] called space-time transmit diversity (STTD), has attracted a lot of attention simply because it represents a practical way to improve the performance of current wireless systems. This technique maximises the diversity gain by transmitting through multiple antennas and uses a very simple receiver over a flat fading channel. Thus, motivated by the spatial and temporal capabilities of a DS-CDMA system, in this chapter, we investigate the potential for a high capacity space-time FEC coded DS-CDMA system by combining MUD and STC. We also suggest the reuse of orthogonal codes to increase the system spectral efficiency.

7.2 System model

We consider a FEC coded DS-CDMA communication system operating with M transmit antennas and only 1 receive antenna (suitable for a mobile downlink) as shown in Fig. 7.1 (a). To reduce the signal processing required in the mobile receiver, the system is implemented with only one receive antenna. The fundamentals will be provided to extend this model to the general case of multiple receive antennas. In this chapter, the system performance is considered over two different types of communication channel: flat fading and multipath fading. A number of U active users operates in the system. The total number of users can be seen as two groups of users transmitting information with the same orthogonal spreading codes used by both groups. To be able to separate the groups, each group is given a separation code $\mathbf{s}_1$ or $\mathbf{s}_2$ as shown in Fig. 7.1 (b). The number of users in the system are split into two groups of K and Q users

respectively. Every user in the system transmits blocks of L data bits for FEC purposes. For the rest of this chapter we will refer to this stream as a *data block*. For the *u*th user every *data block*, $\{d_u(i)\}$; $i \epsilon \{1, 2, \cdots, L\}$, $u \epsilon \{1, 2, \cdots, U\}$, is first encoded by a convolutional encoder with a rate R_0 and constraint length ν.

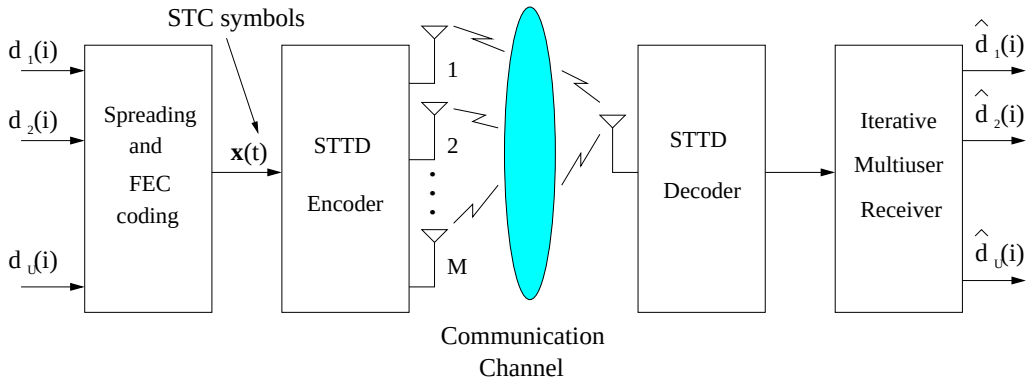

(a)

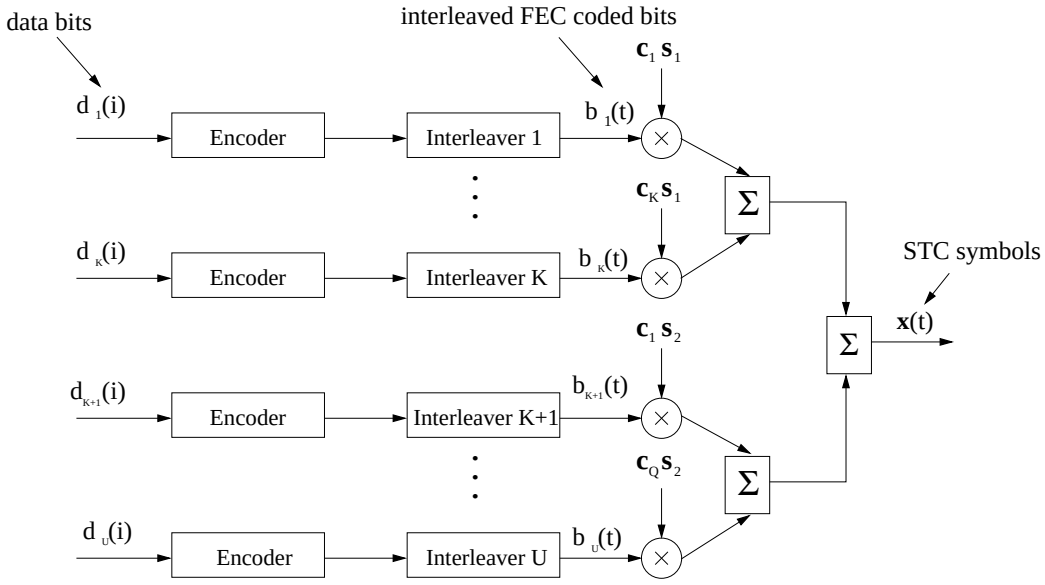

(b)

Figure 7.1: *(a) Space-Time FEC Coded DS-CDMA system architecture and (b) block of spreading FEC coded signals.*

To reduce the effect of burst errors in the input of the FEC decoders, pseudo-random interleaving is applied to the resulting FEC coded bit stream. After interleaving, the stream of

FEC coded bits by the *u*th user appears as $\{b_u(t)\}$; $t \in \{1, 2, \cdots, \frac{L}{R_0}\}$ with $\{b_u(t)\} \in \{-1, 1\}$. Codes of length N are used to spread every user's interleaved FEC coded bits. The multiplexed spreading signals from both groups are then combined to provide with the input to the STTD encoder which at time t can be written as

$$\mathbf{x}(t) = \mathbf{C}\mathbf{b}(t) \tag{7.1}$$

where the user's data vector with dimensions $U \times 1$ is denoted by $\mathbf{b}(t) = [b_1(t), b_2(t), \cdots, b_U(t)]^T$. The $N \times U$ matrix $\mathbf{C}$ contains the spreading and separation codes of the users in the system:

$$\mathbf{C} = \begin{bmatrix} c_{1,1}s_{1,1} & \cdots & c_{K,1}s_{1,1} & c_{1,1}s_{2,1} & \cdots & c_{Q,1}s_{2,1} \\ c_{1,2}s_{1,2} & \cdots & c_{K,2}s_{1,2} & c_{1,2}s_{2,2} & \cdots & c_{Q,2}s_{2,2} \\ \vdots & \ddots & \vdots & \vdots & \ddots & \vdots \\ c_{1,N}s_{1,N} & \cdots & c_{K,N}s_{1,N} & c_{1,N}s_{2,N} & \cdots & c_{Q,N}s_{2,N} \end{bmatrix} \tag{7.2}$$

where the *n*th chip of the spreading and separation code employed by the *u*th user is defined as $c_{u,n}s_{1,n} \in \left\{\frac{-1}{\sqrt{N}}, \frac{1}{\sqrt{N}}\right\}$ for $u \leq K$ and $c_{(u-K),n}s_{2,n} \in \left\{\frac{-1}{\sqrt{N}}, \frac{1}{\sqrt{N}}\right\}$ for $K < u \leq U$, with $s_{1,n}$, $s_{2,n} \in \{-1, 1\}$ as the *n*th element of the group separation code and $n \in \{1, 2, \cdots, N\}$. For the rest of this chapter $\mathbf{x}(t)$ will be referred to as the *STC symbol*. In order to simplify the notation we have also removed the index t in the elements of the spreading codes, *i.e.* for the *u*th user $c_{u,n}(t)$ is replaced by $c_{u,n}$.

The data stream $\{\mathbf{x}(t)\}$; $t \in \{1, 2, \cdots, \frac{L}{R_0}\}$ is then partitioned into blocks of *STC symbols* which are fed to the STTD encoder to yield the data sequence to be transmitted through the M antennas. To guarantee that the overall transmit power is independent of the number of transmit antennas, a factor of $\frac{1}{\sqrt{M}}$ is applied to each of the antennas' signals before transmission. This factor is included in our system by defining the *u*th user amplitude as $b_u(t) \in \left\{\frac{-1}{\sqrt{M}}, \frac{1}{\sqrt{M}}\right\}$.

Similar to section 5.1, we are assuming that the multipath channel spans only one neighbouring data bit, $\alpha < N$. The output of the multipath channel at the chip rate can then be denoted as

$$s(j) = \sum_{m=1}^{M} \sum_{a=0}^{\alpha} h_{m,a}x(j - aT_c) \tag{7.3}$$

where the summations indicate the number of transmit antennas and the channel propagation length (in chips) respectively. To describe the channel output let us first consider the case of

transmitting with only one antenna ($M = 1$). Therefore, with one transmit antenna the channel input is given directly by the data stream $\{\mathbf{x}(t)\}$. Assuming perfect time synchronisation between transmitter and receiver, the received signal which captures all the energy from the information symbol transmitted at time t can alternatively be written as

$$\bar{\mathbf{r}}_t = \mathbf{H}_1^{t+1}\mathbf{x}(t+1) + \mathbf{H}_1^{t}\mathbf{x}(t) + \mathbf{H}_1^{t-1}\mathbf{x}(t-1) + \bar{\boldsymbol{\eta}}(t) \tag{7.4}$$

where the components of the $(N+\alpha)\times 1$ vector $\bar{\mathbf{r}}_t$ are the received signal sampled at the chip rate and $\bar{\boldsymbol{\eta}}(t)$ is a $(N+\alpha)\times 1$ vector with zero mean complex Gaussian noise elements of variance σ^2. The channel response matrix to the transmission of $\mathbf{x}(t)$ is denoted by the $(N+\alpha)\times(N+\alpha)$ Toeplitz matrix

$$\mathbf{H}_1^{t} = \begin{bmatrix} h_{1,0} & 0 & 0 & 0 & \cdots & 0 \\ h_{1,1} & h_{1,0} & 0 & 0 & \cdots & 0 \\ \vdots & & \ddots & & \ddots & \vdots \\ 0 & \cdots & 0 & h_{1,\alpha} & \cdots & h_{1,0} \end{bmatrix}.$$

The terms $\mathbf{H}_1^{t+1}\mathbf{x}(t+1)$ and $\mathbf{H}_1^{t-1}\mathbf{x}(t-1)$ in (7.4) represent the effect of ISI from the next and previous transmitted symbols. The matrices $\mathbf{H}_1^{t+1}$ and $\mathbf{H}_1^{t-1}$ denote $(N+\alpha)\times(N+\alpha)$ Toeplitz matrices given by

$$\mathbf{H}_1^{t+1} = \begin{bmatrix} 0 & 0 & & \cdots & & 0 \\ \vdots & & & \ddots & & \vdots \\ 0 & 0 & & \cdots & & 0 \\ h_{1,0} & 0 & & \cdots & & 0 \\ h_{1,1} & h_{1,0} & 0 & \cdots & & 0 \\ \vdots & & & \ddots & & \vdots \\ h_{1,\alpha-1} & h_{1,\alpha-2} & \cdots & h_{1,0} & 0 \cdots & 0 \end{bmatrix}$$

and

$$\mathbf{H}_1^{t-1} = \begin{bmatrix} 0 & \cdots & 0 & h_{1,\alpha} & h_{1,\alpha-1} & \cdots & h_{1,1} \\ 0 & \cdots & 0 & 0 & h_{1,\alpha} & \cdots & h_{1,2} \\ \vdots & & \ddots & & & \ddots & \vdots \\ 0 & \cdots & 0 & 0 & 0 & \cdots & h_{1,\alpha} \\ 0 & \cdots & 0 & 0 & 0 & \cdots & 0 \\ \vdots & & \ddots & & & \ddots & \vdots \\ 0 & \cdots & 0 & 0 & 0 & \cdots & 0 \end{bmatrix}.$$

When the system transmission is considered over a flat fading channel ($\alpha = 0$), the received signal in (7.4) is simplified to

$$\mathbf{r}(t) = h_{1,0}\mathbf{x}(t) + \boldsymbol{\eta}(t)$$

where $\boldsymbol{\eta}(t)$ is a $N \times 1$ vector of zero mean complex Gaussian noise samples with variance σ^2.

7.3 Reducing the effect of ISI

Orthogonal frequency Division Multiplexing (OFDM) is a modulation technique that resists the effects of a multipath channel when provided with a cyclic prefix (CP) [46]. OFDM uses a CP to preserve orthogonality between narrowband carriers. In a similar fashion, a CP can be appended to each *STC symbol* of the system introduced in Figure 7.1 to avoid the effect of ISI. Figure 7.2 illustrates the effect of incorporating a cyclic prefix for the special case of transmitting with only one antenna ($M = 1$). The two transmit antennas case and the generalisation to more antennas is considered in the next sections. Since ISI occurs only on the first α samples of $\bar{\mathbf{r}}_t$, the ISI effect can be eliminated by simply ignoring the first α samples in the reception of the data vector $\bar{\mathbf{r}}_t$ as shown in Figure 7.2. Therefore, after neglecting the first α samples of the vector $\bar{\mathbf{r}}_t$, the resulting $N \times 1$ vector at the receiver side can be denoted as

$$\hat{\mathbf{r}}_t \stackrel{\text{def}}{=} \bar{\mathbf{r}}_t(\alpha+1, \cdots, \alpha+N) = \mathbf{H}_1\mathbf{x}(t) + \boldsymbol{\eta}(t) \tag{7.5}$$

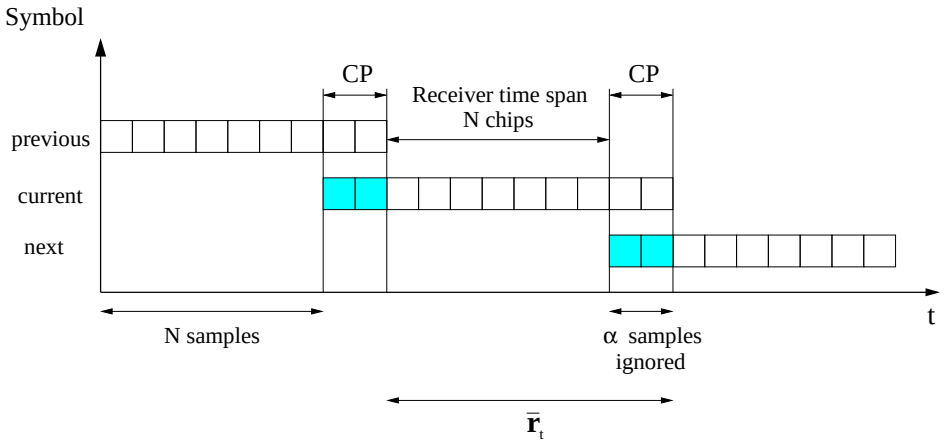

Figure 7.2: *Effect of ISI when a cyclic prefix is incorporated.*

where the channel response matrix $\mathbf{H}_1$ is a $N \times N$ circulant Toeplitz matrix given by

$$\mathbf{H}_1 = \begin{bmatrix} h_{1,0} & 0 & \cdots & 0 & h_{1,\alpha} & h_{1,\alpha-1} & \cdots & h_{1,1} \\ h_{1,1} & h_{1,0} & \cdots & 0 & 0 & h_{1,\alpha} & \cdots & h_{1,2} \\ \vdots & & \ddots & & \ddots & & \ddots & \vdots \\ 0 & \cdots & 0 & 0 & \cdots & h_{1,\alpha} & \cdots & h_{1,0} \end{bmatrix} \tag{7.6}$$

and the noise vector $\boldsymbol{\eta}(t)$ with dimensions $N \times 1$ contains zero-mean complex Gaussian noise samples with variance σ^2.

7.4 Space-time diversity gain

Space-time coding can be implemented either in a trellis form or block form. Space-time trellis coding (STTC) [106] is a recent transmit diversity technique that combines signal processing at the receiver with a specific design of coding technique for multiple transmit antennas. Significant space-time diversity gain is achieved by applying this technique. However, space-time transmit diversity (STTD) [110] is a more remarkable and recent scheme for transmission using two transmit antennas. Despite a loss in performance compared to STTC, the decoding complexity of STTD is much less than STTC. Therefore, in terms of simplicity and performance the STTD scheme is perhaps a better choice for providing space-time diversity gain in real systems. The generalisation of the STTD scheme for more than two transmit antennas is addressed in [111]. For the sake of simplicity, we will focus our attention (unless otherwise stated) mainly

on the case of two transmit antennas and one receive antenna. However, we will provide and establish the fundamentals to extend the scheme to more than two transmit antennas.

7.4.1 STTD encoder for a flat fading channel

Conventional STC encoders with M transmit antennas require the same number of *STC symbol* periods to transmit a block of M *STC symbols*. To clarify exactly how individual *STC symbols* are sent from the transmitter applying the STTD scheme, Figure 7.3 show a layout of the *STC symbols* through the transmit antennas.

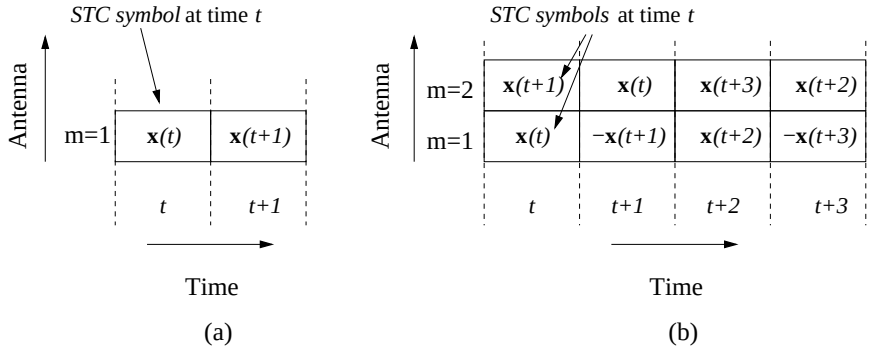

Figure 7.3: *Block transmission through the STC encoder using (a) one transmit antenna ($M = 1$) and (b) two transmit antennas ($M = 2$).*

For comparison purposes, Figure 7.3 (a) shows the scheme for a block transmission using only one transmit antenna. With 2 transmit antennas the scheme is that given in Figure 7.3 (b). Note that when $M = 1$, the STTD encoder output sequence is given directly by its input, *i.e* the stream of *STC symbols* $\{\mathbf{x}(t)\}$, t $\{1, 2, \cdots, L/R_0\}$. For the case of $M = 2$, the *STC symbols* transmitted at the tth time slot are $\mathbf{x}(t)$ and $\mathbf{x}(t+1)$ from antenna 1 and 2 respectively. In the next time slot, $-\mathbf{x}(t+1)$ is transmitted from antenna 1 and $\mathbf{x}(t)$ from antenna 2. The generalisation of the STTD scheme for more than two transmit antennas can be found in [111].

7.4.2 STTD encoder for a multipath fading channel

As described in section 7.3, the ISI effect from the multipath channel can be reduced by incorporating a cyclic prefix (CP) of length equal to the channel length (α) to each *STC symbol*. Figure 7.4 shows the layout of the *STC symbols* through the transmit antennas when the CP is incorporated. Again for comparison purposes the one transmit antenna case is also illustrated.

The CP at time t and antenna m, where $m \,\epsilon\, \{1, 2, \cdots, M\}$, is defined as

$$\text{cyclic prefix} \stackrel{\text{def}}{=} \mathbf{x}(t+N-\alpha+1, \cdots, t+N) \tag{7.7}$$

i.e the last α samples of $\mathbf{x}(t)$. Also to obtain the desired space-time diversity gain, as it will

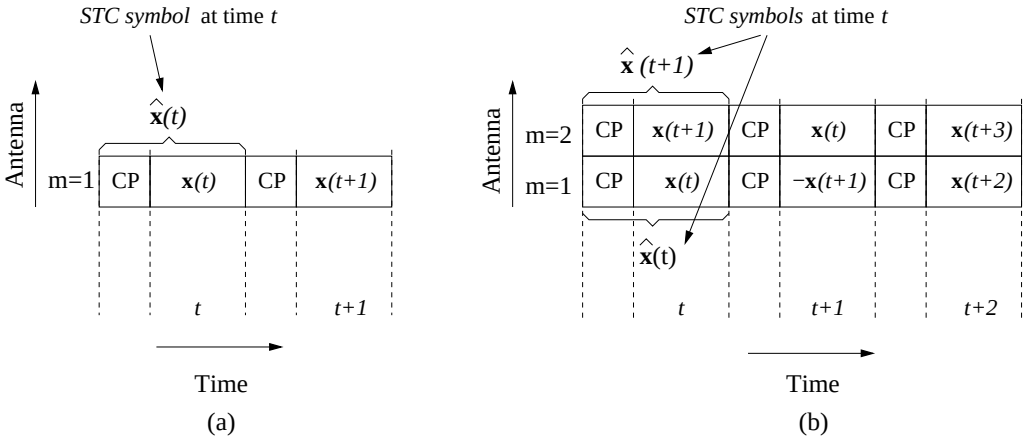

Figure 7.4: *STC encoder scheme for* 1 *and* 2 *transmit antennas with the addition of cyclic prefixes.*

be later described (see section 7.4.4), a real precoding matrix is incorporated into the signal transmitted from each antenna. Therefore, the *t*th *STC symbol* can be now rewritten as follow

$$\hat{\mathbf{x}}(t) \;=\; \mathbf{A}_m \mathbf{C}\mathbf{b}(t) \tag{7.8}$$

where the CP has been incorporated into the precoding matrix $\mathbf{A}_m$. The *m*th matrix $\mathbf{A}_m$ is a $(N+\alpha) \times N$ block matrix defined as

$$\mathbf{A}_m \;=\; \begin{bmatrix} \mathbf{A}_m^0 \\ \mathbf{A}_m^1 \end{bmatrix} \tag{7.9}$$

where the precoding matrix $\mathbf{A}_m^1$ with dimensions $N \times N$ is used to obtain the desired space-time diversity gain as it will be shown in next sections. The $\alpha \times N$ precoding matrix $\mathbf{A}_m^0$, used to incorporate the cyclic prefix, is defined as the last α rows of $\mathbf{A}_m^1$. The matrix $\mathbf{C}$ and vector $\mathbf{b}(t)$ are given as defined in section 7.1.

However, a potential drawback of this scheme is the addition of a CP per *STC symbol* per transmit antenna, with a length at least equal to the channel length. This reduction of the

data throughput is then reflected in a reduction in the overall spectral efficiency of the system. To mitigate this effect we introduce a variation in the scheme by expanding the length of the transmission block from M to $(M \times l)$ *STC symbols*, with $l \in \{1, 2, \cdots\}$. This variation is to reduce the penalty incurred by incorporating a cyclic prefix to every *STC symbol*. As a result, only one cyclic prefix will be required every l *STC symbols*. This new concept can be incorporated in our system by considering a new data stream $\{\bar{\mathbf{x}}(p)\}$; $p \in \{1, 2, \cdots, \frac{L}{R_0 l}\}$ instead of $\{\hat{\mathbf{x}}(t)\}$; $t \in \{1, 2, \cdots, \frac{L}{R_0}\}$. The basic idea is to treat every element in $\{\bar{\mathbf{x}}(p)\}$, which consists of l *STC symbols*, as a new virtual *STC symbol*. Therefore, there are only $\frac{L}{R_0 l}$ virtual *STC symbols* for every *data block*. For this new data scheme, the *p*th element is defined as

$$\bar{\mathbf{x}}(p) = \bar{\mathbf{A}}_m \bar{\mathbf{C}} \bar{\mathbf{b}}(p) \tag{7.10}$$

where

$$\bar{\mathbf{b}}(p) = \begin{bmatrix} \mathbf{b}(t) \\ \mathbf{b}(t+1) \\ \vdots \\ \mathbf{b}(t+l-1) \end{bmatrix} \tag{7.11}$$

is a concatenated vector with dimensions $(U \times l) \times 1$. The $(N \times l) \times (U \times l)$ matrix $\bar{\mathbf{C}}$ is a block diagonal matrix of the form

$$\bar{\mathbf{C}} = \begin{bmatrix} \mathbf{C} & \mathbf{0} & \cdots & \mathbf{0} \\ \mathbf{0} & \mathbf{C} & \cdots & \mathbf{0} \\ \vdots & & \ddots & \vdots \\ \mathbf{0} & \mathbf{0} & \cdots & \mathbf{C} \end{bmatrix} \tag{7.12}$$

in which the $N \times U$ matrix $\mathbf{C}$ is defined by (7.2) and $\mathbf{0}$ is a $N \times U$ null matrix. Similar to (7.8), a real precoding matrix denoted by $\bar{\mathbf{A}}_m$ is included to obtain the desired space-time diversity gain and to incorporate the cyclic prefix. The precoding matrix $\bar{\mathbf{A}}_m$ with $m \in \{1, 2, \cdots, M\}$ is a block matrix of dimensions $(N \times l + \alpha) \times (N \times l)$ defined as

$$\bar{\mathbf{A}}_m = \begin{bmatrix} \bar{\mathbf{A}}_m^0 \\ \bar{\mathbf{A}}_m^1 \end{bmatrix} \tag{7.13}$$

with $\bar{\mathbf{A}}_m^1$ as a $(N \times l) \times (N \times l)$ block diagonal matrix given as

$$\bar{\mathbf{A}}_m^1 = \begin{bmatrix} \mathbf{A}_m^1 & \mathbf{0} & \cdots & \mathbf{0} & \mathbf{0} \\ \mathbf{0} & \mathbf{A}_m^1 & \cdots & \mathbf{0} & \mathbf{0} \\ \vdots & & \ddots & & \vdots \\ \mathbf{0} & \mathbf{0} & \cdots & \mathbf{0} & \mathbf{A}_m^1 \end{bmatrix} \tag{7.14}$$

with $\mathbf{0}$ as a $N \times N$ null matrix. Lastly, the incorporation of the cyclic prefix is denoted by the $\alpha \times (N \times l)$ matrix $\bar{\mathbf{A}}_m^0$ which is defined as the last α rows of $\bar{\mathbf{A}}_m^1$. Notice that only one cyclic prefix will be required every l *STC symbols*, *i.e* one cyclic prefix per virtual *STC symbol*.

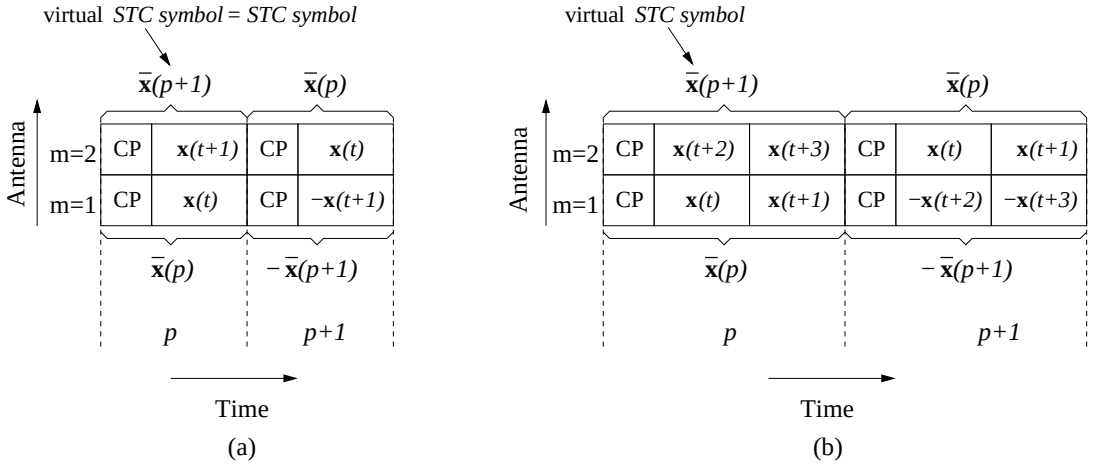

Figure 7.5: *STC encoder scheme with $M = 2$ and a block transmission using (a) $l = 1$ (conventional technique) and (b) $l = 2$.*

To illustrate this new transmission scheme some examples are presented in Figure 7.5. Firstly, Figure 7.5 (a) shows the scheme for a block transmission using $l = 1$ and $M = 2$, *i.e* the number of *STC symbols* is equal to the number of virtual *STC symbols* (conventional technique). On the other hand, a scheme using $l = 2$ is illustrated in Figure 7.5 (b), notice that in this case only the first *STC symbol* of every virtual *STC symbol* requires the incorporation of a cyclic prefix. Therefore, at the *p*th time slot, the virtual *STC symbols* $\bar{\mathbf{x}}(p)$ and $\bar{\mathbf{x}}(p+1)$ are transmitted from antenna 1 and 2 respectively. In the next time slot, *i.e (p+1)*th time slot, $-\bar{\mathbf{x}}(p+1)$ is now transmitted from antenna 1 and $\bar{\mathbf{x}}(p)$ from antenna 2. It is clear that by setting $l = 1$, the STTD encoder scheme incorporate one CP per *STC symbol* transmitted. The criterion for selecting l will depend on two conditions: 1) how rapidly the channel changes and 2) the acceptable receiver complexity. In the following sections the relationship between l and these

two conditions will be explained.

7.4.3 STTD decoder for a flat fading channel

In this section, a flat fading channel is first considered to describe the STTD decoder scheme. With no loss in the generality and in order to illustrate the STTD decoding process, we assume that $M = 2$. It is also assumed that the channel is constant across two consecutive *STC symbols* and that there is a perfect synchronisation between the transmitter and the receiver. For a flat fading channel the block transmission with $M = 2$ is given in Figure 7.3 (b). Therefore, the received signals from the *t*th and (*t*+1)th time slots can be denoted as

$$\begin{aligned} \mathbf{r}_t &= h_{1,0}\mathbf{x}(t) + h_{2,0}\mathbf{x}(t+1) + \boldsymbol{\eta}(t) \\ \mathbf{r}_{t+1} &= h_{2,0}\mathbf{x}(t) - h_{1,0}\mathbf{x}(t+1) + \boldsymbol{\eta}(t+1) \end{aligned} \tag{7.15}$$

where $\mathbf{r}_t$ and $\mathbf{r}_{t+1}$ with dimensions $N \times N$ are the received signals sampled at the chip rate during time t and $t+1$ respectively. The channel effect from the *m*th transmit antenna to the received antenna is modelled by the Rayleigh-distributed random variable $h_{m,0}$ with $m \,\epsilon\, \{1, 2\}$ (no multipath, $\alpha = 0$). The noise vectors $\boldsymbol{\eta}(t)$ and $\boldsymbol{\eta}(t+1)$ with dimensions $N \times 1$ contains zero-mean complex Gaussian noise samples with variance σ^2. For convenience, equation (7.15) can be rewritten in an alternative form by conjugating $\mathbf{r}(t+1)$ and combining the received signal over two consecutive period symbols as follow

$$\begin{bmatrix} \mathbf{r}_t \\ \mathbf{r}^*_{t+1} \end{bmatrix} = \begin{bmatrix} \boldsymbol{\Lambda}_1 & \boldsymbol{\Lambda}_2 \\ \boldsymbol{\Lambda}^*_2 & -\boldsymbol{\Lambda}^*_1 \end{bmatrix} \begin{bmatrix} \mathbf{x}(t) \\ \mathbf{x}(t+1) \end{bmatrix} + \begin{bmatrix} \boldsymbol{\eta}(t) \\ \boldsymbol{\eta}^*(\mathbf{t}+\mathbf{1}) \end{bmatrix} \tag{7.16}$$

where $\boldsymbol{\Lambda}_m = h_{m,0}\mathbf{I}$; $m \,\epsilon\, \{1, 2\}$ and $\mathbf{I}$ as the identity matrix of dimensions $N \times N$. In order to achieve the desired space diversity gain we define

$$\boldsymbol{\Lambda} = \begin{bmatrix} \boldsymbol{\Lambda}_1 & \boldsymbol{\Lambda}_2 \\ \boldsymbol{\Lambda}^*_2 & -\boldsymbol{\Lambda}^*_1 \end{bmatrix} \tag{7.17}$$

and then multiplying (7.16) by $(\boldsymbol{\Lambda}^H\boldsymbol{\Lambda})^{-1}\boldsymbol{\Lambda}^H$, with $()^H$ as the Hermitian operation, we obtain

$$\begin{bmatrix} \mathbf{y}'(t) \\ \mathbf{y}'(t+1) \end{bmatrix} = \begin{bmatrix} \mathbf{x}(t) \\ \mathbf{x}(t+1) \end{bmatrix} + (\boldsymbol{\Lambda}^H\boldsymbol{\Lambda})^{-1}\boldsymbol{\Lambda}^H \begin{bmatrix} \boldsymbol{\eta}(t) \\ \boldsymbol{\eta}(t+1) \end{bmatrix} \tag{7.18}$$

where $\mathbf{y}'(t)$, $\mathbf{y}'(t+1)$ are the estimates of $\mathbf{x}(t)$ and $\mathbf{x}(t+1)$ respectively. Notice that $\mathbf{\Lambda}^H\mathbf{\Lambda}$ is given as $(|h_{1,0}|^2+|h_{2,0}|^2)\mathbf{I}$ with $\mathbf{I}$ as the $2N\times 2N$ identity matrix and $|h_{1,0}|^2+|h_{2,0}|^2$ as the spatial diversity. Taking out the contribution of the signal at time slot t in (7.18) and using (7.1) to replace $\mathbf{x}(t)$, we get

$$\mathbf{y}'(t) \;=\; \mathbf{C}\mathbf{b}(t)+\boldsymbol{\omega}(t) \tag{7.19}$$

where $\boldsymbol{\omega}(t)$ is a $N\times 1$ noise vector. Therefore, we can finish this section by drawing analogies between equation (7.19) and a synchronous DS-CDMA system over an AWGN channel. Since the elements in $\boldsymbol{\eta}(t)$ and $\boldsymbol{\eta}(t+1)$ are complex Gaussian samples, this implies that the elements in $\boldsymbol{\omega}(t)$ are also complex Gaussian samples with zero mean and variance $\sigma^2_{stc}=\sigma^2/(|h_{1,0}|^2+|h_{2,0}|^2)$ as shown in appendix B.3.1.

7.4.4 STTD decoder for a multipath fading channel

Let us consider now the STTD decoder scheme when the transmit signals are propagated through a multipath fading channel. For simplicity we carry on the analysis for the case of $M=2$ and $l=2$ whose block of transmission is presented in Figure 7.5 (b). Therefore, the received signal at the *p*th time slot is denoted by the $(2N+\alpha)\times 1$ vector $\bar{\mathbf{r}}_p$ which includes the effect of the cyclic prefix. Following a similar procedure to that described in section 7.3 to reduce the ISI effect, *i.e* neglecting the first α samples of $\bar{\mathbf{r}}_p$, the resulting $2N\times 1$ vectors from the *p*th and *(p+1)*th time slots are denoted as

$$\begin{aligned}\hat{\mathbf{r}}_p &\overset{\text{def}}{=} \bar{\mathbf{r}}_p(\alpha+1,\cdots,\alpha+2N)\\ \hat{\mathbf{r}}^*_{p+1} &\overset{\text{def}}{=} \bar{\mathbf{r}}^*_{p+1}(\alpha+1,\cdots,\alpha+2N)\end{aligned}$$

or equivalently

$$\begin{aligned}\hat{\mathbf{r}}_p &= \bar{\mathbf{H}}_1\bar{\mathbf{A}}_1^1\bar{\mathbf{C}}\bar{\mathbf{b}}(p)+\bar{\mathbf{H}}_2\bar{\mathbf{A}}_1^1\bar{\mathbf{C}}\bar{\mathbf{b}}(p+1)+\bar{\boldsymbol{\eta}}_p\\ \hat{\mathbf{r}}^*_{p+1} &= \bar{\mathbf{H}}^*_2\bar{\mathbf{A}}_2^1\bar{\mathbf{C}}\bar{\mathbf{b}}(p)-\bar{\mathbf{H}}^*_1\bar{\mathbf{A}}_2^1\bar{\mathbf{C}}\bar{\mathbf{b}}(p+1)+\bar{\boldsymbol{\eta}}^*_{p+1}\end{aligned} \tag{7.20}$$

where the channel responses from each transmit antenna to the receiver antenna are represented by the matrices $\bar{\mathbf{H}}_m$ with $m=1,2$. Similar to (7.6) the *m*th matrix $\bar{\mathbf{H}}_m$ is denoted by a $2N\times 2N$ circulant and Toeplitz matrix with a first row $[h_{m,0},0,\cdots,0,h_{m,\alpha},h_{m,\alpha-1},\cdots,$

$h_{m,1}]$. The properties of these channel matrices allow us to diagonalise them by the FFT basis vectors, *i.e* $\bar{\mathbf{H}}_m$ can be substituted by $\mathbf{W}\mathbf{\Lambda}_m\mathbf{W}^H$ where $\mathbf{W}$ denotes a $2N \times 2N$ matrix whose elements are given as $v_{g,f}$ =exp$(j2\pi gf/2N)/\sqrt{2N}$, with $g, f = 0, \cdots, 2N-1$ and $()^H$ as the Hermitian transpose operation. $\mathbf{\Lambda}_m$ is a $2N \times 2N$ diagonal matrix with $\lambda_{g,g} = \sum_{u=0}^{\alpha} h_{m,u}exp(-j2\pi ug/2N)$ as its diagonal entries and zero elsewhere. Finally, the vectors $\bar{\boldsymbol{\eta}}_p$ and $\bar{\boldsymbol{\eta}}^*_{p+1}$ in (7.20) are $2N \times 1$ complex Gaussian noise vectors.

For convenience the conjugate of $\hat{\mathbf{r}}_{p+1}$, denoted by $*$, is applied in (7.20) and the concatenated vectors $\bar{\mathbf{C}}\bar{\mathbf{b}}(p)$ and $\bar{\mathbf{C}}\bar{\mathbf{b}}(p+1)$ are defined as $\bar{\mathbf{y}}_p$ and $\bar{\mathbf{y}}_{p+1}$ respectively. Thus, multiplying $\hat{\mathbf{r}}_p$ by $\mathbf{W}^H$ and $\hat{\mathbf{r}}^*_{p+1}$ by $\mathbf{W}^T$ in (7.20), we obtain

$$\begin{aligned}
\mathbf{W}^H\hat{\mathbf{r}}_p &= \mathbf{\Lambda}_1\mathbf{W}^H\bar{\mathbf{A}}_1^1\bar{\mathbf{y}}_p + \mathbf{\Lambda}_2\mathbf{W}^H\bar{\mathbf{A}}_1^1\bar{\mathbf{y}}_{p+1} + \mathbf{W}^H\bar{\boldsymbol{\eta}}_p \\
\mathbf{W}^T\hat{\mathbf{r}}^*_{p+1} &= \mathbf{\Lambda}_2^*\mathbf{W}^T\bar{\mathbf{A}}_2^1\bar{\mathbf{y}}_p - \mathbf{\Lambda}_1^*\mathbf{W}^T\bar{\mathbf{A}}_2^1\bar{\mathbf{y}}_{p+1} + \mathbf{W}^T\bar{\boldsymbol{\eta}}^*_{p+1}.
\end{aligned} \tag{7.21}$$

In order to obtain the desired space-time diversity gain, we choose the $N \times N$ precoding matrices $\mathbf{A}_1^1$ as the identity matrix and $\mathbf{A}_2^1$ as defined below

$$\mathbf{A}_2^1 = \begin{bmatrix}
1 & 0 & 0 & \cdots & 0 & 0 & 0 \\
0 & 0 & 0 & \cdots & 0 & 0 & 1 \\
0 & 0 & 0 & \cdots & 0 & 1 & 0 \\
0 & 0 & 0 & \cdots & 1 & 0 & 0 \\
 & \vdots & & & & \vdots & \\
0 & 0 & 1 & \cdots & 0 & 0 & 0 \\
0 & 1 & 0 & \cdots & 0 & 0 & 0
\end{bmatrix}. \tag{7.22}$$

Therefore, using (7.13), (7.14) and (7.22) the matrices $\bar{\mathbf{A}}_1^1$ and $\bar{\mathbf{A}}_2^1$ are obtained. The reason for selecting these precoding matrices is to ensure orthogonality between the signals transmitted from different antennas. This choice of precoding matrices allows us to exploit the equality of $\mathbf{W}^H = \mathbf{W}^T\bar{\mathbf{A}}_2^1$ which is then used to represent $\mathbf{W}^H\hat{\mathbf{r}}_p$ and $\mathbf{W}^T\hat{\mathbf{r}}^*_{p+1}$ in the following form

$$\begin{bmatrix} \mathbf{W}^H\hat{\mathbf{r}}_p \\ \mathbf{W}^T\hat{\mathbf{r}}^*_{p+1} \end{bmatrix} = \begin{bmatrix} \mathbf{\Lambda}_1 & \mathbf{\Lambda}_2 \\ \mathbf{\Lambda}_2^* & -\mathbf{\Lambda}_1^* \end{bmatrix} \begin{bmatrix} \mathbf{W}^H\bar{\mathbf{y}}_p \\ \mathbf{W}^H\bar{\mathbf{y}}_{p+1} \end{bmatrix} + \begin{bmatrix} \mathbf{W}^H\bar{\boldsymbol{\eta}}_p \\ \mathbf{W}^T\bar{\boldsymbol{\eta}}^*_{p+1} \end{bmatrix}. \tag{7.23}$$

It is clear then that by defining

$$\mathbf{\Lambda} = \begin{bmatrix} \mathbf{\Lambda}_1 & \mathbf{\Lambda}_2 \\ \mathbf{\Lambda}_2^* & -\mathbf{\Lambda}_1^* \end{bmatrix} \tag{7.24}$$

and multiplying (7.23) by $\bar{\mathbf{W}}(\mathbf{\Lambda}^H\mathbf{\Lambda})^{-1}\mathbf{\Lambda}^H$, we obtain

$$\begin{bmatrix} \hat{\mathbf{y}}_p \\ \hat{\mathbf{y}}_{p+1} \end{bmatrix} = \begin{bmatrix} \bar{\mathbf{y}}_p \\ \bar{\mathbf{y}}_{p+1} \end{bmatrix} + \bar{\mathbf{W}}(\mathbf{\Lambda}^H\mathbf{\Lambda})^{-1}\mathbf{\Lambda}^H \begin{bmatrix} \mathbf{W}^H\bar{\boldsymbol{\eta}}_p \\ \mathbf{W}^T\bar{\boldsymbol{\eta}}_{p+1}^* \end{bmatrix} \tag{7.25}$$

where $\hat{\mathbf{y}}_p$, $\hat{\mathbf{y}}_{p+1}$ are the estimates of $\bar{\mathbf{y}}_p$ and $\bar{\mathbf{y}}_{p+1}$ respectively. The matrix $\bar{\mathbf{W}}$ is a $4N \times 4N$ block diagonal matrix given as

$$\bar{\mathbf{W}} = \begin{bmatrix} \mathbf{W} & \mathbf{0} \\ \mathbf{0} & \mathbf{W} \end{bmatrix}$$

with $\mathbf{0}$ as a $2N \times 2N$ null matrix. Considering the contribution only of the signal at the *p*th time slot in equation (7.25), we get

$$\hat{\mathbf{y}}_p \;=\; \bar{\mathbf{y}}_p + \boldsymbol{\varphi}_p \tag{7.26}$$

where $\boldsymbol{\varphi}_p$ is a $2N \times 1$ noise vector given as $\boldsymbol{\varphi}_p = \mathbf{W}(|\mathbf{\Lambda}_1|^2 + |\mathbf{\Lambda}_2|^2)^{-1}[\mathbf{\Lambda}_1^*\mathbf{W}^H\bar{\boldsymbol{\eta}}_p - \mathbf{\Lambda}_2\mathbf{W}^T\bar{\boldsymbol{\eta}}_{p+1}^*]$. Since $\bar{\mathbf{b}}(p) = [\mathbf{b}^T(t), \mathbf{b}^T(t+1)]^T$ (see (7.11)) is a concatenated vector and $\bar{\mathbf{y}}_p = \bar{\mathbf{C}}\bar{\mathbf{b}}(p)$, we can further partition (7.26) to extract only the signal related to $\mathbf{b}(t)$, *i.e* as a function of time index t, resulting in

$$\mathbf{y}'(t) \;=\; \mathbf{C}\mathbf{b}(t) + \boldsymbol{\zeta}(t) \tag{7.27}$$

with $\boldsymbol{\zeta}(t)$ the noise vector given by the first N samples of $\boldsymbol{\varphi}_p$. Similar to the previous section, we can draw analogies between equation (7.27) and a synchronous DS-CDMA system over an AWGN channel. The elements in $\bar{\boldsymbol{\eta}}_p$ are complex Gaussian samples then consequently the elements in $\boldsymbol{\zeta}(t)$ are also complex Gaussian samples with zero mean and covariance matrix given by (see appendix B.3.2)

$$\mathbf{V}_{stc} \;=\; \sigma^2\mathbf{W}(|\mathbf{\Lambda}_1|^2 + |\mathbf{\Lambda}_2|^2)^{-1}\mathbf{W}^H. \tag{7.28}$$

The analogy between the model in (7.27) and a synchronous DS-CDMA model for an AWGN channel is then evident. Following the STTD encoding schemes studied in [111] for more that two transmit antennas, a similar process can be used to generalise the procedure presented in this section for $M > 2$.

7.5 Iterative multiuser receiver

The system signals represented in equations (7.19) and (7.27) can be well interpreted as conventional synchronous DS-CDMA systems over an AWGN channel. In this particular case, MAI from the non-orthogonal users and additive noise are the system interference. Therefore, MUD is an approach that can be applied to mitigate these system impairments as suggested in chapter 3. An attractive multiuser receiver structure based on an iterative scheme has been proposed in [92] for interference mitigation in this type of system. In this section, we show that the basic principle is also applicable to the system model introduced in Figure 7.1.

The iterative multiuser receiver structure in [92] has already been described in Figure (4.4) of chapter 4 but where now the input signal is given by the STTD decoder output, $\mathbf{y}'(t)$ (see equations (7.19) and (7.27)), instead of $\mathbf{r}(t)$. As described before, the receiver structure at the first iteration consists of the Wiener detector followed by a single stage of PIC and a block of single FEC decoders. The Wiener detector takes as its input the STTD decoder output, $\mathbf{y}'(t)$, and computes as its output an initial estimate of the logarithm of likelihood (LLR) ratio of the interleaved FEC coded bits for the interfering users, $\hat{P}_a[b_k(t)]$ with $k \neq u$, $k \,\epsilon\, \{1, 2, \cdots, U\}$. The PIC scheme takes the Wiener detector outputs as *a priori* information and yields at its output an improved estimate of $LLRs$ for the users interleaved FEC coded bits, $P_e[b_u(t)]$ with u $\epsilon\, \{1, 2, \cdots, U\}$. The decoding stage, on the other hand, is implemented by a block of identical single SISO MAP decoders. For the *u*th user, this SISO MAP decoder takes as *a priori* input the $LLRs$ of the FEC coded bits, $P_a[b_u(t)]$, from the PIC output (after deinterleaving), and computes at its output the *a posteriori* $LLRs$ of the FEC coded bits, $\hat{P}_e[b_u(t)]$, as well as the *a posteriori* $LLRs$ of the data bits, $\hat{P}_e[d_u(i)]$. The iterative principle is incorporating into the receiver structure by using the *a posteriori* $LLRs$ from the FEC decoders outputs, $\hat{P}_e[b_u(t)]$, as the *a priori* $LLRs$ required at the PIC scheme input for iterations greater than 1. The stream of LLR values for the FEC coded bits at the FEC decoders output are interleaved to yield the appropriate ordering of the data stream at the input of the PIC scheme. Thus, the PIC scheme and the block of single SISO MAP decoders exchange soft information in an iterative

fashion to improve the performance of the multiuser receiver. Finally, after a desired number of iterations, the SISO MAP decoders perform a hard decision on the LLRs, $\hat{P}_e[d_u(i)]$, to recover the original uncoded data stream. Next we describe each of these modules in the context of the system model introduced in Figure 7.1.

7.5.1 Wiener detector

The LLR output of the Wiener detector for the *u*th user is formed as

$$P_e[b_u(t)] \quad = \quad \ln\left(\frac{p(y_u(t)|b_u(t)=\frac{1}{\sqrt{M}})}{p(y_u(t)|b_u(t)=\frac{-1}{\sqrt{M}})}\right) \tag{7.29}$$

where the conditional probabilities, $p(y_u(t)|b_u(t) = b)$ with $b \,\epsilon\, \{\frac{1}{\sqrt{M}}, \frac{-1}{\sqrt{M}}\}$, are calculated assuming Gaussian noise at the output. The scalar $y_u(t) = \mathbf{w}_u^T\{\mathbf{y}'(t)\}_{Re}$ denotes the real part of the Wiener detector output for the *u*th user with mean $\mathbf{w}_u^T\boldsymbol{\phi}_{y'b}^u$ and noise variance $\sigma_w^2(u) = -(\mathbf{w}_u^T\boldsymbol{\phi}_{y'b}^u)^2 + \mathbf{w}_u^T\boldsymbol{\phi}_{y'b}^u$ (see Appendix B.1). The weights of the N tap Wiener filter for the *u*th user, $\mathbf{w}_u = [w_{u,1}, w_{u,2}, \cdots, w_{u,N}]^T$ are given by

$$\mathbf{w}_u \quad = \quad \boldsymbol{\Phi}_{y'y'}^{-1}\boldsymbol{\phi}_{y'b}^u.$$

$\boldsymbol{\Phi}_{y'y'}$ represents the autocorrelation matrix of the input signal with dimensions $N \times N$ which is defined as $\boldsymbol{\Phi}_{y'y'} = \mathbf{C}\mathbf{D}\mathbf{C}^T + \sigma_{stc}^2\mathbf{I}$. The matrix $\mathbf{D}$ is a $U \times U$ matrix with its leading diagonal the power of the users, $\frac{1}{M}$, and zero elsewhere. The matrix $\mathbf{I}$ is the $N \times N$ identity matrix and σ_{stc}^2 the noise variance from the real part of $\boldsymbol{\omega}(t)$ in (7.19) (flat fading channel) or $\boldsymbol{\zeta}(t)$ in (7.27) (multipath fading channel). Since both $\boldsymbol{\omega}(t)$ and $\boldsymbol{\zeta}(t)$ are Gaussian samples with zero mean and covariance matrix $\mathbf{V}_{stc}$, σ_{stc}^2 can be estimated from independent channel realizations and therefore can be precomputed and stored in advance for different cases of signal to noise ratio. The cross-correlation vector $\boldsymbol{\Phi}_{y'b}^u$ is defined as the combination of the user spreading and separation codes (*u*th column of the matrix $\mathbf{C}$) multiplied by the user power ($\frac{1}{M}$).

7.5.2 PIC scheme

The parallel interference cancellation scheme takes soft estimates of the interfering users and subtracts them from the received signal, $\mathbf{y}'(t)$. A matched filter (MF) operation is then applied to generate the output of the PIC scheme. For the *u*th user, this quantity is expressed in the

following form

$$\hat{y}_u(t) = \mathbf{q}_u[\mathbf{b}(t) - \hat{\mathbf{b}}_u(t)] + \psi_u(t) \tag{7.30}$$

where $\mathbf{q}_u$ denotes the *u*th row of the autocorrelation matrix given as $\mathbf{C}^T\mathbf{C}$, the vector $\hat{\mathbf{b}}_u(t)$ corresponds to the soft estimates of the interfering users which are given as $\hat{\mathbf{b}}_u(t) = [\hat{b}_1(t), \cdots, \hat{b}_{u-1}(t), 0, \hat{b}_{u+1}(t), \cdots, \hat{b}_U(t)]$. The soft estimate of user u is formed as

$$\hat{b}_u(t) = \sum_{b\epsilon\{\frac{-1}{\sqrt{M}}, \frac{1}{\sqrt{M}}\}} bp(b_u(t) = b), \quad u = 1, \ldots, U. \tag{7.31}$$

where the conditional probabilities, $p(y_u(t)|b_u(t) = b)$, are taking as the *a priori* probabilities $p(b_u(t) = b)$ required in (7.31), *i.e* $p(b_u(t) = b) = p(y_u(t)|b_u(t) = b)$ with $b \epsilon \{\frac{1}{\sqrt{M}}, \frac{-1}{\sqrt{M}}\}$. Since users from the same group remain orthogonal, we set to zero their contribution in the vector $\hat{\mathbf{b}}_u(t)$. Lastly, $\psi_u(t)$ represents a Gaussian noise sample with zero mean and variance σ^2_{stc}. Since the PIC scheme output for the *u*th user can be modelled on the first iteration by an equivalent AWGN, this output is written in the following form

$$\hat{y}_u(t) = b_u(t) + \mu_u(t) \tag{7.32}$$

with $\mu_u(t)$ as a Gaussian noise sample with zero mean and variance (see Appendix B.2)

$$\sigma^2_\mu(u) = \frac{1}{M}\sum_{\substack{k=1 \\ k\neq u}}^{U} \rho^2_{u,k} + \sigma^2_{stc} \tag{7.33}$$

$\rho_{u,k}$ denotes the cross-correlation factor between user u and user k with $u, k \epsilon \{1, 2, \cdots, U\}$. Finally, the PIC scheme output for user u is then given by

$$P_e[b_u(t)] \quad = \quad \ln\left(\frac{p(\hat{y}_u(t)|b_u(t) = \frac{1}{\sqrt{M}})}{p(\hat{y}_u(t)|b_u(t) = \frac{-1}{\sqrt{M}})}\right). \tag{7.34}$$

7.5.3 Single FEC decoders

FEC coding is provided by employing convolutional codes. The FEC decoder for the *u*th user consists of a single SISO MAP decoder. As shown in Figure 4.4, the $LLRs$ at the output of the PIC scheme, $P_e[b_u(t)]$, are deinterleaved and then passed onto the SISO MAP decoder as *a*

priori information, $P_a[b_u(t)]$. Similar to before, this information is used directly in the MAP's branch metric calculation, *i.e*

$$\gamma_i(\mathbf{Y}_i, s', s) \quad = \quad Pr\{S_i = s/S_{i-1} = s'\} \prod_{t'=n_c(i-1)+1}^{n_c i} p(\hat{y}_u(t')|b_u(t')) \qquad (7.35)$$

where the product is over all the n_c FEC coded bits, $b_u(t)$, values that produce the transition of the MAP decoder from state s' to state s. The MAP decoder algorithm generates as outputs the *a posteriori* $LLRs$ of the data bits, $\hat{P}_e[d_u(i)]$, and also the *a posteriori* LLR's of the FEC coded bits, $\hat{P}_e[b_u(t)]$ as shown in sections 2.5.2.2 and 2.5.2.3. Thus, the LLR outputs $\hat{P}_e[b_u(t)]$ for $u \epsilon \{1, 2, \cdots, U\}$ and $t \epsilon \{1, 2, \cdots, L/(R_0 l)\}$ after interleaving are fed as the *a priori* information required at the PIC scheme input for an iteration greater than 1. Based on the LLR for user u, $\hat{P}_e[d_u(i)]$, a hard decision is performed on the last iteration to recover the uncoded data bits as shown in (3.28).

7.6 Complexity

Since the signal processing required at the transmitter can be easily accommodated in the base stations of current systems, we focus our attention only to the complexity of the receiver structure. In this section, no efforts are made to reduced the computational complexity of the space-time iterative multiuser receiver, instead we highlight the practical implementation of this receiver architecture.

7.6.1 STTD decoder complexity

The complexity of the STTD decoder requires computation of the matrices, $\mathbf{W}^H$ or $\mathbf{W}^T$ (FFT of the received data block), $\mathbf{\Lambda}^H$ and $(\mathbf{\Lambda}^H\mathbf{\Lambda})^{-1}$ (see section 7.4.4). Since $\mathbf{W}$ is known, it can be precomputed and stored in advance. Also $(\mathbf{\Lambda}^H\mathbf{\Lambda})^{-1}$ can be simplified by the fact that $\mathbf{\Lambda}^H\mathbf{\Lambda}$ is a diagonal matrix whose diagonal entries are given by the magnitude of the diagonal elements from the matrices $\mathbf{\Lambda}_m$ with $m = 1, 2, \cdots, M$. Therefore, the computation of $(\mathbf{\Lambda}^H\mathbf{\Lambda})^{-1}$ is then reduced to the scalar inversion of its diagonal elements. It can then be established that the STTD decoder complexity per user is independent of U (the number of users) and mainly determined by the multiplication of matrices, $O((l \times N)^2)$. Since users may be either static or moving, the computation of $\mathbf{\Lambda}^H$ and $(\mathbf{\Lambda}^H\mathbf{\Lambda})^{-1}$ needs to be updated at a higher rate than the

channel Doppler.

In the particular case of a flat fading channel the complexity of this stage is reduced to the multiplication of the matrix $(\mathbf{\Lambda}^H\mathbf{\Lambda})^{-1}\mathbf{\Lambda}^H$. Since $\mathbf{\Lambda}$ is a diagonal matrix, further reduction in complexity is achieved by substituting $\frac{1}{(|h_{1,0}|^2+\cdots+|h_{M,0}|^2)}\mathbf{I}$ instead of $(\mathbf{\Lambda}^H\mathbf{\Lambda})^{-1}$ where the identity matrix $\mathbf{I}$ has the same dimensions as $\mathbf{\Lambda}$.

7.6.2 Iterative multiuser receiver complexity

The complexity per bit per user per iteration of the proposed iterative multiuser receiver is mainly determined by the following operations. Firstly, the major concern in complexity of the Wiener detector is the inversion of the matrix $\mathbf{\Phi}_{y'y'}$, whose complexity is $O(N^3)$ with N as the processing gain. This matrix requires knowledge of the spreading and separation users codes and the noise variance σ^2_{stc} as shown in section 7.5.1. Since the user codes are known, it can be seen that $\mathbf{\Phi}^{-1}_{y'y'}$ mainly changes according to the value of σ^2_{stc}. However, the noise variance σ^2_{stc} can be estimated from independent channel realizations and thus the matrix $\mathbf{\Phi}^{-1}_{y'y'}$ can be precomputed and stored in advance for different cases of σ^2_{stc}. Secondly, the complexity of the constituent convolutional codes of memory ν is $O(G2^{\nu})$. Normally ν is chosen small to reduce the complexity of this stage. Finally, other complexity factors of importance are the complexity contribution from the PIC scheme, which is linear with the number of interfering users G and the processing gain N, $O(GN)$, and the operations required to compute the likelihood metric calculations. For an iteration number > 1, the complexity of the iterative multiuser receiver is reduced to the complexity in the PIC scheme and the SISO MAP decoders. Notice that the complexity in the iterative multiuser receiver structure is independent of the communication channel. In the case of a flat fading channel the input to this stage is given by equation (7.19), while in the multipath fading channel case this is provided by equation (7.27).

7.7 Performance evaluation

Monte Carlo simulations are provided to illustrate the performance of the space-time FEC coded DS-CDMA system proposed in Figure 7.1. To evaluate the performance, the downlink of a synchronous DS-CDMA system with M transmit antennas and 1 receive antenna is considered. Unless otherwise stated, Walsh codes of length $N = 16$ are used to spread the users signals. The channel coefficients, $h_{m,u}$ with $m = 1, 2, \cdots, M$ and $u = 0, 1, \cdots, \alpha$, are sim-

ulated as independent Rayleigh fading random variables. The time-varying impulse response of the channel is power normalised to be $\mathcal{N}(0,1)$. It is assumed that the receiver has perfect knowledge of the fading coefficients.

The model shown in Figure 7.1 allows us to simulate a system with U active users divided into two groups. The separation of the user groups can be done in two different ways: 1) each group with the same number of users, *i.e* $K = Q = U/2$, or 2) a group with K users where $K = N$ if $U > N$ or $K = U$ if $U < N$, and a second group with Q users where $Q = U - K$ if $U > N$ otherwise $Q = 0$. A search through a number of random codes is performed to obtain the group separation codes, $\mathbf{s}_1$ and $\mathbf{s}_2$, of length N. The decision rule to select the separation codes is to have a maximum normalised cross-correlation of $\mathbf{s}_1^T \mathbf{s}_2 \leq 0.5$.

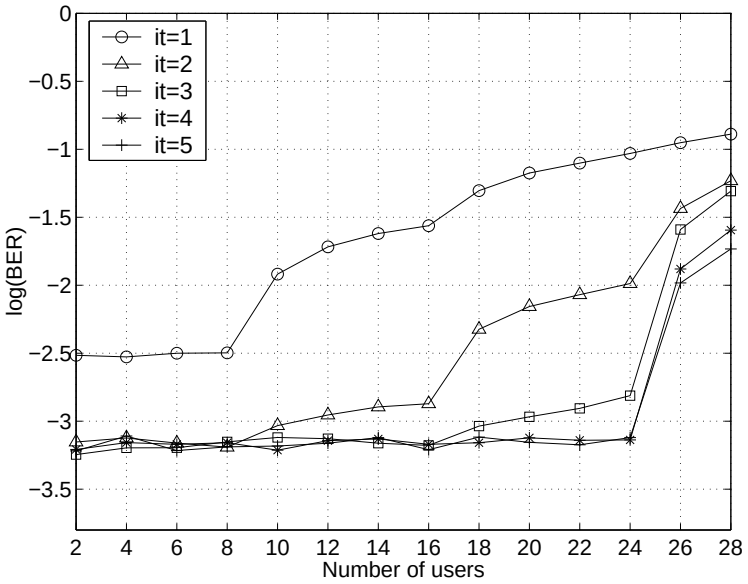

Figure 7.6: *Space-time iterative multiuser receiver BER performance against number of users U in a DS-CDMA system using $M = 2$ with $E_b/N_0 = 5\ dB$.*

7.7.1 Simulation results for a flat fading channel

Let us first evaluate the system performance under the consideration of using $M = 2$ antennas to transmit the multiplexed signals over a flat fading channel ($\alpha = 0$). Every user transmits *data blocks* of $L = 200$ data bits which are then encoded by a recursive systematic convolutional (RSC) code of rate $R_0 = 1/2$, constraint length $\nu = 5$ and generators $(37, 21)$ in octal notation. Figure 7.6 shows the average BER performance of the space-time iterative multiuser receiver

as a function of the number of users U and the number of iterations in the receiver structure. In this case each group in the system is considered to have the same number of users, *i.e* $K = N = U/2$. The system is evaluated using $E_b/N_0 = 5dB$. It is observed from Figure 7.6 that with only 4 iterations in the receiver structure, the system can accommodate up to about $U = 24$ users achieving near single-user performance. This represents a system highly loaded as a total of 24 users are allocated using a processing gain of $N = 16$. When $U > 24$ some degradation appears in the system.

The simulation results in Figure 7.7 shows the average BER performance against the E_b/N_0 for a different number of iterations in the receiver using $M = 2$. Based on the results of Figure 7.6 the number of users is fixed to $U = 24$ divided into two groups, each of 12 users ($K = Q$). To illustrate the diversity gain achieved by using the transmit diversity scheme, Figure 7.7 compares the single-user performance for the cases of $M = 1$ and $M = 2$ transmit antennas.

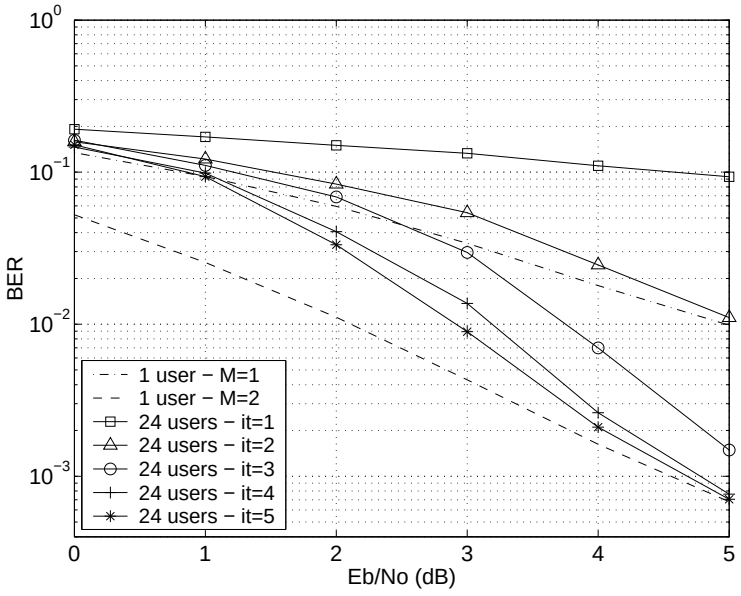

Figure 7.7: *Space-time iterative multiuser receiver BER performance against E_b/N_0 for a DS-CDMA system over a flat fading channel with $M = 2$ and $U = 24$ ($K = Q = U/2$)*

It is seen from the results that significant performance gain is achieved by the proposed space-time DS-CDMA system compared to the conventional DS-CDMA system. Results show that with 4 iterations this highly loaded system in a flat fading channel achieves near single-user performance with diversity from two transmit antennas.

7.7.2 Simulation results for a multipath fading channel

In this section, simulation results are presented for the space-time iterative multiuser receiver over a multipath fading channel. For the rest of this section we will assume that the ISI spans 25% of the symbol period, *i.e* $\alpha = 4$. To illustrate the effect of expanding the STTD encoder input block length as suggested in section 7.4.2, we first present the single-user BER performance versus signal to noise ratio (measured in terms of E_b/N_0) with no FEC coding. Figure 7.8 shows the single-user performance in a multipath fading channel for the cases of 1 and 2 transmit antennas.

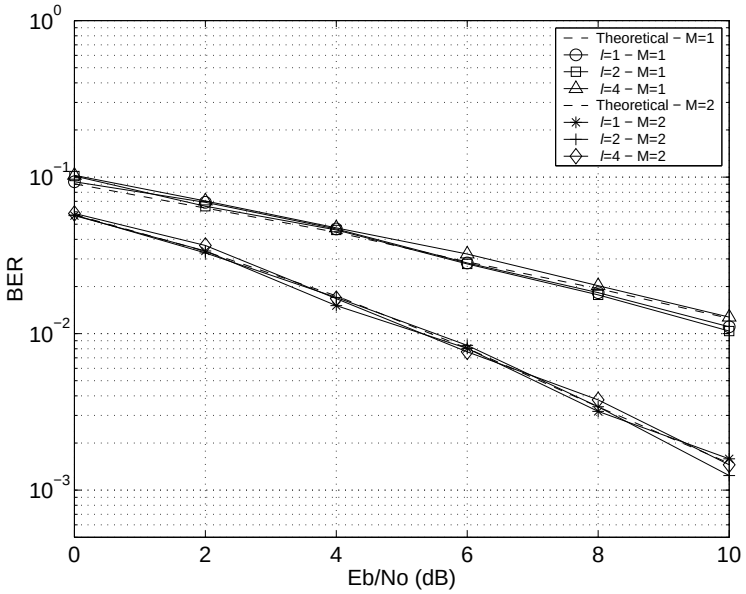

Figure 7.8: *Theoretical and simulated comparison for the single-user BER performance versus E_b/N_0 over a multipath fading channel assuming $\alpha = 4$. The results are obtained for 1 and 2 transmit antennas using $l = 1, 2$ and 4.*

The curves in Figure 7.8 shows the BER performance for a given number of transmit antennas when the STTD encoder input block is set to $l = 1$, $l = 2$ and $l = 4$. From (7.27), after despreading, an expression is derived for the BER performance. Therefore the theoretical performance is also provided to compare with these results. This theoretical BER performance is given as

$$BER = \texttt{erf}\left(\sqrt{\frac{1}{M\sigma_{cw}^2}}\right) \tag{7.36}$$

where the noise power is defined as $\sigma_{cw}^2 = \bar{\mathbf{C}}^T \mathbf{V}_{stc} \bar{\mathbf{C}}$ with $\bar{\mathbf{C}}$ and $\mathbf{V}_{stc}$ as given in equations

(7.12) and (7.28) respectively. An average over $10,000$ independent channel realisations were used to obtain the theoretical BER performance. From the numerical results it can be seen that for a given number of transmit antennas the same performance is obtained in the system regardless of the STTD encoder input block length. Since only one cyclic prefix is required every l *STC symbols* a reduction in the penalty of incorporating cyclic prefixes is achieved. Therefore the higher the block length l the better the throughput in the system.

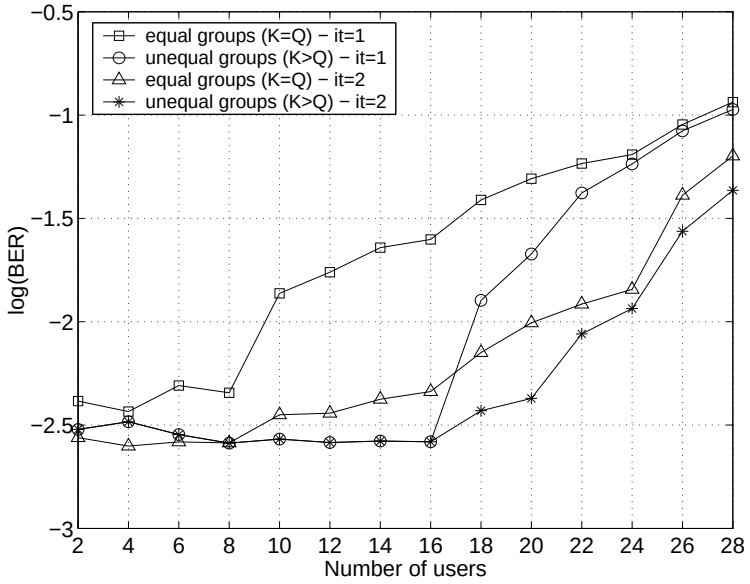

Figure 7.9: *BER versus number of users for a $E_b/N_0 = 4\ dB$ over a multipath fading channel with $\alpha = 4$. The system is implemented for $M = 2$, $l = 1$ with 1 and 2 iterations in the multiuser receiver.*

As mentioned earlier in this section, the total number of active users in the system can be separated in two different ways. To show the system performance under these two schemes, some simulation results are presented in Figure 7.9. FEC coding is implemented by using a RSC code of rate $R_0 = 1/2$, constraint length $\nu = 3$ and generators $(7, 5)$ in octal notation. Every user transmits *data blocks* of $L = 200$ data bits. These results show that when unequal groups ($K > Q$) are considered a better BER performance is obtained in the multiuser receiver. The cases of 1 and 2 multiuser iterations are illustrated. With unequal groups the system can serve up to 16 orthogonal users and the MAI effect does not appear in the system until $U > N$. Even though the BER performance for individuals users can initially differ in each group (the group with Q users faces more MAI that the group with K users), however, this phenomenon is only experienced in the first few iterations of the multiuser receiver as will be shown next.

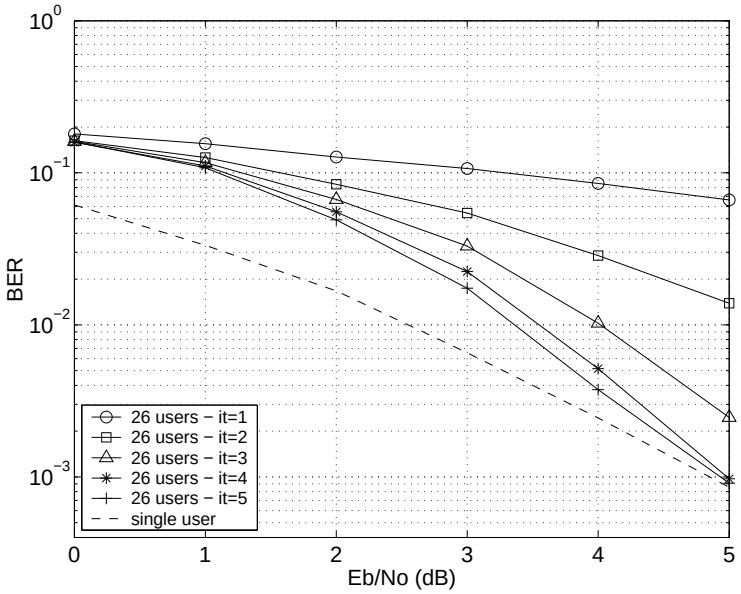

Figure 7.10: *BER against E_b/N_0 for the space-time coded DS-CDMA system over a multipath fading channel with $\alpha = 4$. The system is implemented using $M = 2$, $l = 4$, $N = 16$, $K = 16$, $Q = 10$, $L = 200$ and up to 5 iterations in the multiuser receiver structure.*

Simulation results in Figure 7.10 shows now the average BER performance against E_b/N_0 and the number of iterations in the multiuser receiver. The simulations are performed for a system with $U = 26$ users divided into a group of $K = 16$ and a group of $Q = 10$ users. The system is implemented for $M = 2$ and $l = 4$. Results show that with only four iterations in the multiuser receiver this highly loaded system over a multipath fading channel achieves near single-user performance, *i.e* a probability of error of 10^{-3} with an E_b/N_o of 5 dB.

	Group with K users	Group with Q users	iterations
Best user	0.00107	0.00094	4
Worst user	0.00254	0.00144	4

Table 7.1: *Individual user BER performance for $E_b/N_0 = 5$ dB.*

If we examine the best and worst users, in terms of the BER, from each group after 4 iteration the results for $E_b/N_0 = 5$ dB show that all users converge to about the same average performance as is shown in Table 7.1. This means that no penalty is occurred in individual performances by splitting the users into unequal groups.

7.8 Summary

In this chapter, it has been derived a high capacity space-time FEC coded DS-CDMA system. A space-time iterative multiuser receiver has been proposed to improve the performance and capacity of the system. The main contribution in this work is to combine efficiently MUD and STC techniques to design a receiver capable of mitigating the system impairments. Significant diversity gain is achieved in flat and multipath fading channels by using multiple transmit antennas as compared to the conventional single-antenna systems. The reuse of orthogonal codes is also investigated as a method to enhance further the system capacity.

Numerical results have shown an acceptable performance for systems highly loaded (26 users for a system using a processing gain equal to 16) over a multipath fading channel where the ISI spans 25% of the data symbol. If we were to incorporate cyclic prefixes for each symbol to combat multipath, a reduction in the overall data rate would be yielded. To reduce this penalty a variation in the STTD encoder scheme has been proposed, for instance in the particular case presented in this chapter (choosing $l = 4$) the overall data rate is reduced by only 6.25% instead of 25% as suggested by the conventional scheme (choosing $l = 1$). This penalty can be reduced further if l is made larger still, but at the expense of increasing the complexity at the receiver. It has been assumed that the channel is invariant within a block of symbols, which may not be true for larger blocks. It has also been shown that similar results are obtained by considering a flat fading communication channel.

Chapter 8
Conclusions

The aim of the work presented here was to improve the downlink capacity of DS-CDMA systems by implementing MUD techniques at the mobile receiver. This thesis focuses primarily on new multiuser receiver design using the turbo multiuser detection principle. In this final chapter the main conclusions from the novel findings and future research directions on this work are presented. The following section summarises the work that has been conducted in this thesis which highlights the contributions of this research work. Finally, further research options of this work are discussed in section 8.2.

8.1 Summary and Thesis Contributions

In the last few years, the iterative processing principle used in turbo codes [30] has been successfully applied to a wide variety of problems in wireless communication channels. The approach taken in this thesis is to investigate this principle from the MUD point of view. The aim here is to provide a practical way to increase the possible wireless channel capacity of a DS-CDMA system. Currently, it is a common practise to use MUD in the base stations (uplink), however for 3G cellular, the downlink will be the bottleneck due to constraints in cost, size and weight at the mobile receivers. As the field has matured, non-ideal situations have been gradually incorporated into analysis and simulations to assess their impact on system performance. Today, with the advent of high performance mixed-signal devices, high speed processors, and a better understanding of joint detection structures, the practical implementation of multiuser receivers is actually becoming feasible at the mobile handset.

In chapter 2 we presented a review of key concepts from the existing literature of the communication system of interest. We first review the basic principles of spread spectrum technology and then introduced a general scheme for the downlink of a DS-CDMA system with FEC coding. A detailed description of the basic elements in the communication system, *i.e.* transmitter, communication channel and receiver, is presented. In this chapter the detection of the users is only addressed from the viewpoint of a conventional detector which follows a single user

strategy. The FEC channel coding is also reviewed with a particular interest in turbo codes due to its relationship with the work in this thesis.

In chapter 3 we introduce the turbo multiuser detection principle. A general overview of MUD detection is first presented. Various established MUD techniques are reviewed and compared. It is shown that the optimal multiuser receiver which performs jointly MUD and FEC decoding uses an optimal mapping from the received signals to the original uncoded data symbols. However, it is shown that the computational complexity of this multiuser receiver makes this structure far too complex for practical systems. The prohibitive complexity of this optimum multiuser receiver points to the use of a partitioned scheme that performs signal detection and FEC decoding separately. This implies that the system model can be seen as the serial concatenation of the channel coding (outer code) and the DS-CDMA channel (inner code) where soft information can be exchanged in the same fashion as turbo codes to improve its performance.

In this context, an iterative multiuser receiver for the AWGN channel is introduced in chapter 4 of this thesis. This receiver structure suggests applying a Wiener detector at the front end followed by a block of single FEC decoders. A problem faced when designing a partitioned multiuser receiver with an iterative structure is that of generating the correct single-user input probability information for the FEC decoders and of supplying appropriate *a priori* information to the multiuser detector on each iteration. An accurate noise variance estimate at the Wiener detector output is developed to yield the single-user probabilities required. On the other hand, the iterative principle is introduced by using the output probabilities from the FEC decoders to re-compute the autocorrelation matrix of the input signal in the Wiener detector stage. This is possible by removing the condition of independence between the user's FEC coded bits as shown in section 4.2.1.1. The results show, however, that only a small performance gain is obtained through the iterations in this receiver. With a similar structure, an alternative iterative multiuser receiver is proposed [92]. This new structure incorporates after the Wiener detector a single stage of PIC which aims to provide a more powerful detection stage. In this occasion, a soft-input soft-output PIC scheme based on the single-user probability information is derived to use with the iterative principle. It allows us to obtain and subtract from the desired user an estimate of the MAI which is improved with the number of iterations at the receiver. Also an accurate noise variance estimates at the PIC scheme is developed. It has been shown that this receiver achieves a significant performance improvement over conventional receivers. Furthermore, an overall low-complexity structure is obtained.

The problem with the results in chapter 4 is that we assume a system where a single path is received from the transmitted signal. This almost never occurs in practice so the purpose of chapter 5 is to develop an iterative multiuser receiver that can still remove the system interferences in a multipath channel. The iterative multiuser receiver discussed in chapter 4 applies a Wiener detector at the receiver front end. Linear MUD techniques usually overcome complexity problems but the presence of high levels of MAI and/or ISI due to the multipath scenario results in a poor performance. Such environments make linear techniques incapable of separating the users signals. Therefore, non-linear techniques emerge as the method to improve the receiver performance. Thus, an iterative multiuser receiver based on a hybrid approach is proposed and investigated in chapter 5 for a stationary multipath channel [112]. This receiver explores complexity reduction of the RBF detector by using a scheme based on a pre-selection technique. At the first iteration a Wiener detector is used for detection but this is used solely to establish a level of confidence related to how likely the transmitted information is correctly detected. For further iterations, a reduced complexity RBF detector which includes a pre-selection technique is introduced. The pre-selection approach is developed based on the probability information provided from the FEC decoder outputs in the previous iteration. The iterative multiuser receiver is analysed in terms of performance and complexity. The results revealed that this hybrid receiver almost completely removes the channel interferences despite a large reduction in the receiver complexity as compared to the receiver structure when the full complexity of the RBF detector is included.

In chapter 6, it has been shown that the theoretical limits of a FEC coded DS-CDMA system can be approached by a practical system using the iterative principle [113]. Accordingly, the emphasis is placed on using an iterative multiuser receiver to resolve the interference system problems operating in an AWGN channel. The particular iterative receiver structure considered comprises the concatenation of the RBF detector and a block of FEC turbo decoders. The achievable system performance is investigated with the use of random spreading sequences. A lower bound for a FEC coded DS-CDMA system is derived from the Shannon's sphere packing bound given a data rate R_s and a data block size L. It has been found that the relationship between block size and the required E_b/N_0 is similar to that given by the Shannon's sphere packing bound. From the results, it is determined that the total spectral efficiency of the simulated FEC coded DS-CDMA system is similar to that of an orthogonal system when $U \leq N$. Despite the impractical structure of the receiver considered, its performance is represented as a benchmark for practical systems.

Finally, in chapter 7 the previous work is extended by proposing a novel space-time FEC coded DS-CDMA system which includes antenna arrays [114], [115]. The system spectral efficiency is further enhanced by suggesting a reuse of orthogonal codes. This chapter investigates the performance results for a space-time iterative multiuser receiver operating in two different channels: flat fading and multipath fading. In addition, the STTD technique is described and analysed in both communication channels. The advantage of this technique is its simplicity with regard to its implementation to achieve additional gains over single-antenna systems. Adaption and development of the STTD scheme to reduce the ISI using cyclic prefixes is performed. Also a modified STTD transmission scheme is developed to reduced the penalty of incorporating cyclic prefixes. Results show that a highly spectral efficient DS-CDMA system can be designed by combining MUD and multiple antennas. In particular, we show that near single-user performance can be achieved in a system highly loaded (26 users with a processing gain of 16) operating in a multipath fading channel where the ISI spans 25 % of the data symbol. Additional diversity gains equal to the number of transmit antennas are obtained. Furthermore, a complexity analysis for this receiver is also described. It shows that the receiver architecture can be implemented without a prohibitive complexity.

8.2 Suggestions for future work

Since the invention of Turbo Codes in the past decade, the principle of iterative receivers has been used for various problems in wireless communications. In this thesis, we have only addressed this principle from the viewpoint of multiuser detection. We have studied several interesting iterative multiuser receiver structures which show significant promise in capacity for wireless communication systems. However, there are still open issues concerning the work done in this thesis. In what follows, we present certain points that we consider of great interest for further research work in this topic.

- An important feature which is not considered in this thesis is channel estimation. It would be worth to assess the performance degradation of the various iterative multiuser receivers due to the estimates of the channel parameters.
- For simplicity, certain simplifications and assumptions have been adopted throughout this work. In this thesis, the study of the iterative multiuser receivers is restricted to the binary transmission scheme. However, multi-level transmission schemes are used in

some communication systems in order to increase the bit rate. Therefore, future work in iterative receivers for multi-level transmission scheme would be of great importance.

- An iterative multiuser receiver based on a reduced-complexity RBF detector is addressed in chapter 5. We have shown that using the turbo multiuser detection principle not only performance is improved but also complexity reduction is achieved. However, the results are only obtained using a short spreading factor. For future research, it would be interesting to evaluate the performance and complexity of this iterative multiuser receiver using larger spreading factors. Further complexity reduction in the iterative multiuser receiver could be attempted by exploiting the structural symmetries underlying the generation mechanism of the clusters (centres in the RBF detector) of the received symbols as suggested in [116].

- A non-trivial problem which still remains unsolved is the determination of a closed form solution to the convergence of the iterative multiuser receivers.

- Spatial processing using multiple antennas provides diversity gain which can significantly improve the system capacity and network economics. In chapter 7, we have extended temporal processing techniques to incorporate spatial domain processing. A relatively new but promising area in this direction is the proper exploitation of the coding dimension to achieve better performance of existing space-time algorithms.

Bibliography

[1] W.H. Press, S.A. Teukolsky, W.T. Vetterling, and B.P. Flannery. *Numerical Recipes in C.* Cambridge, USA: Cambridge University Press, second edition, 1992.

[2] L.R. Bahl, J. Cocke, F. Jelinek, and J. Raviv. "Optimal Decoding of Linear Codes for Minimizing Symbol Error Rate". *IEEE Transactions on Information Theory*, IT-20:284–287, March 1974.

[3] B. Sklar. "A Primer on Turbo-Codes Concepts". *IEEE Communications Magazine*, 44(10):94–102, December 1997.

[4] M. Mouly and M.B. Pautet. *The GSM System for Mobile Communications*. Cell&Sys, 1992.

[5] W.C.Y. Lee. *Mobile Communications Engineering:Theory and Applications*. McGraw Hill, 1997.

[6] T. Russell. *Telecommunications Protocols*. McGraw Hill, second edition, 1999.

[7] TIA/EIA/IS-95. *"Mobile Station-Base Station Compatibility Standard for Dual-Mode Wideband Spread Spectrum Cellular System"*. Telecomunication Industry Association, 1993.

[8] V.K. Garg, K. Smolik, and J.E. Wilkes. *Applications of CDMA in Wireless/Personal Communications*. Prentice Hall, 1997.

[9] R. Prasad. *Universal Wireless Personal Communications*. Artech House Publishers: Boston-London, 1998.

[10] S. Pike. "The radio interface for UMTS". In *Proceedings Colloquium on Personal Communications in the 21st Century part I and II, ref no. 1998/214 and 1998/242*, pages 7/1–7/11, February, IEE 1998.

[11] T. Edwards. "Technology trends for personal communications terminals". In *Proceedings of Colloquium on Personal Communications in the 21st Century part I and II, ref no. 1998/214 and 1998/242*, pages 5/1–5/11, February, IEE 1998.

[12] A.J. Viterbi. "The Orthogonal-Random Waveform Dichotomy for Digital Mobile Personal Communication". *IEEE Personal Communications*, 1(1):18–24, First Quarter 1994.

[13] A. Fukasawa, T. Sato, Y. Takizawa, R.E. Fisher, T. Kato, and M. Kawabe. "Wideband CDMA System". In *Proceedings of the 1996 4th International Symposium on Spread Spectrum Techniques and Applications, ISSSTA'96*, volume 1, pages 244–248, IEEE, September 22-25 1996.

[14] E. Dahlman, P. Beming, J. Knutsson, F. Ovesjoe, M. Persson, and C. Roobol. "WCDMA– The Radio Interface for Future Mobile Multimedia Communications". *IEEE Transactions on Vehicular Technology*, 47:1105–1118, November 1998.

[15] E. Dahlman, B. Gudmundson, M. Nilsson, and J. Sköld. "UMTS.IMT-2000 Based on Wideband CDMA". *IEEE Communications Magazine*, pages 70–80, September 1998.

[16] F. Adachi, M. Sawahashi, and H. Suda. "Wideband DS-CDMA for Next Generation Mobile Communications Systems". *IEEE Communications Magazine*, pages 56–69, September 1998.

[17] N. Morinaga, R. Kohno, and S. Sampei. *Wireless Communication Technologies: New Multimedia Systems*. Kluwer International Series in Engineering and Computer Science, Secs 564. Boston: Kluwer Academic Publishers, 2000.

[18] T.S. Rappaport. *Wireless Communications Principles & Practice*. Prentice Hall, 1996.

[19] J.E. Padgett, C.G. Günther, and T. Hattori. "Overview of Wireless Personal Communications. *IEEE Communications Magazine*, pages 28–41, January 1995.

[20] R.A. Scholtz. "The Origins of Spread-Spectrum Communications". *IEEE Transactions on Communications*, 30(5):822–854, May 1982.

[21] R. Price. "Further Notes and Anecdotes on Spread-Spectrum Origins". *IEEE Transactions on Communications*, 31(1):85–97, January 1983.

[22] J. Viterbi. *CDMA: Principles of Spread Spectrum Communication*. Addison-Wesley Wireless Communications, 1995.

[23] P. Jung, P.W. Baier, and A. Steil. "Advantages of CDMA and Spread Spectrum Techniques over FDMA and TDMA". *IEEE Transactions on Vehicular Technology*, 42:357–364, August 1993.

[24] K.S. Gilhousen, I.M. Jacobs, R. Padovani, A.J. Viterbi, L.A. Weaver, Jr., and C.E. Wheatley III. "On the Capacity of the Cellular CDMA System". *IEEE Transactions on Vehicular Technology*, 40(2):303–311, May 1991.

[25] R.L. Pickholtz, D.L. Schilling, and L.B. Milstein. "Theory of Spread-Spectrum Communications—A Tutorial". *IEEE Transactions on Communications*, 30(5):855–884, May 1982.

[26] R.L. Pickholtz, L.B. Milstein, and D.L. Schilling. "Spread Spectrum for Mobile Communications". *IEEE Transactions on Vehicular Technology*, 40(2):313–321, May 1991.

[27] R.C. Dixon. *Spread Spectrum Systems*. Wiley, New York, second edition, 1984.

[28] R. Kohno, R. Meidan, and L. B. Milstein. "Spread Spectrum Access Methods for Wireless Communications". *IEEE Communications Magazine*, pages 58–67, January 1995.

[29] A. Burr. *Modulation and Coding for Wireless Communications*. Prentice Hall, 2001.

[30] C. Berrou and A. Glavieux. "Near Optimum Error Correcting Coding And Decoding: Turbo-Codes". *IEEE Transactions on Communications*, 35(12):1261–1271, October 1996.

[31] C. Heegard and S.B. Wicker. *Turbo Coding*. Kluwer Academic Publishers, 1999.

[32] C. Schlegel and L.C. Perez. "Turbo Codes and Iterative Decoding: Principles and Practice". In *IEEE Vehicular Technology Conference, Houston Tx*, May 1999.

[33] S. Benedetto. "Turbo Codes: Performance, Analysis, Design, Iterative Decoding and Applications". In *IEEE Vehicular Technology Conference Amsterdam, Tutorial 04*, September 1999.

[34] S.S. Pietrobon. "Implementation and performance of a turbo/map decoder". *Int. J. Satellite Communications*, 16:23–46, Jan-Feb 1998.

[35] S.A. Barbulescu and S.S. Pietrobon. "Turbo codes: A tutorial on a new class of powerful error correcting coding schemes Part 1: Code structures and interleaver design, Part

2:Decoder design and performance ". *J. Elec. and Electron. Eng*, 19:129–142, September 1999.

[36] S. Benedetto, D. Divsalar, G. Montorsi, and F. Pollara. "Analysis, Design, and Iterative Decoding Codes with Interleavers". *IEEE Transactions on Selected Areas in Communications*, 16(2):231–244, February 1998.

[37] C. Berrou, A. Glavieux, and P. Thitimajshima. "Near Shannon limit error-correcting coding and decoding:TURBO-CODES". In *IEEE International Conference on Communications*, pages 1064–1070, May 1993.

[38] D. Divsalar and F. Pollara. "Multiple Turbo Codes for Deep-Space Communications". In *TDA Progress Report 42-121*, pages 66–77, May 15 1995.

[39] S. Benedetto and G. Montorsi. "Serial concatenation of block and convolutional codes". *IEE Electronics Letters*, 32(10):887–888, May 1996.

[40] S. Benedetto. "Serial concatenation of interleaved codes: performance analysis, design and iterative decoding". In *ISIT, Ulm Germany*, June 29-July 4 1997.

[41] S. Benedetto and G. Montorsi. "Iterative decoding of serially concatenated convolutional codes". *IEE Electronics Letters*, 32(13):1186–1188, June 1996.

[42] S.A. Barbulescu and S.S. Pietrobon. "Interleaver design for turbo codes". *IEE Electronics Letters*, 30:2107–2108, December 1994.

[43] K.G. Beauchamp. *Walsh Functions and their Applications*. London: Academic Press, 1975.

[44] V.M. DaSilva, E.S. Sousa, and V. Jovanovic. "Effect of Multipath Propagation on the Forward Link pf a CDMA Cellular System". *Wireless Personal Communications*, pages 33–41, 1994.

[45] W. Mohr and M. Kottkamp. "Downlink Performance of IS-95 DS-CDMA under Multipath Propagation Conditions". In *Proceedings of the 1996 4th International Symposium on Spread Spectrum Techniques and Applications, ISSSTA, Mainz, Germany*, pages 1063–1067, IEEE September 1996.

[46] J.G. Proakis. *Digital Communications*. McGraw Hill, fourth edition, 2001.

[47] P.M. Grant, G.J.R. Povey, and R.D. Pringle. "Performance of a Spread Spectrum Rake Receiver Design". In *Proceedings of the 1992 2nd International Symposium on Spread Spectrum Techniques and Applications, ISSSTA*, pages 71–74, IEEE November 1992.

[48] S.R. Saunders. *Antennas and Propagation for Wireless Communication Systems*. Wiley, 1999.

[49] A.J. Viterbi. "Convolutional Codes and Their Performance in Communications Systems". *IEEE Transactions on Communicayions Technology*, COM-19(5):751–772, October 1971.

[50] Hui-Ling Lou. "Implementing the Viterbi Algorithm". *IEEE Signal Processing Magazine*, pages 42–52, September 1995.

[51] C.B. Schlegel. *Trellis Coding*. Piscataway, NJ: IEEE Press, 1997.

[52] J.A. Heller and I.M. Jacobs. "Viterbi Decoding for Satellite and Space Communications". *IEEE Transactions on Communicayions Technology*, COM-19:835–848, October 1971.

[53] M.A. Ambroze. *On turbo codes and other concatenated schemes in communication systems*. PhD Thesis, University of Plymouth, August, 2000.

[54] J. Hagenauer and P. Hoeher. "A Viterbi algorithm with soft-decision outputs and its applications". In *Proceedings Globecom, Dallas, TX*, pages 1680–1686, November 1989.

[55] P. Robertson, E. Villebrun, and P. Hoeher. "A Comparison of Optimal and Sub-optimal MAP Decoding Algorithms Operating in the Log Domain". In *IEEE International Conference on Communications, ICC'95 Seatle*, pages 1009–1013, vol. 2, 1995.

[56] S. Verdu. "Minimum Probability of Error for Asynchronous Gaussian Multiple-Access Channels". *IEEE Transactions on Information Theory*, IT-32:85–96, January 1986.

[57] U. Mitra and H.V. Poor. "Neural Network Techniques for Multiuser Demodulation". In *IEEE International Conference on Neural Networks*, pages 1538–1543, 1993.

[58] B. Mulgrew. "Applying Radial Basis Functions". *IEEE Signal Processing Magazine*, 13(2):50–65, March 1996.

[59] R.O. Duda and P.E. Hart. *Pattern Classification and Scene Analysis*. J. Wiley and Sons, New York, USA, 1st edition, 1973.

[60] K.S. Schneider. "Optimum Detection of Code Division Multiplexed Signals". *IEEE Transaction Aerospace Elect. Systems*, AES-15:181–185, January 1979.

[61] R. Kohno, M. Hatori, and H. Imai. "Cancellation Techniques of Co-Channel Interference in Asynchronous Spread Spectrum Multiple Access Systems". *Elect. and Commun. in Japan*, 66-A(5):20–29, 1983.

[62] R. Lupas and S. Verdu. "Near-Far Resistance of Multi-User Detectors in Asynchronous Channels". *IEEE Transactions on Communications*, 38(4):496–508, April 1990.

[63] R. Lupas and S. Verdu. "Linear Multi-User Detectors for Synchronous Code-Division Multiple-Access Channels". *IEEE Transactions on Information Theory*, 35(1):123–136, January 1989.

[64] S. Moshavi. "Multi-User Detection for DS-CDMA Communications". *IEEE Communications Magazine*, pages 124–136, October 1996.

[65] Z. Xie, R.T. Short, and C.K. Rushforth. "A Family of Suboptimum Detectors for Coherent Multi-User Communications". *IEEE Transactions on Selected Areas in Communications*, 8(4):683–690, May 1990.

[66] R. Lupas-Golaszewski and S. Verdu. "Asymptotic Efficiency of Linear Multi-User Detectors". In *Proc. 25th Conf. on Decision and Control, Athens, Greece*, pages 2094–2100, December, 1986.

[67] S. Verdu. "Multi-User Detection". In *Advances in Statistical Signal Processing, vol. 2, JAI Press*, pages 369–409, 1993.

[68] A. Duel-Hallen, J. Holtzman, and Z. Zvonar. "Multi-User Detection for CDMA Systems". *IEEE Personal Communications*, 2(2):46–58, April 1995.

[69] S. Moshavi. "Survey of Multi-User Detection for DS-CDMA Systems". In *Bellcore pub., IM-555*, August 1996.

[70] S. Verdu. *Multiuser Detection*. Cambridge Univeristy Press, 1998.

[71] S. Haykin. *Adaptive Filter Theory*. Prentice-Hall, 1991.

[72] D.G.M. Cruickshank. "Optimal and Adaptive FIR Filter Receivers for DS-CDMA". In *Personal Indoor and Mobile Radio Communications (PIMRC)*, pages 1339–1343, August 1994.

[73] D.G.M. Cruickshank. "Optimal and Adaptive FIR Filter Receivers for DS-CDMA". In *in Proceedings PIMRC*, pages 1339–1343, 1994.

[74] R. Tanner, D.G.M. Cruickshank, C.Z.W. Hassell Sweatmann, and B. Mulgrew. "Receivers for Nonlinearly Separable Scenarios in DS-CDMA". *IEE Electronics Letters*, 33(25):2103–2105, December 1997.

[75] E.A. Al-Susa and D.G.M. Cruickshank. "Pre-selection Based Reduced Complexity MLMUD for DS-CDMA Systems". In *IEEE Vehicular Technology Conference, VTC 2001 Spring*, pages 491–495, May 2001.

[76] L. Wei, L.K. Rasmussen, and R. Wyrwas. "Near Optimum Tree Search Schemes for Bit Synchronous Multiuser CDMA Systems over Gaussian and Two Path Rayleigh-Fading Channels". *IEEE Transactions on Communications*, 45:691–700, June 1997.

[77] A. AlRustamani. "Greedy Multiuser Detection Over Single-Path Fading Channel". In *Proceedings of the 5th IEEE International Symposium on Spread Spectrum Techniques and Applications (ISSSTA), NY, USA, vol1.*, pages 708–712, September 2000.

[78] M.K. Varanasi and B. Aazhang. "Multistage Detection in Asynchronous Code-Division Multiple-Access Communications". *IEEE Transactions on Communications*, 38(4):509–519, April 1990.

[79] P. Patel and J. Holtzman. "Performance Comparison of a DS/CDMA System Using a Successive Interference Cancellation (IC) Scheme and a Parallel IC Scheme under Fading". In *IEEE International Conference on Communications, New Orleans*, pages 510–514, May 1994.

[80] A. Duel-Hallen. "Decorrelator Decision-Feedback Multi-User Detector for Synchronous Code-Division Multiple-Access Channel". *IEEE Transactions on Communications*, 41(2):285–290, February 1993.

[81] A. Duel-Hallen. "A Family of Multi-User Decision-Feedback Multi-User Detectors for Asynchronous Code-Division Multiple-Access Channels". *IEEE Transactions on Communications*, 43(2/3/4):421–434, February/March/April 1995.

[82] R.M. Buehrer, N.S. Correal, and B.D. Woerner. "A Comparison of Multiuser Receivers for Cellular CDMA". In *in Proceedings of IEEE Global Communications Conference, GLOBECOM'96 (London, UK)*, pages 1571–1577, November 1996.

[83] T.R. Giallorenzi and Stephen G. Wilson. "Suboptimum Multiuser Receivers for Convolutionally Coded Asynchronous DS-CDMA Systems". *IEEE Transactions on Communications*, 44(9):1183–1196, September 1996.

[84] T.R. Giallorenzi and Stephen G. Wilson. "Multiuser ML Sequence Estimator for Convolutionally Coded Asynchronous DS-CDMA Systems". *IEEE Transactions on Communications*, 44(8):997–1008, August 1996.

[85] S. Benedetto, D. Divsalar, G. Montorsi, and F. Pollara. "A Soft-Input Soft-Output APP Module for Iterative Decoding of Concatenated Codes". *IEEE Communications Letters*, 1(1):22–24, January 1997.

[86] H.V. Poor. "Turbo Multiuser Detection: An Overview.

[87] M. Moher. "An Iterative Multiuser Decoder for Near-Capacity Communications". *IEEE Transactions on Communications*, 46(7):870–880, July 1998.

[88] M.C. Reed, C.B. Schlegel, P.D. Alexander, and J.A. Asenstorfer. "Iterative Multiuser Detection for CDMA with FEC: Near-Single-User Performance". *IEEE Transactions on Communications*, 46(12):1693–1699, December 1998.

[89] P.D. Alexander, M.C. Reed, J.A. Asenstorfer, and C.B. Schlegel. "Iterative Multiuser Interference Reduction: Turbo CDMA". *IEEE Transactions on Communications*, 47(7):1008–1014, July 1999.

[90] X. Wang and H.V Poor. "Iterative (Turbo) Soft Interference Cancellation and Decoding for Coded CDMA". *IEEE Transactions on Communications*, 47(7):1046–1060, July 1999.

[91] H.K. Sim and D.G.M. Cruickshank. "An Iterative Multiuser Receiver for FEC Coded CDMA". In *in Proceedings IEEE 6th International Symposium on Spread Spectrum Techniques and Applications (ISSSTA'00), New Jersey, USA*, pages 728–732, September 2000.

[92] J.M. Luna Rivera, D.G.M. Cruickshank, and J.S. Thompson. "Iterative Multiuser Receiver for a Coded DS-CDMA System". In *in Proceedings IEEE Vehicular Technology Conference (VTC 2001 spring), Rhodes Island, Greece*, pages 1518–1522, May 2001.

[93] A.A. AlRustamani, A.D. Damnjanovic, and B.R. Vojcic. "Turbo Greedy Multiuser Detection". *IEEE Transactions on Selected Areas in Communications*, 19(8):1638–1645, August 2001.

[94] D.G.M. Cruickshank. "Suppression of multiple access interference in a DS-CDMA system using Wiener filtering and parallel cancellation.

[95] E.A. Alsusa and D.G.M. Cruickshank. "Pre-selection Based Reduced Complexity MLMUD for DS-CDMA Systems". In *in Proceedings IEEE Vehicular Technology Conference (VTC 2001 spring), Rhodes Island, Greece*, pages 491–495, May 2001.

[96] Z. Xie and C.K. Rushforth. "Multiuser Signal Detection Using Sequential Decoding". *IEEE Transactions on Communications*, 38:578–583, August 1990.

[97] E.A. Alsusa and D.G.M. Cruickshank. "A Comparative Study on Reduced Complexity Maximum Likelihood Based CDMA Multiuser Detectors". In *in Proceedings IEEE Vehicular Technology Conference (VTC 2001 fall), Atlantic City, USA*, pages 1889–1893, October 2001.

[98] D.G.M. Cruickshank. "Radial Basis Funtions Receivers for DS-CDMA". *IEE Electronics Letters*, 32(3):188–190, February 1996.

[99] C. E. Shannon. "Probability of Error for Optimal Codes in a Gaussian Channel". *The Bell System Technical Journal*, XXXVIII(3):611–655, May 1959.

[100] G.J. Foschini. "Layered Space-Time Architecture for Wireless Communication in Fading Environments When Using Multiple Antennas". *Bell Labs Techn. Journal*, 2, Autumn 1996.

[101] D. Agrawal, V. Tarokh, A. Nagui, and N. Seshadri. "Space-Time Code OFDM for High Data Rate Wireless Communication over Wideband Channels". In *in Proceedings IEEE Vehicular Technology Conference (VTC 1998), Ottawa, Ontario, Canada*, pages 2232–2236, May 1998.

[102] V. Tarokh, N. Seshadri, and A.R. Calderbank. "Space-Time Codes for High Data Rate Wireless Communication: Performance criterion and code construction". *IEEE Transactions on Communications*, 47(2):199–207, February 1999.

[103] S. Marinkovic, B. Vucetic, and A. Ushirokawa. "Space-Time Iterative and Multistage Receiver Structures for CDMA Mobile Communications Systems". *IEEE Transactions on Selected Areas in Communications*, 19(8):1594–1604, August 2001.

[104] A.J. Paulraj and C.B. Papadias. "Space-Time Processing for Wireless Communications". *IEEE Signal Processing Magazine*, 14(6):49–83, November 1997.

[105] L.C. Godara. "Applications of Antenna Arrays to Mobile Communications, Part I: Performance Improvement, Feasibility, and System Considerations". *IEEE Proceedings*, 85(7):1031–1060, July 1997.

[106] A.E. Naguib, N. Seshadri, and A.R. Calderbank. "Increasing Data Rate over Wireless Channels". *IEEE Signal Processing Magazine*, pages 76–92, May 2000.

[107] H.E. Gamal and A.R. Hammons, Jr. "A New Approach to Layered Space-Time Coding and Signal Processing". *IEEE Transactions on Information Theory*, 47(6):2312–2334, September 2001.

[108] B. Hochwald, T.L. Marzetta, and C.B. Papadias. "A Transmitter Diversity Scheme for Wideband CDMA Systems Based on Space-Time Spreading". *IEEE Transactions on Selected Areas in Communications*, 19(1):48–59, January 2001.

[109] D. Bevan and R. Tanner. "Performance Comparison of Space-Time Coding Techniques". *IEE Electronics Letters*, 35(20):1707–1708, September 1999.

[110] S.M. Alamouti. "A Simple Transmit Diversity for Wireless Communications". *IEEE Transactions on Selected Areas in Communications*, 16(8):1451–1458, October 1998.

[111] V. Tarokh, H. Jafarkhani, and A.R. Calderbank. "Space-Time Block Codes from Orthogonal Designs". *IEEE Transactions on Information Theory*, 45(5):1456–1467, July 1999.

[112] J.M. Luna Rivera, D.G.M. Cruickshank, and J.S. Thompson. "Hybrid Iterative Multiuser Receiver for a Coded DS-CDMA System". In *in Proceedings IEEE International Symposium on Spread Spectrum Techniques and Applications (ISSSTA'02), Prague, Czech Republic*, September 2002.

[113] J.M. Luna Rivera, D.G.M. Cruickshank, and J.S. Thompson. "Capacity Bounds for a Coded DS-CDMA System as a Function of Block Size". In *in Proceedings IEEE Vehicular Technology Conference (VTC 2001 fall), Atlantic City, USA*, October 2001.

[114] J.M. Luna Rivera, D.G.M. Cruickshank, and J.S. Thompson. “Space-Time Iterative Multiuser Receiver for a Coded DS-CDMA System in a Flat Fading Channel”. In *in Proceedings IEEE Vehicular Technology Conference (VTC 2002 fall), Vancouver, Canada*, September 2002.

[115] J.M. Luna Rivera, D.G.M. Cruickshank, and J.S. Thompson. A High Capacity Space-Time FEC Coded DS-CDMA System for Use over Multipath Channels. *Submitted to IEEE Transactions on Wireless Communications*.

[116] Y. Kopsinis and S. Theodoridis. “A Novel Low Complexity Cluster Based MLSE Equalizar for QPSK Signaling Scheme”. In *in Proceedings IEEE 14th International Conference on Digital Signal Processing*, pages 45–48, 2002.

Appendix A
Derivation of the Wiener detector components

A.1 Autocorrelation matrix

To show the value of matrix $\mathbf{P}'$ in (4.3) let us consider the case of $N = 3$ and $U = 2$. Therefore, equation (4.2) becomes

$$\mathbf{\Phi}_{rr} = E\begin{bmatrix} r_1^2(t) & r_1(t)r_2(t) & r_1(t)r_3(t) \\ r_1(t)r_2(t) & r_2^2(t) & r_2(t)r_3(t) \\ r_1(t)r_3(t) & r_2(t)r_3(t) & r_3^2(t) \end{bmatrix} \tag{A.1}$$

where

$$r_n(t) = \sum_{k=1}^{2} b_k(t)c_{k,n} + n_n(t) \tag{A.2}$$

for all $n \epsilon \{1, 2, 3\}$. Taking the expectation to each element in $\mathbf{\Phi}_{rr}$, this matrix is then denoted as

$$\mathbf{\Phi}_{rr} = \begin{bmatrix} E[r_1^2(t)] & E[r_1(t)r_2(t)] & E[r_1(t)r_3(t)] \\ E[r_1(t)r_2(t)] & E[r_2^2(t)] & E[r_2(t)r_3(t)] \\ E[r_1(t)r_3(t)] & E[r_2(t)r_3(t)] & E[r_3^2(t)] \end{bmatrix} \tag{A.3}$$

with

$$E[r_n(t)r_g(t)] = b_1^2(t)c_{1,n}^2 + b_2^2(t)c_{2,n}^2 + 2E[b_n(t)]E[b_g(t)]c_{1,n}c_{2,n} + \sigma^2 \tag{A.4}$$

in the case that $g = n$ with $g, n \epsilon \{1, 2, 3\}$, otherwise ($g \neq n$)

$$\begin{aligned} E[r_n(t)r_g(t)] = {} & b_1^2(t)c_{1,n}c_{1,g} + b_2^2(t)c_{2,n}c_{2,g} + E[b_1(t)]E[b_2(t)]c_{1,n}c_{2,g} \\ & + E[b_1(t)]E[b_2(t)]c_{1,g}c_{2,n}. \end{aligned} \tag{A.5}$$

Note that we are assuming that $E[b_u(t)] \neq 0$, for $u \, \epsilon \, \{1, 2\}$. Therefore, we can show that by using (A.4) and (A.5) to compute all the elements in $\mathbf{\Phi}_{rr}$, the resulted matrix can be rearrenged in the following form

$$\mathbf{\Phi}_{rr} = \begin{bmatrix} c_{1,1} & c_{2,1} \\ c_{1,2} & c_{2,2} \\ c_{1,3} & c_{2,3} \end{bmatrix} \begin{bmatrix} b_1^2(t) & E[b_1(t)]E[b_2(t)] \\ E[b_1(t)]E[b_2(t)] & b_2^2(t) \end{bmatrix} \begin{bmatrix} c_{1,1} & c_{1,2} & c_{1,3} \\ c_{2,1} & c_{2,2} & c_{2,3} \end{bmatrix} + \sigma^2 \mathbf{I}$$

or equivalently

$$\mathbf{\Phi}_{rr} = \mathbf{C}\mathbf{P}'\mathbf{C}^T + \sigma^2 \mathbf{I} \tag{A.6}$$

where $\mathbf{P}'$ is defined as

$$\mathbf{P}' = \begin{bmatrix} b_1^2(t) & E[b_1(t)]E[b_2(t) \\ E[b_1(t)]E[b_2(t)] & b_2^2(t) \end{bmatrix}. \tag{A.7}$$

The 3×2 matrix $\mathbf{C}$ represents the spreading codes matrix and $\mathbf{I}$ the identity matrix with dimensions 2×2. Using a similar procedure, it can be shown that the generalisation of the matrix $\mathbf{\Phi}_{rr}$ is given by (A.6) but where now P is defined as

$$\mathbf{P} = \begin{bmatrix} b_1^2(t) & E[b_1(t)]E[b_2(t)] & \cdots & E[b_1(t)]E[b_U(t)] \\ E[b_1(t)]E[b_2(t)] & b_2^2(t) & \cdots & E[b_2(t)]E[b_U(t)] \\ \vdots & & \ddots & \vdots \\ E[b_1(t)]E[b_U(t)] & E[b_2(t)]E[b_U(t)] & \cdots & b_U^2(t) \end{bmatrix} \tag{A.8}$$

$\mathbf{C}$ is the $N \times U$ spreading codes matrix and $\mathbf{I}$ the $U \times U$ identity matrix.

A.2 Crosscorrelation vector

Considering again the example described in appendix A.1, *i.e* $N = 3$ and $U = 2$, for the *u*th user the crosscorrelation vector denoted by $\boldsymbol{\phi}_{rb}^u$ is given by

$$\boldsymbol{\phi}_{rb}^u = E\left[b_u(t) \begin{bmatrix} r_1(t) \\ r_2(t) \\ r_3(t) \end{bmatrix} \right]. \tag{A.9}$$

where $r_n(t)$ with $n \epsilon \{1,2,3\}$ is the received signal at the chip rate. For $u = 1$ and using (A.2) to substitute $r_n(t)$ in (A.9) we obtain

$$\boldsymbol{\phi}_{rb}^{u} = E\begin{bmatrix} b_1^2(t)c_{1,1} + b_u(t)b_2(t)c_{2,1} + b_u(t)n_1(t) \\ b_1^2(t)c_{1,2} + b_u(t)b_2(t)c_{2,2} + b_u(t)n_2(t) \\ b_1^2(t)c_{1,3} + b_u(t)b_2(t)c_{2,3} + b_u(t)n_3(t) \end{bmatrix} \tag{A.10}$$

where $\boldsymbol{\phi}_{rb}^{u}$ can be further simplified to

$$\boldsymbol{\phi}_{rb}^{u} = E\begin{bmatrix} b_1^2(t)c_{1,1} + E[b_1(t)]E[b_2(t)]c_{2,1} \\ b_1^2(t)c_{1,2} + E[b_1(t)]E[b_2(t)]c_{2,2} \\ b_1^2(t)c_{1,3} + E[b_1(t)]E[b_2(t)]c_{2,3} \end{bmatrix}. \tag{A.11}$$

It is then straightforward to show that the crosscorrelation vector for the *u*th user in a system with U users becomes

$$\boldsymbol{\phi}_{rb}^{u} = \begin{bmatrix} E[b_u(t)]E[b_1(t)]c_{1,1} \cdots + b_u^2(t)c_{u,1} + \cdots E[b_u(t)]E[b_U(t)]c_{U,1} \\ E[b_u(t)]E[b_1(t)]c_{1,2} \cdots + b_u^2(t)c_{u,2} + \cdots E[b_u(t)]E[b_U(t)]c_{U,2} \\ \vdots \\ E[b_u(t)]E[b_1(t)]c_{1,N} \cdots + b_u^2(t)c_{u,N} + \cdots E[b_u(t)]E[b_U(t)]c_{U,N} \end{bmatrix} \tag{A.12}$$

Appendix B
Noise variance estimates

B.1 Wiener detector output

The minimum mean square error (MMSE) of the Wiener detector output for the *u*th user is given as

$$\begin{aligned} MMSE &= E[(b_u(t) - y_u(t))^2] \\ &= E[b_u^2(t)] - 2E[b_u(t)y_u(t)] + E[y_u^2(t)] \end{aligned} \tag{B.1}$$

where $E[]$ denotes the expected value. The variance of the Wiener detector output is given by

$$\sigma_w^2(u) = E[y_u^2(t)] - E^2[y_u(t)]. \tag{B.2}$$

On the other hand, the Wiener detector output for the *u*th user is $y_u(t) = \mathbf{w}_u^T \mathbf{r}(t)$, therefore, substituting $y_u(t)$ in (B.1) we obtain

$$\begin{aligned} MMSE &= E[(b_u(t) - \mathbf{w}_u^T \mathbf{r}(t))(b_u(t) - \mathbf{w}_u^T \mathbf{r}(t))^T] \\ &= E[b_u^2(t) - 2\mathbf{w}_u^T \mathbf{r}(t) b_u(t) + \mathbf{w}_u^T \mathbf{r}(t) \mathbf{r}^T(t) \mathbf{w}_u] \\ &= E[b_u^2(t)] - 2\mathbf{w}_u^T E[\mathbf{r}(t) b_u(t)] + \mathbf{w}_u^T E[\mathbf{r}(t) \mathbf{r}^T(t)] \mathbf{w}_u \\ &= E[b_u^2(t)] - 2\mathbf{w}_u^T \boldsymbol{\phi}_{rb}^u + \mathbf{w}_u^T \boldsymbol{\Phi}_{rr} \mathbf{w}_u \end{aligned} \tag{B.3}$$

since $\mathbf{w}_u = \boldsymbol{\Phi}_{rr}^{-1} \boldsymbol{\phi}_{rb}^u$, then (B.3) can be further simplified to

$$\begin{aligned} MMSE &= E[b_u^2(t)] - 2\mathbf{w}_u^T \boldsymbol{\phi}_{rb}^u + \mathbf{w}_u^T \boldsymbol{\Phi}_{rr} \boldsymbol{\Phi}_{rr}^{-1} \boldsymbol{\phi}_{rb}^u \\ &= E[b_u^2(t)] - \mathbf{w}_u^T \boldsymbol{\phi}_{rb}^u \end{aligned} \tag{B.4}$$

therefore, by subtracting equation (B.1) from equation (B.2) and substituting $MMSE$ as given in (B.4), we get

$$\begin{aligned}\sigma_w^2(u) &= -E^2[y_u(t)] + 2E[b_u(t)y_u(t)] - E[b_u^2(t)] + MMSE \\ &= -(\mathbf{w}_u^T\boldsymbol{\phi}_{rb}^u)^2 + 2\mathbf{w}_u^T\boldsymbol{\phi}_{rb}^u - E[b_u^2(t)] + E[b_u^2(t)] - \mathbf{w}_u^T\boldsymbol{\phi}_{rb}^u \\ &= -(\mathbf{w}_u^T\boldsymbol{\phi}_{rb}^u)^2 + \mathbf{w}_u^T\boldsymbol{\phi}_{rb}^u \end{aligned} \tag{B.5}$$

B.2 PIC detector output

From (4.12) in section 4.2.1.2 the variance of $\mu_u(t)$ is given as

$$\sigma_\mu^2(u) = E[\mu_u^2(t)] - E^2[\mu_u(t)] \tag{B.6}$$

where again E[] denotes the expected value and $\mu_u(t)$ is given by

$$\mu_u(t) = \sum_{\substack{k=1 \\ k\neq u}}^{U} \rho_{u,k}[b_k(t) - \hat{b}_k(t)] + n_u(t) \tag{B.7}$$

with $\rho_{u,k}$ as the cross-correlation factor between user u and user k. Assuming that $E[b_u(t)] = 0$ but $E[\hat{b}_u(t)] \neq 0$ for $u = 1, 2, \cdots, U$ and using (B.7), we get

$$E^2[\mu_u(t)] = \left(\sum_{\substack{k=1 \\ k\neq u}}^{U} -\rho_{u,k} E[\hat{b}_u(t)] \right)^2 \tag{B.8}$$

and

$$E[\mu_u^2(t)] = \sum_{\substack{k=1 \\ k\neq u}}^{U} \rho_{u,k}^2 E[b_u^2(t)] + \left(\sum_{\substack{k=1 \\ k\neq u}}^{U} -\rho_{u,k} E[\hat{b}_u(t)] \right)^2 + \sigma_n^2 \tag{B.9}$$

therefore it can be shown that the variance σ_μ^2 is then given by

$$\sigma_\mu^2(u) = \sum_{\substack{k=1 \\ k\neq u}}^{U} \rho_{u,k}^2 + \sigma_n^2 \tag{B.10}$$

B.3 STTD decoder output

B.3.1 Flat fading channel

In a flat fading channel the output of the STTD decoder is shown in equation (7.18) of section 7.4.3. The matrix $\mathbf{\Lambda}$ is defined in (7.17) where $\mathbf{\Lambda}_m = h_{m,0}\mathbf{I}$; $m \,\epsilon\, \{1, 2\}$ with the identity matrix $\mathbf{I}$ of equal dimensions than $\mathbf{\Lambda}_m$. Therefore, the noise vector in (7.18) can also be expressed as follow

$$(\mathbf{\Lambda}^H\mathbf{\Lambda})^{-1}\mathbf{\Lambda}^H \begin{bmatrix} \boldsymbol{\eta}(t) \\ \boldsymbol{\eta}(t+1) \end{bmatrix} = \frac{1}{|h_{1,0}|^2 + |h_{2,0}|^2} \begin{bmatrix} \mathbf{\Lambda}_1^* & \mathbf{\Lambda}_2 \\ \mathbf{\Lambda}_2^* & -\mathbf{\Lambda}_1 \end{bmatrix} \begin{bmatrix} \boldsymbol{\eta}(t) \\ \boldsymbol{\eta}(t+1) \end{bmatrix}. \quad \text{(B.11)}$$

Thus, it is easy to show that the noise vector at time t can be denoted as

$$\begin{aligned} \boldsymbol{\omega}(t) &= \frac{1}{|h_{1,0}|^2 + |h_{2,0}|^2}(\mathbf{\Lambda}_1^*\boldsymbol{\eta}(t) + \mathbf{\Lambda}_2\boldsymbol{\eta}(t+1)) \\ &= \frac{1}{|h_{1,0}|^2 + |h_{2,0}|^2}(h_{1,0}^*\boldsymbol{\eta}(t) + h_{2,0}\boldsymbol{\eta}(t+1)). \end{aligned} \quad \text{(B.12)}$$

Therefore, the variance of the *n*th element in $\boldsymbol{\omega}(t)$, denoted by $\omega_n(t)$ with $n \,\epsilon\, \{1, 2, \cdots, N\}$, is defined as

$$\sigma_{stc}^2 = E[\omega_n^2(t)] - E^2[\omega_n(t)] \quad \text{(B.13)}$$

where E[] denotes the expected value. Since $\boldsymbol{\eta}(t)$ and $\boldsymbol{\eta}(t)$ are noise vectors with zero-mean complex Gaussian noise samples and variance σ^2, then we can obtain σ_{stc}^2 as follow

$$\sigma_{stc}^2 = E\left[\left(\frac{h_{1,0}^*\eta_n(t) + h_{2,0}\eta_n(t+1)}{|h_{1,0}|^2 + |h_{2,0}|^2}\right)\left(\frac{h_{1,0}\eta_n^*(t) + h_{2,0}^*\eta_n^*(t+1)}{|h_{1,0}|^2 + |h_{2,0}|^2}\right)\right]$$

or equivalenlty

$$\begin{aligned} \sigma_{stc}^2 &= \frac{1}{(|h_{1,0}|^2 + |h_{2,0}|^2)^2} E\left[|h_{1,0}|^2|\eta_n(t)|^2 + |h_{2,0}|^2|\eta_n(t+1)|^2\right] \\ &= \frac{1}{(|h_{1,0}|^2 + |h_{2,0}|^2)^2}\left(|h_{1,0}|^2 E[|\eta_n(t)|^2] + |h_{2,0}|^2 E[|\eta_n(t+1)|^2]\right) \\ &= \frac{|h_{1,0}|^2 + |h_{2,0}|^2}{(|h_{1,0}|^2 + |h_{2,0}|^2)^2}\sigma^2 \end{aligned}$$

where $\eta_n(t)$ and $\eta_n(t+1)$ are the *n*th samples from the noise vectors $\boldsymbol{\eta}(t)$ and $\boldsymbol{\eta}(t+1)$ respectively. Thus, the variance of the noise samples at the STTD decoder output can be expressed

as

$$\sigma^2_{stc} = \frac{\sigma^2}{|h_{1,0}|^2 + |h_{2,0}|^2} \tag{B.14}$$

B.3.2 Multipath fading channel

In the case of the multipath fading channel, the STTD decoder output is represented by equation (7.27), where the noise vector at time t, $\boldsymbol{\zeta}(t)$, is given by the first N samples of $\boldsymbol{\varphi}_p$ which is defined as

$$\begin{aligned} \boldsymbol{\varphi}_p &= \mathbf{W}(|\boldsymbol{\Lambda}_1|^2 + |\boldsymbol{\Lambda}_2|^2)^{-1}[\boldsymbol{\Lambda}_1^* \mathbf{W}^H \bar{\boldsymbol{\eta}}_p - \boldsymbol{\Lambda}_2 \mathbf{W}^T \bar{\boldsymbol{\eta}}^*_{p+1}] \\ &= \mathbf{W}(|\boldsymbol{\Lambda}_1|^2 + |\boldsymbol{\Lambda}_2|^2)^{-1}\boldsymbol{\Psi} \end{aligned} \tag{B.15}$$

where $[\boldsymbol{\Lambda}_1^* \mathbf{W}^H \bar{\boldsymbol{\eta}}_p - \boldsymbol{\Lambda}_2 \mathbf{W}^T \bar{\boldsymbol{\eta}}^*_{p+1}]$ is substituted by $\boldsymbol{\Psi}$. Thus, the covariance of $\boldsymbol{\varphi}_p$ is given by

$$\mathbf{V}_{stc} = E[\boldsymbol{\varphi}_p \boldsymbol{\varphi}_p^H] - E[\boldsymbol{\varphi}_p] E^H[\boldsymbol{\varphi}_p] \tag{B.16}$$

considering that $\bar{\boldsymbol{\eta}}_p$ and $\bar{\boldsymbol{\eta}}^*_{p+1}$ contains zero-mean complex Gaussian noise samples, (B.16) is simplified to

$$\mathbf{V}_{stc} = E[\boldsymbol{\varphi}_p \boldsymbol{\varphi}_p^H] \tag{B.17}$$

substituting (B.15) into (B.15) we get

$$\begin{aligned} \mathbf{V}_{stc} &= E[(\mathbf{W}(|\boldsymbol{\Lambda}_1|^2 + |\boldsymbol{\Lambda}_2|^2)^{-1}\boldsymbol{\Psi})(\mathbf{W}(|\boldsymbol{\Lambda}_1|^2 + |\boldsymbol{\Lambda}_2|^2)^{-1}\boldsymbol{\Psi})^H] \\ &= E[(\mathbf{W}(|\boldsymbol{\Lambda}_1|^2 + |\boldsymbol{\Lambda}_2|^2)^{-1}\boldsymbol{\Psi})(\boldsymbol{\Psi}^H[\mathbf{W}(|\boldsymbol{\Lambda}_1|^2 + |\boldsymbol{\Lambda}_2|^2)^{-1}]^H)] \\ &= E[\mathbf{W}(|\boldsymbol{\Lambda}_1|^2 + |\boldsymbol{\Lambda}_2|^2)^{-1}\boldsymbol{\Psi}\boldsymbol{\Psi}^H(|\boldsymbol{\Lambda}_1|^2 + |\boldsymbol{\Lambda}_2|^2)^{-1}\mathbf{W}^H]. \end{aligned} \tag{B.18}$$

Considering that $\boldsymbol{\Psi} = \boldsymbol{\Lambda}_1^* \mathbf{W}^H \bar{\boldsymbol{\eta}}_p - \boldsymbol{\Lambda}_2 \mathbf{W}^T \bar{\boldsymbol{\eta}}^*_{p+1}$ we obtain that

$$\begin{aligned} \boldsymbol{\Psi}\boldsymbol{\Psi}^H &= (\boldsymbol{\Lambda}_1^* \mathbf{W}^H \bar{\boldsymbol{\eta}}_p - \boldsymbol{\Lambda}_2 \mathbf{W}^T \bar{\boldsymbol{\eta}}^*_{p+1})(\boldsymbol{\Lambda}_1^* \mathbf{W}^H \bar{\boldsymbol{\eta}}_p - \boldsymbol{\Lambda}_2 \mathbf{W}^T \bar{\boldsymbol{\eta}}^*_{p+1})^H \\ &= (\boldsymbol{\Lambda}_1^* \mathbf{W}^H \bar{\boldsymbol{\eta}}_p - \boldsymbol{\Lambda}_2 \mathbf{W}^T \bar{\boldsymbol{\eta}}^*_{p+1})(\bar{\boldsymbol{\eta}}_p^H \mathbf{W} \boldsymbol{\Lambda}_1^T - \bar{\boldsymbol{\eta}}^T_{p+1} \mathbf{W}^* \boldsymbol{\Lambda}_2^H) \\ &= \boldsymbol{\Lambda}_1^* \mathbf{W}^H \bar{\boldsymbol{\eta}}_p \bar{\boldsymbol{\eta}}_p^H \mathbf{W} \boldsymbol{\Lambda}_1^T - \boldsymbol{\Lambda}_2 \mathbf{W}^T \bar{\boldsymbol{\eta}}^*_{p+1} \bar{\boldsymbol{\eta}}_p^H \mathbf{W} \boldsymbol{\Lambda}_1^T - \boldsymbol{\Lambda}_1^* \mathbf{W}^H \bar{\boldsymbol{\eta}}_p \bar{\boldsymbol{\eta}}^T_{p+1} \mathbf{W}^* \boldsymbol{\Lambda}_2^H + \\ &\quad \boldsymbol{\Lambda}_2 \mathbf{W}^T \bar{\boldsymbol{\eta}}^*_{p+1} \bar{\boldsymbol{\eta}}^T_{p+1} \mathbf{W}^* \boldsymbol{\Lambda}_2^H \end{aligned} \tag{B.19}$$

substituting (B.19) into (B.18) and taking the expectation we get

$$\begin{aligned}
\mathbf{V}_{stc} &= \sigma^2\mathbf{W}(|\mathbf{\Lambda}_1|^2+|\mathbf{\Lambda}_2|^2)^{-1}(\mathbf{\Lambda}_1^*\mathbf{W}^H\mathbf{W}\mathbf{\Lambda}_1^T+\mathbf{\Lambda}_2\mathbf{W}^T\mathbf{W}^*\mathbf{\Lambda}_2^H)(|\mathbf{\Lambda}_1|^2+|\mathbf{\Lambda}_2|^2)^{-1}\mathbf{W}^H \\
&= \sigma^2\mathbf{W}(|\mathbf{\Lambda}_1|^2+|\mathbf{\Lambda}_2|^2)^{-1}(\mathbf{\Lambda}_1^*\mathbf{\Lambda}_1^T+\mathbf{\Lambda}_2\mathbf{\Lambda}_2^H)(|\mathbf{\Lambda}_1|^2+|\mathbf{\Lambda}_2|^2)^{-1}\mathbf{W}^H \\
&= \sigma^2\mathbf{W}(|\mathbf{\Lambda}_1|^2+|\mathbf{\Lambda}_2|^2)^{-1}(|\mathbf{\Lambda}_1|^2+|\mathbf{\Lambda}_2|^2)(|\mathbf{\Lambda}_1|^2+|\mathbf{\Lambda}_2|^2)^{-1}\mathbf{W}^H \qquad \text{(B.20)}
\end{aligned}$$

which finally becomes

$$\mathbf{V}_{stc} = \sigma^2\mathbf{W}(|\mathbf{\Lambda}_1|^2+|\mathbf{\Lambda}_2|^2)^{-1}\mathbf{W}^H \qquad \text{(B.21)}$$

Appendix C
Publications

- J.M. Luna Rivera, D.G.M. Cruickshank and J.S. Thompson. *"Iterative Multiuser Receiver for a Coded DS-CDMA system"*. Proceedings of the IEEE Vehicular Technology Conference (VTC'01 Spring), vol. 2, pp. 1518-1522, Rhodes Island, Greece, May 2001

- J.M. Luna Rivera, D.G.M. Cruickshank and J.S. Thompson. *"Capacity Bounds for a Coded DS-CDMA system as a function of block size"*. Proceedings of the IEEE Vehicular Technology Conference (VTC'01 Fall), Atlantic city, USA, October 2001

- J.M. Luna Rivera, D.G.M. Cruickshank and J.S. Thompson. *"Hybrid Iterative Multiuser Receiver for a Coded DS-CDMA system"*. Proceeding of the IEEE International Symposium on Spread Spectrum Techniques and Applications (ISSSTA'02), Prague, Czech Republic, September 2002

- J.M. Luna Rivera, D.G.M. Cruickshank and J.S. Thompson. *"Space-Time Iterative Multiuser Receiver for a Coded DS-CDMA System in a Flat Fading Channel"*. Proceedings of the IEEE Vehicular Technology Conference (VTC'02 Fall), Vancouver, Canada, September 2002

- J.M. Luna Rivera, D.G.M. Cruickshank and J.S. Thompson. *"A High Capacity Space-Time FEC Coded DS-CDMA System for use over Multipath Channels"*. Submitted to IEEE Transactions on Wireless Communications, July 2002

ITERATIVE MULTIUSER RECEIVER FOR A CODED DS-CDMA SYSTEM

J. M. Luna Rivera, D.G.M. Cruickshank and J.S. Thompson

University of Edinburgh
Department of Electronics and Electrical Engineering
The King's Buildings, Mayfield Rd., Edinburgh, EH9 3JL, UK
email: mlr@ee.ed.ac.uk, dgmc@ee.ed.ac.uk, jst@ee.ed.ac.uk

Abstract — *A new iterative multiuser receiver structure for a direct-sequence code division multiple access (DS-CDMA) system with forward error correction (FEC) coding is proposed. This structure employs the turbo multiuser detection principle in a soft multi-access interference cancellation scheme. The receiver first uses a Wiener filter to demodulate and despread the received signal, this process yields the initial coded data estimates. Based on these estimates, the parallel cancellation scheme and the channel decoding are coupled to exchange soft information in an iterative fashion. Simulation results show that performance approaches the single-user performance even in highly loaded systems. It is also shown that the use of Wiener filtering on the first iteration of the iterative receiver yields a substantial performance gain in the system.*

I. INTRODUCTION

The standardisation of DS-CDMA technology in mobile communications (third generation) has raised a lot of interest in the research community in trying to increase the capacity of this type of system. The major problems faced in these type of multi-access environments are intersymbol interference (ISI) and multiple-access interference (MAI). These obstacles arise mainly due to the fact that multiuser receivers deal with signals which are not transmitted by a single source but by several uncoordinated sources and geographically separated receivers (non-orthogonal signals). Since DS-CDMA capacity is only interference limited, any reduction in interference converts directly into an increase in capacity.

In [1], the optimal multiuser receiver for the asynchronous coded DS-CDMA was introduced. Here the multiuser detection and the channel decoding are performed jointly. However, its prohibitive complexity (which rises exponentially with the number of active users and the constraint length of the convolutional code) made this structure impractical. Motivated by this high cost in complexity, a search for a satisfactory sub-optimum multiuser receiver which can mitigate such a complexity handicap is still ongoing.

Perhaps the most exciting development in coding theory in recent years has been the announcement of turbo codes [2]. This new scheme achieves near Shannon capacity performance (in the power limited region of an AWGN channel) combining two or more recursive convolutional codes (RSC) in an iterative scheme and using interleavers. Since then a lot of work has been developed in iterative processing techniques. Recently, this technique has been applied to the multiuser detection/decoding field with very promising results [4]-[8].

A partitioned multiuser receiver scheme which performs the multiuser detection and decoding channel processes separately has shown to be a viable structure to reduce complexity [3]. An important result which was obtained in [4] established that asymptotically single-user performance can be achieved even in a highly loaded multiuser system. It was proved theoretically that the combination of FEC coding and random interleavers overcame the limitation of a multiuser detector/decoder in a highly loaded system. In this paper we propose a new iterative multiuser receiver structure which combines a subtractive interference cancellation scheme with single-user *Maximum Aposteriori Probability* (MAP) decoders by exchanging soft information in an iterative fashion. It is shown how the combination of Wiener filtering with FEC coding, iterative decoding and random interleavers can improve the multiuser receiver performance to the single-user performance in the presence of high levels of MAI. It is also important to point out that the proposed structure requires low complexity for each of the stages involved.

The paper has been organised as follow. In the next section the system description is presented. Section III describes the iterative process through the multiuser detector/decoder structure. Simulation results and conclusions are contained in Section IV and V re-

spectively.

II. SYSTEM DESCRIPTION

We consider the model depicted in Fig. 1. The scheme shows a discrete-time DS-CDMA communication system with FEC coding for K active users. The channel model is both chip and symbol synchronous with the samples taken at the chip rate. The kth user transmits a data block of i.i.d[1] binary data, $\{b_i^k\}$; $i \epsilon \{i = 1, 2, \ldots, L\}$, where b_i^k is referred to as the data symbol of user k at time index i. Each data symbol of user k is passed through a non-recursive convolutional code with constraint length v and a code rate $R_0 = 1/R$. The resulting coded sequence at the output of the kth encoder is interleaved (π_k) to reduce the effect of error bursts at the input of the decoder channel. A BPSK technique is used to modulate the interleaved coded symbols, yielding the user symbols $\{d_t^k\}$; $t \epsilon \{t = 1, 2, \ldots, RL\}$. Every user symbol of the kth user is then modulated by a unique spreading waveform and transmitted through an AWGN channel. The nth chip of the spreading waveform employed by the kth user is defined as $s_{k,n} \epsilon \left\{ \frac{-1}{\sqrt{N}}, \frac{1}{\sqrt{N}} \right\}$ where N is the processing gain and $n \epsilon \{n = 1, 2, \ldots, N\}$. The spreading codes employed are random and non-orthogonal to simulate the effect of a multipath channel.

It is assumed that all the users transmit with equal and constant power. It is also assumed that the spreading codes for every user are known exactly by the receiver. The received signal at the chip rate is then given by

$$y_{t,n} = \sum_{k=1}^{K} d_t^k s_{k,n} + w_n \qquad (1)$$

where w_n is a Gaussian noise sample with distribution, $\mathcal{N}(0, \sigma^2)$.

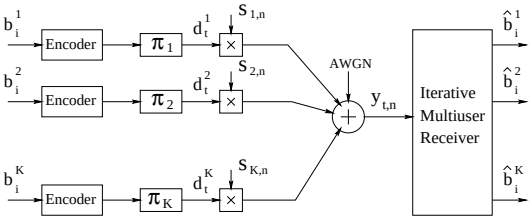

Fig. 1. Scheme of a DS-CDMA system with FEC coding.

III. ITERATIVE MULTIUSER RECEIVER

In this section we introduce the iterative multiuser receiver which is shown in Fig. 2. This structure comprises a multiuser detection stage, a parallel cancellation scheme and a FEC decoding stage which exchange soft information in an iterative fashion. The main issue faced in this type of structure is to generate the correct single-user probabilities for the FEC decoders and supplying appropriated *a priori* information to the multiuser detector on each iteration.

A. Multiuser detection and parallel cancellation

In the multiuser detection field it is well known that Wiener filtering gives better performance than any other conventional linear detector and the combination of such detector with a single stage of parallel cancellation gives even better performance than any linear technique in isolation [9]. Therefore we exploit this quality and thus Wiener filtering together with parallel cancellation is used as the multiuser detector in the first stage of the iterative receiver.

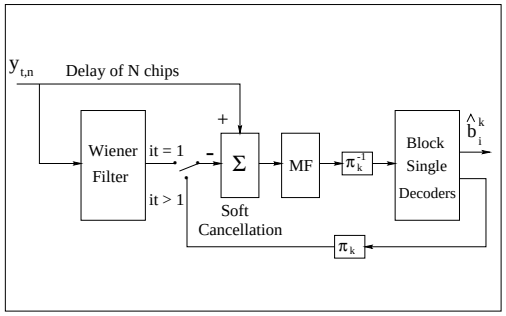

Fig. 2. Iterative multiuser receiver.

Firstly, the Wiener filter [10] delivers the initial soft estimates of the user symbols, $\{\tilde{d}_t^k\}$, at time index t which are then passed to the parallel cancellation scheme. These soft estimates are yielded by forming the expectation of the user symbols for every user as define these quantities straight below in eqn 2.

$$\tilde{d}_t^k = \sum_{d \epsilon \{1,-1\}} dp(d), \quad k = 1, \ldots, K. \qquad (2)$$

The distribution of the Wiener filter output is assumed to be Gaussian. Hence such expectations are computed by taking the conditional probabilities, $p(y_t^k / d_t^k = d)$, which are delivered by the Wiener filter as the *a priori* probabilities $p(d)$ required for user k at time index t. However, to yield these conditional probabilities it is required to know the variance at the Wiener filter output. In [9] it is shown that a good approximation

[1] independent and identically distributed

of this parameter can be achieved, therefore we follow the same procedure.

Using the parallel cancellation scheme the soft estimates of the interfering user symbols (MAI) are then subtracted from the received signal yielded a resulted signal which is passed through a Matched Filter (MF). The signal at the output of the MF can be expressed as

$$\tilde{y}_t^k = R_k[d_t - \tilde{d}_t] + \eta_k,$$

where $R_k \epsilon C^{1\times K}$ denotes the kth row of the autocorrelation matrix $R \epsilon C^{K\times K}$. The vectors d_t and $\tilde{d}_t$ are defined as follows:

$$\begin{aligned} d_t &= \{d_t^1, d_t^2, \ldots, d_t^K\}, \\ \tilde{d}_t &= \{\tilde{d}_t^1, \tilde{d}_t^2, \ldots, \tilde{d}_t^{k-1}, 0, \tilde{d}_t^{k+1}, \ldots, \tilde{d}_t^K\}, \end{aligned}$$

and η_k is the noise sample. Thus the desired user signal at the MF output is denoted as

$$\tilde{y}_t^k = R_{k1}[d_t^1 - \tilde{d}_t^1] + \ldots + d_t^k + \ldots + R_{kK}[d_t^K - \tilde{d}_t^K] + \eta_k$$

where R_{ij} corresponds to the element in the ith row and jth column of the matrix R. It has been showed that iterative receivers based on soft information provide excellent performance. Therefore, the conditional probabilities, $p(\tilde{y}_t^k/d_t^k = d)$, at the MF output are used as the soft information provided to the single-user decoders. To obtain such probabilities it is assumed that the output of the MF can be represented as a AWGN channel with input d_t^k. This equivalent channel is denoted as

$$\tilde{y}_t^k = d_t^k + z_k \tag{3}$$

where z_k is a Gaussian noise sample with distribution $\sim N(m_{z_k}, \sigma_{z_k}^2)$. Then to yield the probabilities, $p(\tilde{y}_t^k/d_t^k = d)$, we must first calculate the noise variance, $\sigma_{z_k}^2$. Derived from eq. 3 (see the Appendix) $\sigma_{z_k}^2$ can be computed by using eq. 4.

$$\sigma_{z_k}^2 = \sum_{\substack{u=1 \\ u\neq k}}^{K} (R_{ku}^2 - R_{ku}^2 \tilde{d_t^u}^2 + R_{ku}\tilde{d_t^u}) + \sigma^2 \tag{4}$$

B. Decoding

The decoding consists of a block of K soft-input soft-output (SISO) single user decoders. As every user makes use of the same decoding algorithm, we base the discussion only on the kth user.

The input sequence for the kth decoder consists of the logarithm of the likelihood ratio (LLR_{in}) of the data symbols (soft input) defined as,

$$LLR_{in}(d_t^k) = \ln \frac{p(\tilde{y}_t^k/d_t^k = 1)}{p(\tilde{y}_t^k/d_t^k = -1)}. \tag{5}$$

While the output sequences given by the kth decoder are the LLR_{out} (soft output) of the *a posterior* probabilities (APP) for both the data symbols, $p(b_i^k = b/Y_i^k)$, and the user symbols, $p(d_t^k = d/Y_i^k)$. These APP can be calculated by using a slight modification of the MAP algorithm [2]. The input sequence is given by $\{Y_i^k\}$; $i \epsilon \{i = 1, 2, \ldots, L\}$, where $Y_i^k = (y_{(i-1)R+1}^k, \cdots, y_{Ri}^k)$.

In this section we outline the procedure to estimate the $LLR'_{out}s$ of the user and data symbols. The APP of the data symbols b_i^k is derived from the joint probability $\lambda_i^b(m) = Pr\{b_i^k = b, S_i = m/Y^k\}$. Thus the APP of the data symbol for the kth user at time index i is defined as

$$Pr\{b_i^k = b/Y_i^k\} = \sum_m \lambda_i^b(m) \tag{6}$$

where $\{b_i^k\}$; $i \epsilon \{1, 2, \cdots, L\}$, $b \epsilon \{1, -1\}$ and m is the index of all possible states in the trellis representation at time i.

As in [2] the forward $\alpha_i(m)$ and backward $\beta_i(m)$ state probabilities can be recursively obtained as follow

$$\alpha_i(m) = H_\alpha^k \sum_{m'} \sum_b \gamma_b(Y_i, m', m)\alpha_{i-1}(m') \tag{7}$$

$$\beta_i(m) = H_\beta^k \sum_{m'} \sum_b \gamma_b(Y_{i+1}, m', m)\beta_{i+1}(m') \tag{8}$$

where H_α^k and H_β^k are normalisation constants such that

$$H_\alpha^k \rightarrow \sum_m \alpha_i(m) = 1$$

$$H_\beta^k \rightarrow \sum_m \beta_i(m) = 1.$$

The transition probability $\gamma_b(Y_i, m', m)$ from state $S_{i-1} = m'$ to state $S_i = m$ at time index i is given as

$$\gamma_b(Y_i^k, m', m) = (\Pi_{l=(i-1)R+1}^{Ri} p(\tilde{y}_l^k/b_i^k = b))Pr\{b_i^k = b\}$$

with $p(y_{(i-1)R+1}^k/b_i^k = b) \cdots p(y_{Ri}^k/b_i^k = b)$ as the conditional probabilities of the codeword associated with the transition. Since there are only two possible transitions from each state and they are with the same probability, then the *a priori* probabilities $Pr\{b_i^k = 1\} = Pr\{b_i^k = -1\} = 1/2$. Using eq. 7 and eq. 8 the joint probability $\lambda_i^b(m)$ is computed as follow

$$\lambda_i^b(m) = \alpha_i(m)\beta_i(m). \tag{9}$$

The boundary conditions are $\alpha_0^k(0) = 1$ and $\alpha_0^k(m) = 0$ $\forall m \neq 0$ and $\beta_L^k(m) = \frac{1}{L}$ $\forall m$.

An analogous procedure can be used to yield the APP's for the user symbols [11]. Eq. 6 is slightly modified to yield APP's

$$Pr\{d_t^k = d/Y_i^k\} = \sum_m \lambda_i^d(m)$$

where $\{d_t^k\}$; $t \epsilon \{1, 2, \cdots, RL\}$, $d \epsilon \{1, -1\}$ and $\{Y_i^k\}$; $i \epsilon \{1, 2, \cdots, L\}$.

C. Iterative principle

In a similar fashion to turbo codes [2], we make use of the single-user decoder output probabilities from iteration n to yield the user symbols estimation, $\{\tilde{d}_t^k\}$, required in the cancellation scheme for iteration $n+1$. Therefore, for an iteration number > 1 the estimates of these values are now delivered from the decoder outputs instead of the Wiener filter. Then by applying once again eq. 2 such estimates can be obtained, but this time the APP of the user symbols (coded bits) at the output of every single-user decoder are used as the *a priori* information, $p(d) = Pr\{d_t^k = d/Y_i^k\}$. It is important to mention that the sequence supplied to the cancellation scheme for an iteration number > 1 must be interleaved in order to yield the appropriate ordering of the information sequence at that point.

IV. SIMULATION RESULTS

The performance of the system was evaluated in terms of the bit error rate (BER) using Monte-Carlo simulations. Graphs show the average BER over all users in the system. We considered a channel model that was both chip and symbol synchronous with equal power users. The same FEC coding channel was employed for all users, it consists of a non-recursive convolutional code with rate, $R_o = 1/2$, constraint length, $v = 3$, and generators $(7, 5)$. The block size was set to $L = 128$ data symbols, giving $RL = 256$ coded symbols in a block which were transmitted with different sets of random spreading codes.

The simulation results in Fig. 3 shows the performance of the multiuser receiver for a different number of iterations. The simulation was performed with a processing gain $N = 15$, $K = 15$ active users and random interleavers of depth RL with different patterns for every user. The results shows that multiuser receiver performance approaches the single-user performance even in this heavily loaded system. Although the major improvement of the receiver occurs in the second and third iterations, the system performance at the first iteration plays an important factor in the final result as it indicates how rapidly the system performance will converge to the single-user performance.

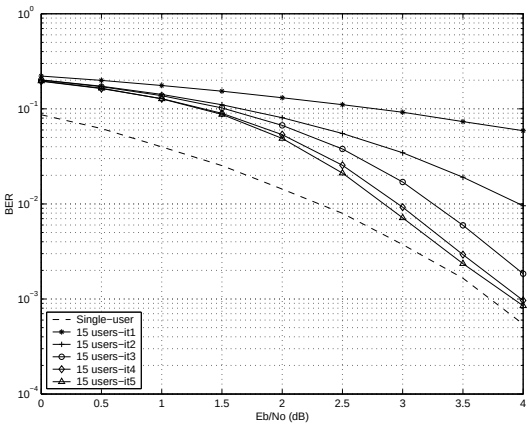

Fig. 3. Iterative multiuser performance

Fig. 4 shows the average BER against number of users for a different number of iterations. Comparing the graphs we can observe that for an iteration number bigger than three the system performance remains closely to a constant value (single-user bound) up to a number of users equal to the processing gain ($K = N$). Further number of users in the system ($K/N > 1$) push the system performance away from the single-user bound, as is expected.

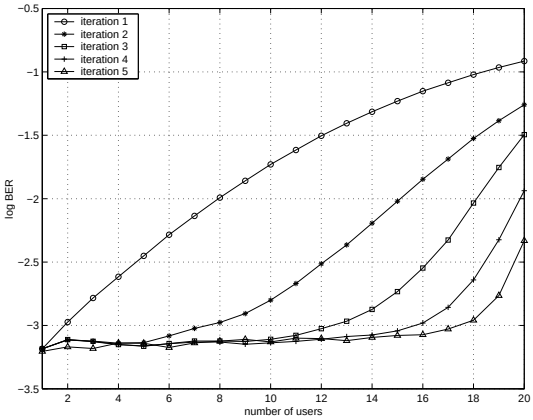

Fig. 4. Number of users against BER averaged over all users for Eb/No=4dB and N=15.

V. CONCLUSIONS

The combination of a good multiuser detection stage at the first iteration and the principle of turbo multi-

user detection yields a multiuser receiver performance close to single-user performance even in highly loaded systems. A further important result is that this structure employs a minimum of complexity in every stage, yielding a final structure with low complexity.

Appendix

The variance of the noise sample, z_k, in eq. 3 is denoted as

$$\sigma^2_{z_k} = E(z_k^2) - E(z_k)^2. \quad (10)$$

where E[] denotes the expected value and z_k is given by:

$$z_k = MAI_k + n_k - M\tilde{A}I_k \quad (11)$$

with $MAI_k = \sum_{u \neq k} R_{ku} d_t^u$, $M\tilde{A}I_k = \sum_{u \neq k} R_{ku} \tilde{d}_t^u$ ($u \epsilon \{1, \cdots, K\}$) and n_k is a noise sample with distribution, $N(0, \sigma^2)$.

Then substituting eq. 11 in eq. 10 and taking in consideration that E(η_k)=E(MAI)=0 it yields

$$\sigma^2_{z_k} = E(MAI^2) + E(\eta_k^2) + E(M\tilde{A}I_k{}^2) - E(M\tilde{A}I_k). \quad (12)$$

To reduce complexity in computing $\sigma^2_{z_k}$ we can truncate E($M\tilde{A}I_k{}^2$) to contain only the square terms, therefore the final expression for $\sigma^2_{z_k}$ is given by:

$$\sigma^2_{z_k} = \sum_{\substack{u=1 \\ u \neq k}}^{K} (R_{ku}^2 - R_{ku}^2 \tilde{d}_t^{u\,2} + R_{ku} \tilde{d}_t^u) + \sigma^2. \quad (13)$$

References

[1] T.R. Giallorenzi and S.G. Wilson. "*Multiuser ML Sequence Estimator for Convolutionally Coded Asynchronous DS-CDMA Systems*". IEEE Transactions on Communications, vol. 44, no. 8, pp. 997-1008, August 1996.

[2] Claude Berrou, Alain Glavieux. "*Near Optimum Error-Correcting Coding and Decoding: Turbo-Codes*". IEEE Transactions on Communications, vol. 44, no. 10, pp. 1261-1271, October 1996.

[3] T.R. Giallorenzi and S.G. Wilson. "*Suboptimum Multiuser Receivers for Convolutionally Coded Asynchronous DS-CDMA Systems*". IEEE Transactions on Communications, vol. 44, no. 9, pp. 1183-1196, September 1996.

[4] Michael Moher. "*An Iterative Multiuser Decoder for Near-capacity Communications*". IEEE Transaction on Communications, vol. 46, no. 7, pp. 870-880, July 1998.

[5] Mark C. Reed, Christian B. Schlegel, Paul D. Alexander, and John A. Asenstorfer. "*Iterative Multiuser Detection for CDMA with FEC: Near-Single-User Performance*". IEEE Transactions on Communications, vol. 46, no. 12, pp. 1693-1699, December 1998.

[6] Xiaodong Wang, and H. Vincent Poor. "*Iterative (Turbo) Soft Interference Cancellation and Decoding for Coded CDMA*". IEEE Transactions on Communications, vol. 47, no. 7, pp. 1046-1060, July 1999.

[7] Paul D. Alexander, Mark C. Reed, John Asenstorfer, Christian B. Schlegel. "*Iterative Multiuser Interference Reduction: Turbo CDMA*". IEEE Transactions on Communications, vol 47, no. 7, July 1999, pp. 1008-1014.

[8] H.K. Sim, and D.G.M. Cruickshank. "*An iterative Multiuser Receiver for FEC Coded CDMA*". IEEE 6th Int. Symp. on Spread-Spectrum Tech. & Appli., NJIT, New Jersey, USA, September 2000.

[9] D.G.M. Cruickshank. "*Suppression of Multiple Access Interference in a DS-CDMA System using Wiener Filtering and Parallel Cancellation*". IEE Proceedings (Communications), vol. 143, no. 4, pp. 226-230, August 1996.

[10] D.G.M. Cruickshank. "*Optimal and Adaptive FIR Filter Receivers for DS-CDMA*". Personal, Indoor and Mobile Radio Communications PIMRC 1994, pp. 1339-1343.

[11] S. Benedetto, D. Divsalar, G. Montorsi, and F. Pollara. "*A Soft-Input Soft-Output Maximum A Posteriori (MAP) Module to Decode Parallel and Serial Concatenated Codes*". JPL TDA Progress Report 42-127, November 15, 1996.

Capacity bounds for a coded DS-CDMA system as a function of block size

J. M. Luna Rivera, D. G. M. Cruickshank and J. S. Thompson

University of Edinburgh
Department of Electronics and Electrical Engineering
The King's Buildings, Mayfield Rd., Edinburgh, EH9 3JL, UK
email: mlr@ee.ed.ac.uk, dgmc@ee.ed.ac.uk, jst@ee.ed.ac.uk

Abstract — **This paper examines the capacity bounds for a direct sequence code division multiple access (DS-CDMA) system with forward error correction (FEC) coding in an additive white Gaussian noise (AWGN) channel. Using Shannon's sphere-packing bounds, the capacity for this type of system as a function of the block size is shown. Furthermore, its analysis provides a comparison baseline for DS-CDMA communication channels. We compare these limits with the achievable capacity of a DS-CDMA system based on an iterative multiuser receiver (IMR).**

I. INTRODUCTION

A CDMA system based on direct sequence spread spectrum offers certain distinct advantages such as dynamic channel sharing, robustness to time variations in the channel, ease of cellular planning, etc. As the development of such schemes are mainly for capacity reasons, in the information theory of a multiple-access channel the main goal is to find its capacity limit. This limit represents the set of information rates at which simultaneous reliable communication of the messages of each user is possible. Since normal applications impose constraints on the maximum block length of information symbols, an analysis of the system as a function of this parameter is desirable. Based on Shannon's sphere packing bound [1] the behaviour of these bounds as a function of the block size in a DS-CDMA communication channel is investigated.

On the other hand, with the advent of turbo codes [2] a lot of work has been carried out in iterative processing techniques for multiuser receivers [3]-[7]. In [3] a multiuser receiver scheme for synchronous coded CDMA based on iterative techniques is introduced. Therefore, we make use of this type of structure to show a comparison of the theoretical bounds with the simulated performance achieved by a DS-CDMA system. We compare the signal to noise ratio, E_b/N_o, required to achieve a particular codeword error probability, P_w, operating over a binary-input AWGN channel.

The paper has been organised as follows. In the next section the capacity bounds for a DS-CDMA system are derived. For the purpose of a comparison, section III introduces a DS-CDMA system based on an iterative multiuser receiver. Then section IV shows the comparison between the theoretical bounds and the simulation performance achieved by the DS-CDMA system. Finally the conclusions of the paper are drawn in Section V.

II. CAPACITY BOUNDS

A. Shannon's bound

It is well known that the Shannon's sphere packing bound establishes a lower bound on the error probability for codes with a particular block size [1]. The development of this bound assumes a spherical block code that contains a collection of $2^k = M$ equal power codewords where k is the number of information symbols. Each codeword is represented by a sequence of n code symbols (geometrically it represents a point in $n-$dimensional Euclidean space) with a signal power nP_s per codeword (then each codeword is on the surface of a sphere of radius $\sqrt{nP_s}$). The communication channel adds independently to each channel symbol Gaussian noise with distribution $\mathcal{N}(0, N_o/2)$.

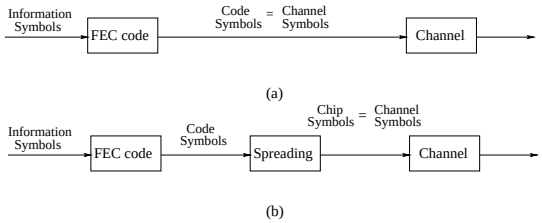

Fig. 1. Communication system: a)no-spreading model b) spreading model.

In a typical digital communication system additional functions such as a modulation scheme and error control coding (channel coding) are both included in Shannon's coding theory, see Fig. 1 (a). The code rate, R, is then

defined as the ratio of the number of information symbols to the number of channel symbols where the number of information symbols, k, is measured in bits for a binary input. Thus the code rate, $R = k/n$, represents the number of information bits per channel symbol.

In what follows, an outline of the fundamentals of Shannon's sphere packing lower bound is discussed in the context of DS-CDMA. Only the expressions of interest to our problem are displayed, more analysis on these bounds can be found in [1]. This fundamental lower bound is expressed in the following form

$$P_w \geq Q(\theta_1, A, n) \tag{1}$$

where P_w is the codeword error probability, $A = \sqrt{2RE_b/N_o}$ is the amplitude corresponding to the signal to noise ratio per channel symbol. The scalar $Q(\theta, A, n)$ is the probability that a point X in $n-$dimensional space, at distance $A\sqrt{n}$ from the origin, falls outside an $n-$dimensional cone of half angle θ with vertex at the origin O and axis OX. The perturbation of noise is according to a spherical Gaussian distribution with covariance $\mathbf{I}_{n\times n}$ (identity matrix of dimension $n \times n$). Then θ_1 represents the half angle of an $n-$dimensional cone that satisfies

$$\begin{aligned} \Omega_n(\theta_1) &= \frac{\Omega(\theta_1)}{\Omega(\pi)} \\ &= \frac{1}{M} \end{aligned} \tag{2}$$

where $\Omega(\theta_1)/\Omega(\pi)$ denotes the ratio of the solid angle within an $n-$dimensional cone of half angle θ_1 to the total solid angle of $n-$dimensional Euclidean space (full solid angle of an sphere). The expressions for the solid angle function $\Omega_n(\theta)$ and the probability function $Q(\theta, A, n)$ are given by

$$\Omega_n(\theta) = \int_0^{\theta} \frac{n-1}{n} \frac{\Gamma(\frac{n}{2}+1)}{\Gamma(\frac{n+1}{2})} (sin\phi)^{n-2} d\phi$$

and

$$\begin{aligned} Q(\theta, A, n) = & \int_{\theta}^{\phi} \frac{n-1}{2^{n/2}} \frac{(sin\phi)^{n-2}}{\sqrt{\pi}\Gamma(\frac{n+1}{2})} \int_0^{\infty} x^{n-1} \cdot \\ & \exp^{-(x^2+nA^2-2x\sqrt{n}Acos\phi)/2} \, dx d\phi \end{aligned}$$

where $\Gamma(a)$ is the gamma function defined by the integral $\int_0^{\infty} e^{-t} t^{(a-1)} dt$. Rather than these complex integrals, asymptotic expressions are derived for these bounds when n is large. These approximations are denoted in the following form

$$\Omega_n(\theta) \approx \frac{\Gamma(\frac{n}{2}+1)(sin\theta)^{n-1}}{n\Gamma(\frac{n+1}{2})\sqrt{\pi}cos\theta} \tag{3}$$

and

$$\begin{aligned} Q_n(\theta, A, n) \approx & \frac{(G(\theta, A)sin\theta e^{-(A^2 - AG(\theta,A)cos\theta)/2})^n}{\sqrt{n\pi}\sqrt{1+G^2(\theta, A)}} \cdot \\ & \frac{1}{sin\theta(AG(\theta, A)sin^2\theta - cos\theta)} \end{aligned} \tag{4}$$

where $G(\theta) = \frac{1}{2}(Acos\theta + \sqrt{A^2cos^2\theta + 4})$. Therefore, a lower bound on the error performance of a code of rate R can be computed using (2), (3) and (4).

B. CDMA bound

The incorporation of the CDMA scheme, where the spreading is imposed, yields a multiple access communication channel that can be interpreted in a similar manner to Shannon's model, Fig. 1 (b). However, this representation instead yields an overall "code" rate given by

$$R_s = \frac{Uk}{nN} = \frac{U}{N} R \tag{5}$$

where U is the number of users in the system, k represents the information block size (in bits) per user, n the number of FEC coded symbols per information block and N the number of chips per coded symbol (spreading factor). Assuming a multiuser detection strategy where the multiuser receiver knows exactly the spreading waveforms of all users and jointly demodulates and detects all users' signals, each channel symbol is then corrupted only by a Gaussian noise with variance $N_o/2$. Consequently, the Shannon's sphere packing bound (1)-(4) is applicable to this multiple access model but with a signalling rate R_s instead of R.

By applying Shannon's expressions these bounds are obtained for the DS-CDMA communication model. These asymptotic bounds allow us to determine the minimum E_b/N_o required given a particular signalling rate (R_s) and a desired codeword error probability (P_w) as a function of the information block length (k). In section IV these bounds will be showed as a function of the block size and the number of users in the system.

III. SIMULATED DS-CDMA SYSTEM

In this section we consider the simulation of a discrete time coded DS-CDMA communication system in an AWGN channel. In Fig 2 the system model is shown. This communication system operates with U active users that transmit simultaneously through a channel. The users are both chip and symbol synchronous. Every user transmits a block of k independent and identically distributed data bits, $\{b_j^i\}$; $j \in \{j = 1, 2, \ldots, k\}$, $i \in \{i = 1, 2, \ldots, U\}$, which are encoded with a code rate R. After BPSK modulation the resulting coded sequence is given by $\{d_t^i\}$; $t \in \{t = 1, 2, \ldots, k/R\}$. Every user symbol is then modulated by a unique spreading waveform

of N chips length and transmitted through an AWGN channel (assuming that all the users transmit with equal and constant power). The mth chip of the spreading waveform employed by the ith user is defined as $s_{i,m} \epsilon \left\{-1/\sqrt{N}, 1/\sqrt{N}\right\}$ where $m \epsilon \{m = 1, 2, \ldots, N\}$. The spreading codes employed are randomly chosen and non-orthogonal. The received signal at the chip rate is then given by

$$y_{t,m} = \sum_{i=1}^{U} d_t^i s_{i,m} + w_m \tag{6}$$

where w_m is a Gaussian noise sample with distribution, $\mathcal{N}(0, N_o/2)$.

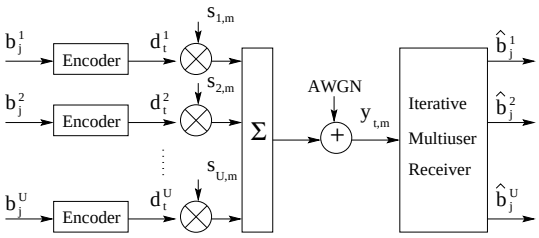

Fig. 2. System model

In a multiple access system with FEC coding the complexity of the optimal multiuser receiver increases exponentially with the number of users U and the memory of the convolutional code ν, $O(2^{U\nu})$. The analysis of a jointly optimum multiuser detector and forward error correction coding process will yield the minimum achievable probability of error and optimum asymptotic multiuser efficiency in this type of scheme but is far too complex to be practical. For complexity reasons we consider a partitioned multiuser receiver which performs the multiuser detection and channel decoding processes separately but exchanging soft information in an iterative fashion (multiuser iterations) to improve the performance in the receiver [3]-[7], see Fig. 3.

In an iterative multiuser receiver structure an essential issue is the method of exchanging information between the detection stage and the channel decoding. In a similar fashion to [3]-[7] soft information is output by the multiuser detector which is then supplied as the soft-input to the FEC decoders. Equally, the information yielded at the decoder outputs is used as *a priori* information into the multiuser detector on each iteration. In this paper the soft information for multiuser iteration p is represented using the *logarithm likelihood ratio* (LLR) as given in the following expression

$$LLR(x^i)_p = \ln \frac{P_{+1}}{P_{-1}} \tag{7}$$

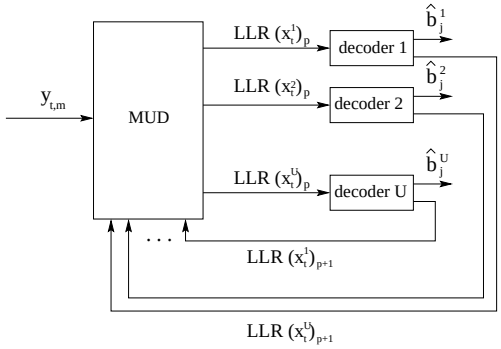

Fig. 3. Iterative multiuser receiver

where x^i can be either the information symbols or coded symbols of the ith user and P_{+1}, P_{-1} are the probability information (marginal or *a posteriori* probabilities) of detecting $x^i = +1$ and $x^i = -1$ respectively. To obtain the probabilities as a function of the LLR we solve (7) for either P_{+1} or P_{-1} as shown in (8) and (9).

$$pr(x^i = +1) = \frac{\exp(LLR(x^i))}{1 + \exp(LLR(x^i))} \tag{8}$$

$$pr(x^i = -1) = \frac{1}{1 + \exp(LLR(x^i))} \tag{9}$$

A. Optimal multiuser detector

For the detection process it has been shown that radial basis function detector (RBF) can be implemented as the optimal multiuser detector in a DS-CDMA system [8], [9]. Therefore we select this type of multiuser detector to demodulate the users signals in the receiver.

The RBF detector output for the ith user can be expressed by the ratio of the conditional probability as is shown in the following equation

$$\frac{p(\underline{y}_t/d_t^i = +1)}{p(\underline{y}_t/d_t^i = -1)} = \frac{\sum_{l=1}^{2^{U-1}} \exp\left(-\frac{||\underline{y}_t - \underline{a}_l||^2}{2\sigma^2}\right)}{\sum_{l=1}^{2^{U-1}} \exp\left(-\frac{||\underline{y}_t - \underline{a}_l||^2}{2\sigma^2}\right)} \tag{10}$$

where the conditional probabilities are generated by the multivariate Gaussian probability density function [10] as given below

$$p(\underline{y}_t/d) = \frac{1}{2^{U-1}} \sum_{l=1}^{2^{U-1}} \frac{\exp\left(-\frac{||\underline{y}_t - \underline{a}_l||^2}{2\sigma^2}\right)}{(2\pi)^{N/2}\sigma^N} \tag{11}$$

with $d \epsilon \{+1, -1\}$, $\underline{y}_t = [y_{t,1}, y_{t,2}, \cdots, y_{t,N}]$ is the input vector consisting of the N chip spaced input samples (6), $\underline{a}_l = [c_1, c_2, \cdots, c_N]$ is the lth centre in the RBF network and σ^2 is the noise variance.

B. Channel decoder

On the other hand, it has been established that turbo codes [2] represents one of the most powerful classes of error correcting codes as they achieve near Shannon capacity performance (in the power limited region of an AWGN channel). Therefore, this type of FEC coding is used to decode the information symbols of every user in the system.

The channel decoding for the DS-CDMA system consists of a block of U single user turbo decoders. The input sequence to the ith turbo decoder are the *a priori* LLR's of the coded symbols yielded by the RBF detector. As an output it delivers an update of the LLR's based on the *a posteriori* probabilities (APP) of the coded symbols as well as the information symbols. When the last multiuser iteration in the receiver structure has been reached a hard decision is accomplished at the decoder output

$$\hat{b}_j^i = \begin{cases} +1 & \text{if } LLR(b_j^i) > 0 \\ -1 & \text{otherwise} \end{cases}$$

where

$$LLR(b_j^i) = \ln \frac{p(b_j^i = +1/\underline{y})}{p(b_j^i = -1/\underline{y})}$$

with b_j^i as the jth information symbol of user i and $\underline{y}$ is the input sequence of coded symbols corresponding to k information symbols. But if the last multiuser iteration has not been reached yet then the decoder yields as output the LLRs for the coded bits

$$LLR(d_t^i) = \ln \frac{p(d_t^i = +1/\underline{y})}{p(d_t^i = -1/\underline{y})}$$

where d_t^i is the tth coded symbol of user i. These values are then supplied as *apriori* information to the multiuser detector in the next iteration.

The LLR's values are obtained after a desired number of turbo decoder iterations have been accomplished in the decoder structure. The APPs are calculated in a similar fashion as it is shown in [2] but with a slight modification to yield the APPs for the coded symbols, see [11].

C. Turbo multiuser detection principle

Turbo multiuser detection refers to multiuser detection and channel decoding using an iterative exchange of soft information between the two processes. In a similar fashion to [4] this principle is applied to the RBF detector by calculating the conditional probability $p(\underline{y}_t/d_t^i = d)$ as follows:

$$p(\underline{y}_t/d_t^i = d) = \sum_{\substack{\underline{d}_t \\ (d_t^i = d)}} p(\underline{y}_t/\underline{d}_t) \prod_{\substack{r=1 \\ r \neq i}}^{U} pr(d_t^i). \qquad (12)$$

where $d \in \{+1, -1\}$ and $pr(d_t^i)$ is the *a priori* probability of the ith user at time index t. In multiuser iteration p, the APPs of the coded symbol at the output of every single-user decoder are used as *a priori* probabilities which are provided into (12) for a multiuser iteration $p+1$. For $p = 1$ these *a priori* probabilities are set to 0.5 for every user.

D. Simulation

As an example of the IMR performance we simulate a DS-CDMA system in an AWGN channel. In Fig. 4 the performance of the IMR is shown for different numbers of multiuser iterations. The system considered is a DS-CDMA system with $U = 5$ active users and a processing gain $N = 7$. For the FEC coding every user uses a turbo code of rate $R = 1/2$ and generators $G1 = 37$ and $G = 21$ in octal notation and where every user transmits a block of $k = 200$ information bits. In the decoder structure the number of turbo decoder iterations were set to 4. In this scenario, the 5 user case performance is very close to the single-user bound after 4 multiuser iterations.

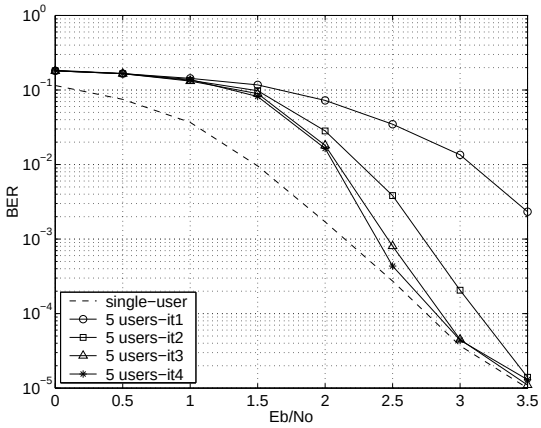

Fig. 4. Iterative multiuser receiver performance

IV. COMPARISON

To enable us to compare the bounds derived in section 2, we simulate the DS-CDMA system introduced in the previous section in an identical scenario. Although in practical applications the computational complexity in the system receiver is still prohibitive, $O(2^U) + O(2^v)$, it can be useful for understanding how closely a practical system can approach the theoretical limits.

The simulation results are shown in Fig. 5. The parameters used to compare the achievable performance of this practical system with the theoretical bounds are:

$R = 1/3$, $N = 7$, with $U = 5$, 7 and 9 attaining a $P_w = 10^{-2}$. Pseudo-noise sequences are employed to spread the users' signals. The FEC coding includes an encoder with memory $v = 4$ and generators $G_1 = 37$, $G_2 = 21$, the same encoder is employed for all users. A combination of 5 turbo decoder iterations and 5 multiuser iterations are applied in the receiver structure. The performance is measured by averaging the codeword error rate (or frame error rate FER) across all the users.

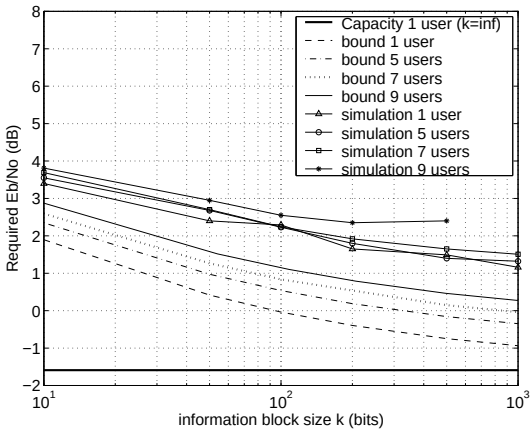

Fig. 5. Asymptotic bounds for a DS-CDMA system as a function of the information block length for $R = 1/3$, $N = 7$ and $U = 5$, 7 and 9 achieving a $P_w = 10^{-2}$.

These results show us that a small block length for these systems puts up the minimum E_b/N_o required for reliable communications. Also it is illustrated that increasing U (the number of users) also increases the minimum E_b/N_0 required for reliable communications. From the simulation results it can be note that for $U > N$ (*i.e.* 9 users) the minimum E_b/N_o required does not show a similar behaviour as the cases when $U < N$. The possible reason for this is the behaviour of the FEC coding performance when the multiuser interference gets very high. The improvement in the BER performance with larger block sizes is a well known characteristic of turbo codes (also maintained for the FER), however, it does not continue at low signal to interference plus noise ratios, which is the case in our simulation results for 9 users in the system.

V. CONCLUSIONS

The capacity bounds for a DS-CDMA system as a function of the information block length were derived. Using an iterative multiuser receiver we show that the performance of this type of system has a similar relationship between block length and required E_b/N_o as that given by Shannon's sphere packing bound. Furthermore, it was shown that by using the iterative multiuser receiver the total spectral efficiency in the system (number of information bits per chip transmitted reliably for all the users) is similar to an orthogonal DS-CDMA system. Good performance is maintained in systems with a ratio $U/N \leq 1$.

References

[1] C.E. Shannon. "*Probability of Error for Optimal Codes in a Gaussian Channel*". Bell System Technical Journal, vol. 38, pp. 611-656, 1959.

[2] Claude Berrou, Alain Glavieux. "*Near Optimum Error-Correcting Coding and Decoding: Turbo-Codes*". IEEE Transactions on Communications, vol. 44, no. 10, pp. 1261-1271, October 1996.

[3] Michael Moher. "*An Iterative Multiuser Decoder for Near-capacity Communications*". IEEE Tran. on Commun., pp. 870-880, July 1998.

[4] Mark C. Reed, Christian B. Schlegel, Paul D. Alexander, and John A. Asenstorfer. "*Iterative Multiuser Detection for CDMA with FEC: Near-Single-User Performance*". IEEE Transactions on Communications, vol. 46, no. 12, pp. 1693-1699, December 1998.

[5] Xiaodong Wang, and H. Vincent Poor. "*Iterative (Turbo) Soft Interference Cancellation and Decoding for Coded CDMA*". IEEE Transactions on Communications, vol. 47, no. 7, pp. 1046-1060, July 1999.

[6] Paul D. Alexander, Mark C. Reed, John Asenstorfer, Christian B. Schlegel. "*Iterative Multiuser Interference Reduction: Turbo CDMA*". IEEE Transactions on Communications, vol 47, no. 7, July 1999, pp. 1008-1014.

[7] H.K. Sim, and D.G.M. Cruickshank. "*An iterative Multiuser Receiver for FEC Coded CDMA*". IEEE 6th Int. Symp. on Spread-Spectrum Tech. & Appli., NJIT, New Jersey, USA, September 2000.

[8] U. Mitra and H. Vincent Poor. "*Neural Network Techniques for Adaptive Multiuser Demodulation*". IEEE Journal on Selected Areas in Communications, vol. 12, no. 9, December 1994.

[9] D.G.M. Cruickshank. "*Radial Basis function Receivers for DS-CDMA*". Electronics Letters, vol. 32, no. 3, february 1996.

[10] J. G. Proakis, *Digital Communications*, 4th edition. New York: McGrawHill 2001.

[11] S. Benedetto, D. Divsalar, G. Montorsi, and F. Pollara. "*A Soft-Input Soft-Output Maximum A Posteriori (MAP) Module to Decode Parallel and Serial Concatenated Codes*". JPL TDA Progress Report 42-127, November 15, 1996.

Hybrid Iterative Multiuser Receiver for a Coded DS-CDMA System

J.M. Luna Rivera, D.G.M. Cruickshank and J.S. Thompson
The University of Edinburgh
Department of Electronics and Electrical Engineering
The King's Buildings, Mayfield Rd., Edinburgh, EH9 3JL, UK
mlr@ee.ed.ac.uk, dgmc@ee.ed.ac.uk, jst@ee.ed.ac.uk

Abstract — **This paper presents a suboptimum multiuser receiver for a multipath direct-sequence code division multiple access (DS-CDMA) system with forward error correction (FEC) coding. The complexity of the optimal joint receiver is well known to be exponential with the number of users and the memory of the FEC code. Therefore, we propose a hybrid structure which applies the turbo multiuser detection principle not only to improve performance in the system but also to reduce complexity in the receiver. This structure uses a moderate-complexity detector (MCD), based on a linear detection technique on the first iteration of the receiver and then for further iterations a suboptimal radial basis function detector (SRBF) is applied. The aim of the MCD is solely to establish a level of confidence related to how likely the transmitted information can be correctly detected. Using this information a preselection technique is applied to reduce the complexity of the optimal radial basis function detector which is used for subsequent iterations. These two modules together operate as the SRBF detector. Numerical results show that good performance is achieved by this hybrid receiver at a significantly reduced complexity.**

I. INTRODUCTION

The 3rd generation of mobile communications will be based upon DS-CDMA technology with both long and short spreading sequences [1], [2]. Therefore many researchers are trying to increase the capacity that this technology can deliver. In DS-CDMA systems the presence of intersymbol interference (ISI) due to the multipath nature of the wireless channels together with multiple access interference (MAI) that originates from asynchronous transmission and/or multipath, constitutes the major impediments to the overall system performance.

In [3], the optimal multiuser receiver for the asynchronous convolutionally coded DS-CDMA was introduced. However, the prohibitive complexity of this receiver, $O(2^{U\nu})$, which rises exponentional with the number of users U and the encoder memory ν, makes this structure far from practical. To reduce this obstacle, a partitioned structure is proposed in [4] where the complexity factor is reduced to $O(2^U) + O(2^\nu)$. As v is normally small, the receiver complexity is basically dominated by the multiuser detector $O(2^U)$. However, even with a small number of users in the system the complexity of this structure becomes impractical. While linear multiuser detection techniques overcome this problem of complexity, the presence of a high level of MAI and/or ISI gives poor performance in the receiver. This degradation is mainly caused by the fact that in such scenarios the desired signals are no longer linearly separable. Therefore, nonlinear receiver structures have to be used. However, these structures usually involve a high cost in complexity which motivates the current research into a search for sub-optimum nonlinear receiver structures of comparable performance to that of the optimal receiver but at a significantly reduced complexity.

Iterative processing techniques have been recently applied in the field of multiuser detection (MUD) [5–9] with the *turbo multiuser detection principle*. Essentially this principle consists of an iterative exchange of *extrinsic information* among the receiver modules (detector/decoder) to achieve an improved performance. The results show that in order to exploit fully this principle instead of using powerful error correction codes, for example turbo codes, to overcome the system interferences, it may in fact be better to use a simpler encoder combined with more advanced MUD detectors. In [10], it is shown that the optimal radial basis function (RBF) network can be implemented as the optimum detector for a DS-CDMA system. However in a multipath scenario, even assuming that significant ISI spans only one neighbouring symbol, its complexity is proportional to 2^{3U} [11]. With this in mind, in this paper we introduce a hybrid iterative multiuser receiver (HIMR) that exploits the *turbo multiuser detection principle* not only to improve the bit error rate (BER) perform-

ance but also to reduce the multiuser receiver complexity. We propose to use a moderate-complexity multiuser detector structure at the first iteration of the scheme and then to make use of a suboptimal radial basis function (SRBF) detector for further iterations. The objective of the first stage is to identify by means of a *pre-selection* technique those signals that are most likely to be correctly detected. Based upon these confidence values a reduced-complexity method is applied to the receiver for subsequent iterations.

The paper has been organised as follows. In the next section the system model is discussed. Section III introduces the hybrid iterative multiuser receiver. Numerical results and final conclusions are drawn in section IV and V respectively.

II. SYSTEM MODEL

We consider the downlink of a DS-CDMA system with FEC coding in a stationary multipath scenario. The system model is shown in Fig. 1. In this communication system U users transmit simultaneously and are both chip and symbol synchronous as in a mobile downlink. Every user transmits a frame of L independent and identically distributed data bits, $\{\mathbf{b_i^k}\}$; $i \in \{1,2,\ldots,L\}$, $k \in \{1,2,\ldots,U\}$, which are convolutionally encoded with a rate $R_0 = 1/R$ and memory ν. The same encoder is employed for all users and BPSK modulation is applied. To reduce the effect of error bursts at the input of the channel decoding, the coded sequence of the kth user is interleaved (π_k) with a distinct pattern which yields the coded symbols $\{d_t^k\}$; $t \in \{1,2,\ldots,RL\}$. The coded symbols are then modulated by a unique spreading waveform of length N chips and transmitted through the multipath channel. The nth chip of the spreading code employed by the kth user at time t is defined as $s_{t,n}^k \in \left\{\frac{-1}{\sqrt{N}}, \frac{1}{\sqrt{N}}\right\}$ where $n \in \{1,2,\ldots,N\}$. The spreading codes employed are randomly chosen and non-orthogonal to simulate the effect of a severe multipath channel.

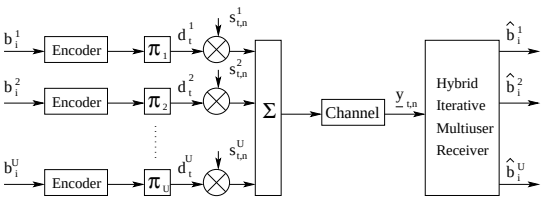

Fig. 1. Scheme of a DS-CDMA system with FEC coding.

The transmitted signal propagates through a multipath channel with impulse response $M(z) = \sum_{l=0}^{W-1} h_l z^{-l}$ where the channel length W denotes the number of chips. Therefore, assuming that the multipath channel spans only one neighbouring data symbol the receiver signal at the chip rate is then given by

$$\underline{y}_t = \underline{H}\,\underline{C}\,\underline{d} + \underline{\eta} \qquad (1)$$

where $\underline{H}$ is the channel matrix with dimensions $(N+W-1)\times(N+2W-2)$. The matrix with the spreading codes $\underline{C}$ has dimension $(N+2W-2)\times(3U)$. $\underline{d}$ and $\underline{\eta}$ are the data and noise vectors of length $3U$ and $(N+W-1)$ respectively. For $W=3$ the matrices in (1) are represented by

$$\underline{d} = \left[\; d_{t-1}^1, d_t^1, d_{t+1}^1, \cdots, d_{t-1}^U, d_t^U, d_{t+1}^U \;\right]^T.$$

$$\underline{C} = \begin{bmatrix} s_{t-1,N-1}^1 & 0 & 0 & s_{t-1,N-1}^2 & \cdots \\ s_{t-1,N}^1 & 0 & 0 & s_{t-1,N}^2 & \cdots \\ 0 & s_{t,1}^1 & 0 & 0 & \cdots \\ 0 & s_{t,2}^1 & 0 & 0 & \cdots \\ \vdots & \vdots & \vdots & \vdots & \cdots \\ 0 & s_{t,N}^1 & 0 & 0 & \cdots \\ 0 & 0 & s_{t+1,1}^1 & 0 & \cdots \\ 0 & 0 & s_{t+1,2}^1 & 0 & \cdots \end{bmatrix}$$

and $\underline{H}$ is a Toeplitz matrix with first row $[h_2, h_1, h_0, 0, \cdots, 0]$ and first column $[h_2, 0, \cdots, 0]^T$. The noise samples in $\underline{\eta}$ are Gaussian with distribution $\mathcal{N}(0,\sigma^2)$. This gives the output vector $\underline{y}_t$ of length $(N+W-1)$. It is assumed that all the users transmit with equal and constant power. It is also assumed that the spreading codes for every user are known exactly by the receiver.

III. ITERATIVE MULTIUSER RECEIVER

The structure of the HIMR is shown in Fig. 2. It consists of a soft-input soft-output multiuser detector followed by FEC decoding which operate separately but exchanging information in an iterative fashion. The implementation of this receiver can be viewed as using two different multiuser receivers: one that uses a moderate-complexity detector at the first iteration of the scheme and a second which is a SRBF detector for subsequent iterations.

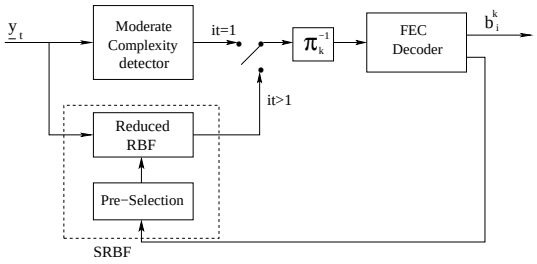

Fig. 2. Hybrid iterative multiuser receiver.

The multiuser detector output for the kth user is given by the *logarithm likelihood ratio* (LLR)

$$\Omega_{out}(d_t^k) = \ln\left(\frac{p(\underline{y}_t/d_t^k=+1)}{p(\underline{y}_t/d_t^k=-1)}\right) \qquad (2)$$

where $p(\underline{y}_t/d_t^k)$ are the conditional probabilities of detecting $d_t^k = +1$ or $d_t^k = -1$. This information is then supplied to the FEC decoding which consists of a block of U single-user decoders. The kth decoder output delivers the LLRs of the *a-posteriori* probabilities (APP) either for the coded bits (d_t^k) or the information bits (b_i^k),

$$\Omega_{in}(x) = \ln \frac{p(x = +1/\underline{y})}{p(x = -1/\underline{y})}. \tag{3}$$

where x represents either d_t^k or b_i^k and $\underline{y}$ is the input sequence of symbols corresponding to L information bits (frame length) in the kth decoder [12].

A. Multiuser receiver for the first iteration

On the first iteration all coded bit sequences are assumed to be equiprobable and therefore it is not possible to use the SRBF at this point because it would be required to implement the optimal RBF with full complexity. Hence, for this first iteration we suggest applying a moderate-complexity linear structure in the multiuser detection process followed by the FEC decoding. This moderate-complexity structure can be implemented by using any linear detection technique, *e.g.* matched filter, decorrelator, Wiener filter, etc. However, the better the performance the more reliable the information provided to the FEC decoder. It is well known that Wiener filtering provides the best performance among these linear techniques and this is what we will use. As mentioned previously, the multiuser detector must deliver a soft-input for the kth single-user decoder. For the Wiener filter detector this quantity is obtained as follows

$$\Omega_{out}(d_t^k) = \ln \frac{p(\hat{y}_t^k/d_t^k = +1)}{p(\hat{y}_t^k/d_t^k = -1)}. \tag{4}$$

where the scalar $\hat{y}_t^k$ represents the Wiener filter output corresponding to the kth user and $d_t^k = \pm 1$ the transmitted signal. Assuming Gaussian noise at the Wiener filter output these conditional probabilities can be obtained in a similar fashion to [13]. Once the LLR values of the coded bits have been computed, they are passed to the block of single-user decoders which update these LLR's to yield the multiuser receiver output at the first iteration.

B. FEC decoding

The input sequence to the kth single-user decoder is a vector whose components are given by (2) where $t \in \{1, 2, \cdots, RL\}$. The output sequence of the FEC decoder is obtained using a slight modification of the maximum *a-posteriori* (MAP) algorithm, as shown in [12]. For the kth user the APPs of the information (uncoded) bits are defined as follows

$$Pr\{b_i^k = b/\underline{y}^k\} = \sum_m \lambda_i^b(m) \tag{5}$$

where $\{b_i^k\}$; $i \in \{1, 2, \cdots, L\}$, $b \in \{1, -1\}$, and m is the index of all possible states in the trellis of the convolutional codes at time i. The APP is derived from the joint probability $\lambda_i^b(m)$ which can be obtained in a similar fashion to [12]. The vector $\underline{y}^k$ is the input sequence of a block of RL coded bits corresponding to the kth user. An analogous procedure can be applied to yield the APPs for the coded bits,

$$Pr\{d_t^k = d/\underline{y}^k\} = \sum_m \lambda_i^d(m) \tag{6}$$

where $\{d_t^k\}$; $t \in \{1, 2, \cdots, RL\}$, $d \in \{1, -1\}$ and $\underline{y}^k$ is the same as defined for (5).

C. Pre-selection technique

A *pre-selection* technique [14] is applied to reduce the complexity of the optimal RBF detector (applied in iterations > 1) based upon the LLRs of the coded bits $(\Omega_{in}(d_t^k))$ at the decoder outputs. The absolute value of these LLR values are used to yield a *confidence* value, $|\Omega_{in}(d_t^k)|$, for each coded bit of all users at time t. These *confidence* values are supplied to the multiuser detector so they can be used to reduce the complexity.

In the multipath scenario the vector used to obtain the centres of the RBF detector is given as $\underline{d}_t = [d_{t-1}^1, d_t^1, d_{t+1}^1, \cdots, d_{t-1}^U, d_t^U, d_{t+1}^U]$. The *confidence* of each coded bit provides a measure of how likely these bits can be correctly detected. The function of this stage is to establish an order of precedence among all these *confidence* values from the decoders' outputs. A large *confidence* value will mean that that bit can be detected correctly with a very high probability. Therefore, those bits with a high *confidence* value can be fixed to $+1$ in the case that $\Omega_{in}(d_t^k) > 0$ or -1 otherwise. To illustrate this technique an example for the case of two users is examined, we shall consider that the vector $\underline{d}_t = [d_{t-1}^1, d_t^1, d_{t+1}^1, d_{t-1}^2, d_t^2, d_{t+1}^2]$ has been received with the following *confidence* values

$$LLR(\underline{d}_t) = \begin{bmatrix} |\Omega_{in}(d_{t-1}^1)| \\ |\Omega_{in}(d_t^1)| \\ |\Omega_{in}(d_{t+1}^1)| \\ |\Omega_{in}(d_{t-1}^2)| \\ |\Omega_{in}(d_t^2)| \\ |\Omega_{in}(d_{t+1}^2)| \end{bmatrix} = \begin{bmatrix} |-10.38| \\ |5.33| \\ |9.18| \\ |1.20| \\ |-3.16| \\ |-6.38| \end{bmatrix} \begin{matrix} \\ \\ \\ \leftarrow \\ \leftarrow \\ \\ \end{matrix} \tag{7}$$

in this particular example a full search in the optimal RBF detector to find the most likely transmitted information would consider 2^6 possible combinations. However, a constraint in complexity can be given to allow only a desired level of complexity in the detector. For example fixing the search to only 3 bits in the vector $\underline{d}_t$ (those with the lowest *confidence* values as indicated in (7)), the total search would be reduced to complexity 2^3. Therefore the search in the RBF detector is done only for those bits with

the lowest *confidence* of being correctly detected, in our example the vector $\underline{d}_t = [-1, d_t^1, 1, d_{t-1}^2, d_t^2, -1]$ would be sent to the RBF.

D. Multiuser receiver for iteration > 1

The structure of the receiver for subsequent iterations is obtained by replacing the moderate-complexity detector with the SRBF detector which includes the *pre-selection* technique and the reduced RBF detector as shown in Fig. 2. The SRBF detector output for the kth user is yielded by (2) where the ratio of probabilities is obtained as follows

$$\frac{p(\underline{y}_t/d_t^k=+1)}{p(\underline{y}_t/d_t^k=-1)} = \frac{\sum_{l=1}^{2^{3U-1}} \exp\left(-\frac{||\underline{y}_t-\underline{a}_l||^2}{2\sigma^2}\right)}{\sum_{l=1}^{2^{3U-1}} \exp\left(\frac{-||\underline{y}_t-\underline{a}_l||^2}{2\sigma^2}\right)}. \quad (8)$$

The conditional probabilities are generated by the multivariate Gaussian probability density function [15] as given below

$$p(\underline{y}_t/d) = \frac{1}{2^{3U-1}} \sum_{l=1}^{2^{3U-1}} \frac{\exp\left(-\frac{||\underline{y}_t-\underline{a}_l||^2}{2\sigma^2}\right)}{(2\pi)^{N/2}\sigma^N} \quad (9)$$

where $d \in \{+1, -1\}$, $\underline{y}_t = [y_{t,1}, y_{t,2}, \cdots, y_{t,N}]$ is the received input vector consisting of the N chip spaced input samples, $\underline{a}_l = [c_1, c_2, \cdots, c_N]$ is the lth centre in the SRBF network and σ^2 is the noise variance. Note that in eq. (8) the numerator and denominator expressions are not equal since the centres $\underline{a}_l$ are computed with different values of d_t^k.

In a similar fashion to [5–9] we apply the turbo multiuser detection principle to the SRBF detector by modifying the probability $p(\underline{y}_t/d_t^k = d)$ as follow

$$p(\underline{y}_t/d_t^k=d) = \sum_{\substack{\underline{d}_t \\ (d_t^k=d)}} p(\underline{y}_t/\underline{d}_t) \prod_{\substack{r=1 \\ r\neq k}}^{U} pr(d_t^r) \quad (10)$$

where the *a priori* probabilities, $pr(d_t^k = d)$, are taken from the *confidence* values supplied at the decoder output in the previous iteration.

E. Complexity

In terms of complexity the Wiener filter has a complexity $O(N^3)$ regardless of the number of users. The MAP decoder algorithm's complexity increases exponentially with the encoder memory $O(2^v)$, but v is normally small. We can show that the full complexity of the receiver is basically dominated by the complexity in the SRBF detector, which has complexity 2^c operations per symbol interval where c is the desired level of complexity in the detector. By taking the number of centres (2^c) in the SRBF detector as the measure of complexity, we will show that using the *pre-selection* technique and the turbo multiuser detection principle, we not only get good performance but a significant complexity reduction can be obtained in the receiver structure compared with full RBF receivers where the complexity factor is 2^{3U}.

IV. NUMERICAL RESULTS

In this section we show performance of the system in terms of the bit error rate (BER) averaged over all users using Monte-Carlo simulations. We assume that the channel model is both chip and symbol synchronous (downlink scenario) with perfect power control. Also it is assumed that all users employ the same FEC encoder/decoder which consists of a non-recursive convolutional code of rate $R_o = 1/2$, memory $\nu = 4$, and generators $(37, 21)$ in octal notation. Each user transmits a block size of $L = 200$ information bits. A unique random interleaver (π) is used for every user. The user's spreading codes are chosen in a pseudo-random fashion on a symbol by symbol basis. The channel impulse response used in the simulations is given as $H(z) = 0.3482 + 0.8704z^{-1} + 0.3482z^{-2}$.

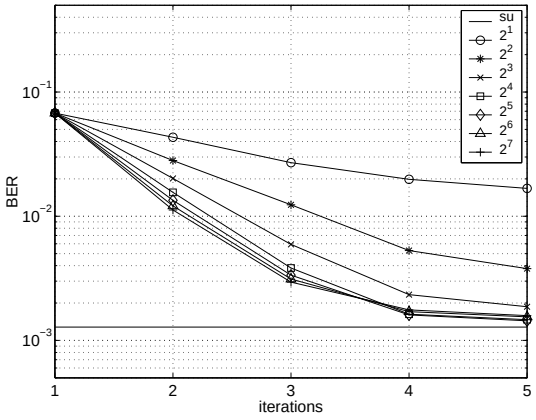

Fig. 3. BER performance against the number of iterations for $E_b/N_o = 4dB$. The curves show the performance when the complexity of the SRBF is constant at several values.

Fig 3 shows the BER performance of the HIMR for different number of iterations. The simulation was performed with a spreading code length of $N = 7$ and with $U = 5$ active users for $E_b/N_o = 4dB$. We show the cases when the complexity in the SRBF detector is kept constant at 2^c where $c \in \{1, 2, \cdots, 7\}$ (note that the full complexity of the optimal RBF detector is 2^{15} with 5 users). The case of *su* refers to the single-user performance. Here it is illustrated that the SRBF suffers performance degradation if the complexity is set too low. For example, the curve corresponding to 2^1 refers to the case when the complexity (number of centres) in the SRBF detector is kept constant at 2. It is shown that a better BER perform-

ance is achieved when a higher number of centres are included in the SRBF detector, as is expected. It is also shown that little improvement in performance is yielded if the SRBF complexity is increased beyond 2^4. It indicates that the performance of the optimal RBF detector can be achieved although some of the centres in the RBF network have not been considered at all. Therefore, by applying this hybrid structure we are avoiding making redundant and unnecessary operations.

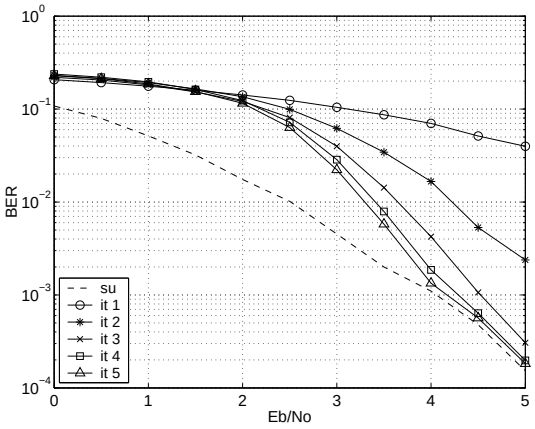

Fig. 4. HIMR performance with a fixed complexity in the SRBF of 2^4

A second simulation is carried out to illustrate the HIMR performance as a function of the E_b/N_o. Fig. 4 shows the HIMR performance for different numbers of iterations. Based on the results obtained in Fig. 3, the complexity in the SRBF is kept constant at 2^4 in a system with $N = 7$ and $U = 5$. As before *su* refers to the case of the single-user performance. It can be seen that with only 4 iterations in the receiver the single-user performance is achieved for a system with 5 users and spreading $N = 7$ providing $E_b/N_o > 4dB$.

V. CONCLUSIONS

In this paper we have derived a hybrid iterative multiuser receiver which achieved single-user performance even for large system loads in a multipath scenario. The extremely high complexity of the optimal joint receiver makes it an impractical choice for DS-CDMA systems. We apply the turbo multiuser detection principle not only to improve performance but also to reduce complexity in the RBF receiver.

Numerical results show the performance with a large number of users relative to the spreading factor. Using the turbo multiuser detection principle the receiver achieves single-user performance and reduces its complexity significantly, for example in the particular case presented in this paper the complexity is reduced from $2^{15} = 32768$ to $2^4 = 16$ operations per symbol required in the detection stage. Therefore, we can conclude that a good BER-complexity trade off is achieved by the hybrid iterative multiuser receiver proposed in this paper.

References

[1] A. Baier, U. Fiebig, W. Granzow, W. Knoch, P. Teder, and J. Thielecke. "*Design Study for a CDMA-Based Third-Generation Mobile Radio System*". IEEE J. Select. Areas in Commun., vol. 12, pp. 733-743, May 1994.

[2] S. Pike. "*The radio interface for UMTS*". In Proceedings Colloquium on Personal Commun. in the 21st Century part I and II, ref no. 1998/214 and 1998/242. IEE Feb. 1998, pp7/1-7/11.

[3] T.R. Giallorenzi and S.G. Wilson. "*Multiuser ML Sequence Estimator for Convolutionally Coded Asynchronous DS-CDMA Systems*". IEEE Trans. on Commun., vol. 44, no. 8, pp. 997-1008, Aug. 1996.

[4] Thomas R. Giallorenzi and Stephen G. Wilson. "*Suboptimum Multiuser Receivers for Convolutionally Coded Asynchronous DS-CDMA Systems*". IEEE Trans. on Commun., vol. 44, no. 9, Sept. 1996.

[5] H. Vincent Poor. "*Turbo Multiuser Detection: An Overview*". IEEE 6th Int. Symp. on Spread-Spectrum Tech. & Appli., NJIT, New Jersey, USA, Sept. 6-8, 2000.

[6] Michael Moher. "*An Iterative Multiuser Decoder for Near-capacity Communications*". IEEE Trans. on Commun., vol. 46, no. 7, pp. 870-880, July 1998.

[7] Mark C. Reed, Christian B. Schlegel, Paul D. Alexander, and John A. Asenstorfer. "*Iterative Multiuser Detection for CDMA with FEC: Near-Single-User Performance*". IEEE Trans. on Commun., vol. 46, no. 12, pp. 1693-1699, Dec. 1998.

[8] Xiaodong Wang, and H. Vincent Poor. "*Iterative (Turbo) Soft Interference Cancellation and Decoding for Coded CDMA*". IEEE Trans. on Commun., vol. 47, no. 7, pp. 1046-1060, July 1999.

[9] J.M. Luna Rivera, D.G.M. Cruickshank, and J.S. Thompson. "*Iterative Multiuser Receiver for a Coded DS-CDMA System*". IEEE VTC (Spring), Rhodes, Greece, May 2001.

[10] U. Mitra and H. Vincent Poor. "*Neural Network Techniques for Adaptive Multiuser Demodulation*". IEEE J. Select. Areas in Commun., vol. 12, no. 9, Dec. 1994.

[11] D.G.M. Cruickshank. "*Radial Basis function Receivers for DS-CDMA*". Electronics Letters, vol. 32, no. 3, Feb. 1996.

[12] S. Benedetto, D. Divsalar, G. Montorsi, and F. Pollara. "*A Soft-Input Soft-Output Maximum A Posteriori (MAP) Module to Decode Parallel and Serial Concatenated Codes*". JPL TDA Progress Report 42-127, Nov. 15, 1996.

[13] D.G.M. Cruickshank. "*Suppression of multiple access interference in a DS-CDMA system using Wiener filtering and parallel cancellation*". IEE Proc. Commun., vol. 143, no. 4, pp. 226-230 Aug. 1996.

[14] Emad A. Alsusa, D.G.M. Cruickshank. "*Pre-selection based reduced complexity MLMUD for DS-CDMA systems*". IEEE VTC (Spring), Rhodes, Greece, May 2001.

[15] J. G. Proakis, *Digital Communications*, 4th edition. New York: McGrawHill 2001.

Space-Time Iterative Multiuser Receiver for a Coded DS-CDMA System in a Flat Fading Channel

J. M. Luna Rivera, D.G.M. Cruickshank, and J.S. Thompson
The University of Edinburgh
Department of Electronics and Electrical Engineering
The King's Buildings, Mayfield Rd., Edinburgh, EH9 3JL, UK
email: mlr@ee.ed.ac.uk, dgmc@ee.ed.ac.uk, jst@ee.ed.ac.uk

Abstract — **In this paper, we consider a space-time iterative multiuser (STIM) receiver for a flat fading channel and examine its application in a DS-CDMA mobile communication system with forward error correction (FEC) coding. This multiuser receiver structure exploits its spatial and temporal capabilities to overcome interference. Numerical results shows that a significant increase in capacity over flat fading channels is achieved by combining efficient space-time coding (STC), multiuser detection (MUD), iterative signal processing techniques and the reuse of orthogonal spreading codes.**

I. INTRODUCTION

THE third generation (3G) of mobile communications aims to enhance system capacity, quality and data rate compared with currently available systems. Since DS-CDMA systems are adopted as the main technology for 3G, a significant interest exists in enhancing data rates and capacity. However, multiple access interference (MAI) is one of the major factors that limits the capacity and performance of DS-CDMA systems. Over the last decade, MUD techniques have been applied to mitigate this type of interference. Recently, iterative processing techniques have particularly received considerable attention in this field. As a result, a substantial number of sub-optimum multiuser receivers have been proposed with some remarkably good results [1–4]. On the other hand, antenna arrays have shown to be an effective and practical technique to provide spatial diversity allowing a significant capacity gain over conventional single-antenna systems [5–7]. For downlink transmissions a major concern is with the constraints in cost and size of the receiver. Therefore, transmit diversity techniques tend to provide an effective solution in these scenarios.

Motivated by the spatial and temporal capabilities of a DS-CDMA system, we exploit further this potential to design a space-time iterative multiuser receiver for a coded DS-CDMA system over a flat fading channel. In this paper, we suggest reuse of orthogonal codes to increase the system spectral efficiency. To distinguish between those users with same orthogonal codes, a separation code is proposed. Therefore, the users with the same orthogonal codes but with a different separation code will introduce into the system a MAI factor due to the cross-correlation terms between non-orthogonal users. To remove this MAI term, we derive a multiuser detector based on an iterative technique.

An attractive iterative multiuser structure is obtained, as shown [4], by using the Wiener filter (WF) detector followed by a soft cancellation (SC) scheme and a block of FEC decoders since this receiver has reasonable complexity and good performance. In a moderate loaded system the convergence of an iterative receiver will rely on the signal to noise and interference ratio (SNIR) required to obtain a "good" performance at the first iteration (normally it requires a bit error rate (BER) lower than 10^{-1} to converge). However, increasing the number of users in the system will increase significantly the SNIR required at the first iteration to achieve the same performance and consequently the convergence of the iterative receiver. It is therefore crucial to effectively combat or reduce the effect of adding more users into the system. Hence, in this paper a space-time iterative multiuser receiver is derived. A simple STC technique is used to achieved the desired diversity at the receiver [8], [9]. This diversity technique maximises the gain introduced into the signals by transmitting through multiple antennas.

The rest of the paper is organised as follow. The next section describes the system model. In section III, the STC encoder/decoder structure used to obtain the desired spatial diversity gain is introduced. Then the iterative multiuser receiver is discussed in section IV. Finally, simulation results and conclusions are presented in section V and VI respectively. Throughout this paper, scalars are denoted by *italic* font, lowercase **bold** for vectors and uppercase **bold** for matrices.

II. SYSTEM MODEL

In Fig. 1 a FEC coded DS-CDMA system model with M transmit antennas is shown in a flat fading channel. Without loss of generality, only one receive antenna is considered (suitable for downlink transmissions). A total number of U active users operates in the system. The total number of users can be seen as two groups of users transmitting information with the same orthogonal spreading codes used by both groups. To distinguish the groups,

each group is given a separation code as shown in Fig. 1. The users' information stream is transmitted in FEC

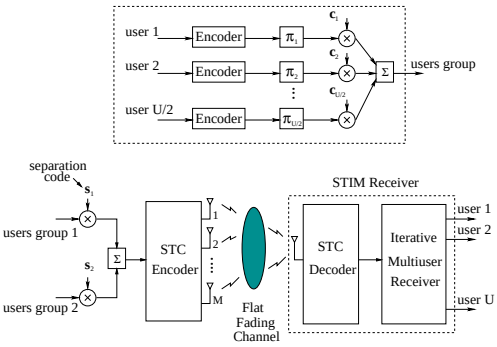

Fig. 1. DS-CDMA System model with FEC coding in a flat fading channel.

blocks of L data bits, referred to as a *data block*. For the kth user every *data block*, $\{d_k(i)\}$; $i \in \{1, 2, \cdots, L\}$, $k \in \{1, 2, \cdots, U\}$, is first encoder by a convolutional encoder with a rate n_0 and memory ν. To reduce the effect of burst errors in the FEC decoder's input, an interleaver (π_k) is applied to the resulting FEC coded bit stream. After interleaving, the stream of FEC coded bits by the kh user appears as $\{b_k(t)\}$; $t \in \{1, 2, \cdots, L/n_0\}$ with $b_k(t) \in \{-1, 1\}$. Codes of length N are used to spread the user's interleaved FEC coded bits. Thus, the STC encoder input at time t can be written as

$$\mathbf{x}_t = \mathbf{C}\mathbf{b}_t \tag{1}$$

where $\mathbf{b}_t = [b_1(t), b_2(t), \cdots, b_U(t)]^T$ denotes the users data vector with dimensions $U \times 1$. The matrix $\mathbf{C}$ with dimensions $N \times U$ has as its columns the users codes combined with the separation codes, *i.e* the element in the nth row and kth column of $\mathbf{C}$ is defined as

$$C_{n,k} = \begin{cases} c_{g,n}\, s_{1,n} & \text{if } k \leq U/2 \\ c_{g,n}\, s_{2,n} & \text{otherwise} \end{cases}$$

where $c_{g,n} \in \left\{\frac{-1}{\sqrt{N}}, \frac{1}{\sqrt{N}}\right\}$ and $s_{1,n}$, $s_{2,n} \in \{-1, 1\}$ for all $n \in \{1, 2, \cdots, N\}$ and $g \in \{1, 2, \cdots, U/2\}$. For the rest of the paper $\mathbf{x}_t$ will be referred to as a *STC symbol*. The data stream $\{\mathbf{x}_t\}$; $t \in \{1, 2, \cdots, L/n_0\}$ is then partitioned into blocks of *STC symbols* which are fed to the STC encoder to yield the data sequence to be transmitted through the M antennas. To guarantee that the overall transmit power is independent of the number of transmit antennas, a factor of $1/\sqrt{M}$ is applied to each of the antenna's signals before transmission. This factor is included in our system by defining the kth user amplitude as $b_k(t) \in \left\{\frac{-1}{\sqrt{M}}, \frac{1}{\sqrt{M}}\right\}$.

III. SPACE-TIME DIVERSITY GAIN

Space-time trellis coding (STTC) [10] is a recent transmit diversity technique that combines signal processing at the receiver with a specific design of coding for multiple transmit antennas. Significant space-time diversity gain is achieved by applying this technique. However, space-time transmit diversity (STTD) [8] is a more remarkable and recent scheme for transmission using two transmit antennas. Despite a loss in performance compared to STTC, the decoding complexity of STTD is much less than STTC. Therefore, in terms of simplicity and performance the STTD scheme is perhaps a better choice for providing space-time diversity gain in real systems.

A. STC Encoder

Conventional STC encoders with M transmit antennas require the same number of *STC symbol* periods to transmit a block of M *STC symbols*. To clarify exactly how individual *STC symbols* are sent from the transmitter, Fig. 2 shows a layout of the *STC symbols* through the transmit antennas. Fig. 2 (a) illustrates the scheme for a block

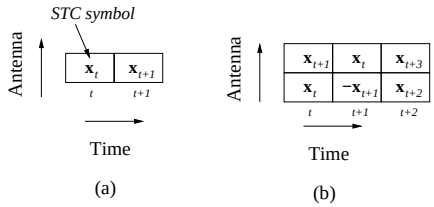

Fig. 2. Block transmission through the STC encoder using (a) $M = 1$ and (b) $M = 2$.

transmission using only one transmit antenna ($M = 1$). With 2 transmit antennas ($M = 2$) the scheme is that given in Fig. 2 (b). Notice that in the former the block of transmission is given directly by the data stream $\{\mathbf{x}_t\}$; $t \in \{1, 2, \cdots, L/n_0\}$. The latter transmits in the tth time slot the *STC symbols* $\mathbf{x}_t$ and $\mathbf{x}_{t+1}$ from antenna 1 and 2 respectively. In the next time slot (t+1), $-\mathbf{x}_{t+1}$ is transmitted from antenna 1 and $\mathbf{x}_t$ from antenna 2. The generalisation of the STTD scheme for more than two transmit antennas is addressed in [9].

B. STC Decoder

With no loss in the generality and in order to illustrate the STC decoder procedure, we assume the case of $M = 2$. It is also assumed that the channel is constant across two consecutive *STC symbols* and there is perfect time synchronisation between the transmitter and receiver, therefore, the received signals from the tth and $(t+1)$th time slots can be written as

$$\begin{aligned} \mathbf{r}_t &= h_1\mathbf{x}_t + h_2\mathbf{x}_{t+1} + \boldsymbol{\eta}_t \\ \mathbf{r}_{t+1} &= h_2\mathbf{x}_t - h_1\mathbf{x}_{t+1} + \boldsymbol{\eta}_{t+1} \end{aligned} \tag{2}$$

where the components of the vectors $\mathbf{r}_t$ and $\mathbf{r}_{t+1}$ with dimensions $N \times 1$ are the received signals at time t and $t+1$ respectively which are sampled at the chip rate. The channel effect from the mth transmit antenna to the receive

antenna is modelled by the Rayleigh-distributed random variable h_m with $m \epsilon \{1,2\}$. Finally, the noise vectors $\boldsymbol{\eta}_t$ and $\boldsymbol{\eta}_{t+1}$ with dimensions $N \times 1$ contains zero-mean complex Gaussian noise samples with variance σ^2. For convenience, (2) can be rewritten in an alternative form by conjugating $\mathbf{r}_{t+1}$ and combining the received signal over two consecutive period symbols in the following way

$$\begin{bmatrix} \mathbf{r}_t \\ \mathbf{r}^*_{t+1} \end{bmatrix} = \begin{bmatrix} \boldsymbol{\Lambda}_1 & \boldsymbol{\Lambda}_2 \\ \boldsymbol{\Lambda}^*_2 & -\boldsymbol{\Lambda}^*_1 \end{bmatrix} \begin{bmatrix} \mathbf{x}_t \\ \mathbf{x}_{t+1} \end{bmatrix} + \begin{bmatrix} \boldsymbol{\eta}_t \\ \boldsymbol{\eta}^*_{t+1} \end{bmatrix} \quad (3)$$

where $\boldsymbol{\Lambda}_m = h_m \mathbf{I}$; $m \epsilon \{1,2\}$ with $\mathbf{I}$ as the identity matrix of dimensions $N \times N$. In order to achieve the desired space diversity gain we define

$$\boldsymbol{\Lambda} = \begin{bmatrix} \boldsymbol{\Lambda}_1 & \boldsymbol{\Lambda}_2 \\ \boldsymbol{\Lambda}^*_2 & -\boldsymbol{\Lambda}^*_1 \end{bmatrix} \quad (4)$$

and then multiplying (3) by $(\boldsymbol{\Lambda}^H \boldsymbol{\Lambda})^{-1} \boldsymbol{\Lambda}^H$, with $()^H$ as the Hermitian operation, we obtain

$$\begin{bmatrix} \hat{\mathbf{x}}_t \\ \hat{\mathbf{x}}_{t+1} \end{bmatrix} = \begin{bmatrix} \mathbf{x}_t \\ \mathbf{x}_{t+1} \end{bmatrix} + (\boldsymbol{\Lambda}^H \boldsymbol{\Lambda})^{-1} \boldsymbol{\Lambda}^H \begin{bmatrix} \boldsymbol{\eta}_t \\ \boldsymbol{\eta}_{t+1} \end{bmatrix} \quad (5)$$

where $\hat{\mathbf{x}}_t$, $\hat{\mathbf{x}}_{t+1}$ are the estimates of $\mathbf{x}_t$ and $\mathbf{x}_{t+1}$ respectively. Notice that $\boldsymbol{\Lambda}^H \boldsymbol{\Lambda}$ is given as $(|h_1|^2 + |h_2|^2)\mathbf{I}$ with $\mathbf{I}$ as the $2N \times 2N$ identity matrix and $|h_1|^2 + |h_2|^2$ as the space diversity gain factor. Taking out the contribution in eq. (5) of the signal at time slot t and using (1) to replace $\mathbf{x}_t$, we get

$$\hat{\mathbf{x}}_t \quad = \quad \mathbf{C}\mathbf{b}_t + \boldsymbol{\omega}_t \quad (6)$$

where $\boldsymbol{\omega}_t$ is a $N \times N$ noise vector. Therefore, we can finish this section by drawing analogies between eq. (6) and a synchronous DS-CDMA system over an AWGN channel. Since the elements in $\boldsymbol{\eta}_t$ and $\boldsymbol{\eta}_{t+1}$ are complex Gaussian samples, this implies that the elements in $\boldsymbol{\omega}_t$ are also complex Gaussian samples with zero mean and variance $\sigma^2_{stc} = \sigma^2/(|h_1|^2 + |h_2|^2)$.

IV. ITERATIVE MULTIUSER RECEIVER

MUD techniques can be applied to eq. (6) in order to mitigate MAI in the system. An attractive iterative multiuser structure was proposed in [4] for interference mitigation in a DS-CDMA system. In this section, we show that the basic principle is also applicable to the DS-CDMA system proposed in this paper. The iterative multiuser receiver structure is illustrated in Fig. 3. It consists of a Wiener fileter (WF) multiuser detector, followed by a soft cancellation (SC) scheme and a block of parallel MAP convolutional decoders. The cancellation/decoders are separated by interleavers and deinterleavers. Next we describe each of these modules in the receiver structure.

A. Wiener based multiuser detector

Firstly, the WF detector takes as its input the STC decoder output, $\hat{\mathbf{x}}_t$, and computes as its output an initial estimate of the *a priori* logarithm of likelihood ratios

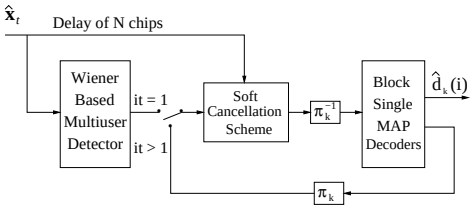

Fig. 3. Iterative multiuser receiver structure.

(LLR's) of the interleaved FEC coded bits for the desired user and the interfering users, $LLR_{wf}(b_k(t))$ with $k \epsilon \{1, 2, \cdots, U\}$. These estimates are formed as

$$LLR_{wf}(b_k(t)) \quad = \quad \ln\left(\frac{p(y_k(t)|b_k(t) = \frac{1}{\sqrt{M}})}{p(y_k(t)|b_k(t) = \frac{-1}{\sqrt{M}})}\right) \quad (7)$$

where the conditional probabilities $p(y_k(t)|b_k(t) = b)$ with $b \epsilon \{\frac{1}{\sqrt{M}}, \frac{-1}{\sqrt{M}}\}$, are calculated assuming Gaussian noise at the WF detector output. The scalar $y_k(t) = \boldsymbol{\psi}^T \{\hat{\mathbf{x}}_t\}_{Re}$ denotes the real part of the WF detector output for the kth user with mean $\boldsymbol{\psi}^T \boldsymbol{\phi}^k_{\hat{x}b}$ and noise variance $\sigma^2_{wf}(k) = -(\boldsymbol{\psi}^T \boldsymbol{\phi}^k_{\hat{x}b})^2 + \boldsymbol{\psi}^T \boldsymbol{\phi}^k_{\hat{x}b}$ (see [11]). The vector $\boldsymbol{\psi}$ is an N tap filter given by $\boldsymbol{\psi} = \boldsymbol{\Phi}^{-1}_{\hat{x}\hat{x}} \boldsymbol{\phi}^k_{\hat{x}b}$, where $\boldsymbol{\Phi}_{\hat{x}\hat{x}}$ represents the $N \times N$ autocorrelation matrix of the input signal which is given as $\boldsymbol{\Phi}_{\hat{x}\hat{x}} = \mathbf{C}\mathbf{D}\mathbf{C}^T + \sigma^2_{stc}/2\mathbf{I}$. The matrix $\mathbf{D}$ is a $U \times U$ matrix with its leading diagonal as the power of the users, *i.e* $1/M$, and zero elsewhere. The matrix $\mathbf{I}$ is the $N \times N$ identity matrix and $\sigma^2_{stc}/2$ the noise variance from the real part of $\boldsymbol{\omega}_t$ (see eq. (6)).

The cross-correlation vector $\boldsymbol{\phi}^k_{\hat{x}b}$ with dimensions $N \times 1$ is defined as the combination between the user spreading and separation codes (kth column of $\mathbf{C}$) multiplied by $1/M$.

B. Soft parallel cancellation scheme

The SC scheme, which incorporates the iterative principle, yields at its output an improved estimate of the LLR's of the interleaved FEC coded bits, $LLR^{\pi}_{sc}(b_k(t))$. These estimates are computed by taking soft estimates of the interfering users and subtracts them from the received signal $\hat{\mathbf{x}}_t$. A matched filter (MF) is then applied to yield the output of the SC scheme. For the kth user, this quantity is expressed in the following form

$$\hat{y}_k(t) = \mathbf{q}_k[\mathbf{b}_t - \hat{\mathbf{b}}^k_t] + \zeta_k(t) \quad (8)$$

where $\mathbf{q}_k$ denotes the kth row of the autocorrelation matrix given as $\mathbf{C}^T\mathbf{C}$, the vector $\hat{\mathbf{b}}^k_t$ corresponds to the soft estimates of the interfering users which are given as $\hat{\mathbf{b}}^k_t = [\hat{b}_1(t), \cdots, \hat{b}_{k-1}(t), 0, \hat{b}_{k+1}(t), \cdots, \hat{b}_U(t)]$. The soft estimate of a user is formed as

$$\hat{b}_k(t) = \sum_{b \epsilon \{\frac{-1}{\sqrt{M}}, \frac{1}{\sqrt{M}}\}} bp(b), \quad k = 1, \ldots, U. \quad (9)$$

where the conditional probabilities at the WF detector output, $p(y_k(t)|b_k(t)=b)$, are taking as the *a priori* probabilities $p(b)$ required in eq. (9), *i.e* $p(b)=p(y_k(t)|b_k(t)=b)$ with $b \in \{\frac{1}{\sqrt{M}}, \frac{-1}{\sqrt{M}}\}$. Since the users from the same group are orthogonal, we set to zero their contribution in the vector $\hat{\mathbf{b}}_t^k$. Lastly, $\zeta_k(t)$ represents a Gaussian noise sample with zero mean and variance $\sigma_{stc}^2/2$. Since the SC scheme output for the kth user can be well modelled by an equivalent AWGN, it can then be written as

$$\hat{y}_k(t) = b_k(t) + \mu_k(t) \tag{10}$$

with $\mu_k(t)$ as a Gaussian noise sample with zero mean and variance (see Appendix I)

$$\sigma_\mu^2(k) = \frac{1}{M}\sum_{\substack{k_1=1 \\ k_1\neq k}}^{U} q_{k,k_1}^2 + \sigma_{stc}^2/2. \tag{11}$$

q_{k,k_1} denotes the cross-correlation factor between user k and user k_1.q_{k,k_1}. Similar to (7), the LLR_{sc}^{π}'s at the SC scheme output are obtained by computing the conditional probabilities $p(\hat{y}_k(t)|b_k(t)=b)$ for $b=1/\sqrt{M}$ and $b=-1/\sqrt{M}$.

C. MAP Decoding

In our proposed system, convolutional codes are chosen as the channel code. In this section we just briefly describe the kth user's single decoder, which consists of a MAP decoder. As shown in Fig. 3, the deinterleaved *extrinsic* LLR's values, $LLR_{sc}^{\pi^{-1}}(b_k(t))$, are fed as input to the MAP convolutional decoder. This information is used directly in the MAP's branch metric calculation which is modified as in [1–4] to

$$\gamma_i(m_1', m_1) = Pr \prod_{t'=(i-1)n_0+1}^{in_0} p(\hat{y}_k(t')|b_k(t')) \tag{12}$$

where $Pr = Pr\{S_i = m_1/S_{i-1} = m_1'\}$. The product in (12) is over all the $b_k(t)$ values that produce the transition of the MAP decoder from state m_1' to state m_1. At the first iteration no *a prior* information is available, therefore $Pr\{S_j = m_1/S_{j-1} = m_1'\} = 1/2$. Thus, the MAP decoder computes the *a posteriori* probabilities (APP) LLR's of the data bits, $LLR_{MAP}(d_k(t))$, based on the estimated FEC coded bits given by the SC scheme. Also, the APP LLR's of the FEC coded bits, $LLR_{MAP}(b_k(t))$, are computed from the MAP algorithm.

D. Iterative scheme

To incorporate the iterative principle in the multiuser receiver structure, we make use of the soft APP's from the channel code, $a_k^t = LLR_{MAP}(b_k(t))$, which then can be used as *a priori* information for the SC scheme in eq. (9) if $p(b_k(t)=b) = e^{a^t}/M$ or $1/(1+e^{a_k^t})$ if $b=-1/\sqrt{M}$. For the first iteration, the WF detector provides the required *a priori* probabilities to compute the soft estimates of interfering users. Therefore, at time t these *a priori* probabilities must be generated only for the FEC coded bits of those interfering users. On subsequent iterations, these quantities are computed by the MAP decoder based on the extrinsic LLR's values, $LLR_{MAP}(b_k(t))$. Note that for an iteration number >1 these extrinsic LLR's values have to be interleaved to yield the appropriate ordering of the data stream at that stage. Finally, after a desired number of iterations the MAP decoder performs a hard decision on the LLR's of the data bits, $LLR_{MAP}(d_k(t))$, to recover the original uncoded data stream.

V. SIMULATIONS RESULTS

In this section, we present the performance of the proposed STIM receiver. To evaluate the performance we simulate the downlink of a synchronous DS-CDMA system with $M=2$ transmit antennas over a flat fading channel. The channel coefficients denoted by h_m with $m=1,2$, are modelled as independent Rayleigh fading random variables with distribution $\mathcal{N}(0,1)$. It is assumed that the receiver has perfect knowledge of the channel coefficients. Every user transmits *data blocks* of $L=200$ information

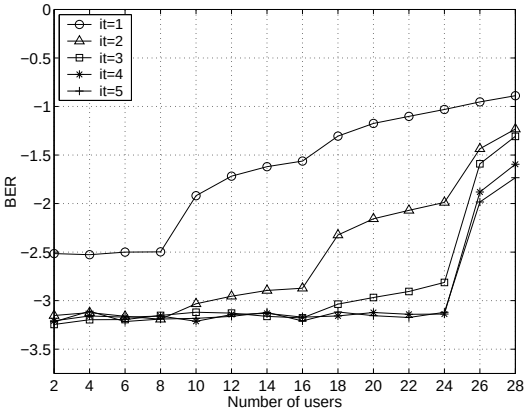

Fig. 4. STIM receiver performance with M=2

bits which are encoded by a recursive systematic convolutional code of rate $n_0=1/2$ with memory $\nu=4$ and generators $(37,21)$ in octal notation. To spread the signals, Walsh-Hadamard codes of length $N=16$ are applied. Random interleavers (π) are used to reduce the effect of burst errors in the decoders' input. The group separation codes $\mathbf{s}_1$ and $\mathbf{s}_2$ of length N are chosen by generating random codes of length N and then the cross-correlation $\mathbf{s}_1^T\mathbf{s}_2$ is checked. The separation codes generated here have a maximum normalised cross-correlation of $\mathbf{s}_1^T\mathbf{s}_2 \leq 0.5$. Fig. 4 shows the average BER performance of the STIM receiver as a function of the number of users for a different number of iterations. Each group in the system is considered to have the same number of users, *i.e* given a

total number of users U each group contains $U/2$ users. From Fig. 4 it is observed that using only 4 iterations in the STIM receiver, the system achieves near single-user performance up to about 24 users (a system 150 % loaded, *i.e* $U = 24$, $N = 16$).

Simulation results in Fig. 5 shows the average BER performance against the E_b/N_0 for different number of iterations using $M = 2$. The simulations are performed for a system with $U = 24$ users divided into two groups, each of 12 users. To illustrate the performance gain by using the transmit diversity scheme, Fig. 5 includes the single-user performance over the conventional single-antenna case ($M = 1$). As defined before, the group separation codes ($\mathbf{s}_1$ and $\mathbf{s}_2$) are limited to those with a normalised cross-correlation of $\mathbf{s}_1^T \mathbf{s}_2 \leq 0.5$. Results show that with only 4 iterations in the STIM receiver this highly loaded system in a flat fading channel achieves near single-user performance.

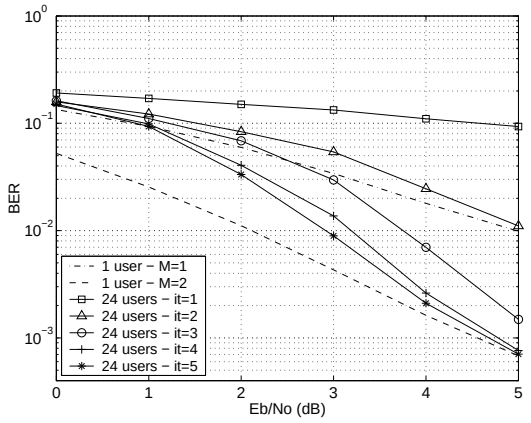

Fig. 5. STIM receiver BER performance for a DS-CDMA system in a flat fading channel

VI. CONCLUSIONS

In this paper a space-time iterative multiuser receiver has been presented to improve the capacity and performance of a DS-CDMA system in a flat fading channel. The main contribution is in combining MUD with antenna array techniques to design a STIM receiver structure capable of mitigate interferences and achieving a significant capacity improvement. The capacity is further enhance by the reuse of orthogonal spreading codes, *i.e* the STIM receiver allows to achieve an improvement in the spectral efficiency of the system as only $U/2$ orthogonal spreading codes are required for a system with U users.

Appendix

I. Noise variance at the SC scheme output

From eq. (10) the variance of $\mu_k(t)$ is expressed as $\sigma_\mu^2(k) = E[\mu_k^2(t)] - E^2[\mu_k(t)]$. Where E[] denotes the expected value and $\mu_k(t)$ is given by

$$\mu_k(t) = \sum_{\substack{k_1=1 \\ k_1 \neq k}}^{U} q_{k,k_1}[b_{k_1}(t) - \hat{b}_{k_1}(t)] + \zeta_k(t) \qquad (13)$$

with q_{k,k_1} as the cross-correlation factor between user k and user k_1. Considering $E[b_k(t)] = 0$ for all k and using (13), we get

$$E^2[\mu_k(t)] = \left(\sum_{\substack{k_1=1 \\ k_1 \neq k}}^{U} -q_{k,k_1} E[\hat{b}_k(t)] \right)^2$$

and

$$E[\mu_k^2(t)] = \left(\sum_{\substack{k_1=1 \\ k_1 \neq k}}^{U} q_{k,k_1}^2 E[b_k^2(t)] \right) + E^2[\mu_k(t)] + \sigma_{stc}^2/2$$

therefore it can be shown that the variance σ_μ^2 is then given by

$$\sigma_\mu^2(k) = \frac{1}{M} \sum_{\substack{k_1=1 \\ k_1 \neq k}}^{U} q_{k,k_1}^2 + \sigma_{stc}^2/2 \qquad (14)$$

References

[1] M. Moher. "*An Iterative Multiuser Decoder for Near-capacity Communications*". IEEE Transactions on Communications, vol. 46, no. 7, pp. 870-880, July 1998.

[2] M.C. Reed, C.B. Schlegel, P.D. Alexander, and J.A. Asenstorfer. "*Iterative Multiuser Detection for CDMA with FEC: Near-Single-User Performance*". IEEE Transactions on Communications, vol. 46, no. 12, pp. 1693-1699, December 1998.

[3] X. Wang, and H.V. Poor. "*Iterative (Turbo) Soft Interference Cancellation and Decoding for Coded CDMA*". IEEE Transactions on Communications, vol. 47, no. 7, pp. 1046-1060, July 1999.

[4] J.M. Luna Rivera, D.G.M. Cruickshank, and J.S. Thompson. "*Iterative Multiuser Receiver for a Coded DS-CDMA System*". IEEE Vehicular Technology conference (VTC 2001 spring), vol. 2, pp. 1518-1522, Rhodes Island, Greece, May 2001.

[5] G.J. Foschini. "*Layered space-time architecture for wireless communication in fading environments when using multiple antennas*". Bell Labs. Techn. J., vol. 2, Autumn 1996.

[6] V. Tarokh, N. Seshadri, and A.R. Calderbank. "*Space-time codes for high data rate wireless communication: Performance criterion and code construction*". IEEE Transaction on Communications, vol. 47, No. 2, pp. 199-207, February 1999.

[7] D. Agrawal, V. Tarokh, A. Nagui, and N. Seshadri. "*Space-time coded OFDM for high data-rate wireless communication over wideband channels*". IEEE Vehicular Technology Conference (VTC 1998), vol. 3, pp. 2232-2236, Ottawa, Ontario, Canada, May 1998.

[8] S. M. Alamouti. "*A Simple Transmit Diversity Technique for Wireless Communications*". IEEE Journal on Selected Areas in Communications, vol. 16, no. 8, pp. 1451-1458, October 1998.

[9] V. Tarokh, H. Jafarkhani, and A.R. Calderbank. "*Space-Time Block Codes from Orthogonal Designs*". IEEE Transactions on Information Theory, vol. 45, no. 5, pp. 1456-1467, July 1999.

[10] A.F. Naguib, N. Seshadri and A.R. Calderbank. "*Increasing data rate over wireless channels*". IEEE Signal Processing Magazine, vol. 17, No. 3, pp. 76-92, May 2000.

[11] D.G.M. Cruickshank. "*Suppression of multiple access interference in a DS-CDMA system using Wiener filtering and parallel cancellation*". IEE Proc. Commun., vol. 143, no. 4, pp. 226-230 Aug. 1996.

A High Capacity Space-Time FEC Coded DS-CDMA System for use over Multipath Channels

J. M. Luna Rivera[†], D.G.M. Cruickshank, and J.S. Thompson

Submitted to *IEEE Transactions on Wireless Communications*, June 26, 2002.

Index Terms — *DS-CDMA, space time coding, multiuser detection, iterative processing techniques, multipath fading channel.*

Abstract — **Antenna array techniques and multiuser detection are very promising approaches for obtaining substantial capacity increases in wireless channels. In this paper, we propose a novel space-time architecture for the downlink of a forward error correction (FEC) coded direct-sequence code division multiple access (DS-CDMA) system for use in multipath fading channels. In particular, we exploit the spatial and temporal capabilities of the system to design the transmitter/receiver. Significant increase in capacity over multipath fading channels is achieved by combining efficient space-time coding (STC), multiuser detection (MUD), iterative signal processing techniques and the reuse of orthogonal spreading codes. Analysis and simulation results are provided to demonstrate the capacity improvement. To illustrate the practical implementation of this architecture an analysis of complexity is presented.**

I. Introduction

The rapid growth in mobile wireless communications creates the need for enhanced system capacity and quality in mobile systems. Since DS-CDMA systems are adopted as the main technology for the third generation (3G) of mobile communications, a significant interest exists in enhancing data rates and capacity. However, reliable wireless communication is always difficult over time-varying multipath fading channels. The channel causes multiple access interference (MAI) and intersymbol interference (ISI) which are two major factors that limit the capacity and performance of DS-CDMA systems. Over the last decade, MUD techniques have been applied to mitigate these interference effects. Recently, iterative processing techniques have received considerable attention in this field. As a result, a substantial number of sub-optimum multiuser receivers have been proposed with some remarkably good results [1–5]. On the other hand, antenna arrays have shown to be an effective and practical technique to provide spatial diversity, allowing a significant capacity gain over conventional single-antenna systems [6–9]. For downlink transmissions a major concern is with the constraints in cost and size of the receiver. Therefore, transmit diversity techniques tend to provide an effective solution in these scenarios.

More recently, an efficient space-time transmit diversity (STTD) scheme has been proposed in [10] and has attracted a lot of attention. This is because it represents a practical way to improve the performance of current systems. The STTD technique maximises the diversity gain by transmitting through multiple antennas and uses a very simple receiver for flat fading channels. A generalisation to time dispersive channels has been recently proposed in [11]. This new approach not only provides full space diversity gain but is also capable of reducing the MAI and ISI factors. The approach relies upon incorporating a cyclic prefix in the user transmission. However, a potential drawback of this scheme is the incorporation of a cyclic

[†]The authors are with: Signals and Systems Group, Electronics & Electrical Eng. Depart., University of Edinburgh. The King's Buildings, Mayfield Rd. Edinburgh, EH9 3JL, UK. Tel.: +44 131 650 5556, Fax: +44 131 650 6554 and E-mail mlr@ee.ed.ac.uk

prefix per data symbol, with length at least equal to the channel length. This reduction in the data throughput is then reflected in a reduction in the overall spectral efficiency of the system. Analysis of the scheme in [11] shows that if the processing gain is equal to N, the system spectral efficiency as a function of the number of users is limited to N users since this is the maximum number of orthogonal codes available in the system.

Motivated by the spatial and temporal capabilities of a DS-CDMA system, we exploit further the potential to design a high capacity space-time coded DS-CDMA system. In this paper, we suggest the reuse of orthogonal codes to increase the system spectral efficiency. To distinguish those users with the same orthogonal codes, a separation code is proposed. Similar to [11], a cyclic prefix is used to combat the ISI effect from the channel. As distinct from [11], a MAI factor will appear at the receiver side as a consequence of the cross-correlation terms between non-orthogonal users. To remove this MAI term, we derive a multiuser detector based on an iterative technique. For this structure, we derive the Wiener filter (WF) solution followed by a cancellation scheme and a block of single forward error correction (FEC) decoders which are combined using the iterative decoding principle [12]. Furthermore, to reduce the penalty of including the cyclic prefixes, a new transmission scheme using blocks of data is also proposed. To illustrate the practical application of the system, we analyse the receiver structure complexity.

The rest of the paper is organised as follow. The system model is described in Section II. In Section III, we introduce the STC encoder/decoder structure proposed for the desired spatial diversity gain. Section IV is devoted to describing the iterative multiuser detector scheme. In Section V, we provide an analysis of the receiver complexity. Simulation results are presented in Section VI to demonstrate the system performance. Finally, Section VII concludes the paper. Throughout this paper, scalars are denoted by *italic* font, lowercase bold for vectors and uppercase bold for matrices.

II. System model

We consider a multiple antenna DS-CDMA communication system operating over a multipath fading channel with M transmit antennas and only 1 receive antenna (suitable for a mobile downlink) as shown in Fig. 1. A number of U active users operates in the system. The total number of users can be seen as two groups of users transmitting information with the same orthogonal spreading codes used by both groups. To be able to separate the groups, each group is given a separation code $\mathbf{s}_1$ or $\mathbf{s}_2$ as shown in Fig. 1. The number of users in the system are split into two groups of K and Q users respectively. In the system the users' information stream is transmitted in blocks of L data bits for FEC purposes. For the rest of the paper we will refer to this as a *data block*. For the kth user every *data block*, $\{d_k(i)\}$; $i \in \{1, 2, \cdots, L\}$, $k \in \{1, 2, \cdots, U\}$, is first encoded by a convolutional encoder with a rate n_0 and memory ν. To reduce the effect of burst errors in the FEC decoders input, an interleaver (π_k) is applied to the resulting FEC coded bit stream. Each interleaved FEC coded bit is BPSK modulated yielding the stream, $\{b_k(t)\}$; $t \in \{1, 2, \cdots, \frac{L}{n_0}\}$. Codes of length N are used to spread the user's interleaved FEC coded bits. In a similar fashion to [11], a cyclic prefix of length equal to the channel length, α, is incorporated to combat the ISI effect of the channel. Also to obtain the desired space-time diversity gain, a real precoding matrix is incorporated into the signal transmitted from each antenna. Therefore, the space-time encoder input at time t (given by the superposition of the users' signal from both groups) is denoted by

$$\mathbf{x}_t = \mathbf{A}_m \mathbf{C} \mathbf{b}_t. \quad (1)$$

For the rest of the paper $\mathbf{x}_t$ will be referred to as a *STC symbol*. The $N \times U$ matrix $\mathbf{C}$

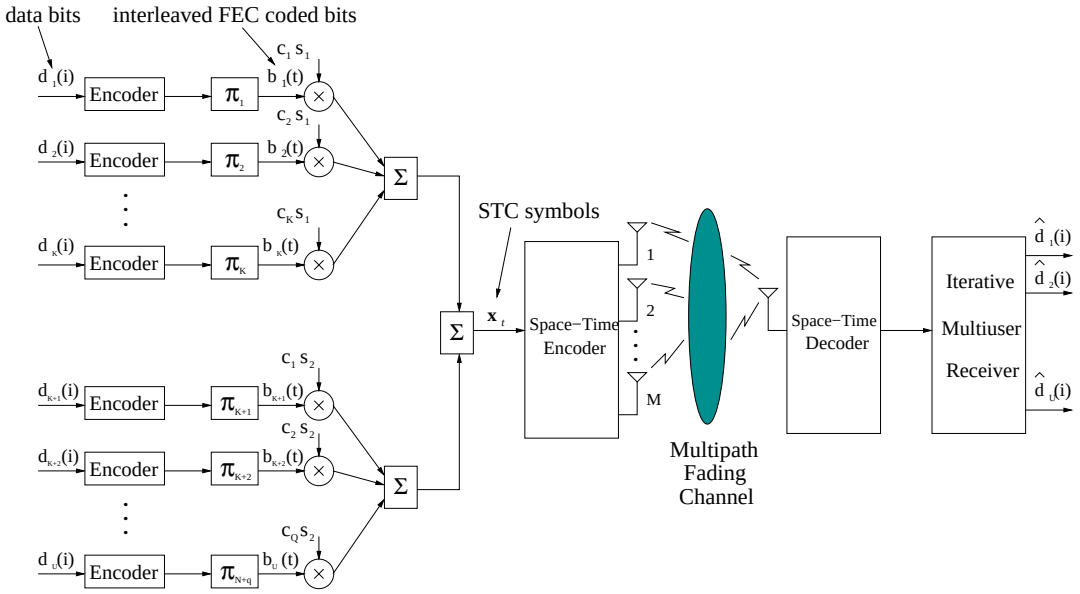

Fig. 1. Space-Time FEC Coded DS-CDMA system architecture.

contains the users' spreading and separation codes:

$$\mathbf{C} = \begin{bmatrix} c_{1,1}s_{1,1} & \cdots & c_{K,1}s_{1,1} & c_{1,1}s_{2,1} & \cdots & c_{Q,1}s_{2,1} \\ c_{1,2}s_{1,2} & \cdots & c_{K,2}s_{1,2} & c_{1,2}s_{2,2} & \cdots & c_{Q,2}s_{2,2} \\ \vdots & \ddots & \vdots & \vdots & \ddots & \vdots \\ c_{1,N}s_{1,N} & \cdots & c_{K,N}s_{1,N} & c_{1,N}s_{2,N} & \cdots & c_{Q,N}s_{2,N} \end{bmatrix} \tag{2}$$

where the nth chip of the spreading and separation code employed by the kth user is defined as $c_{k,n}s_{1,n} \in \left\{\frac{-1}{\sqrt{N}}, \frac{1}{\sqrt{N}}\right\}$ for $k \leq K$ and $c_{(k-K),n}s_{2,n} \in \left\{\frac{-1}{\sqrt{N}}, \frac{1}{\sqrt{N}}\right\}$ for $K < k \leq U$, with $s_{1,n}$, $s_{2,n}$ $\in \{-1, 1\}$ as the nth element of the group separation code and $n \in \{1, 2, \cdots, N\}$. The matrix $\mathbf{A}_m$ with $m \in \{1, 2, \cdots, M\}$, is a $(N + \alpha) \times N$ block matrix defined as

$$\mathbf{A}_m = \begin{bmatrix} \mathbf{A}_m^0 \\ \mathbf{A}_m^1 \end{bmatrix} \tag{3}$$

where the precoding matrix $\mathbf{A}_m^1$ with dimensions $N \times N$ is used to obtain the desired space-time diversity gain as it will be shown in section III B. The $\alpha \times N$ precoding matrix $\mathbf{A}_m^0$, used to incorporate the cyclic prefix, is defined as the last α rows of $\mathbf{A}_m^1$. Finally, $\mathbf{b}_t = [b_1(t), b_2(t), \cdots, b_U(t)]^T$ denotes the users data vector at time t with dimensions $U \times 1$. The data stream $\{\mathbf{x}_t\}$; $t \in \{1, 2, \cdots, \frac{L}{n_0}\}$ is then partitioned into blocks of *STC symbols* which are fed to the STC encoder to yield the data sequence to be transmitted through the M antennas. To guarantee that the overall transmit power is independent of the number of transmit antennas, a factor of $\frac{1}{\sqrt{M}}$ is applied to each of the antenna's signals before transmission. This factor is included in our system by defining the kth user amplitude as $b_k(t) \in \left\{\frac{-1}{\sqrt{M}}, \frac{1}{\sqrt{M}}\right\}$.

To illustrate the effect of the cyclic prefix, we first analyse the case of transmitting with only one antenna ($M = 1$). The two transmit antennas case and the generalisation to more antennas is considered in the next section. Therefore, with 1 transmit antenna the channel input is given directly by the data stream $\{\mathbf{x}_t\}$. Assuming perfect time synchronisation between transmitter and receiver, the channel output at discrete time t can be written as

$$\mathbf{r}_t = \mathbf{H}_1^d \mathbf{x}_t + \mathbf{H}_1^{ISI} \mathbf{x}_{t-1} \tag{4}$$

where the components of the vector $\mathbf{r}_t$ are the received signal sampled at the chip rate. The channel response matrix to the transmission of $\mathbf{x}_t$ is denoted by the $(N+\alpha)\times(N+\alpha)$ Toeplitz matrix

$$\mathbf{H}_1^d = \begin{bmatrix} h_{1,0} & 0 & 0 & 0 & \cdots & 0 \\ h_{1,1} & h_{1,0} & 0 & 0 & \cdots & 0 \\ \vdots & & \ddots & & \ddots & \vdots \\ 0 & \cdots & 0 & h_{1,\alpha} & \cdots & h_{1,0} \end{bmatrix}.$$

The term $\mathbf{H}_1^{ISI}\mathbf{x}_{t-1}$ in eq. (4) represents the effect of ISI, where $\mathbf{H}_1^{ISI}$ denotes a $(N+\alpha)\times(N+\alpha)$ Toeplitz matrix given by

$$\mathbf{H}_1^{ISI} = \begin{bmatrix} 0 & \cdots & 0 & h_{1,\alpha} & h_{1,\alpha-1} & \cdots & h_{1,1} \\ 0 & \cdots & 0 & 0 & h_{1,\alpha} & \cdots & h_{1,2} \\ \vdots & & \ddots & & & \ddots & \vdots \\ 0 & \cdots & 0 & 0 & 0 & \cdots & h_{1,\alpha} \\ 0 & \cdots & 0 & 0 & 0 & \cdots & 0 \\ \vdots & & \ddots & & & \ddots & \vdots \\ 0 & \cdots & 0 & 0 & 0 & \cdots & 0 \end{bmatrix}.$$

Since ISI occurs only on the first α samples of $\mathbf{r}_t$, the ISI effect can be eliminated by simply ignoring the first α samples in the reception of the data vector $\mathbf{r}_t$. Therefore, after neglecting the first α samples, the resulting $N \times 1$ vector at the receiver side is expressed as

$$\hat{\mathbf{r}}_t \overset{\text{def}}{=} \mathbf{r}_t(\alpha+1,\cdots,\alpha+N) = \mathbf{H}_1\mathbf{A}_1^1\mathbf{y}_t + \boldsymbol{\eta}_t \tag{5}$$

where the channel response matrix $\mathbf{H}_1$ is a $N \times N$ circulant Toeplitz matrix given by

$$\mathbf{H}_1 = \begin{bmatrix} h_{1,0} & 0 & \cdots & 0 & h_{1,\alpha} & h_{1,\alpha-1} & \cdots & h_{1,1} \\ h_{1,1} & h_{1,0} & \cdots & 0 & 0 & h_{1,\alpha} & \cdots & h_{1,2} \\ \vdots & & \ddots & & \ddots & & \ddots & \vdots \\ 0 & \cdots & 0 & 0 & \cdots & h_{1,\alpha} & \cdots & h_{1,0} \end{bmatrix}. \tag{6}$$

whereas $\mathbf{A}_1^1\mathbf{y}_t$ represents the last N samples of $\mathbf{x}_t$ with $\mathbf{y}_t = \mathbf{C}\mathbf{b}_t$. Finally, the noise vector $\boldsymbol{\eta}_t$ with dimensions $N \times 1$ contains zero-mean complex Gaussian noise samples with variance σ^2.

III. Space-Time Diversity Gain

Space-time trellis coding (STTC) [13] is a recent transmit diversity technique that combines signal processing at the receiver with a specific design of coding technique for multiple transmit antennas. Significant space-time diversity gain is achieved by applying this technique. However, space-time transmit diversity (STTD) [10] is a more remarkable and recent scheme for transmission using two transmit antennas. Despite a loss in performance compared to STTC, the decoding complexity of STTD is much less than STTC. Therefore, in terms of simplicity and performance the STTD scheme is perhaps a better choice for providing space-time diversity gain in real systems. The generalisation of the STTD scheme for more than two transmit antennas is addressed in [14]. For the sake of simplicity, we analyse our system for the case of two transmit antennas and one receive antenna. However, we provide and establish the fundamentals to extend the scheme to more than two transmit antennas.

A. STC Encoder

Conventional STC encoders with M transmit antennas require the same number of *STC symbol* periods to transmit a block of M *STC symbols*. However, as distinct from [10], in this paper we introduce a slight variation in the scheme by expanding the length of this block from M to $l \times M$ *STC symbols*, with $l \in \{1, 2, \cdots\}$. This variation is to reduce the penalty incurred by incorporating a cyclic prefix to every *STC symbol* as was suggested in [11]. As a result, only one cyclic prefix will be required every l *STC symbols*. Therefore, this new concept can be incorporated in our system by considering a new data stream $\{\bar{\mathbf{x}}_p\}$; $p \in \{1, 2, \cdots, \frac{L}{n_0 l}\}$ instead of $\{\mathbf{x}_t\}$; $t \in \{1, 2, \cdots, \frac{L}{n_0}\}$. The basic idea is to treat every element in $\{\bar{\mathbf{x}}_p\}$, which consists of l *STC symbols*, as a new virtual *STC symbol*. Therefore, there are totally only $\frac{L}{n_0 l}$ virtual *STC symbols* for every *data block*. For this new data stream, the pth element is given as

$$\bar{\mathbf{x}}_p = \bar{\mathbf{A}}_m \bar{\mathbf{C}} \bar{\mathbf{b}}_p \tag{7}$$

where $\bar{\mathbf{b}}_p = [\mathbf{b}_t^T, \mathbf{b}_{t+1}^T, \cdots, \mathbf{b}_{t+l-1}^T]^T$ is a concatenated vector with dimensions $(U \times l) \times 1$. The $(N \times l) \times (U \times l)$ matrix $\bar{\mathbf{C}}$ is a block diagonal matrix of the form

$$\bar{\mathbf{C}} = \begin{bmatrix} \mathbf{C} & \mathbf{0} & \cdots & \mathbf{0} \\ \mathbf{0} & \mathbf{C} & \cdots & \mathbf{0} \\ \vdots & & \ddots & \vdots \\ \mathbf{0} & \mathbf{0} & \cdots & \mathbf{C} \end{bmatrix} \tag{8}$$

in which the $N \times U$ matrix $\mathbf{C}$ is defined in section II (see (2)) and $\mathbf{0}$ as a $N \times U$ null matrix. Whereas the precoding matrix $\bar{\mathbf{A}}_m$ now becomes a block matrix of dimensions $(N \times l + \alpha) \times (N \times l)$ defined as

$$\bar{\mathbf{A}}_m = \begin{bmatrix} \bar{\mathbf{A}}_m^0 \\ \bar{\mathbf{A}}_m^1 \end{bmatrix} \tag{9}$$

with $\bar{\mathbf{A}}_m^1$ as a $(N \times l) \times (N \times l)$ block diagonal matrix given as

$$\bar{\mathbf{A}}_m = \begin{bmatrix} \mathbf{A}_m^1 & \mathbf{0} & \cdots & \mathbf{0} & \mathbf{0} \\ \mathbf{0} & \mathbf{A}_m^1 & \cdots & \mathbf{0} & \mathbf{0} \\ \vdots & & \ddots & & \vdots \\ \mathbf{0} & \mathbf{0} & \cdots & \mathbf{0} & \mathbf{A}_m^1 \end{bmatrix} \tag{10}$$

with $\mathbf{0}$ as a $N \times N$ null matrix. Lastly, the incorporation of the cyclic prefix is denoted by the $\alpha \times (N \times l)$ matrix $\bar{\mathbf{A}}_m^0$ which is defined as the last α rows of $\bar{\mathbf{A}}_m^1$. Notice that only one cyclic prefix will be required every l *STC symbols*, *i.e* one cyclic prefix per virtual *STC symbol*. To clarify exactly how individual *STC symbols* are sent from the transmitter, a layout of the *STC symbols* through the antennas is shown in Fig. 2. Firstly Fig. 2 (a) shows the scheme for a block transmission using $l = 1$, *i.e* the number of *STC symbols* is equal to the number of virtual *STC symbols* (conventional technique). On the other hand, a scheme using $l = 2$ is illustrated in Fig. 2 (b), notice that in this case only the first *STC symbol* of every virtual *STC symbol* requires the incorporation of a cyclic prefix. Therefore, in the pth time slot the $\bar{\mathbf{x}}_p$ and $\bar{\mathbf{x}}_{p+1}$ are the virtual *STC symbols* transmitted from antenna 1 and 2 respectively. In the next time slot (p+1), $-\bar{\mathbf{x}}_{p+1}$ is transmitted from antenna 1 and $\bar{\mathbf{x}}_p$ from antenna 2. It is clear that by setting $l = 1$, the STC encoder scheme is reduced to that given in [10, 11]. The criterion for selecting l will depend on two conditions: 1) how rapidly the channel changes and 2) the acceptable receiver complexity. In the following sections the relationship between l and these two conditions will be explained.

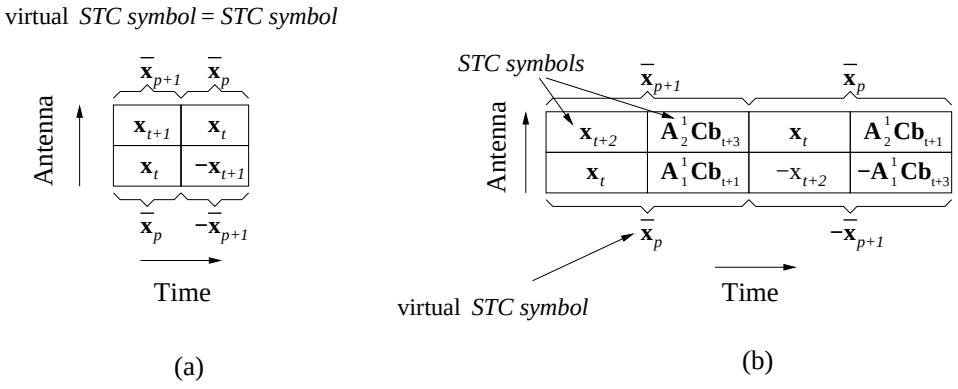

Fig. 2. STC encoder scheme with $M = 2$ and a block transmission using (a) $l = 1$ (conventional technique) and (b) $l = 2$.

B. STC Decoder

With no loss in the generality and in order to illustrate the STC decoder procedure, we carry on with the analysis for $M = 2$ and $l = 2$. Therefore, following a similar procedure to that presented for the derivation of eq. (5), the received signals from the pth and $(p+1)$th time slots can be written as

$$\begin{aligned} \hat{\mathbf{r}}_p &\stackrel{\text{def}}{=} \bar{\mathbf{r}}_p(\alpha+1,\cdots,\alpha+2N) = \bar{\mathbf{H}}_1\bar{\mathbf{A}}_1^1\bar{\mathbf{y}}_p + \bar{\mathbf{H}}_2\bar{\mathbf{A}}_1^1\bar{\mathbf{y}}_{p+1} + \bar{\boldsymbol{\eta}}_p \\ \hat{\mathbf{r}}_{p+1}^* &\stackrel{\text{def}}{=} \bar{\mathbf{r}}_{p+1}^*(\alpha+1,\cdots,\alpha+2N) = \bar{\mathbf{H}}_2^*\bar{\mathbf{A}}_2^1\bar{\mathbf{y}}_p - \bar{\mathbf{H}}_1^*\bar{\mathbf{A}}_2^1\bar{\mathbf{y}}_{p+1} + \bar{\boldsymbol{\eta}}_{p+1}^* \end{aligned} \tag{11}$$

where $\bar{\mathbf{y}}_p = \bar{\mathbf{C}}\bar{\mathbf{b}}_p$ and $\bar{\mathbf{y}}_{p+1} = \bar{\mathbf{C}}\bar{\mathbf{b}}_{p+1}$ are concatenated vectors with dimensions $2N \times 1$. The vectors $\bar{\boldsymbol{\eta}}_p$ and $\bar{\boldsymbol{\eta}}_{p+1}^*$ are $2N \times 1$ complex Gaussian noise vectors. The channel responses from each transmit antenna to the receiver antenna are represented by the matrices $\bar{\mathbf{H}}_m$ with $m = 1, 2$. Similar to (6) the mth matrix $\bar{\mathbf{H}}_m$ is denoted by a $2N \times 2N$ circulant and Toeplitz matrix with a first row $[h_{m,0}, 0, \cdots, 0, h_{m,\alpha}, h_{m,\alpha-1}, \cdots, h_{m,1}]$. As is shown in [11], due to the properties of the channel matrices, they can be diagonalised by the FFT basis vectors, *i.e* $\bar{\mathbf{H}}_m$ can be substituted by $\mathbf{W}\boldsymbol{\Lambda}_m\mathbf{W}^H$ where $\mathbf{W}$ denotes a $2N \times 2N$ matrix whose elements are given as $w_{g,f} = \exp(j2\pi gf/2N)/\sqrt{2N}$, with $g, f = 0, \cdots, 2N-1$ and $()^H$ as the Hermitian transpose operation. $\boldsymbol{\Lambda}_m$ is a $2N \times 2N$ diagonal matrix with $\lambda_{g,g} = \sum_{u=0}^{\alpha} h_{m,u}\exp(-j2\pi gu/2N)$ as its diagonal entries and zero elsewhere. For convenience the conjugate of $\hat{\mathbf{r}}_{p+1}$, denoted by $*$, is applied in (11). Multiplying $\hat{\mathbf{r}}_p$ by $\mathbf{W}^H$ and $\hat{\mathbf{r}}_{p+1}^*$ by $\mathbf{W}^T$ in (11), we obtain

$$\begin{aligned} \mathbf{W}^H\hat{\mathbf{r}}_p &= \boldsymbol{\Lambda}_1\mathbf{W}^H\bar{\mathbf{A}}_1^1\bar{\mathbf{y}}_p + \boldsymbol{\Lambda}_2\mathbf{W}^H\bar{\mathbf{A}}_1^1\bar{\mathbf{y}}_{p+1} + \mathbf{W}^H\bar{\boldsymbol{\eta}}_p \\ \mathbf{W}^T\hat{\mathbf{r}}_{p+1}^* &= \boldsymbol{\Lambda}_2^*\mathbf{W}^T\bar{\mathbf{A}}_2^1\bar{\mathbf{y}}_p - \boldsymbol{\Lambda}_1^*\mathbf{W}^T\bar{\mathbf{A}}_2^1\bar{\mathbf{y}}_{p+1} + \mathbf{W}^T\bar{\boldsymbol{\eta}}_{p+1}^*. \end{aligned} \tag{12}$$

In order to obtain the desired space-time diversity gain, we choose the precoding matrices $\mathbf{A}_1^1$ as the identity matrix and $\mathbf{A}_2^1$ as defined below

$$\mathbf{A}_2^1 = \begin{bmatrix} 1 & 0 & 0 & \cdots & 0 & 0 \\ 0 & 0 & 0 & \cdots & 0 & 1 \\ 0 & 0 & 0 & \cdots & 1 & 0 \\ \vdots & & & \ddots & \vdots & \vdots \\ 0 & 1 & 0 & \cdots & 0 & 0 \end{bmatrix}. \tag{13}$$

Therefore, using (9) and (10) the matrices $\bar{\mathbf{A}}_1^1$ and $\bar{\mathbf{A}}_2^1$ can be obtained. As shown in [11], the reason for selecting these precoding matrices is to ensure orthogonality between the signals

transmitted from different antennas. Thus, this choice of precoding matrices allows us to exploit the equality of $\mathbf{W}^H = \mathbf{W}^T\bar{\mathbf{A}}_2^1$ which then is used to represent $\mathbf{W}^H\hat{\mathbf{r}}_p$ and $\mathbf{W}^T\hat{\mathbf{r}}_{p+1}^*$ in the following form

$$\begin{bmatrix} \mathbf{W}^H\hat{\mathbf{r}}_p \\ \mathbf{W}^T\hat{\mathbf{r}}_{p+1}^* \end{bmatrix} = \begin{bmatrix} \mathbf{\Lambda}_1 & \mathbf{\Lambda}_2 \\ \mathbf{\Lambda}_2^* & -\mathbf{\Lambda}_1^* \end{bmatrix} \begin{bmatrix} \mathbf{W}^H\bar{\mathbf{y}}_p \\ \mathbf{W}^H\bar{\mathbf{y}}_{p+1} \end{bmatrix} + \begin{bmatrix} \mathbf{W}^H\bar{\boldsymbol{\eta}}_p \\ \mathbf{W}^T\bar{\boldsymbol{\eta}}_{p+1}^* \end{bmatrix}. \tag{14}$$

It is clear then that by defining

$$\mathbf{\Lambda} = \begin{bmatrix} \mathbf{\Lambda}_1 & \bar{\mathbf{\Lambda}}_2 \\ \mathbf{\Lambda}_2^* & -\bar{\mathbf{\Lambda}}_1^* \end{bmatrix} \tag{15}$$

and multiplying (14) by $\bar{\mathbf{W}}(\mathbf{\Lambda}^H\mathbf{\Lambda})^{-1}\mathbf{\Lambda}^H$, we obtain

$$\begin{bmatrix} \hat{\mathbf{y}}_p \\ \hat{\mathbf{y}}_{p+1} \end{bmatrix} = \begin{bmatrix} \bar{\mathbf{y}}_p \\ \bar{\mathbf{y}}_{p+1} \end{bmatrix} + \bar{\mathbf{W}}(\mathbf{\Lambda}^H\mathbf{\Lambda})^{-1}\mathbf{\Lambda}^H \begin{bmatrix} \mathbf{W}^H\bar{\boldsymbol{\eta}}_p \\ \mathbf{W}^T\bar{\boldsymbol{\eta}}_{p+1}^* \end{bmatrix} \tag{16}$$

where $\hat{\mathbf{y}}_p$, $\hat{\mathbf{y}}_{p+1}$ are the estimates of $\bar{\mathbf{y}}_p$ and $\bar{\mathbf{y}}_{p+1}$ respectively. The matrix $\bar{\mathbf{W}}$ is a $4N \times 4N$ block diagonal matrix given as

$$\bar{\mathbf{W}} = \begin{bmatrix} \mathbf{W} & \mathbf{0} \\ \mathbf{0} & \mathbf{W} \end{bmatrix}$$

with $\mathbf{0}$ as a $2N \times 2N$ null matrix. Taking out the contribution in eq. (16) of the signal at time slot p, we get

$$\hat{\mathbf{y}}_p \;=\; \bar{\mathbf{y}}_p + \boldsymbol{\varphi}_p \tag{17}$$

where $\boldsymbol{\varphi}_p$ is a $2N \times 1$ noise vector given as $\boldsymbol{\varphi}_p = \mathbf{W}(|\mathbf{\Lambda}_1|^2 + |\mathbf{\Lambda}_2|^2)^{-1}[\mathbf{\Lambda}_1^*\mathbf{W}^H\bar{\boldsymbol{\eta}}_p - \mathbf{\Lambda}_2\mathbf{W}^T\bar{\boldsymbol{\eta}}_{p+1}^*]$. Since $\bar{\mathbf{b}}_p = [\mathbf{b}_t^T, \mathbf{b}_{t+1}^T]^T$ (see (7)) is a concatenated vector and $\bar{\mathbf{y}}_p = \bar{\mathbf{C}}\bar{\mathbf{b}}_p$, we can further partition eq. (17) to extract only the signal related to $\mathbf{b}_t$, *i.e* as a function of time index t, resulting in

$$\mathbf{y}_t' \;=\; \mathbf{C}\mathbf{b}_t + \boldsymbol{\zeta}_t \tag{18}$$

with $\mathbf{y}_t'$ as an estimate of $\mathbf{y}_t$ and $\boldsymbol{\zeta}_t$ the noise vector given by the first N samples of $\boldsymbol{\varphi}_p$. Thus, we can finish this section by drawing analogies between eq. (18) and a synchronous DS-CDMA system over an AWGN channel. Since the elements in $\bar{\boldsymbol{\eta}}_p$ are complex Gaussian samples, this implies that the elements in $\boldsymbol{\zeta}_t$ are also complex Gaussian samples with zero mean and covariance matrix given by

$$\Omega \;=\; \sigma^2\mathbf{W}(|\mathbf{\Lambda}_1|^2 + |\mathbf{\Lambda}_2|^2)^{-1}\mathbf{W}^H. \tag{19}$$

The analogy between the model in eq. (18) and a synchronous DS-CDMA model for a AWGN channel is then evident. Following the STC encoding schemes studied in [14] for more that two transmit antennas, a similar process can be used to generalise the procedure presented in this section for $M > 2$.

IV. Iterative Multiuser Receiver

MUD techniques can be applied to eq. (18) since it represents a conventional signal model for a synchronous DS-CDMA system over an AWGN channel. In this particular case, MAI interference from the non-orthogonal users and additive noise are the interference factors. An attractive iterative multiuser structure was proposed in [5] for interference mitigation in a DS-CDMA system. In this section, we show that the basic principle is also applicable to the

space-time FEC coded DS-CDMA system proposed in this paper. The iterative multiuser receiver structure is illustrated in Fig. 3. It consists of a Wiener filter (WF) detector, followed by a soft cancellation (SC) scheme and a block of parallel MAP convolutional decoders. The cancellation/decoders are separated by interleavers and deinterleavers. The WF detector takes as its input the STC decoder output, $\mathbf{y}'_t$, and computes as its output an initial estimate of the *a priori* logarithm of likelihood ratios (LLR's) of the interleaved FEC coded bits for the desired user and the interfering users, $LLR_{wf}(b_k(t))$ with $k \in \{1, 2, \cdots, U\}$. Then the SC

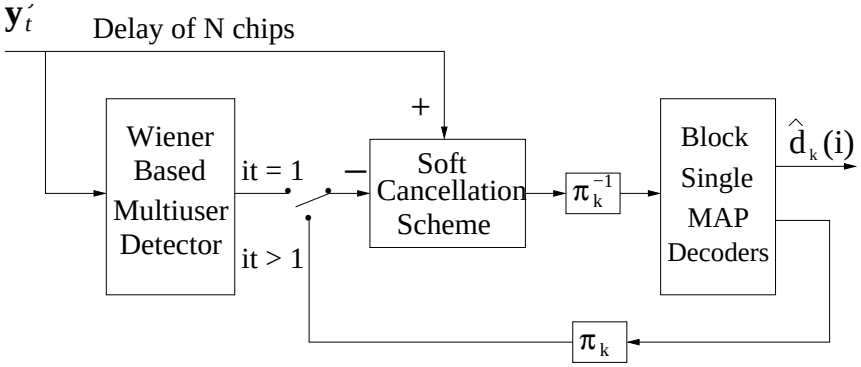

Fig. 3. Iterative multiuser receiver structure.

scheme, which incorporates the iterative principle, yields at its output an improved estimate of the LLR's of the interleaved FEC coded bits for the same group of users, $LLR^{\pi}_{sc}(b_k(t))$. The MAP decoder for the kth user takes as input the *a priori* LLR's of the deinterleaved FEC coded bits, $LLR^{\pi^{-1}}_{sc}(b_k(t))$, and computes at its output the *a posteriori* LLR's of the FEC coded bits as well as the *a posteriori* LLR's of the data bits. Lastly, the SC scheme and the block of single MAP decoders exchange soft information in an iterative fashion to improve the performance of the multiuser receiver. Next we describe each of these modules in the receiver structure.

A. Multiuser Detector

Firstly, the $LLR_{wf}(b_k(t))$ estimates are formed as

$$LLR_{wf}(b_k(t)) = \ln\left(\frac{p(y_k(t)|b_k(t) = \frac{1}{\sqrt{M}})}{p(y_k(t)|b_k(t) = \frac{-1}{\sqrt{M}})}\right) \tag{20}$$

where the conditional probabilities at the WF detector output, $p(y_k(t)|b_k(t) = b)$ with $b \in \{\frac{1}{\sqrt{M}}, \frac{-1}{\sqrt{M}}\}$, are calculated assuming Gaussian noise at the WF detector output. The scalar $y_k(t) = \boldsymbol{\psi}^T\{\mathbf{y}'_t\}_{Re}$ denotes the real part of the WF detector output for the kth user with mean $\boldsymbol{\psi}^T\boldsymbol{\phi}^k_{y'b}$ and noise variance $\sigma^2_n(k) = -(\boldsymbol{\psi}^T\boldsymbol{\phi}^k_{y'b})^2 + \boldsymbol{\psi}^T\boldsymbol{\phi}^k_{y'b}$ (see Appendix I). The vector $\boldsymbol{\psi} = [\psi_1, \psi_2, \cdots, \psi_N]^T$ is an N tap filter given by

$$\boldsymbol{\psi} = \boldsymbol{\Phi}^{-1}_{y'y'}\boldsymbol{\phi}^k_{y'b}.$$

$\boldsymbol{\Phi}_{y'y'}$ represents the autocorrelation matrix of the input signal with dimensions $N \times N$ which is $\boldsymbol{\Phi}_{y'y'} = \mathbf{CDC}^T + \sigma^2_{stc}\mathbf{I}$. The matrix $\mathbf{D}$ is a $U \times U$ matrix with its leading diagonal as the power of the users, $\frac{1}{M}$, and zero elsewhere. The matrix $\mathbf{I}$ is the $N \times N$ identity matrix and σ^2_{stc} the noise variance from the real part of $\boldsymbol{\zeta}_t$ (see eq. (18)). Since $\boldsymbol{\zeta}_t$ are Gaussian samples with zero mean and covariance matrix Ω, σ^2_{stc} can be estimated from independent channel realizations and therefore can be precomputed and stored in advance for different cases of

signal to noise ratio (SNR). The cross-correlation vector $\Phi^k_{y'b}$ is defined as the combination of the user spreading and separation codes (kth column of the matrix $\mathbf{C}$) multiplied by $\frac{1}{M}$.

B. Soft parallel cancellation scheme

The parallel cancellation scheme takes soft estimates of the interfering users and subtracts them from the received signal, $\mathbf{y}'_t$. Then a matched filter (MF) operation is applied to yield the output of the SC scheme. For the kth user, this quantity is expressed in the following form

$$\hat{y}_k(t) = \mathbf{q}_k[\mathbf{b}_t - \hat{\mathbf{b}}^k_t] + n_k(t) \tag{21}$$

where $\mathbf{q}_k$ denotes the kth row of the autocorrelation matrix given as $\mathbf{C}^T\mathbf{C}$, the vector $\hat{\mathbf{b}}^k_t$ corresponds to the soft estimates of the interfering users which are given as $\hat{\mathbf{b}}^k_t = [\hat{b}_1(t), \cdots, \hat{b}_{k-1}(t), 0, \hat{b}_{k+1}(t), \cdots, \hat{b}_U(t)]$. The soft estimate of a user is formed as

$$\hat{b}_k(t) = \sum_{b\epsilon\{\frac{-1}{\sqrt{M}}, \frac{1}{\sqrt{M}}\}} bp(b), \quad k = 1, \ldots, U. \tag{22}$$

where the conditional probabilities at the WF detector output, $p(y_k(t)|b_k(t) = b)$, are taking as the *a priori* probabilities $p(b)$ required in eq. (22), *i.e* $p(b) = p(y_k(t)|b_k(t) = b)$ with $b \epsilon \{\frac{1}{\sqrt{M}}, \frac{-1}{\sqrt{M}}\}$. Since the users from the same group still remain orthogonal, we set to zero their contribution in the vector $\hat{\mathbf{b}}^k_t$. Lastly, $n_k(t)$ represents a Gaussian noise sample with zero mean and variance σ^2_{stc}. Since the SC scheme output for the kth user can be well modelled by an equivalent AWGN, it can then be written in the following form

$$\hat{y}_k(t) = b_k(t) + z_k(t) \tag{23}$$

with $z_k(t)$ as a Gaussian noise sample with zero mean and variance (see Appendix II)

$$\sigma^2_z(k) = \frac{1}{M} \sum_{\substack{k_1=1 \\ k_1 \neq k}}^{U} q^2_{k,k_1} + \sigma^2_{stc} \tag{24}$$

q_{k,k_1} denotes the cross-correlation factor between user k and user k_1. Finally, the LLR^{π}_{sc}'s at the SC scheme output are then given by

$$LLR^{\pi}_{sc}(b_k(t)) \quad = \quad \ln\left(\frac{p(\hat{y}_k(t)|b_k(t) = \frac{1}{\sqrt{M}})}{p(\hat{y}_k(t)|b_k(t) = \frac{-1}{\sqrt{M}})}\right). \tag{25}$$

C. MAP Decoding

In our proposed system, convolutional codes are chosen as the channel code. In this section we just briefly describe the kth user's single decoder, which consists of a MAP decoder. As shown in Fig. 3, the deinterleaved *extrinsic* LLR's values, $LLR^{\pi^{-1}}_{sc}(b_k(t))$, are fed as input to the MAP convolutional decoder. This information is used directly in the MAP's branch metric calculation [15] which is modified as in [1–5] to

$$\gamma_i(m'_1, m_1) \quad = \quad Pr\{S_i = m_1/S_{i-1} = m'_1\} \prod_{t'=(i-1)n_0+1}^{in_0} p(\hat{y}_k(t')|b_k(t')) \tag{26}$$

where the product is over all the $b_k(t)$ values that produce the transition of the MAP decoder from state m'_1 to state m_1. At the first iteration no *a prior* information is available, therefore $Pr\{S_j = m_1/S_{j-1} = m'_1\} = 1/2$. Thus, the MAP decoder algorithm computes the *a posteriori* LLR's of the data bits, $LLR_{MAP}(d_k(t))$, based on the estimated FEC coded bits given by the soft cancellation scheme. Also, the *a posteriori* LLR's of the FEC coded bits, $LLR_{MAP}(b_k(t))$, are computed from the MAP algorithm.

D. Iterative scheme

To incorporate the iterative principle in the multiuser receiver structure, we make use of the soft *a posteriori* probabilities from the channel code, $a_k^t = LLR_{MAP}(b_k(t))$, which then can be used as *a priori* information for the soft cancellation scheme in eq. (22), *i.e* $p(b_k(t) = b) = e^{a_k^t}/(1+e^{a_k^t})$ if $b = 1/\sqrt{M}$ and $p(b_k(t) = b) = 1/(1+e^{a_k^t})$ if $b = -1/\sqrt{M}$. For the first iteration, the WF detector provides the required *a priori* probabilities to compute the soft estimates of interfering users. Therefore, at time t these *a priori* probabilities must be generated only for the FEC coded bits of those interfering users. On subsequent iterations, these quantities are computed by the MAP decoder based on the extrinsic LLR's values, $LLR_{MAP}(b_k(t))$. Note that for an iteration number > 1 these extrinsic LLR's values have to be interleaved to yield the appropriate ordering of the data stream at that stage. Finally, after a desired number of iterations the MAP decoder performs a hard decision on the LLR's of the data bits, $LLR_{MAP}(d_k(t))$, to recover the original uncoded data stream.

V. Complexity

For the complexity we focus our attention only on the space-time iterative multiuser receiver since the signal processing required at the transmitter can be easily accommodated in the base stations of current systems. In this paper we make no effort to reduce the complexity in the space-time iterative multiuser receiver, instead we highlight the practical implementation of the receiver architecture.

A. STC Decoder Complexity

Firstly, the STC decoder requires computation of the matrices, $\mathbf{W}^H$ or $\mathbf{W}^T$ (FFT of the received data block), $\mathbf{\Lambda}^H$ and $(\mathbf{\Lambda}^H\mathbf{\Lambda})^{-1}$ (see section III B). Since $\mathbf{W}$ is known it can be precomputed and stored in advance. Also $(\mathbf{\Lambda}^H\mathbf{\Lambda})^{-1}$ can be simplified by the fact that $\mathbf{\Lambda}^H\mathbf{\Lambda}$ is a diagonal matrix whose diagonal entries are given by the magnitude of the diagonal elements from the matrices $\mathbf{\Lambda}_m$ with $m = 1, 2, \cdots, M$ (see section III B). Therefore, the computation of $(\mathbf{\Lambda}^H\mathbf{\Lambda})^{-1}$ is then reduced to the scalar inversion of its diagonal elements. It can then be established that the STC decoder complexity per user is independent of U (the number of users) and mainly determined by the multiplication of matrices, $O((l \times N)^2)$. Since users may be either static or moving, the computation of $\mathbf{\Lambda}^H$ and $(\mathbf{\Lambda}^H\mathbf{\Lambda})^{-1}$ needs to be updated at a higher rate than the channel Doppler.

B. Iterative Multiuser Receiver Complexity

The complexity per bit per user per iteration of the proposed iterative multiuser receiver is mainly determined by the following operations. Firstly, the major concern in complexity from the WF detector is the inversion of the matrix $\mathbf{\Phi}_{y'y'}$, whose complexity is $O(GN^3)$ with G as the number of interfering users plus one (notice that $G < N$), this matrix requires knowledge of the spreading and separation users codes and the noise variance σ_{stc}^2, see section IV A. Since the user codes are known, it can be seen that $\mathbf{\Phi}_{y'y'}^{-1}$ mainly changes according to the value of σ_{stc}^2. However, the noise variance σ_{stc}^2 can be estimated from independent channel realizations and therefore the matrix $\mathbf{\Phi}_{y'y'}^{-1}$ can be precomputed and stored in advance for different cases of σ_{stc}^2. Secondly, for the constituent convolutional codes of memory ν, the decoding complexity is $O(G2^\nu)$. Normally ν is chosen small to reduce the complexity of this part of the receiver. Finally, other complexity factors of importance are the complexity contribution from the SC scheme, which is linear with the number of interfering users $O(G)$, and the operations required to compute the likelihood metric calculations. For a number of iteration > 1, the complexity of the iterative multiuser receiver is reduced to the complexity in the SC scheme and the MAP decoders.

VI. Simulation Results

Monte Carlo simulations are provided to illustrate the performance of the proposed space-time FEC coded DS-CDMA system. To evaluate the performance we simulate the downlink of a synchronous DS-CDMA system with M transmit antennas and 1 receive antenna. Unless otherwise stated, Walsh codes of length $N = 16$ are used for the spreading. The channel coefficients, $h_{m,u}$ with $m = 1, 2, \cdots, M$ and $u = 0, 1, \cdots, \alpha$, are modelled as Rayleigh fading random variables. The time-varying impulse response of the channel is power normalised to be $\mathcal{N}(0, 1)$. It is assumed that the receiver has perfect knowledge of the fading coefficients. For the rest of this section it is also assumed that the ISI spans 25% of the symbol period ($\alpha = 4$). To demonstrate the effect of expanding the STC encoder input block length as suggested in section III A, we first present the single-user BER performance versus SNR (measured in terms of the E_b/N_0) with no FEC coding. Fig. 4 shows the single-user performance in a multipath fading channel for 1 and 2 transmit antennas. The curves in Fig. 4 shows the BER performance for a given number of transmit antennas when the STC encoder input block is set with $l = 1$, $l = 2$ and $l = 4$. From eq. (18) after despreading an expression can be derived

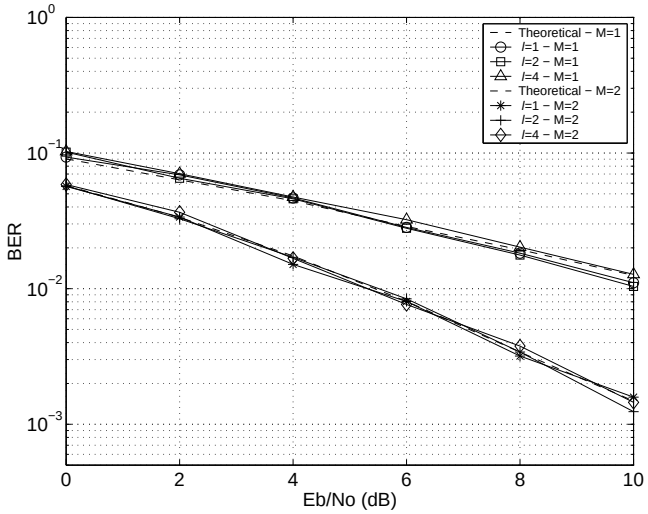

Fig. 4. Theoretical and simulated results for the single-user BER performance versus E_b/N_0 over a multipath fading channel with $\alpha = 4$ and $N = 16$. The results are obtained for 1 and 2 transmit antennas when the STC encoder input block length is set to $l = 1, 2$ and 4.

for the BER performance, therefore the theoretical performance is also provided to compare with these results. The theoretical BER performance is given as

$$BER = \texttt{erf}\left(\sqrt{\frac{1}{M\sigma_{cw}^2}}\right) \tag{27}$$

where the noise power is defined as $\sigma_{cw}^2 = \bar{\mathbf{C}}^{\mathbf{T}}\Omega\bar{\mathbf{C}}$ with $\bar{\mathbf{C}}$ and Ω as given in equations (8) and (19) respectively. An average over 10000 independent channel realisations were used to obtain the theoretical BER performance. From the results it can be seen that for a given number of transmit antennas the same performance is obtained in the system regardless of the STC encoder input block length. Since only one cyclic prefix is required every l *STC symbols* a reduction in the penalty of incorporating cyclic prefixes is achieved. Therefore the higher the block length l the better the throughput in the system.

The model shown in Fig. 1 allows us to simulate a system with U active users divided into two groups. The separation of the user groups can be done in two different ways: 1) Each group with the same number of users, *i.e* $K = Q = U/2$, or 2) A group with K users where $K = N$ if $U > N$ or $K = U$ if $U < N$, and a second group with Q users where $Q = U - K$ if $U > N$ otherwise $Q = 0$. To illustrate the effect of the way the user groups are split, Fig. 5 shows the average BER performance as a function of the number of users for $E_b/N_0 = 4$ dB. The system is implemented for $M = 2$ and $l = 1$. For the FEC coding each user employs a recursive systematic convolutional (RSC) code of rate $n_0 = 1/2$, memory $\nu = 2$ and generators $(7, 5)$ in octal notation. Every user transmits *data blocks* of $L = 200$ information bits. The group separation codes, $\mathbf{s}_1$ and $\mathbf{s}_2$, of length N are chosen by generating random codes of length N and then calculating the cross-correlation $\mathbf{s}_1^T\mathbf{s}_2$. The separation codes generated here have a maximum normalise cross-correlation of $\mathbf{s}_1^T\mathbf{s}_2 \leq 0.5$. Random interleavers (π) are used to reduce the effect of burst errors in the decoders' input. Fig. 5 shows that a better performance is obtained when the user groups are unequal *i.e* $K > Q$. With unequal groups the system can serve up to 16 orthogonal users and the MAI effect does not appear in the system until $U > N$. Even though the BER performance for individuals users can initially differ from each group (the group with Q users faces more MAI that the group with K users), however this phenomenon is only experienced in the first few iterations of the multiuser receiver as will be shown next.

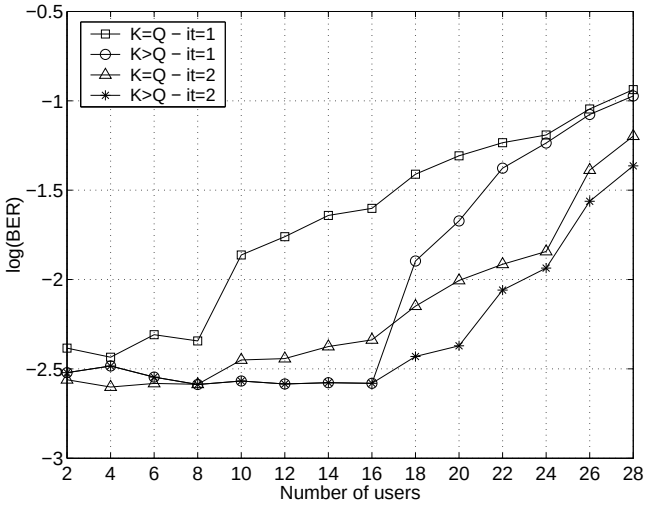

Fig. 5. Probability of error versus number of users for a $Eb/No = 4dB$ over a multipath fading channel with $\alpha = 4$. The system is implemented for $M = 2$, $L = 200$, $l = 1$, $N = 16$ and using 1 and 2 iterations in the iterative multiuser receiver. The FEC consists of a RSC with $n_0 = 1/2$, $\nu = 2$ and generators $(7, 5)$.

Simulation results in Fig. 6 shows now the average BER performance against the number of iterations in the multiuser receiver. The simulations are performed for a system with $U = 26$ users divided into a group of $K = 16$ and a group of $Q = 10$ users. As defined before every user transmits *data blocks* of $L = 200$ data bits which are encoded by a RSC code of rate $1/2$, $\nu = 2$ with generator polynomials $(7, 5)$ and then randomly interleaved. N Walsh-Hadamard codes are used for the spreading and the group separation codes $\mathbf{s}_1$ and $\mathbf{s}_2$ are also limited to those with a normalised cross-correlation of $\mathbf{s}_1^T\mathbf{s}_2 \leq 0.5$. The system is implemented for $M = 2$ and $l = 4$.

Results show that with only four iterations in the multiuser receiver this highly loaded

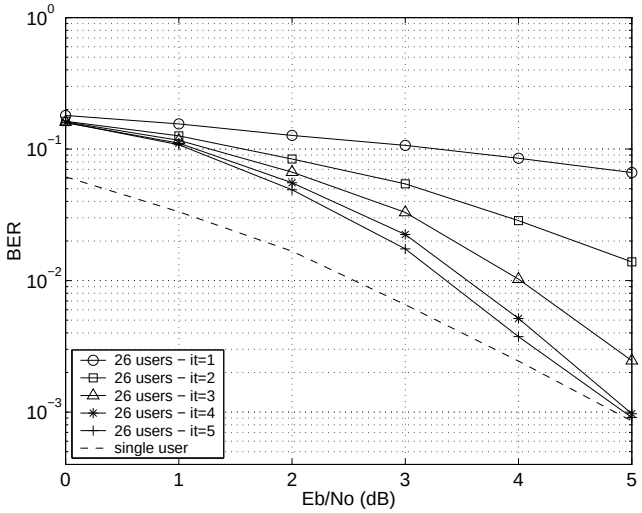

Fig. 6. Probability of error for the space-time coded DS-CDMA system as a function of the Eb/No over a multipath fading channel with $\alpha = 4$. The system is implemented for $M = 2$ and 1 receive antenna using $l = 4$, $N = 16$, $K = 16$, $Q = 10$, $L = 200$ and up to 5 iterations in the iterative multiuser receiver. The FEC consists of a RSC with $n_0 = 1/2$, $\nu = 2$ and generators $(7, 5)$.

system over a multipath fading channel achieves near single-user performance, *i.e* a probability of error of 10^{-3} with an E_b/N_o of 5 dB. If we examine the best and worst users, in terms of the BER, from each group and after 4 iteration the results for $E_b/N_o = 5$ dB show that all users converge to about the same average performance as is shown in Table 1. This means that no penalty is occurred in individual performances by splitting the users into unequal groups.

	Group with K users	Group with Q users	iterations
Best user	0.00107	0.00094	4
Worst user	0.00254	0.00144	4

Table 1
Individual user BER performance for $E_b/N_0 = 5$ dB.

VII. Conclusions

In this paper we have presented a high capacity space-time coded DS-CDMA system over multipath fading channels. The main contribution is in combining antenna array and iterative processing techniques to design a space-time transmitter/receiver capable of mitigating interference and multipath to achieve a significant spectral efficiency improvement. The reuse of orthogonal codes is investigated as a method to enhance further the system capacity. Also we have derived a multiuser receiver which approaches single-user performance for very large system loads, *i.e* a spectrally efficient system.

Simulation results show acceptable performance for a system 160% loaded over a multipath fading channel where the ISI spans 25% of the data symbol. If we were to incorporate cyclic prefixes for each symbol to combat multipath, a reduction in the overall data rate would be yielded. To reduce this penalty a variation in the STC encoder scheme is proposed, for

instance in the particular case presented in this paper (choosing $l = 4$) the overall data rate is reduced by only 6.25% instead of 25% as suggested in [11] (choosing $l = 1$). This penalty can be reduced further if l is made larger still, but at the expense of increasing the complexity at the receiver. We are assuming that the channel is invariant within a block of symbols, which may not be true for larger blocks.

Appendix

I. Noise variance at the WF detector output

The minimum mean square error (MMSE) at the output of the WF detector is given as

$$\begin{aligned} MMSE &= E[(b_k(t) - y_k(t))^2] \\ &= E[b_k^2(t)] - 2E[b_k(t)y_k(t)] + E[y_k^2(t)] \end{aligned} \tag{28}$$

where $E[]$ denotes the expected value. The variance of the WF detector output is given by

$$\sigma_n^2(k) = E[y_k^2(t)] - E^2[y_k(t)]. \tag{29}$$

On the other hand, substituting $y_k(t) = \boldsymbol{\psi}^T\{\mathbf{y}'_t\}_{Re}$ (see section IV A) in (28) we obtain

$$\begin{aligned} MMSE &= E[(b_k(t) - \boldsymbol{\psi}^T\mathbf{y}'_t)(b_k(t) - \boldsymbol{\psi}^T\mathbf{y}'_t)^T] \\ &= E[b_k^2(t)] - 2\boldsymbol{\psi}^T E[\mathbf{y}'_t b_k(t)] + \boldsymbol{\psi}^T E[\mathbf{y}'_t(\mathbf{y}'_t)^T]\boldsymbol{\psi} \\ &= E[b_k^2(t)] - 2\boldsymbol{\psi}^T\boldsymbol{\phi}^k_{y'b} + \boldsymbol{\psi}^T\boldsymbol{\Phi}_{y'y'}\boldsymbol{\psi} \end{aligned} \tag{30}$$

where for simplicity we denote $\mathbf{y}'_t = \{\mathbf{y}'_t\}_{Re}$. Since $\boldsymbol{\psi} = \boldsymbol{\Phi}^{-1}_{y'y'}\boldsymbol{\phi}^k_{y'b}$, eq. (30) can be simplified to

$$\begin{aligned} MMSE &= E[b_k^2(t)] - 2\boldsymbol{\psi}^T\boldsymbol{\phi}^k_{y'b} + \boldsymbol{\psi}^T\boldsymbol{\Phi}_{y'y'}\boldsymbol{\Phi}^{-1}_{y'y'}\boldsymbol{\phi}^k_{y'b} \\ &= E[b_k^2(t)] - \boldsymbol{\psi}^T\boldsymbol{\phi}^k_{y'b} \end{aligned} \tag{31}$$

therefore, by subtracting eq. (28) from eq. (29) and substituting $MMSE$ as given in (31), we get

$$\begin{aligned} \sigma_n^2(k) &= -E^2[y_k(t)] + 2E[b_k(t)y_k(t)] - E[b_k^2(t)] + MMSE \\ &= -(\boldsymbol{\psi}^T\boldsymbol{\phi}^k_{y'b})^2 + 2\boldsymbol{\psi}^T\boldsymbol{\phi}^k_{y'b} - E[b_k^2(t)] + E[b_k^2(t)] - \boldsymbol{\psi}^T\boldsymbol{\phi}^k_{y'b} \\ &= -(\boldsymbol{\psi}^T\boldsymbol{\phi}^k_{y'b})^2 + \boldsymbol{\psi}^T\boldsymbol{\phi}^k_{y'b} \end{aligned} \tag{32}$$

II. Noise variance at the SC scheme output

From eq. (23) in section IV B the variance of $z_k(t)$ is given as

$$\sigma_z^2 = E[z_k^2(t)] - E^2[z_k(t)] \tag{33}$$

where again E[] denotes the expected value and $z_k(t)$ is given by

$$z_k(t) = \sum_{\substack{k_1=1 \\ k_1 \neq k}}^{U} q_{k,k_1}[b_{k_1}(t) - \hat{b}_{k_1}(t)] + n_k(t) \tag{34}$$

with q_{k,k_1} as the cross-correlation factor between user k and user k_1. Considering the fact that $E[b_k(t)] = 0$ for $k = 1, 2, \cdots, U$ and using eq. (34), we get

$$E^2[z_k(t)] = \left(\sum_{\substack{k_1=1 \\ k_1 \neq k}}^{U} -q_{k,k_1} E[\hat{b}_k(t)] \right)^2 \tag{35}$$

and

$$E[z_k^2(t)] = \sum_{\substack{k_1=1 \\ k_1 \neq k}}^{U} q_{k,k_1}^2 E[b_k^2(t)] + \left(\sum_{\substack{k_1=1 \\ k_1 \neq k}}^{U} -q_{k,k_1} E[\hat{b}_k(t)] \right)^2 + \sigma_{stc}^2 \tag{36}$$

therefore it can be shown that the variance σ_z^2 is then given by

$$\sigma_z^2(k) = \frac{1}{M} \sum_{\substack{k_1=1 \\ k_1 \neq k}}^{U} q_{k,k_1}^2 + \sigma_{stc}^2 \tag{37}$$

References

[1] M. Moher, "An Iterative Multiuser Decoder for Near-capacity Communications," IEEE Transactions on Communications, vol. 46, no. 7, pp. 870-880, July 1998.

[2] M.C. Reed, C.B. Schlegel, P.D. Alexander, and J.A. Asenstorfer, "Iterative Multiuser Detection for CDMA with FEC: Near-Single-User Performance," IEEE Transactions on Communications, vol. 46, no. 12, pp. 1693-1699, December 1998.

[3] X. Wang, and H.V. Poor, "Iterative (Turbo) Soft Interference Cancellation and Decoding for Coded CDMA," IEEE Transactions on Communications, vol. 47, no. 7, pp. 1046-1060, July 1999.

[4] P.D. Alexander, M.C. Reed, J.A. Asenstorfer, C.B. Schlegel, "Iterative Multiuser Interference Reduction: Turbo CDMA," IEEE Transactions on Communications, vol 47, no. 7, pp. 1008-1014, July 1999.

[5] J.M. Luna Rivera, D.G.M. Cruickshank, and J.S. Thompson, "Iterative Multiuser Receiver for a Coded DS-CDMA System," in *Proc.* IEEE Vehicular Technology conference (VTC 2001 spring), vol. 2, pp. 1518-1522, Rhodes Island, Greece, May 2001.

[6] G.J. Foschini, "Layered space-time architecture for wireless communication in fading environments when using multiple antennas," Bell Labs. Techn. J., vol. 2, Autumn 1996.

[7] V. Tarokh, N. Seshadri, and A.R. Calderbank, "Space-time codes for high data rate wireless communication: Performance criterion and code construction," IEEE Transaction on Communications, vol. 47, No. 2, pp. 199-207, February 1999.

[8] S. Marinkovic, B. Vucetic and A. Ushirokawa, "Space-Time Iterative and Multistage Receiver Structures for CDMA Mobile Communications Systems," IEEE Journal on Selected Areas in Communications, vol. 19, No. 8, pp. 1594-1604, August 2001.

[9] D. Agrawal, V. Tarokh, A. Nagui, and N. Seshadri, "Space-time coded OFDM for high data-rate wireless communication over wideband channels," in *Proc.* IEEE Vehicular Technology Conference (VTC 1998), vol. 3, pp. 2232-2236, Ottawa, Ontario, Canada, May 1998.

[10] S. M. Alamouti, "A Simple Transmit Diversity Technique for Wireless Communications," IEEE Journal on Selected Areas in Communications, vol. 16, no. 8, pp. 1451-1458, October 1998.

[11] S. Barbarossa and F. Cerquetti, "Simple Space-Time Coded SS-CDMA Systems Capable of Perfect MUI/ISI Elimination," IEEE Communications Letters, vol. 5, No. 12, pp. 471-473, December 2001.

[12] C. Berrou, A. Glavieux, "Near Optimum Error-Correcting Coding and Decoding: Turbo-Codes," IEEE Transactions on Communications, vol. 44, no. 10, pp. 1261-1271, October 1996.

[13] A.F. Naguib, N. Seshadri and A.R. Calderbank, "Increasing data rate over wireless channels," IEEE Signal Processing Magazine, vol. 17, No. 3, pp. 76-92, May 2000.

[14] V. Tarokh, H. Jafarkhani, and A.R. Calderbank, "Space-Time Block Codes from Orthogonal Designs," IEEE Transactions on Information Theory, vol. 45, no. 5, pp. 1456-1467, July 1999.

[15] L.R. Bahl, J. Cocke, F. Jelinek, and J. Raviv, "Optimal decoding of linear codes for minimizing symbol error rate," IEEE Transaction on Information Theory, vol. 20, pp. 284-287, March 1974.